

UNCLASSIFIED

AD NUMBER
AD864964
NEW LIMITATION CHANGE
TO Approved for public release, distribution unlimited
FROM Distribution authorized to U.S. Gov't. agencies and their contractors; Administrative/Operational Use; Oct 1969. Other requests shall be referred to U.S. Army Aviation Material Laboratories, Fort Eustis, VA 23604.
AUTHORITY
USAAMRDL ltr, 28 Apr 1971

THIS PAGE IS UNCLASSIFIED

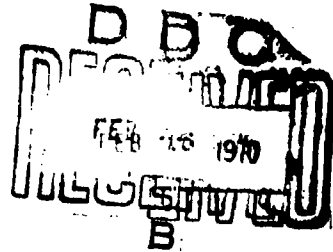
AD 864964

AD

USAAVLABS TECHNICAL REPORT 69-75

**ADVANCEMENT OF STRAIGHT AND SPIRAL BEVEL GEAR
TECHNOLOGY**

By
W. Coleman
E. P. Lohmann
D. W. Mollis
D. M. Pool



October 1969

**U. S. ARMY AVIATION MATERIEL LABORATORIES
FORT EUSTIS, VIRGINIA**

**CONTRACT DAAJ02-68-C-0032
THE GLEASON WORKS
ROCHESTER, NEW YORK**

This document is subject to special export controls, and each transmittal to foreign governments or foreign nationals may be made only with prior approval of US Army Aviation Materiel Laboratories, Fort Eustis, Virginia 23604.



Reproduced by the
CLEARINGHOUSE
for Federal Scientific & Technical
Information Springfield Va. 22151

292

DISCLAIMER NOTICE

THIS DOCUMENT IS BEST QUALITY PRACTICABLE. THE COPY FURNISHED TO DTIC CONTAINED A SIGNIFICANT NUMBER OF PAGES WHICH DO NOT REPRODUCE LEGIBLY.

Disclaimers

The findings in this report are not to be construed as an official Department of the Army position unless so designated by other authorized documents.

When Government drawings, specifications, or other data are used for any purpose other than in connection with a definitely related Government procurement operation, the United States Government thereby incurs no responsibility nor any obligation whatsoever; and the fact that the Government may have formulated, furnished, or in any way supplied the said drawings, specifications, or other data is not to be regarded by implication or otherwise as in any manner licensing the holder or any other person or corporation, or conveying any rights or permission, to manufacture, use, or sell any patented invention that may in any way be related thereto.

Trade names cited in this report do not constitute an official endorsement or approval of the use of such commercial hardware or software.

Disposition Instructions

Destroy this report when no longer needed. Do not return it to the originator.

PROPERTY OF	
FORM	DATE ACTION <input type="checkbox"/>
NO.	OFF ACTION <input type="checkbox"/>
CLASSIFICATION	<input type="checkbox"/>
DISPOSITION	
BY	
DISTRIBUTION/CLASSIFICATION CODE	
EXT. + AVAIL. AND/OR SPECIAL	
2	



DEPARTMENT OF THE ARMY
HEADQUARTERS US ARMY AVIATION MATERIAL LABORATORIES
FORT EUSTIS, VIRGINIA 22604

This report presents part of a continuing program to derive more accurate and uniform gear design formulas for aircraft propulsion systems than are currently available. Included are the results of an analytical and experimental program conducted to derive improved formulas for predicting the strength of bevel gears and to furnish a usable computer program that would enable a gear designer to effectively design high-capacity gear sets.

This command concurs in the conclusions made by the contractor.

Task IG162204A01401
Contract DAAJ02-68-C-0032
USAAVLABS Technical Report 69-75
October 1969

ADVANCEMENT OF STRAIGHT AND SPIRAL BEVEL GEAR
TECHNOLOGY

Final Report

By

W. Coleman
E. P. Lehmann
D. W. Mellis
D. M. Peel

Prepared by

The Gleason Works
Rochester, New York

for

U. S. ARMY AVIATION MATERIEL LABORATORIES
FORT EUSTIS, VIRGINIA

This document is subject to special export controls, and each transmittal to foreign governments or foreign nationals may be made only with prior approval of U. S. Army Aviation Materiel Laboratories, Fort Eustis, Virginia 23604.

SUMMARY

The purpose of this project was to review existing formulas for the strength of bevel gear teeth, to select the method that is currently considered to be the best, to determine what factors in this method need further study and development, to outline a program for improving the method, and to carry out a program of theoretical and experimental investigation to develop this improved method.

Four methods for analyzing gear strength were reviewed. One of these was selected as the most reliable starting point for the project, and six factors were selected for further analysis.

Basic test gear geometry was chosen to be consistent with current-day practice and to permit fatigue testing on the three major pieces of available equipment.

Four types of tests were selected that would provide sufficient information concerning the fatigue properties of gears.

The conclusions of this report are summarized as follows:

1. A new, improved method for the stress determination of bevel gears was found.
2. The basic material strength curve for carburized AMS-6265 was established.
3. A design S-N curve for AMS-6265 was established.
4. An improved formula for effective face width was developed.
5. The correction factor for locating the position of the point of load application has been modified.
6. An improved formula for the load distribution factor was derived.
7. A new formula for size factor has been introduced in the equation for working stress.
8. Lengthwise tooth curvature was found to have the most significant effect on gear tooth strength and is recognized for the first time in a gear tooth strength formula.

9. A computer program has been provided for the gear designer.

A significant improvement in the formulas for the strength of bevel gear teeth has been achieved, which will materially aid in the design of future bevel gear drives.

FOREWORD

This is the final report on the Gleason project entitled "Advancement of Straight and Spiral Bevel Gear Technology". This project was conducted during the 16-month period from 23 February 1968 through 23 June 1969 for the U. S. Army Aviation Materiel Laboratories (USAAVLABS) under Contract DAAJ02-69-C-0032, Task IG162204A01401.

USAAVLABS technical direction was provided by Mr. R. Givens.

Outside consultants consisted of Professor Frank Mc Clintock of the Massachusetts Institute of Technology and Mr. Eugene Shipley of Mechanical Technology Incorporated, whose suggestions were very useful.

Special acknowledgement is given to Mr. Charles B. King of the Gleason Works, who managed the project until his retirement.

TABLE OF CONTENTS

	<u>Page</u>
SUMMARY	iii
FOREWORD	v
LIST OF ILLUSTRATIONS	x
LIST OF TABLES	xviii
INTRODUCTION	1
PRELIMINARY ANALYSIS	3
Historical Background	3
Comparison of Bevel Gear Strength Standards	4
TEST GEAR DESIGN	7
Tooth Design	7
Blank Design	13
TEST GEAR MANUFACTURE	17
Blanks	17
Teeth	17
Material Evaluation	19
GEAR TESTING	21
Types of Tests	21
Test Equipment	22
Test Procedure	32
RESULTS OF TESTS	40
Documentation of Results	40
Test Failures	40
Metallurgical Investigations	48

	Page
NEW STRENGTH FORMULAS	60
Effective Face Width	60
Position of Point of Load Application	62
Load Distribution Factor	62
Size Factor	64
Final Strength Formulas	65
ANALYSIS OF RESULTS	68
Torque Vs Life Diagrams	68
Stress Vs Life Diagrams	77
Torque Vs Stress	77
R. R. Moore Analysis	78
Comparison of R. R. Moore and Dynamic Tests	85
Comparison of R. R. Moore and Pulsing Tests	87
Effect of Cutter Diameter	88
Endurance Limit for AISI 9310 Vacuum-Melt Steel	88
Fatigue Test Data From Past Dynamic Tests	90
Endurance Limit for Air-Melt Steel	90
Slope of the S-N Diagrams	90
Peak Stress	93
Validation of New Strength Formula	94
COMPUTER PROGRAM	95
Stress Formula Documentation	95
Input-Output Data	95
Program Listing	96
CONCLUSIONS	97
LITERATURE CITED	99
APPENDIXES	
I. Gear Manufacturing Data	101
II. Gear Testing Data	136
III. Effective Face Width	157
IV. Load Distribution Factor	185

	<u>Page</u>
V. Stress Formula Documentation	203
VI. Computer Program	216
VII. Comparison of AGMA and German Methods of Strength Determination for Bevel Gears	249
• DISTRIBUTION	268
•	

LIST OF ILLUSTRATIONS

<u>Figure</u>		<u>Page</u>
1	Spiral Bevel Gear Dimension Sheet for the 17/51 Combination, Test Gears Produced With 12-Inch Cutter Diameter	8
2	Spiral Bevel Gear Dimension Sheet for the 17/51 Combination, Test Gears Produced With 7-1/2-Inch Cutter Diameter	9
3	Deflection Testing Machine With Test Box . . .	24
4	Gleason No. 510 Axle Test Machine Used for Dynamic Testing	24
5	Schematic Diagram of Gleason No. 510 Axle Test Machine	25
6	Test Box Used for the Gleason No. 510 Axle Test Machine for Dynamic Testing	27
7	Sketch of Test Box for Dynamic Tests	28
8	Gleason Bevel Gear Pulser.	30
9	Schematic Diagram of Gleason Bevel Gear Pulser	31
10	Test Box Showing Indicators Mounted for Measuring Deflections	34
11	Typical Bending Fatigue Crack in Root of Gear Tooth	44
12	Typical Bending Fatigue Crack in Root of Gear Tooth	44
13	Typical Bending Fatigue Crack in Root of Pinion Tooth	45
14	Typical Bending Fatigue Crack in Root of Pinion Tooth	45

<u>Figure</u>		<u>Page</u>
15	Fatigue Cracks on the Profile of a Gear Tooth	46
16	Fatigue Fracture Resulting From Cracks on the Tooth Profile of a Gear Tooth	46
17	Typical Bending Fatigue Crack in the Root of the Pinion Tooth on Pulser Test	47
18	Typical Bending Fatigue Crack in the Root of the Gear Tooth on Pulser Test	47
19	Hardness Traverse on Test Gear No. 123	49
20	Photomicrograph of Case Structure in Test Gear No. 123	50
21	Photomicrograph of Core Structure in Test Gear No. 123	50
22	Case Depth Vs Hardness Traverse for R. R. Moore Specimens 3 and 16	51
23	Photomicrograph of Case Structure in R. R. Moore Specimens	53
24	Photomicrograph of Core Structure in R. R. Moore Specimens	53
25	Hardness Traverse on Test Gear No. 122	54
26	Case Microstructure on Test Gear No. 122	55
27	Core Microstructure on Test Gear No. 122	55
28	Photograph Showing Location of Microhardness Traverse on Test Gear No. 178	57
29	Case Depth Vs Hardness Traverse for Test Gear No. 178	57

<u>Figure</u>	<u>Page</u>
30 Photograph of Profile Crack on Test Gear No. 172	58
31 Photograph Showing Location of Microhardness Traverse on Test Gear No. 172	58
32 Photograph From Electron-Beam Scanning Microscope on Test Gear No. 120	59
33 Loading Matrix on Tooth Models	61
34 Gear Torque Vs Life in Cycles for Dynamic Tests on 17/51 Test Gears	69
35 Calculated Bending Stress Vs Life in Cycles for Dynamic Tests on 17/51 Test Gears Using New, Improved Strength Formulas With the Size Factor Omitted.	70
36 Gear Torque Vs Life in Cycles for Pulsing Tests on 17/51 Test Gears	71
37 Calculated Bending Stress Vs Life in Cycles for Pulsing Tests on 17/51 Test Gears Using New, Improved Strength Formulas With the Size Factor Omitted	72
38 Calculated Bending Stress Vs Life in Cycles for Dynamic Tests on 17/51 Test Gears Using New, Improved Strength Formulas With the Old Size Factor Included	73
39 Calculated Bending Stress Vs Life in Cycles for Dynamic Tests on 17/51 Test Gears Using AGMA Strength Formulas With the Old Size Factor Included	74
40 Calculated Bending Stress Vs Life in Cycles for Pulsing Tests on 17/51 Test Gears Using New, Improved Strength Formulas With the Old Size Factor Included	75

<u>Figure</u>	<u>Page</u>
41 Calculated Bending Stress Vs Life in Cycles for Pulsing Tests on 17/51 Test Gears Using AGMA Strength Formulas With the Old Size Factor Included	76
42 Bending Stress Vs Life in Cycles From the R. R. Moore Tests on AISI 9310 Vacuum-Melt Steel Corrected for Single-Direction Bending	79
43 Diagram Showing Reverse Bending (a) and Single-Direction Bending (b)	81
44 Bending Stress Vs Life in Cycles From R. R. Moore Tests on AISI 9310 Vacuum-Melt Steel Under Reverse Bending on a Polished Specimen	82
45 Modified Goodman Diagram Showing Method for Converting From Reverse Bending to Single-Direction Bending	83
46 Bending Stress Vs Life in Cycles From the R. R. Moore Analysis	84
47 Comparison of the 7-1/2-Inch and 12-Inch Cutter Diameter Gear Designs at Load Levels I and II, as in Figure 35	89
48 Calculated Bending Stress Vs Life in Cycles for Results of Previous Dynamic Tests Using the New, Improved Strength Formulas With the Old Size Factor Included	91
49 Calculated Bending Stress Vs Life in Cycles for Results of Previous Dynamic Tests Using the AGMA Strength Formulas With the Old Size Factor Included	92
50 Pinion Drawing for 7-1/2-Inch Cutter Diameter Test Gear Set	115

<u>Figure</u>		<u>Page</u>
51	Pinion Drawing for 12-Inch Cutter Diameter Test Gear Set	117
52	Pinion Drawing for 12-Inch Cutter Diameter Pulser Gear Set	119
53	Gear Drawing for 7-1/2-Inch Cutter Diameter Test Gear Set	121
54	Gear Drawing for 12-Inch Cutter Diameter Test Gear Set	123
55	Test Gear Routing Sheets	125
56	Test Pinion Routing Sheets	127
57	Ground Spiral Bevel Summary for 7-1/2-Inch Cutter Diameter Test Gears	129
58	Ground Spiral Bevel Summary for 12-Inch Cutter Diameter Test Gears	131
59	Drawing for R. R. Moore Test Specimens . .	133
60	R. R. Moore Specimen Routing Sheet	135
61	Deflection Test Gear Tooth Contacts on 12- Inch Cutter Diameter Gear Design - Friction Load at Start of Test on Gear Convex Tooth Surface	143
62	Deflection Test Gear Tooth Contacts on 12- Inch Cutter Diameter Gear Design - Friction Load at Start of Test on Gear Concave Tooth Surface	143
63	Deflection Test Gear Tooth Contacts on 12- Inch Cutter Diameter Gear Design - 35,800 Lb-In. Gear Torque on Gear Convex Tooth Surface	144

<u>Figure</u>	<u>Page</u>
64 Deflection Test Gear Tooth Contacts on 12-Inch Cutter Diameter Gear Design - 50,000 Lb-In. Gear Torque on Gear Convex Tooth Surface	144
65 Deflection Test Gear Tooth Contacts on 12-Inch Cutter Diameter Gear Design - 71,600 Lb-In. Gear Torque on Gear Convex Tooth Surface	145
66 Deflection Test Gear Tooth Contacts on 12-Inch Cutter Diameter Gear Design - 100,000 Lb-In. Gear Torque on Gear Convex Tooth Surface	145
67 Deflection Test Gear Tooth Contacts on 12-Inch Cutter Diameter Gear Design - Friction Load at End of Test on Gear Convex Tooth Surface	146
68 Deflection Test Gear Tooth Contacts on 12-Inch Cutter Diameter Gear Design - Friction Load at End of Test on Gear Concave Tooth Surface	146
69 Deflection Test Gear Tooth Contacts on 7-1/2-Inch Cutter Diameter Gear Design - Friction Load at Start of Test on Gear Convex Tooth Surface	147
70 Deflection Test Gear Tooth Contacts on 7-1/2-Inch Cutter Diameter Gear Design - 35,800 Lb-In. Gear Torque on Gear Convex Tooth Surface	148
71 Deflection Test Gear Tooth Contacts on 7-1/2-Inch Cutter Diameter Gear Design - 50,000 Lb-In. Gear Torque on Gear Convex Tooth Surface	148

<u>Figure</u>	<u>Page</u>
72 Deflection Test Gear Tooth Contacts on 7-1/2-Inch Cutter Diameter Gear Design - 71,600 Lb-In. Gear Torque on Gear Convex Tooth Surface	149
73 Deflection Test Gear Tooth Contacts on 7-1/2-Inch Cutter Diameter Gear Design - 100,000 Lb-In. Gear Torque on Gear Convex Tooth Surface	149
74 Deflection Test Gear Tooth Contacts on 7-1/2-Inch Cutter Diameter Gear Design - Friction Load at End of Test on Gear Convex Tooth Surface	150
75 Deflection Test Gear Tooth Contacts on 7-1/2-Inch Cutter Diameter Gear Design - Friction Load at End of Test on Gear Concave Tooth Surface	150
76 Side Elevation of Pinion Mounted in Test Box Showing Locations of Indicators for Measuring Displacements	151
77 Front Elevation of Gear Mounted in Test Box Showing Locations of Indicators for Measuring Displacements	153
78 Plan View of Gear and Pinion Mounted in Test Box Showing Locations of Indicators for Measuring Displacements	155
79 Mean Section Through Tooth Showing Load Height, h_N	158
80 Location of Contact Lines on Tooth Models for Uniform Loading	164
81 Sketch Showing Location of 15 Contact Lines Used in the Analysis for Effective Face Width . .	167

<u>Figure</u>		<u>Page</u>
82	Curve Fit for Strain Distribution Along the Tooth Root on the Tooth Models	178
83	Assumed Position of the Tooth Contact Pattern Under No Load	187
84	Assumed Position of the Tooth Contact Pattern Under Peak Load	187
85	Sign Convention Used in Analysis of Deflection Test Results	192
86	Correlation Between Calculated and Measured Contact Shift, 12-Inch Cutter Diameter Design	197
87	Correlation Between Calculated and Measured Contact Shift, 7-1/2-Inch Cutter Diameter Design	198
88	Relationship Between Face Width and Tooth Length on a Spiral Bevel Gear Tooth	200
89	Load Distribution Factor Vs Contact Shift for the Concave Tooth Surface	201
90	Load Distribution Factor Vs Contact Shift for the Convex Tooth Surface	202
91	S-N Diagram Based on AGMA Method	256
92	S-N Diagram Based on German (DIN) Method .	257
93	Tooth Layout Used to Determine Weakest Section by German Method	265
94	Graph Showing Strength Factor, q_k , in Terms of Tooth Number, Z_v , and Addendum Factor, x , for Gears With 20° Pressure Angle (From DIN 3990)	266

LIST OF TABLES

<u>Table</u>	<u>Page</u>
I Summary of Calculated Tooth Stresses for Test Gears	15
II Summary of Calculated Tooth Stresses for Pulser Gears	16
III Load Data for Deflection and Tooth Contact Tests	33
IV Operating Speed for Dynamic Tests	36
V Test Results, No. 510 Axle Test Machine	37
VI Pulser Test Results	41
VII Fatigue Test Results for R. R. Moore Specimens	42
VIII Allowable Stress Vs Working Stress for AISI 9310 Vacuum-Melt Steel	86
IX Summary of Calculated Tooth Stresses for Pulser Gears	102
X Heat-Treatment Batch Grouping	103
XI Inspection Record of Pinions	105
XII Inspection Record of Gears	109
XIII Raw Material Examination Records	113
XIV Inspection Records for R. R. Moore Fatigue Specimens	114
XV Deflection Test Summary	138
XVI Pairing of Ground Test Gears and Pinions, 12-Inch Cutter Diameter	141

<u>Table</u>	<u>Page</u>
XVII Pairing of Ground Test Gears and Pinions, 7-1/2-Inch Cutter Diameter	142
XVIII Gear Tooth Configurations	160
XIX U_i as Calculated From the Data Analysis Program	165
XX Coordinates of Contact Lines in the Axial Plane	169
XXI V_i as Calculated From the Data Analysis Program	170
XXII Geometric Variables for U_i	177
XXIII Geometric Variables for V_i	181
XXIV E, P, G, and α for the 12-Inch Cutter Diameter Design	194
XXV E, P, G, and α for the 7-1/2-Inch Cutter Diameter Design	194
XXVI List of Symbols	226
XXVII Output Symbols	244
XXVIII Straight Bevel Gears With 20° Pressure Angle	252
XXIX Spiral Bevel Gears With 20° Pressure Angle and 35° Spiral Angle	253
XXX Selected Automotive Spiral Bevel Gears	254
XXXI Life Data for Ratios in Table.	258
XXXII Factors Affecting Gear Tooth Strength	259

BLANK PAGE

INTRODUCTION

The purpose of this project was to review existing formulas for the strength of bevel gear teeth, to select the method that is currently considered to be the best, to determine what factors in this method need further study and development, to outline a program for improving the method, and to carry out a program of theoretical and experimental investigation to develop this improved method.

A review of past and present methods was undertaken with the object of selecting the best method for further study. This method was analyzed for possible areas of improvement. From this analysis it was apparent that the complexity of bevel gear geometry made the complete solution to the problem a formidable task. Therefore, it was decided to select certain specific areas where immediate improvement of the formulas would result in substantial benefit to the gear designer.

The basic procedure for developing new formulas consisted of the following steps:

1. Derivation of new theoretical formulas to reflect the observed behavior of the gears under load and to provide stresses that correlate with the strength of the material.
2. Design of a test program and test gears that would evaluate the effects of changes in the gear design parameters.
3. A carefully controlled manufacturing and testing program to provide reliable data.
4. Use of previously generated test data for the solution of problems related to stress distribution in the gear tooth roots.
5. An analysis and evaluation of the test results using the new theoretical formulas.
6. A final review of the formulas to assure correlation with the gear test data.
7. Writing of a computer program incorporating the newly developed formulas for use on the IBM 7090/7094 Computer.

8. Testing of the computer program on a series of gear designs including spiral bevel, Zerol[®] bevel, and straight bevel gears to assure the usefulness of the program and formulas.
9. Evaluation of vacuum-melt 9310 steel (AMS-6265) to determine the endurance limit for bevel gear design.

[®] Registered trademark of the Gleason Works

PRELIMINARY ANALYSIS

HISTORICAL BACKGROUND

The first serious attempt to compute the strength of a gear tooth was the work performed by Wilfred Lewis, Reference 1, in 1892. Lewis treated the gear tooth as a cantilever beam and attempted to solve for the bending stress in the root of the tooth. The use of the inscribed parabola for locating the weakest section of the tooth, which was introduced by Lewis, is still the basis for present-day formulas for gear tooth strength. The basic flexure formula derived by Lewis is still in use.

In 1922, McMullen and Durkan, Reference 2, proposed a significant change in the Lewis formula: To consider the load applied at the highest point of single tooth contact rather than at the tip of the tooth. This was first applied to bevel gear teeth and eventually was adopted for analyzing spur gear teeth.

Carl G. Barth introduced the first factor for the consideration of the dynamic effects of tooth load on an elastic system. Through his influence, an ASME Special Research Committee on Strength of Gear Teeth was established under the leadership of Wilfred Lewis. Much of the actual work was carried out under the direction of Professor Earle Buckingham, Reference 3.

General Motors Research Laboratories, under the direction of John O. Almen, conducted extensive fatigue tests on automotive spiral bevel gears and later on transmission gears, which resulted in the first use of S-N diagrams for gear design, References 4 and 5.

In 1941, Candee, Reference 6, introduced at an AGMA meeting a geometrical method for arriving at the tooth form factor to replace the graphical method that had been in common use up to that time. At the same meeting, Messrs. Dolan and Broghamer, Reference 7, presented a concise review of their photoelastic studies of gear tooth models. Their work resulted in a combined stress concentration and stress correction term, which compensated for the inaccuracies in the inscribed parabola as a means for locating the weakest section of the tooth, corrected the stress values in the root fillet, and considered the radial component of the normal tooth load. This factor is widely used in current gear strength formulas.

The first attempt at a unique formula for the strength of bevel gear teeth was the work of Coleman, Reference 8. Previously, formulas for the strength of bevel gears were adaptations of spur gear formulas. In the method presented by Coleman, an attempt was made to analyze the load sharing between teeth, to determine the most damaging position of the load on the tooth, to consider the load distribution along the line of instantaneous contact and its effect on the root stress by means of the concept of effective face width, to incorporate a change in allowable stress with a change in gear tooth size, and to introduce a factor for the effect of temperature on gear tooth strength. Many of these factors were introduced for the first time in a gear tooth strength formula.

Wellauer and Seireg, Reference 9, have investigated the effects of load distribution and effective face width on helical gear teeth using the cantilever-plate theory. Their work has led to the latest bending strength formulas for helical gears, Reference 10. Kelley and Pedersen, Reference 11, have extended the investigation of root fillet stresses by photoelastic means.

A significant advance in the analysis of bevel gear tooth strength was made by Baxter, References 12 and 13, in his study and mathematical analysis of tooth contact conditions between mating gear teeth and the effects of misalignment on the same. This work is the basis of the present analysis of load distribution factor.

Work recently performed by Hoogenboom, Reference 14, under the direction of the contractor in an effort to extend the work of Wellauer and Seireg, Reference 9, has added much new knowledge to the concept of effective face width and load distribution. This work also was used in the present study.

Other workers too numerous to name have contributed to the overall knowledge of gear tooth strength.

COMPARISON OF BEVEL GEAR STRENGTH STANDARDS

In addition to the AGMA strength standards for bevel gear teeth, References 15 and 16, three other methods were reviewed by the contractor prior to the initiation of, or during, the present contract. These were the following:

1. German Standard, DIN3990, Reference 17.
2. Kelley-Pedersen Method, Reference 11.
3. British Standard, BS545, Reference 18.

German Standard

This method is based on an adaptation of the spur and helical gear tooth formulas. A detailed comparison of the AGMA standards and the German standard was made by the contractor and is included in Appendix VII. From the conclusions it can be seen that this method lacks many of the features contained in the AGMA standards.

Kelley-Pedersen Method

In 1961, the contractor attempted to incorporate the Kelley-Pedersen formulas into the AGMA method for bevel gear tooth strength. The stresses resulting from the combined method were found to be essentially the same as those from the AGMA standards except for a generally higher stress level (approximately 20 percent higher). Since no reduction in the scatter of the plotted results over that of the existing method was found, this combined method was not adopted.

British Standard

This method is based on an adaptation of the British formulas for spur and helical gear teeth to bevel gears. The method is based on the original Lewis method with various modifications. However, it has not been updated over the years and lacks many of the features included in the latest AGMA bevel gear strength standards. Therefore, only a cursory analysis was made.

Summary of Existing Standards

Upon completion of the review of the various strength standards in current use, it is concluded that the AGMA bevel gear strength standards should furnish the most reliable starting point for improving the formulas. Accordingly, for the work conducted under the present contract, the following factors were selected for further analysis:

1. Improved formulas for effective face width, which were to be based on experimental data.

2. Correction of the formula for point of load application to improve the strength balance between gear and mating pinion.
3. Improved formulas for load distribution factor, which would incorporate the effects of lengthwise tooth curvature and mounting deflections on the load distribution on the tooth.
4. Transferral of the size factor from the equation for calculated stress to the equation for working stress in order to calculate true stress values more accurately.
5. Determination of the S-N diagram and endurance limit stress for AMS-6265 steel.
6. Establishment of a base line on a bevel gear pulser.

TEST GEAR DESIGN

TOOTH DESIGN

Selection of Gear Parameters

The basic gear geometry was chosen with two factors in mind. First, the size and ratio should be consistent with current-day practice in high-speed power drive line applications such as helicopters. Second, the gear must be of a size to permit fatigue testing on available equipment so that the program cost could be minimized.

The gear parameters are shown on the dimension sheets in Figures 1 and 2. The dimension sheets were produced on a computer using the contractor's Program No. A101. This program is based upon American Gear Manufacturers Association formulas, References 16, 19, and 20.

Additional data on the output format are in agreement with present industry-wide standards. The above program is in regular use in the contractor's engineering department to produce data for bevel gear users all over the Free World and is also in use at many companies where bevel gears are used. Therefore, the basic gear tooth geometry is consistent with current-day practice, and no special formulas have been introduced that could alter the results, except as noted later.

The following items of input to the computer program were chosen for the test gears:

Gear Size

The gear size was selected to be within the capacity limitation of the Gleason No. 510 Axle Test Machine and the available test boxes. It was also selected to be within the range of helicopter power drive gears. Therefore, a gear diameter of 12.5 inches was chosen.

Ratio and Tooth Numbers

The gear ratio and tooth numbers were chosen to make the test meaningful to the helicopter industry. A three-to-one speed-reducing ratio was selected since this corresponds to a typical VTOL power transmission application. The numbers of teeth in gear and pinion were based upon data given in Reference 21. The

SPIRAL BEVEL GEAR DIMENSIONS

NO. 139-887A B

DATA SHEET

FORM F

CUSTOMER - FORT EUSTIS - DAAGJ08-68-C-0032

	PINION	GEAR
NUMBER OF TEETH	17	51
PART NUMBER		
DIAMETRAL PITCH	4.000	
FACE WIDTH	1.500"	1.500"
PRESSURE ANGLE	20° 0'	
SHAFT ANGLE	90° 0'	
TRANSVERSE CONTACT RATIO . .		1.212
FACE CONTACT RATIO		1.948
MODIFIED CONTACT RATIO		1.966
OUTER CONE DISTANCE		6.988"
MEAN CONE DISTANCE		5.838"
CIRCULAR PITCH770"	
WORKING DEPTH417"	
WHOLE DEPTH463"	.463"
CLEARANCE044"	.046"
PITCH DIAMETER	4.167"	12.500"
ADDENDUM293"	.123"
DEDENDUM169"	.339"
OUTSIDE DIAMETER	4.725"	12.578"
PITCH APEX TO CROWN	8.187"	1.966"
MEAN CIRCULAR THICKNESS441"	.232"
OUTER NORMAL TOP LAND135"	.111"
MEAN NORMAL TOP LAND138"	.114"
INNER NORMAL TOP LAND146"	.102"
PITCH ANGLE	18° 26'	71° 34'
FACE ANGLE OF BLANK	31° 23'	73° 2'
ROOT ANGLE	16° 38'	68° 37'
DEDENDUM ANGLE	1° 28'	2° 57'
OUTER SPIRAL ANGLE		38° 46'
MEAN SPIRAL ANGLE		35° 0'
INNER SPIRAL ANGLE		31° 36'
HAND OF SPIRAL LH		RH
DRIVING MEMBER PIN		
DIRECTION OF ROTATION REV		
OUTER NORMAL BACKLASH MIN	.006" MAX	.008"
TOOTH TAPER STD		
CUTTING METHOD SB		
GEAR TYPE GENERATED		
FACE WIDTH IN PERCENT OF CONE DISTANCE		22.768

	PINION	GEAR
THEORETICAL CUTTER RADIUS	5.526"	
CUTTER RADIUS	6.000"	
CALC. GEAR FINISH. PT. WIDTH148"
GEAR FINISHING POINT WIDTH150"
ROUGHING POINT WIDTH050"	.140"
OUTER SLOT WIDTH086"	.150"
MEAN SLOT WIDTH087"	.150"
INNER SLOT WIDTH076"	.150"
FINISHING CUTTER BLADE POINT050"	.080"
STOCK ALLOWANCE026"	.010"
MAX. RADIUS-CUTTER BLADES058"	.103"
MAX. RADIUS-MUTILATION061"	.135"
MAX. RADIUS-INTERFERENCE054"	.054"
CUTTER EDGE RADIUS	0.00"	.080"
CALC. CUTTER NUMBER	3	10
MAX. NO. BLADES IN CUTTER	17.479	
CUTTER BLADES REQUIRED STD. DEPTH	STD. DEPTH	STD. DEPTH
DUPLX SUM OF DEDENDUM ANG	4° 58'	
ROUGHING RADIAL	5.468"	
GEOMETRY FACTOR-STRENGTH-J2737	.2730
STRENGTH FACTOR-Q	3.356	1.121
FACTOR KI	1.0174	
STRENGTH BALANCE DESIRED STRS		
STRENGTH BALANCE OBTAINED STRS		.002
GEOMETRY FACTOR-DURABILITY-I1228	
DURABILITY FACTOR-Z	2259	1290
GEOMETRY FACTOR-SCORING-Q004409	
SCORING FACTOR - K2679	
PROFILE SLIDING FACTOR004653	.006970
ROOT LINE FACE WIDTH	1.500"	1.500"
AXIAL FACTOR-DRIVER CW OUT	.436	OUT .036
AXIAL FACTOR-DRIVER CCW IN	.284	OUT .116
SEPARATING FACTOR-DRIVER CW SEP	.108	SEP .145
SEPARATING FACTOR-DRIVER C'W SEP	.348	ATT .095
GEAR ANGULAR FACE - CONCAVE		16° 52'
GEAR ANGULAR FACE - CONVEX		18° 14'
GEAR ANGULAR FACE - TOTAL		20° 36'

*THIS FACTOR IS USED IN THE NEW 1965 SCORING FORMULA

CHECKED BY - *PC*

DATE 02/16/68

Figure 1. Spiral Bevel Gear Dimension Sheet for the 17/51 Combination, Test Gears Produced With 12-Inch Cutter Diameter.

SPIRAL BEVEL GEAR DIMENSIONS			N: 139-698A B	DATA SHEET	FORM G
CUSTOMER - FORT RUS. IS - 9AAJ02-68-C-0082				PINION	GEAR
	PINION	GEAR			
NUMBER OF TEETH	17	51			
PART NUMBER					
DIAMETRAL PITCH	6.000				
FACE WIDTH	1.900"	1.900"			
PRESSURE ANGLE	20° 0'				
SHAFT ANGLE	90° 0'				
TRANSVERSE CONTACT RATIO		1.212			
FACE CONTACT RATIO		1.948			
MODIFIED CONTACT RATIO		1.966			
OUTER CONE DISTANCE		6.588"			
MEAN CONE DISTANCE		9.830"			
CIRCULAR PITCH770"				
WORKING DEPTH374"				
WHOLE DEPTH421"	.421"			
CLEARANCE046"	.046"			
PITCH DIAMETER	4.167"	12.900"			
ADDENDUM266"	.109"			
DEDENDUM153"	.812"			
OUTSIDE DIAMETER	4.671"	12.969"			
PITCH APEX TO CROWN	6.166"	1.980"			
MEAN CIRCULAR THICKNESS440"	.232"			
OUTER NORMAL TOP LAND146"	.093"			
MEAN NORMAL TOP LAND137"	.114"			
INNER NORMAL TOP LAND131"	.097"			
PITCH ANGLE	18° 26'	71° 34'			
FACE ANGLE OF BLANK	19° 17'	71° 53'			
ROOT ANGLE	18° 51'	70° 43'			
DEDENDUM ANGLE	0° 21'	0° 51'			
OUTER SPIRAL ANGLE		44° 11'			
MEAN SPIRAL ANGLE		35° 0'			
INNER SPIRAL ANGLE		26° 19'			
HAND OF SPIRAL	LH	RH			
DRIVING MEMBER	PIN				
DIRECTION OF ROTATION	REV				
OUTER NORMAL BACKLASH006" MAX	.008"			
TOOTH TAPER	TRLM				
CUTTING METHOD	SB				
GEAR TYPE	GENERATED				
FACE WIDTH IN PERCENT OF CONE DISTANCE		22.768			
CHECKED BY - <i>A.C.</i>		DATE 02/16/58			
			THEORETICAL CUTTER RADIUS	3.750"	
			CUTTER RADIUS	3.750"	
			CALC. GEAR FINISH. PT. WIDTH140"
			GEAR FINISHING POINT WIDTH190"
			ROUGHING POINT WIDTH065"	.140"
			OUTER SLOT WIDTH049"	.150"
			MEAN SLOT WIDTH087"	.150"
			INNER SLOT WIDTH072"	.150"
			FINISHING CUTTER BLADE POINT045"	.080"
			STOCK ALLOWANCE024"	.010"
			MAX. RADIUS-CUTTER BLADES041"	.105"
			MAX. RADIUS-NULLIFICATION057"	.150"
			MAX. RADIUS-INTERFERENCE053"	.095"
			CUTTER EDGE RADIUS040"	.080"
			CALC. CUTTER NUMBER	1	2
			MAX. NO. BLADES IN CUTTER	10.778	
			CUTTER BLADES REQUIRED	STD. DEPTH	STD. DEPTH
			DUPLEX SUM OF DEDENDUM ANG	1° 12'	
			ROUGHING RADIAL	4.799"	
			GEOMETRY FACTOR-STRENGTH-J2751	.2728
			STRENGTH FACTOR-Q	3.363	1.122
			FACTOR	1.0174	
			STRENGTH BALANCE DESIRED	STRS	
			STRENGTH BALANCE OBTAINED	STRS	0.000
			GEOMETRY FACTOR-DURABILITY-I1229	
			DURABILITY FACTOR-2	2239.	1296.
			GEOMETRY FACTOR-SCORING-B004485	
			SCORING FACTOR - K2678	
			PROFILE SLIDING FACTOR004681	.006970
			ROOT LINE FACE WIDTH	1.506"	1.530"
			AXIAL FACTOR-DRIVER CW	OUT .436	OUT .036
			AXIAL FACTOR-DRIVER CCW	IN .284	OUT .116
			SEPARATING FACTOR-DRIVER CW SEP100	SEP .148
			SEPARATING FACTOR-DRIVER CCW SEP348	ATT .095
			GEAR ANGULAR FACE - CONCAVE		26° 36'
			GEAR ANGULAR FACE - CONVEX		30° 7'
			GEAR ANGULAR FACE - TOTAL		33° 24'
			*THIS FACTOR IS USED IN THE NEW 1966 SCORING FORMULA		

Figure 2. Spiral Bevel Gear Dimension Sheet for the 17/51 Combination, Test Gears Produced With 7-1/2-Inch Cutter Diameter.

graph given in this reference indicates that a 15-tooth pinion is recommended for general work; however, for high-speed applications, more teeth are usually chosen to reduce a scoring tendency and to decrease noise. Thus a 17-tooth pinion was selected for this design. The resulting number of teeth in the gear was 51. The combination of 17/51 agrees with current aircraft practice.

Face Width

The face width is generally chosen to be 30 percent of the outer cone distance or less. In this case, it was reduced to 22 percent to cause breakage to occur on the available test equipment. This reduction in face width will not affect the results of this analysis. A face width of 1.5 inches was selected.

Pressure Angle

A pressure angle of 20° was selected, which is in accordance with recommended design for a power gear application, Reference 21.

Spiral Angle

The spiral angle was chosen to give a face contact ratio sufficient for smooth-running gears. Generally, a contact ratio between 1.5 and 2.0 is adequate. For quieter, smoother running gears, a contact ratio closer to 2.0 is more desirable, but for this test program a lower value was selected to permit tooth failure within the capacity of the test equipment. For the test gears, a spiral angle of 35° was selected, which resulted in a face contact ratio of 1.548. See Reference 21.

Hand of Spiral

The hand of spiral was selected to yield an outward thrust on both members. This was accomplished by consideration of the driving member and the direction of rotation. This resulted in the selection of a left-hand pinion and a right-hand gear.

Cutter Diameter

The cutter diameter for spiral bevel gears, which determines the lengthwise tooth curvature, is usually chosen approximately equal

to, or slightly smaller than, twice the outer cone distance. The outer cone distance of the test gears is 6.588 inches. Twice this value is 13.176 inches. Cutters are made with standard diameters, and those in the range of this gear set are of 9-inch, 12-inch, and 16-inch diameters. A 12-inch cutter diameter was selected for these gears in accordance with the generally accepted standard since it was the next smaller diameter than twice the outer cone distance.

On the other hand, the use of this cutter diameter results in a tooth contact that tends to shift toward the heel as load is applied. The amount of shift is a function of the cutter diameter, the applied load, and the deflection characteristics of the gear mountings. The above rule for selection of the cutter diameter yields a reasonable balance between cost and performance and has been the accepted method of selection by the gear industry.

For comparative purposes, a second, smaller cutter diameter was also selected. It has been observed that when the cutter diameter approaches the product of the mean cone distance times twice the sine of the mean spiral angle, the tooth contact tends to resist a movement to the heel of the tooth as load is applied. As a result, the contact pattern can be lengthened and more tooth area can be used under light and intermediate loads. For the test gears, a second cutter diameter as determined by the above formula was

$$D_c = 2(5.838)(0.57358) = 6.697$$

A cutter diameter that is slightly larger than the calculated value was chosen. Some earlier observations indicated that if the cutter diameter becomes too small, the contact pattern tends to move toward the small end of the tooth, which is undesirable. To avoid such a condition, a 7-1/2-inch cutter diameter was selected.

Tooth Proportions

The tooth proportions for the 12-inch cutter diameter design are in accordance with Reference 19 and are the generally accepted standard for the given diametral pitch and combination. Long and short addendums are specified, since they eliminate undercut and yield the best balance among strength, pitting resistance, scoring resistance, and contact ratio. The tooth thickness of pinion and mating gear has been adjusted by the AGMA method of stress analysis to obtain approximately equal bending stress on both

members.

The tooth proportions for the 7-1/2-inch cutter diameter design were modified to obtain the optimum pinion point width taper. Point width taper (frequently called slot width taper) refers to the change in the maximum limit point width (slot width) of a V-shaped cutting tool of nominal pressure angle whose sides are tangent to the two sides of a tooth space and whose tip is tangent to the root line along the tooth length. The tooth proportions were modified by altering the depthwise taper until the outer and inner slot widths of the pinion member were nearly equal. Depthwise taper refers to the change in tooth depth along the tooth length measured perpendicular to the pitch surface. This change affects the face angles and root angles of both the pinion and the mating gear and is referred to as "tilting the root lines". The tooth depth, addendum, and dedendum of both members remain the same at the middle of the face width but are smaller at the outer cone distance and larger at the inner cone distance when compared to a tooth with standard depthwise taper. The latter refers to a tooth in which the depth of the tooth in any section is proportional to the distance of the section from the pitch cone apex.

Fillet Radius

In the roots of the gear teeth, the fillet radius should be as large as possible. Therefore, the cutter edge radius was chosen by the computer program to meet the following three criteria: (1) the maximum radius that can physically be manufactured on the cutter blades, (2) the maximum radius that can be cut into the tooth before the clearance side of the cutter blade mutilates the fillet on the opposite side of the tooth space, and (3) the maximum radius that can be used before an interference occurs between the root fillet of one member and the tooth tip of the mating member. The final cutter edge radius is selected to be approximately 0.010 inch less than the smallest of the above three values.

Undercut and Fillet Interference

Undercut and fillet interference were checked using another computer program previously developed by the contractor. This program uses the actual machine settings and cutter specifications. The data obtained from this program indicate the location of undercut along the tooth length, the height of the undercut up from the root of the tooth, the angle of intersection of the undercut with reference to the tooth

profile, and the location of any interference. Inspection of the data showed that undercut and interference would not exist for either tooth design.

Selection of Gear Quality

The gear tooth accuracy was established in accordance with Reference 22 as AGMA Class 13 by contractual agreement. This is currently the highest quality obtainable in production on bevel gears and was specified here in order to assure maximum strength. Generally high accuracy is necessary for high-speed heavily loaded gears to reduce detrimental dynamic effects.

The selection of gear blank tolerances is dependent upon the accuracy requirements of the teeth. The detail drawings indicate the tolerances on the locating and centering surfaces that are required to obtain the specified gear tooth accuracy.

Preliminary Stress Analysis

The bending stresses, compressive stresses, and scoring indexes were calculated for the test gears produced with both 7-1/2-inch and 12-inch cutter diameters using the American Gear Manufacturers Association and the contractor's manuals that are in current use. The stress formulas contained in these manuals had been previously programmed on a computer by the contractor and resulted in Dimension Sheet No. 139.898AB for the 7-1/2-inch cutter diameter design and Dimension Sheet No. 139.887AB for the 12-inch cutter diameter design. A summary of the calculated stresses is shown in Table I for the four load levels used in the dynamic tests and in Table II for the maximum, minimum, and an intermediate level used in the static test (pulsing tests). (See Table IX in Appendix I for complete load-stress spectrum used in the static tests.)

BLANK DESIGN

The gear and pinion blank configurations were chosen to permit the use of existing rigid test boxes in the possession of the contractor.

The pinion shank size and length, as well as the front pilot, were identical on all pinion designs. Pinions used in the pulser contained an additional 0.750-inch-diameter hole through the shank at right angles to the pinion axis. The three pinion designs are shown in Figures 50, 51, and 52 in Appendix I, which includes the pertinent data for each

design.

Similarly, the gear blanks were made as nearly identical as possible. No special provision was necessary for the gears tested in the pulser. The two gear designs are shown in Figures 53 and 54 in Appendix I.

TABLE I. SUMMARY OF CALCULATED TOOTH STRESSES FOR TEST GEARS *

CUTTER DIAMETER		12"		7.5"			
DIMENSION SHEET NO.		139.887AB		139.898AB			
Load Level	Member	Torque (in. -lb)	Speed (rpm)	Calculated Bending Stress (psi)	Calculated Contact Stress (psi)	Calculated Bending Stress (psi)	Calculated Contact Stress (psi)
I	Pinion	33,330	950	111,866	408,050	112,099	408,050
	Gear	100,000	317	112,100	-	112,200	-
II	Pinion	23,867	1300	80,098	365,205	80,265	365,205
	Gear	71,600	433	80,264	-	80,335	-
III	Pinion	20,000	1600	67,120	343,986	67,260	343,986
	Gear	60,000	533	67,260	-	67,320	-
IV	Pinion	16,667	1900	55,934	323,584	56,050	323,584
	Gear	50,000	633	56,050	-	56,100	-

* Calculated stresses in above table are based on AGMA formulas.

**TABLE II. SUMMARY OF CALCULATED TOOTH STRESSES*
FOR PULSER GEARS**

Based on Static Loading
Dimension Sheet No. 139.887AB

Test Number	Member	Torque (in. -lb)	Calculated Bending Stress (psi)	Calculated Compressive Stress (psi)
4	Pinion	20,000	66,000	316,000
	Gear	60,000	66,100	-
9	Pinion	33,300	109,900	407,900
	Gear	99,900	110,100	-
21	Pinion	50,000	165,000	499,700
	Gear	150,000	165,300	-

See Appendix 1 for complete listing of stresses
for the full range of test loadings.

*Calculated stresses in above table are based on AGMA
formulas.

TEST GEAR MANUFACTURE

BLANKS

Sequence of Operations

Routing sheets indicating the sequence of operations are included in Figure 55 in Appendix I. Since all of the gear members followed the identical processing procedure, only one set of routing sheets is shown for the gear member. Similarly, only one set of routing sheets is included for the pinion in Figure 56 in Appendix I since the pinions are also nearly identical.

Inspection of Blanks

During the machining processes, each operation was inspected on the first piece before proceeding with the balance of the parts. Upon completion of the blanks to the point of cutting the teeth, each member was individually inspected 100 percent, and records have been maintained.

TEETH

Data for Gear Manufacturing

Information regarding the gear dimensions, the cutter specifications, machine settings for cutting and grinding both gear and pinion, inspection data, and machine sequencing data including speed and feed information is given on a Summary. Copies of the developed Summaries for both designs are included as Figures 57 and 58 in Appendix I.

The Summaries were calculated using a computer program developed by the contractor. This program is used regularly to provide Summaries for bevel gear users throughout the world. The gear member of the pair was cut and ground by the "spread-blade" method, in which an alternate-blade face-mill cutter is used to cut a slot of uniform width from toe to heel. The pinion was cut and ground by the "fixed-setting" method, in which independent control of each side of the tooth space is maintained by individual machine settings and separate face-mill cutters for the concave and convex sides of the tooth.

Another computer program, the Tooth Contact Analysis Program, previously developed by the contractor, provides a kinematic analysis of the tooth contact between mating tooth surfaces based upon the actual

machine settings. This provides the gear engineer with a means to modify the tooth contact before cutting begins. This procedure saves time and decreases the cost of a cutting development since the proper cutter blade angles and point diameters can be specified with greater certainty.

Gear Tooth Cutting

Upon completion of the gear blank manufacture, the tooth slots were roughed and semifinished in a conventional spiral bevel gear generating machine.

Heat Treatment

Due to the lack of capacity of the carburizing and quenching facilities at the contractor's plant, it was not possible to heat-treat all of the gears or all of the pinions in one batch. Therefore, it was necessary to separate the gears into smaller quantities for processing. A schedule was established whereby the gears were split into two groups for carburizing and four groups for quenching. Similarly, the pinions were also split into two groups for carburizing and quenching. Each gear and pinion was serialized before carburizing so that the heat-treat processing group could be identified for each part. The purpose of these records was to minimize the effect of heat-treatment variation when the gears were paired for testing.

Heat-treatment batch groupings are shown in Table X in Appendix I.

Gear Tooth Grinding - Contact Pattern Development

Some modifications of tooth contact pattern are generally required to suit the deflection characteristics of the gearbox. Several pairs of dummy gears and pinions of both the 7-1/2-inch and 12-inch cutter diameter designs were processed prior to the processing of the test gears. They were manufactured in the same manner as the test gears, and their tooth profiles were ground to give a normally acceptable contact pattern. To verify this, the dummy gears were mounted in the test boxes and were checked for tooth contact under the range of loads scheduled in the fatigue test. If the tooth contact pattern ground on dummy gears was acceptable, the test gears were ground with the same grinding machine settings to produce the same tooth shape. These machine settings were recorded on the developed Summaries shown

in Appendix I.

Gear Tooth Grinding - Stock Removal Control

After the completion of heat treatment and process grinding of the hardened parts, the gears were ready for grinding the teeth. This operation was performed in a standard spiral bevel gear grinding machine. Prior to the grinding of the test gear or pinion teeth, tooth thickness measurements were made at three points along the face width: one near the toe (inner end of the tooth), one at the center of the tooth, and the third at the heel (outer end of the tooth) on each piece. In addition, the tooth whole depth was measured prior to the grinding. Identical measurements were made after gear tooth grinding. The difference between before and after values established the amount of stock removed. On the gear member, since both sides of the tooth are ground simultaneously, it is not possible to determine the amount of material removed from each side individually, but every effort was made to divide the stock evenly. On the pinion, measurements were made after grinding each side of the tooth. In this manner the stock removal on each surface can be controlled. Tabulation of stock removal at mid-face is shown in Tables XI and XII in Appendix I.

Inspection of Test Gears

Inspection of the runout and pitch variation are also shown in Tables XI and XII in Appendix I.

MATERIAL EVALUATION

Selection and Inspection of Material

The gears were made from AMS-6265 steel which is a consumable-electrode vacuum-melted material in general use in the aircraft industry. This material was specified in the contract. The forgings were purchased, inspected, and processed in the normal manner for precision spiral bevel gears. This included metallurgical inspection of the forgings, hardness checks, and certification of the chemical analysis. These are recorded in Table XIII in Appendix I.

R. R. Moore Specimen Manufacture

The contract called for performing R. R. Moore rotating-beam tests on the same steel used for the test gears in order to establish

confidence that the material was comparable with material used for other tests. The material for these R. R. Moore specimens was received at the contractor's facility, where it went through the same metallurgical and chemical inspection as the gear forgings. These bars were sent to the John Stulen Company, located in Pittsburgh, Pennsylvania, for machining. A drawing of the part, Figure 59, is shown in Appendix I. Also included in the appendix is the routing sheet, Figure 60, used to produce the specimens.

To duplicate the heat treatment of the R. R. Moore specimens and the test gears as closely as possible, the carburizing, hardening, and stress-relieving operations of the specimens for all parts were performed at the contractor's plant. Upon completion of the manufacture of the test specimens, they were inspected. A compilation of the inspection results is shown in Table XIV in Appendix I.

GEAR TESTING

In the following sections will be found a brief description of the test equipment used on this project together with the test procedure.

TYPES OF TESTS

Tooth Contact and Deflection Tests

The purpose of a tooth contact test and deflection test is to determine the suitability of the gear and pinion development and their mountings.

For the tooth contact tests, the gears are rotated very slowly in their mountings under various loads from friction load (no load) to full load. At each load level the teeth of the gear are painted with a gear marking compound while the gears are rotating. In this manner a true picture of the tooth contact at the specified load is obtained. There is no carry-over of the tooth contact pattern from operation at other loads. The machine is stopped at each load level, and tape transfers and/or photographs are made of the gear tooth pattern.

For the deflection test, indicators are placed at strategic positions in the housing to measure the deflections within the housing and to measure the relative shift of the positions of gear and pinion with respect to one another.

The data obtained from these two tests were used to determine the suitability of the tooth bearing development when the gears operate under load. These data were also used to derive the formulas for load distribution factor, which is described in greater detail elsewhere in this report.

Dynamic Tests

The purpose of the dynamic tests is to determine the behavior of the gears at operating speeds and to establish a stress-life curve (S-N diagram).

The primary reason for this series of tests was to obtain sufficient information to:

1. Establish an S-N curve for spiral bevel gears made from carburized AISI 9310 vacuum-melt steel.

2. Establish the difference in fatigue life between spiral bevel gears made with a 12-inch cutter diameter and those made with a 7-1/2-inch cutter diameter.
3. Confirm the validity of the new formulas for effective face width and load distribution factor developed on this project.

Pulser Tests

The purpose of the pulser tests is to determine the suitability of gear tooth pulsing on spiral bevel gears and to establish a base line for future testing.

On the gear tooth pulser the gear member of the pair is rigidly locked against rotation. Therefore, the contact between the pinion and gear tooth is that represented by an instantaneous line of contact during gear rotation. For these tests, a position of the line of contact was selected from theoretical calculations, which indicated that only one tooth in the pair of gears would be supporting the load and that its position would produce the highest stress in the root of the tooth. No measurements of root stresses were made on the gears used in these tests to confirm this theoretical result. Furthermore, under the high torque loads imposed on these gears, the instantaneous line of contact spread over an enlarged area because of the gear tooth and mounting deflections. Adjacent teeth on the gear were removed to assure that all of the load would be carried by a single tooth.

The actual pulsing tests performed in this program serve as a base line for future testing. It is believed that with further testing to confirm the theoretical calculations, a practical procedure for testing spiral bevel gear teeth can ultimately be achieved.

R. R. Moore Tests

The purpose of performing R. R. Moore tests on the material used for these gear tests is to determine the true material strength and to show that the particular heat of material is comparable to that used in other similar tests.

TEST EQUIPMENT

The test equipment used on this project includes the deflection testing machine, dynamic testing machine, and bevel gear pulser.

Deflection Testing Machine

The deflection testing machine is shown in Figure 3. The input shaft is driven through a universal joint shaft arrangement connected to a reduction gearbox driven by a 10-horsepower electric motor. The output shafts are connected to brake units which consist of conventional hydraulic truck brakes with the master cylinders controlled by air valves. Lever systems are used to measure the torque reactions of the brakes in pounds of force on two platform scales.

Dynamic Testing Machine

The dynamic testing machine, Figure 4, was primarily designed and built for automotive and truck axle testing. The versatility of the machine makes it ideal for testing any right-angle bevel gear drive application within the maximum torque range of 300,000 lb-in. total output torque and output shaft speeds of up to 1500 rpm.

Figure 5 shows a schematic diagram of the dynamic testing machine.

This machine incorporates a four-square arrangement with two torque loops, a test gearbox, and a slave gearbox, both gearboxes containing the same gear ratio and assembled at opposite ends of the machine to close the two torque loops. The load is applied by increasing the torsion in the machine shafting by means of a windup mechanism on one of the corner transmission units. The windup is actuated from the machine console, and when the proper torque load has been applied, the windup mechanism is deactivated; the torque then remains constant in the loop until a failure occurs.

The drive line is rotated by a center drive motor and transmission unit incorporating an infinitely variable speed range up to a maximum speed of 5000 rpm on the input shaft.

A motor-generator unit provides power to the main motor and coolant motors. All operating controls are located at the machine console and consist of speed, load, and operating on-off switches. Also included are indicators for reading DC current, drive motor speed, and test gear driven speed.

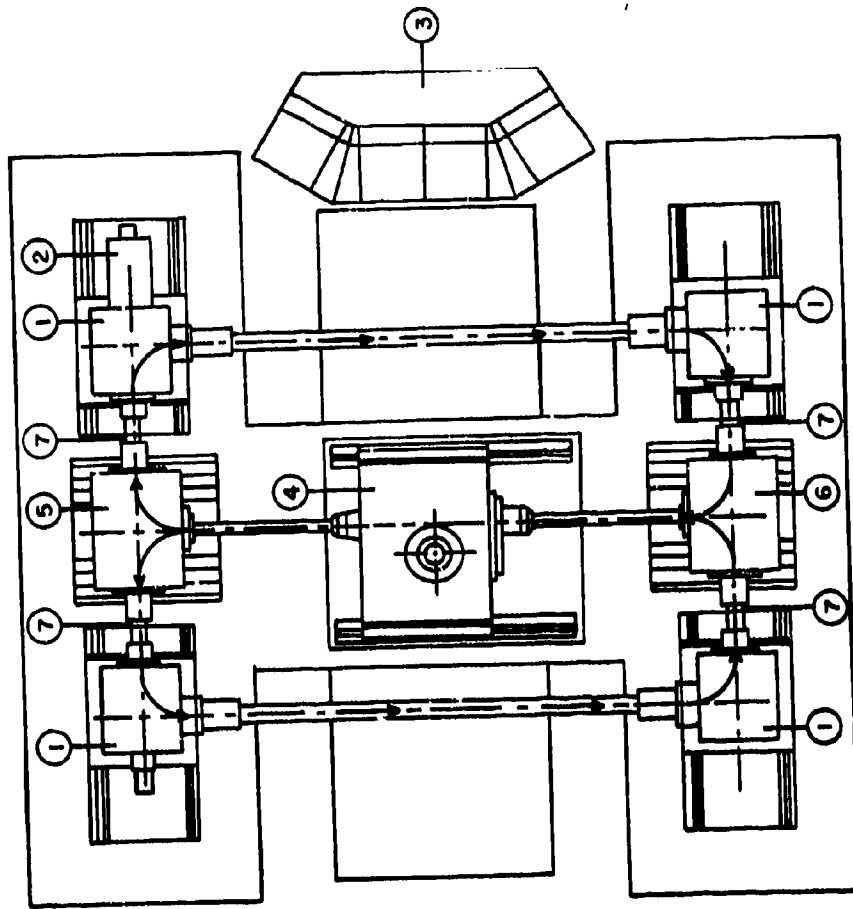
A safety interlock system is coordinated with the console controls to protect the machine from serious damage and to insure more accurate test results. This system provides automatic shutdown of the machine upon failure of a part of the test unit or for a variety of other causes,



Figure 3. Deflection Testing Machine With Test Box.



Figure 4. Gleason No. 510 Axle Test Machine Used for Dynamic Testing.



- 1. CORNER TRANSMISSIONS
 - 2. WINDUP UNIT
 - 3. CONTROL CONSOLE
 - 4. MAIN POWER AND SPEED CHANGE DRIVE
 - 5. TEST GEARBOX
 - 6. SLAVE GEARBOX
 - 7. STRAIN GAGE TORQUE SENSOR
- ARROWS INDICATE POWER
 FLOW THROUGH THE TWO
 TORQUE LOOPS

Figure 5. Schematic Diagram of Gleason No. 510 Axle Test Machine.

such as over-torque, under-torque, overheating, excessive vibration, overspeed, underspeed, and loss of oil pressure in any of the machine components.

The vibration indicators attached to the test boxes and slave boxes are the primary detection devices for tooth failure. The vibration indicator unit is adjusted for the ambient vibration at the beginning of each test and is then set for some known sensitivity. As the test progresses, and tooth failure begins, even the smallest crack in the tooth is indicated by a rise in the vibration level, alerting the operator that failure has occurred. A visual inspection of the unit then follows to confirm the failure.

Description of Dynamic Testing Machine Test Box

The test box consists of an enclosed gear drive, Figure 6, having a right-angle spiral bevel gear set. A sketch of the test box is shown in Figure 7.

The pinion is straddle-mounted on a double-row taper roller bearing behind the pinion, which locks this member against thrust in both directions, and a straight roller bearing in front of the pinion. The pinion assembly is mounted in an eccentric sleeve which permits the pinion to be moved in a direction at right angles to the plane containing the gear and pinion axes. Shims are provided to adjust the pinion mounting distance to obtain the optimum tooth contact pattern.

The gear shaft is straddle-mounted on straight roller bearings to support the gear and hub assembly. The hub assembly consists of a four-pinion differential, which splits the torque between the two side gears splined to the two output shafts. Shims are provided to adjust the gear for the proper backlash.

The slave box at the other end of the test machine has no differential, so torque can be transmitted from each torque loop on the machine back into the center drive box, thereby completing the closed loops.

The gears in the test box are lubricated by a splash system in which the gear member dips into the oil sump in the bottom of the box. The bearings are pressure-lubricated. Internal channels within the box return the oil to the sump. The sump oil is circulated to an external oil reservoir where it is filtered and returned to the box at the required

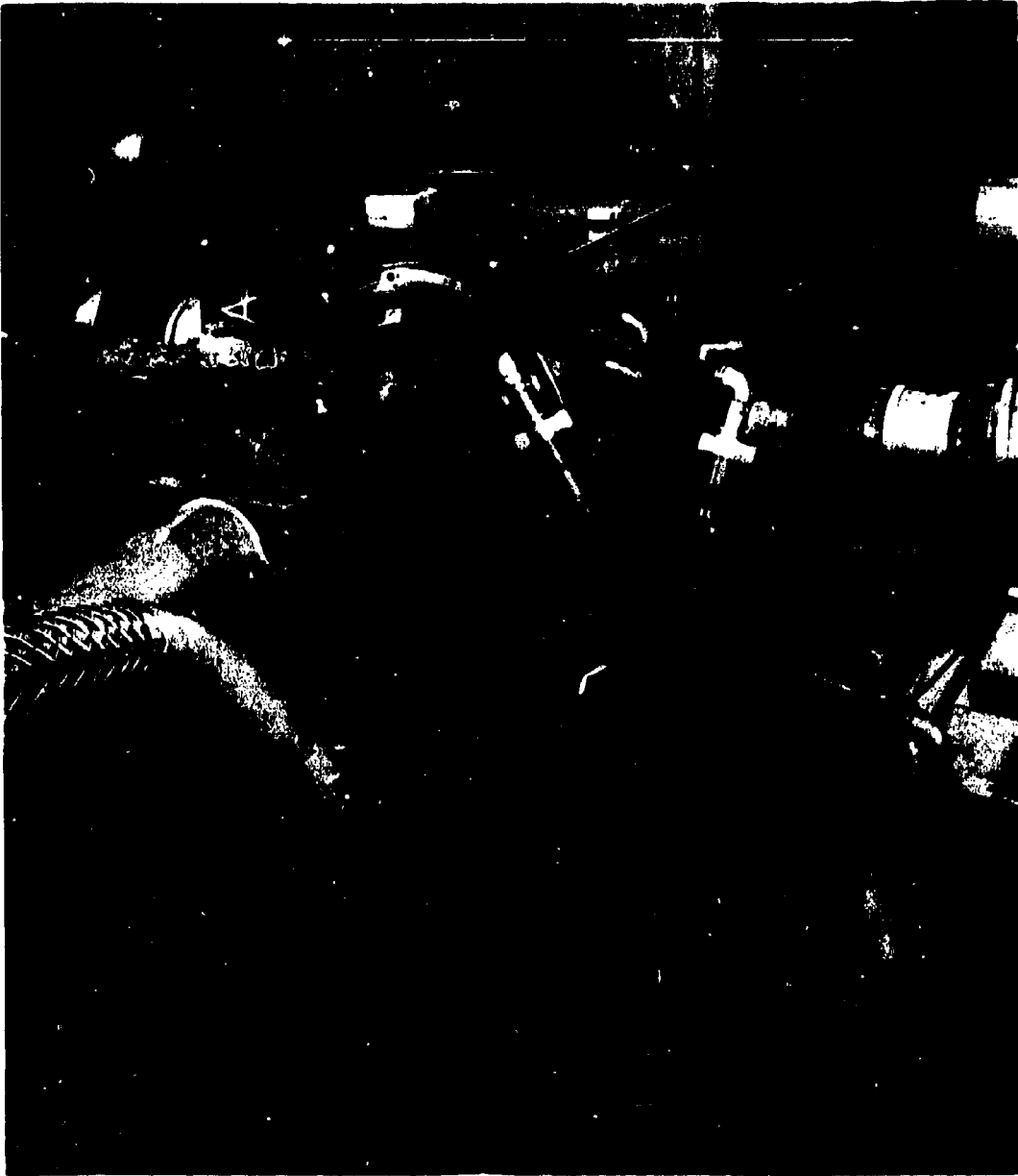


Figure 6. Test Box Used for the Gleason No. 510 Axle Test Machine for Dynamic Testing.

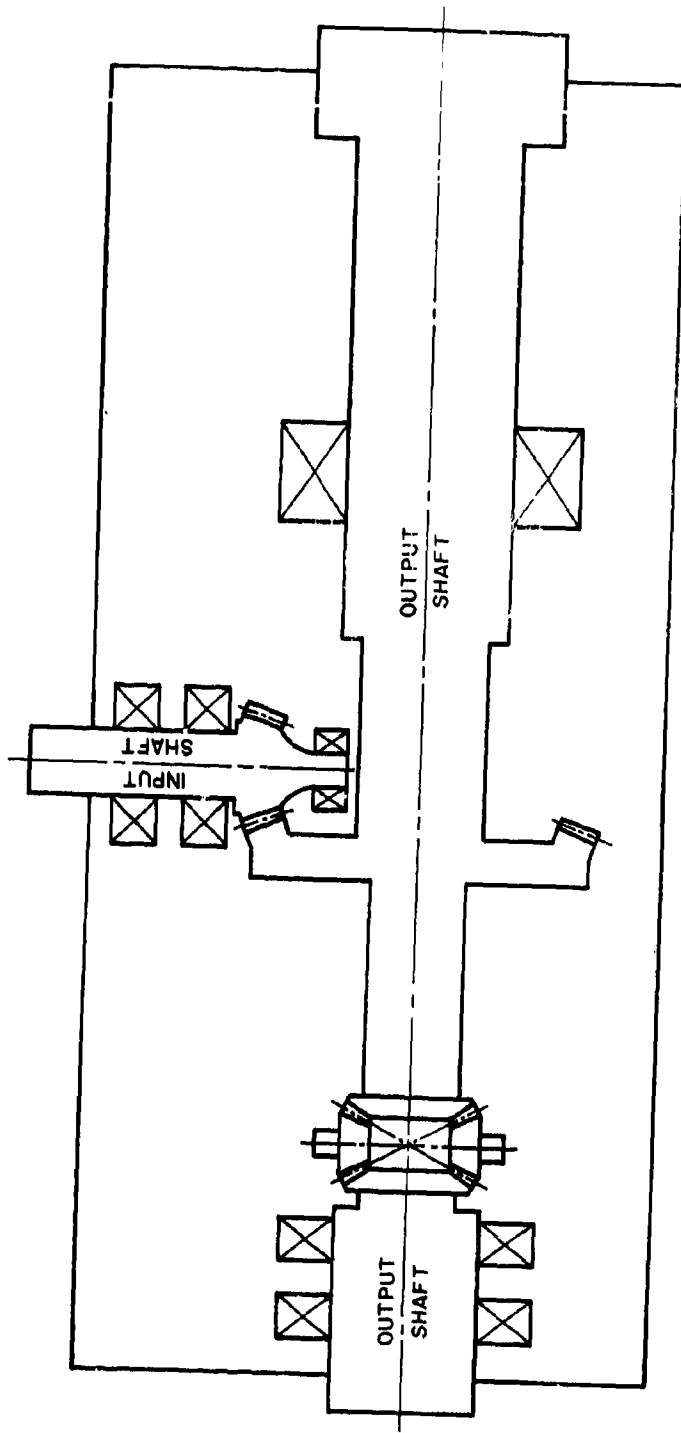


Figure 7. Sketch of Test Box for Dynamic Tests.

oil temperature, which was maintained at a level of 150°F to 160°F.

Failure Detection Devices

The N-I bearing test set, Model BTS 101, is designed to check and evaluate the condition of equipment and machinery while in operation. It detects vibration caused by excessive clearances, ball checks, shaft galling, and misalignment. The gain control positions of the switch provide five graduated levels of gain so that successive tests of any bearing can be conducted under identical conditions. The meter of the bearing test set provides a numerical indication of relative bearing noise picked up by the probe through an amplified electronic system of the instrument. Indications are presented on a scale of zero to 100 and are not intended to represent any particular absolute units but to provide relative measures of bearing noise. The reference gain setting is established and recorded at the start of each bearing inspection program. The headset permits a qualitative evaluation of bearing condition and is especially useful when the operator is familiar with the different sounds associated with a smooth-running bearing and one that requires replacement.

The vibra-switch-malfunction detector is designed for protecting rotating equipment against damage in the event that malfunctions occur, which may be detected as an increase in vibration. An alarm is activated which indicates a probable failure, requiring an inspection by the operator.

Thermocouples are mounted in the test box. The signal is monitored on the temperature recorder-controller used to control the oil temperature in the test box. In the event that the temperature exceeds the set point, an alarm system is activated which shuts off the main drive motor.

Bevel Gear Pulser

The pulser, Figure 8, was designed and built to cause fatigue failure in pinion or gear teeth by the application of a cyclic load, which has come to be known as pulsing.

A schematic diagram of the Gleason gear pulser is shown in Figure 9. Item 1 on this diagram is an 1800-rpm, 5-horsepower electric motor, which is the drive motor for the pulser. Item 2 is a gear tooth pulley and belt assembly connecting the motor to the pulser drive shaft. An



Figure 8. Gleason Bevel Gear Pulser.

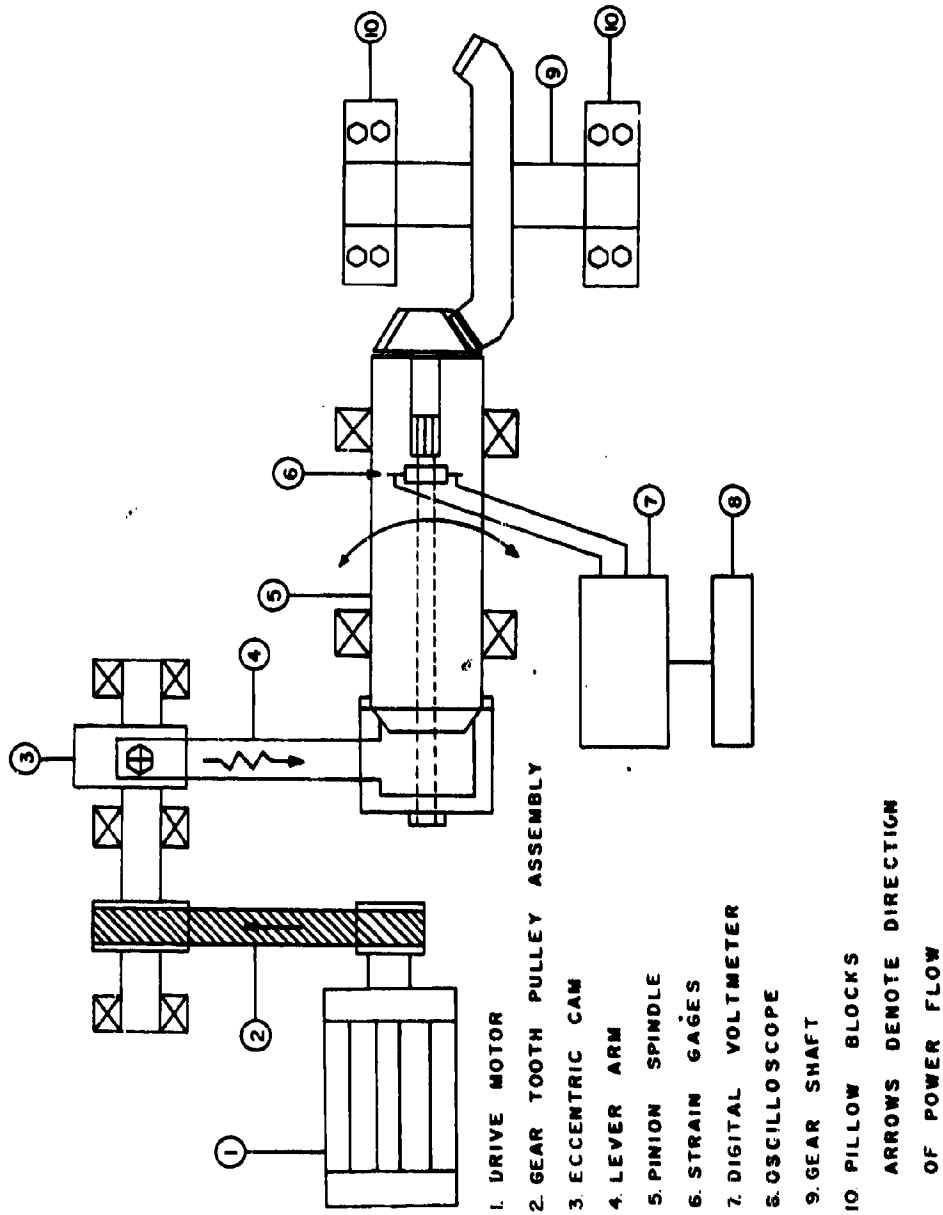


Figure 9. Schematic Diagram of Gleason Bevel Gear Pulser.

eccentric cam, Item 3, mounted on this shaft has an adjustable throw which can be set to apply the proper torque load through the lever arm, Item 4, to the pinion spindle, Item 5. The applied torque is measured through strain gages, Item 6, mounted on the pinion spindle. The signal output of the strain bridge is read out on a digital voltmeter, Item 7, and visually monitored by the height of the wave form on an oscilloscope, Item 8. The gear shaft, Item 9, is rigidly supported at each end by the pillow blocks, Item 10, which provide resistance to torque as well as to radial and axial movement.

In order to pulse the pinion and gear teeth, the cam is rotated at the desired speed, and during each revolution the cam applies and releases through the lever arm the torque load on the pinion and gear teeth.

The phase angle of engagement of the teeth is held the same on each test by observing the contact pattern under load. A vernier and scale provide minute adjustments in the rotation angle of the gear shaft.

Failure is detected by a reduction in the wave height on the screen of the oscilloscope, which indicates a loss in torque in the system and, hence, the beginning of tooth fatigue failure.

TEST PROCEDURE

Below are listed the test procedures employed on the three machines; namely, the deflection testing machine, the dynamic testing machine, and the pulser.

Tooth Contact and Deflection Tests

The test box was assembled with the ground spiral bevel test gear pair. The pinion bearing preload was 50 lb-in. torque with a backlash of .007 inch to .008 inch. The assembly was mounted in a deflection testing machine, and tooth contact tests were made on gear sets for both the 7-1/2-inch and 12-inch cutter diameters.

Torque loads in accordance with Table III were applied on the convex side of the gear (concave side of the pinion). Photographs were made of the gear tooth contacts at each torque load. See Figures 61 through 75 in Appendix II. Following the tooth contact test, the test box was disassembled, and holes were drilled in the main housing so that dial indicators could be mounted to register gear and pinion displacements.

The unit was reassembled with the spiral bevel gears, and an indicator anchorage system was mounted on the housing. See Figure 10. All dial indicators were mounted from this anchorage, and their respective locations are shown on the indicator diagrams, Figures 76, 77 and 78 in Appendix II. Torque loads were applied in the same manner as in the tooth contact test. See Table III. Indicator readings were recorded at each torque load as shown in Table XV in Appendix II.

TABLE III. LOAD DATA FOR DEFLECTION AND TOOTH CONTACT TESTS		
Load Level	Gear Torque (lb-in.)	Pinion Torque (lb-in.)
I	100,000	33,333
II	71,600	23,867
III	50,000	16,667
IV	35,800	11,933

Test Objectives

1. To provide a grinding development of tooth contact that would be satisfactory in the test boxes.
2. To observe and photograph the gear tooth contacts under the specified loads.
3. To record the displacements of the gear and pinion under the specified loads.

Test Outline

Tooth contact test - 12-inch cutter diameter.

Tooth contact test - 7-1/2-inch cutter diameter.

Deflection test gear sets with 12-inch and 7-1/2-inch cutter diameters.



Figure 10. Test Box Showing Indicators Mounted for Measuring Deflections.

The final grinding developments for the spiral bevel test gears manufactured with both 7-1/2-inch and 12-inch cutter diameters had a length, position, and shape suitable for the displacements registered in the deflection test.

The gear and pinion displacements are summarized in Appendix II, Table XV.

Testing Loads on Dynamic Testing Machine

In order to produce an S-N diagram for gears made from AMS-6265 steel, four load levels were selected. For a satisfactory S-N diagram, a range of two to one in the load levels at which tests are to be conducted is required. The highest load level was based on the capacity of the No. 510 Axle Test Machine, which has a maximum capacity of 300,000 lb-in. torque on the gear shaft. However, because of the design of the existing test boxes it was not feasible to use this upper limit of the No. 510 machine. A limit value of 100,000 lb-in. torque was established as load level I for these tests. Load level IV was to be the torque corresponding to the endurance limit of the gears. An initial prediction of this level was 35,800 lb-in. gear torque. This value was 33 percent above the presently used endurance limit for air-melt steel. The two intermediate gear torques were selected as 71,600 lb-in. (twice the minimum torque) and 50,000 lb-in. (one-half the maximum torque). These were tentatively established as load levels II and III, respectively. This produced nearly uniform spacing on logarithmic plotting paper.

Testing was initiated at the highest loads and extended downward by steps, thereby producing a rough S-N curve with single points at the three upper load levels. By projecting this S-N line down to the lowest load level (load level IV), it appeared that the 35,800 lb-in. gear torque would be below the endurance limit. Therefore, the initial test at load level IV was performed at a gear torque of 40,000 lb-in. At this load no failure was experienced within the 30,000,000-cycle limit. Further testing indicated that the endurance limit was close to a gear torque of 50,000 lb-in. (load level III). Therefore, the remainder of the testing at load level IV was performed in the gear torque range of 45,000 to 50,000 lb-in.

A new load level III was established at 60,000 lb-in. gear torque, which was roughly halfway between load levels II and IV.

It had been planned to test all of the gears (eight sets) produced with a 7-1/2-inch-diameter cutter at load level II (71,600 lb-in. gear torque). However, after testing two sets of these gears at this level, it became apparent that this was too close to the endurance limit for this design. Therefore, only four sets were tested at this load level. The remaining four sets were tested at load level I (1000,000 lb-in. gear torque).

By this means it was possible to establish roughly the fatigue curve for gears produced with a 7-1/2-inch-diameter cutter.

The load levels finally used are presented in Table V.

The sets of test gears and pinions were paired in such a manner as to cancel the effect of batch hardening. The heat-treatment pairing is shown in Appendix II, Tables XVI and XVII.

Operating Speeds on the Dynamic Testing Machine

Operating speeds for the dynamic tests were selected to be compatible with the vibration characteristics of the machine and to suit the test program best.

Load levels and gear and pinion speeds are listed in Table IV.

TABLE IV. OPERATING SPEED FOR DYNAMIC TESTS		
Load Level	Pinion Speed (rpm)	Gear Speed (rpm)
I	950	317
II	1300	433
III	1900	633
IV	2600	867

Tests were terminated at 30,000,000 pinion cycles or when failure was experienced, whichever occurred first. From previous testing it had been established that a life of 30,000,000 cycles represents a close approximation to the endurance limit for dynamic gear testing.

Testing Loads on the Pulser

In order to produce an S-N diagram for gears made from AMS-6265 steel and to roughly correlate the results with the running tests performed on the No. 510 Axle Test Machine, it was necessary to use approximately the same range of loads. However, it was decided that the torque loads applied in the pulser should be higher to compensate for the absence of the dynamic effects felt in the axle test machine. The first tests were performed at a load level of 100,000 lb-in. gear torque. From here the loads were extended upward and downward in an effort to obtain a complete S-N diagram and to establish an endurance limit. No attempt was made to operate the pulser at four predetermined load levels, as was done on the running tests on the No. 510 Axle Test Machine. The range of torques covered by the pulser tests extended from 60,000 lb-in. to 150,000 lb-in.

Operating Speeds on the Pulser

The cycle rate of pulsing was selected to be compatible with the vibration characteristics of the pulser machine. For the high-load short-run tests, the speed was selected at 1,200 stress cycles per minute to minimize the percentage of error in life when fatigue occurred. For the light-load long-cycle runs, the cycle rate was increased to 2,700 cycles per minute to minimize the length of the tests.

Tests were terminated at 10,000,000 cycles or when failure was experienced, whichever occurred first. From previous testing it had been established that a life of 10,000,000 cycles represents a close approximation to the endurance limit for pulsing gear testing.

Test Gears Used on the Pulser

The gears used for the pulser tests were produced with a 12-inch cutter diameter. Tooth geometry was identical with the gears used for dynamic testing. However, gear teeth adjacent to the tooth being stressed were removed from the gear prior to testing so that the load would be carried by a single gear tooth.

TABLE V. TEST RESULTS NO. 510 AXLE TEST MAC

Load Level Gear Torque Pinion Speed Cutter Diam.	I 100,000 lb-in. 950 rpm 12 in.					II 71,600 lb-in. 1,300 rpm 12 in.				
	Test	Serial	Pinion Cycles	Failure* Pinion Gear		Test	Serial	Pinion Cycles	P	
	1	8-108	89,190	B	A	5	6-106	401,000		
	2	12-112	122,900	B	A	7	9-109	406,000		
	8	3-103	103,700	B	A	10	35-135	399,900		
	11	21-121	109,900	B	A	27	17-117	485,800		
	14	34-134	111,700	B	A	28	20-120	429,300		
	30	26-126	147,000	B	A	31	27-127	421,500		
	35	37-137	136,300	B	A	34	46-146	442,900		
	39	41-141	118,700	B	A	38	45-145	368,500		
Load Level Gear Torque Pinion Speed Cutter Diam.	IV 50,000 lb-in. 1,900 rpm 12 in.					I 100,000 lb-in. 950 rpm 7.500 in.				
	Test	Serial	Pinion Cycles	Failure* Pinion Gear		Test	Serial	Pinion Cycles	P	
	3	1-105	2,753,000	None	B	19	72-172	478,800		
	4	19-119	2,861,000	None	{ A B	21	78-178	254,900		
	6	4-104	30,000,000**	None	None	23	79-179	173,500		
	9	10-110	1,981,000	None	B	25	71-171	314,000		
	12	14-114	30,000,000	None	{ A B					
	13	15-115	30,000,000†	None	None					
	16	30-130	30,000,000†	None	None					
	26	44-144	23,320,000	None	A					
<p>* A = Fatigue cracks on profile near root B = Fatigue cracks in root fillet</p>										

A

510 AXLE TEST MACHINE

II 71,600 lb-in. 1,300 rpm 12 in.				III 60,000 lb-in. 1,900 rpm 12 in.				
Serial	Pinion Cycles	Failure* Pinion Gear		Test	Serial	Pinion Cycles	Failure* Pinion Gear	
6-106	401,000	B	A	15	7-107	550,500	B	None
9-109	406,000	B	A	20	31-131	517,500	B	A
35-135	399,900	B	A	22	18-118	284,900	B	A
17-117	485,800	B	A	24	22-122	884,700	None	B
20-120	429,300	B	A	29	36-136	2,244,000	None	A
27-127	421,500	B	A	32	32-132	1,756,000	None	B
46-146	442,900	B	None	33	39-139	3,083,000	None	A
45-145	368,500	B	None	37	47-147	1,881,000	None	A

I 100,000 lb-in. 950 rpm 7.500 in.				II 71,600 lb-in. 2,000 rpm 7.500 in.				
Serial	Pinion Cycles	Failure* Pinion Gear		Test	Serial	Pinion Cycles	Failure* Pinion Gear	
72-172	478,800	None	A	17	69-169	5,055,000	None	B
78-178	254,900	B	A	18	70-170	6,358,000	A	None
79-179	173,500	None	A	36	73-173	10,260,000	None	A
71-171	314,000	B	A	40	80-180	4,446,000	None	A

** 40,000 lb-in. gear torque
 † 45,000 lb-in. gear torque
 ‡ 47,500 lb-in. gear torque

B

RESULTS OF TESTS

From the three series of fatigue tests conducted during the program, data have been accumulated on the dynamic fatigue life of representative gears (dynamic tests), the static fatigue life of the same representative gears (pulser tests), and the material fatigue strength (R. R. Moore tests).

DOCUMENTATION OF RESULTS

Dynamic Tests

Table V shows the results of the dynamic tests. This table contains the data from the six series of tests - four load levels for the 12-inch cutter diameter gears and two load levels for the 7-1/2-inch cutter diameter gears. For each series, the test number, the pinion and gear serial numbers, the pinion life, and the type of failure on both pinion and gear are listed.

Pulsing Tests

Table VI shows the results of the pulser tests. This table lists the gear torque the life, and the member on which failure was first observed.

R. R. Moore Tests

Table VII shows the results of the R. R. Moore tests. This table lists the specimen number, the stress level, and the life to failure.

Tooth Contact and Deflection Tests

Results of the tooth contact and deflection tests were reported in the Test Procedure section. Pictures of the tooth contacts are shown in Figures 61 through 75 in Appendix II.

TEST FAILURES

An extensive analysis of the test failures was performed, including visual and metallurgical inspections. Every effort was made to pinpoint the origin of the failure and to explain the causes. This section deals with the visual inspection of these failures.

TABLE VI. PULSER TEST RESULTS

Gear Torque (lb-in.)	Life (cycles)	Failure
60,000	10,215,000	None
70,000	10,000,000	None
73,500	1,051,200	Pinion
73,500	566,400	Gear
73,500	10,000,000	None
76,500	536,400	Pinion
79,500	649,780	Pinion
100,000	69,600	Pinion-Gear
100,000	63,600	Pinion-Gear
100,000	103,250	Pinion
103,500	48,290	Gear
103,500	62,100	Pinion-Gear
111,000	28,050	Gear
111,000	47,870	Pinion-Gear
111,000	50,250	Pinion
115,500	45,450	Gear
120,000	18,420	Gear
129,000	21,210	Gear
135,000	17,900	Gear
135,000	20,850	Gear
135,000	13,600	Gear
135,000	11,120	Gear
150,000	3,540	Gear

TABLE VII. FATIGUE TEST RESULTS FOR R. R. MOORE SPECIMENS

Serial Number	Calculated Stress (ksi)	Cycles to Failure ($\times 10^{-6}$)
10	100.0	10.200 *
12	120.0	29.340 *
14	130.0	11.580 *
8	140.0	10.716 *
1	145.0	12.980 *
5	148.0	11.330 *
15	150.0	2.905
13	151.0	2.281
2	155.0	8.678
4	160.0	0.392
3	160.0	0.101
11	160.0	11.109 *
16	160.0	4.839
6	170.0	1.156
9	171.0	0.410
7	172.0	0.400

*Did not fail (run-out)

Dynamic Tests

In the dynamic tests, two types of bending fatigue failures were observed: failures in the root fillet and failures on the tooth profile near the root area. These are indicated in Table V. Figures 11 and 12 illustrate representative bending fatigue failures in the root fillet of the gear. The cracks extend along the root of the tooth for two-thirds of the distance from the toe toward the heel. Figures 13 and 14 illustrate representative bending fatigue failures in the root fillet of the pinion. Here also it will be seen that the cracks extend along the root of the tooth for approximately two-thirds of the tooth length. On many parts, several teeth showed cracks when treated with Spot-Check after the failure was first detected. With two or three exceptions, no failures progressed to the point where the teeth were physically broken out. One of these exceptions is shown in Figure 16.

As indicated in Table V, many of the gears failed from bending fatigue on the tooth profile near the root area. This is illustrated in Figure 15. The crack is well above the root fillet and is on the working profile of the tooth. A further analysis of these failures is made in the Metallurgical Investigations section.

Pulsing Tests

On the pulsing tests, only bending fatigue failures in the root fillet were experienced. See Figures 17 and 18. This no doubt was due to the fact that the line of contact between gear and mating pinion did not pass through the area of the tooth where cracks were observed on the gears that were tested dynamically.

Although both gear and pinion failures were observed on this series of tests, gear failures outnumbered pinion failures by nearly two to one. In four cases both gear and pinions cracked at approximately the same time. This would indicate that the lives of pinion and gear teeth were nearly equal under the particular test conditions. It will be evident from an examination of Table VI that the pinions generally failed at the lower torque loads, whereas the gears failed at the higher torque loads. In the middle-load range both members failed. This would appear to be at variance with the results of the dynamic tests, in which gear failures were most prevalent at the lower torque loads.



Figure 11. Typical Bending Fatigue Crack in Root of Gear Tooth.



Figure 12. Typical Bending Fatigue Crack in Root of Gear Tooth.



Figure 13. Typical Bending Fatigue Crack in Root of Pinion Tooth.



Figure 14. Typical Bending Fatigue Crack in Root of Pinion Tooth.

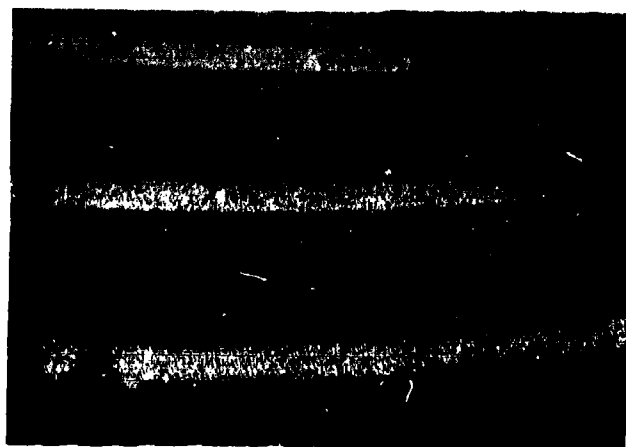


Figure 15. Fatigue Cracks on the Profile of a Gear Tooth.



Figure 16. Fatigue Fracture Resulting From Cracks on the Tooth Profile of a Gear Tooth.



Figure 17. Typical Bending Fatigue Crack in the Root of the Pinion Tooth on Pulsar Test.



Figure 18. Typical Bending Fatigue Crack in the Root of the Gear Tooth on Pulsar Test.

R. R. Moore Tests

The R. R. Moore tests were used primarily to establish that the material used in these test gears was of a quality suitable for comparison with other test results.

The R. R. Moore specimens failed in fatigue because of the reverse bending encountered in this type of test. The failures experienced in this test are not representative of failures experienced on gear teeth. Gears are seldom subjected to reverse bending. In addition, the size of the cross-sectional area of the R. R. Moore specimens was selected to be within the capacity of the standard R. R. Moore testing machine and was not related to the cross-sectional area of the gear teeth. Finally, the polished surfaces used on the R. R. Moore specimens were not representative of the ground fillets used on the test gears.

The failures experienced here occurred in the central area of the specimens. The scatter in the location of the failures was about normal for this type of test. Tests were run for 10,000,000 cycles or until failure, whichever occurred first. Table VII includes the results of the R. R. Moore fatigue tests.

METALLURGICAL INVESTIGATIONS

Preliminary Examinations of Test Gears

Metallurgical examinations of test gears and pinions were conducted prior to fatigue testing to insure that the gear sets were properly heat-treated. One gear or pinion from each of the four carburizing loads was sectioned. The results of surface hardness and case depth checks for gear No. 123 are shown plotted in Figure 19. The microhardness traverse was made normal to the root fillet. The core hardness of the gear was 38 R_C. Similar results were obtained from the other three specimens.

The heat-treatment requirements were:

1. Case hardness, R_C 60 minimum.
2. Effective case depth at root radius, 0.045"-0.055".
3. Core hardness, R_C 34 to 38.

It was concluded that the test gears and pinions were properly heat-treated. The metallurgical structure of the carburized case is shown in Figure 20. The structure consists of martensite and a small quantity of retained austenite. The core structure, Figure 21, consists of low carbon martensite with no evidence of proeutectoid ferrite.

Examination of Failed R. R. Moore Specimens

Two R. R. Moore specimens, No. 3 and No. 16, were fatigue-tested at the same stress level of 160,000 psi. Specimen No. 16 ran 4.8×10^6 cycles before it failed, while specimen No. 3 lasted only 0.1×10^6 cycles. A metallurgical investigation was conducted to determine the reason for the difference in specimen life during the fatigue test. A microhardness traverse on a Leitz tester under a load of 1 Kg was run; refer to Figure 22. The case depth vs hardness traverse shows the case hardness, effective depth of case, and the core hardness of each specimen to be nearly identical.

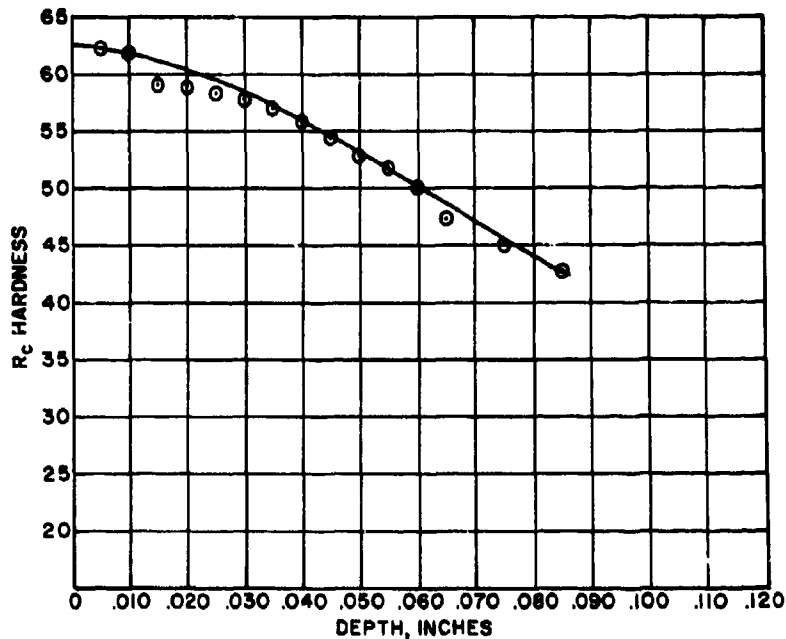


Figure 19. Hardness Traverse on Test Gear No. 123.



Figure 20. Photomicrograph of Case Structure in Test Gear No. 123 (X 500).



Figure 21. Photomicrograph of Core Structure in Test Gear No. 123 (X 500).

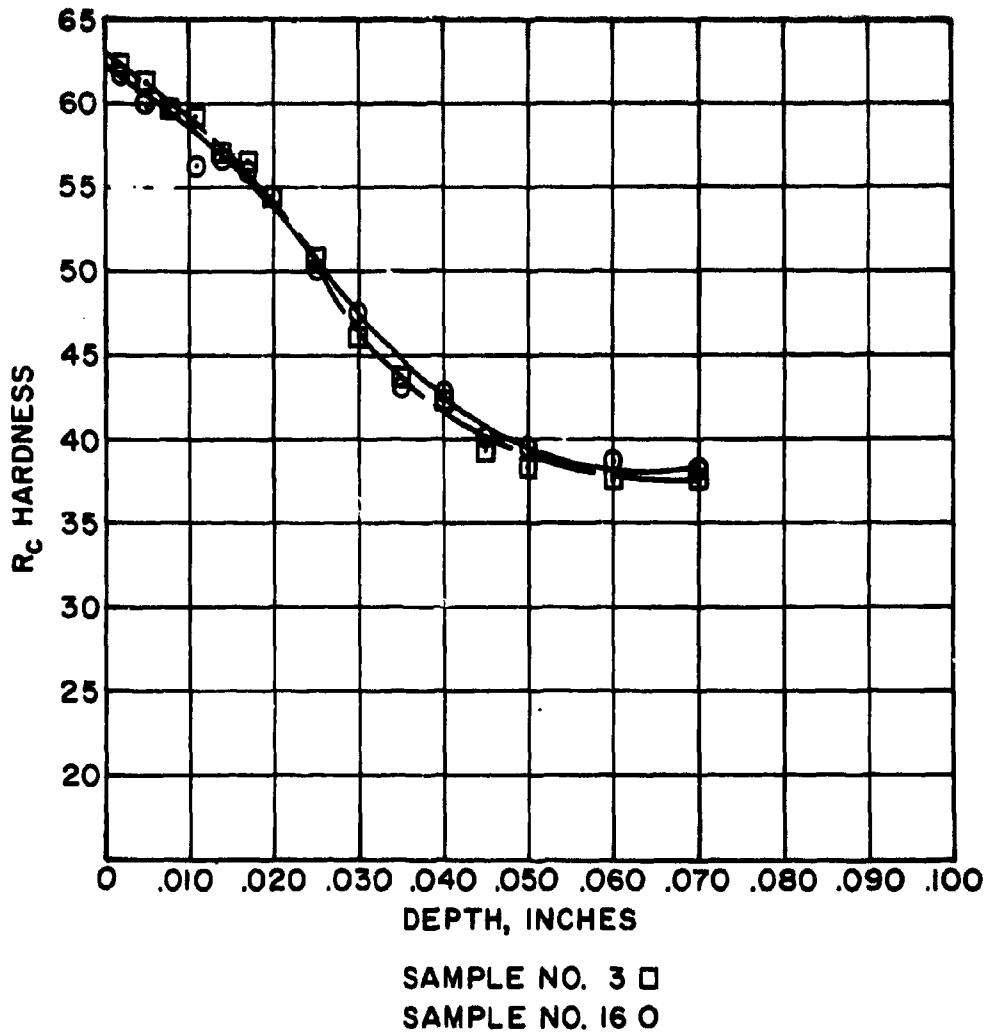


Figure 22. Case Depth Vs Hardness Traverse for R. R. Moore Specimens 3 and 16.

Visual examination showed the two samples to be almost identical in metallurgical structure. Representative photomicrographs of the case and core structures are shown in Figures 23 and 24. The retained austenite in both specimens was estimated to be about 15 to 20 percent. It was concluded that the metallurgical examination did not reveal any gross discrepancies that could be held accountable for the difference in specimen life. It is believed that stress concentration at grain boundaries and at inclusions, and strength variations due to grain orientation are the factors most likely to have affected the difference in life between the two specimens.

Examination of Failed Test Gears

During the test program, bending fatigue cracks on the test gears were observed at two locations: one in the tensile fillet and the other slightly higher on the tensile profile of the tooth. Usually, bending fatigue cracks occur in the tensile fillet and originate at the surface. An extensive effort was made to determine whether the cracks that occurred higher up on the profile were initiated at the surface or below the surface (subsurface).

Gear No. 122 was typical of the test gears that failed because of bending fatigue cracks in the tensile fillet. The cracked tooth was removed from this gear and sectioned. Microhardness traverses were made normal to the convex (tensile side) surface both in the root of the tooth below the crack and at the pitch line and normal to the concave surface in the root. See Figure 25. Photomicrographs typical of the case and core structure of this tooth are shown in Figures 26 and 27. The case and core structures are essentially the same as the structures examined prior to testing.

Gear No. 178 had profile cracks on about half the teeth. One tooth on this gear that did not show any surface cracks under either the "Spot-Check Technique" or the microscopic examination was removed. A normal section slice was made near the heel end of the tooth, and the section was examined for the presence of subsurface cracks. None were found. An additional 0.010 inch of stock was carefully ground off the normal section, and the specimen was reexamined. This process was repeated on this tooth until the area of probable damage had been completely examined. Another tooth was selected at random from the same gear, and the process was repeated. In neither case were subsurface cracks visible.



Figure 23. Photomicrograph of Case Structure in R. R. Moore Specimens (X 500).



Figure 24. Photomicrograph of Core Structure in R. R. Moore Specimens (X 500).

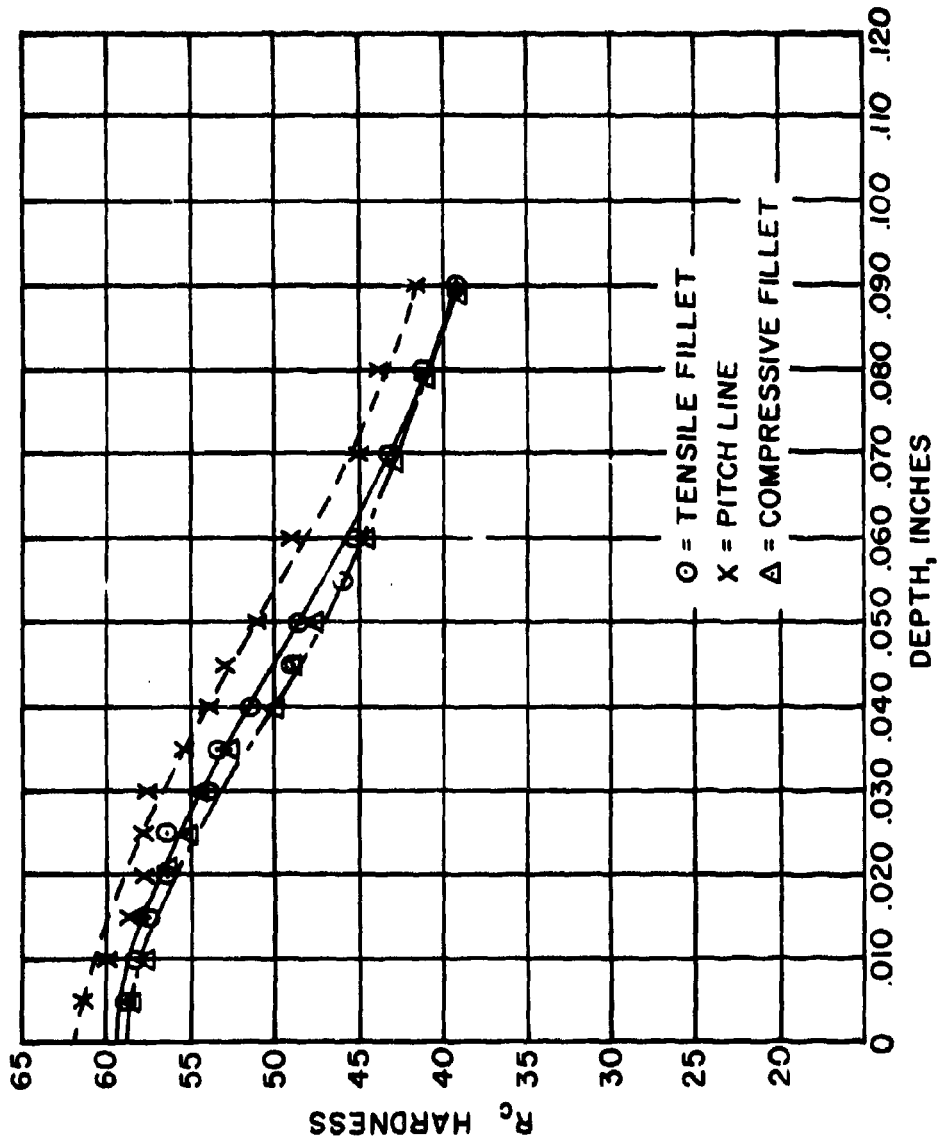


Figure 25. Hardness Traverse on Test Gear No. 122.



Figure 26. Case Microstructure on Test Gear No. 122 (X 500).



Figure 27. Core Microstructure on Test Gear No. 122 (X 500).

A tooth from gear No. 178 that had a surface crack on the tooth profile was removed and sectioned. A microhardness traverse was made in the normal section slightly above the crack; see Figure 28. The plot of hardness versus depth is shown in Figure 29. This traverse, like all the others made on failed test gears, showed a reduction in the value of effective case depth from that measured prior to fatigue testing. This is explained by the removal of stock during the final tooth-grinding operation which followed the preliminary metallurgical examinations of the test gears.

Gear No. 172 also had a few teeth with profile cracks. One tooth with a profile crack was removed (Figure 30) and a normal section was made near the heel end. Figure 31 shows where the microhardness traverse was taken. The hardness versus case depth was almost identical to the plot shown in Figure 29.

Stock was carefully ground off the normal section in successive steps going from heel to toe. What may have appeared as a subsurface crack in one section joined the surface crack in another section. It can be concluded that no cracks were seen which did not at some point along the tooth length come to the surface. It was not possible to prove conclusively the true origin of these cracks.

X-ray diffraction techniques were used to determine the amount of retained austenite on the tooth surface both in the tensile fillet and on the profile approximately where the higher cracks were located. The concave side of pinion No. 35 and the convex side of gears Nos. 122 and 118 all showed about 8 to 11 percent retained austenite.

Pinion No. 35 and gear No. 122 had fatigue cracks in the root of the tooth. Profile fatigue cracks were observed on the teeth of gear No. 118.

There did not appear to be any metallurgical difference between the gears with root cracks and the gears with profile cracks. The gears made of vacuum-melt material are able to run longer at higher stress levels; therefore, it is possible that the tensile surface stresses surrounding the area of high contact stress near the root of the gear tooth combine with the bending stresses to cause bending fatigue failure on the tooth profile rather than in the root fillet. No other explanation for this difference has been found to date.



Figure 28. Photograph Showing Location of Microhardness Traverse on Test Gear No. 178 (X 100).

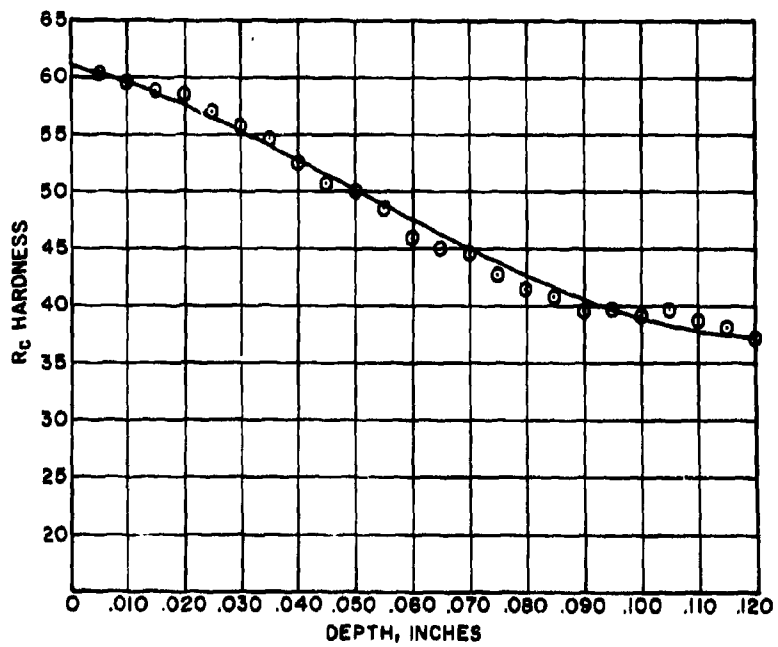


Figure 29. Case Depth Vs Hardness Traverse for Test Gear No. 178.



Figure 30. Photograph of Profile Crack on Test Gear No. 172 (X 6).



Figure 31. Photograph Showing Location of Microhardness Traverse on Test Gear No. 172 (X 100).

Finally, a high-magnification photograph of a typical profile fracture is shown in Figure 32. This photograph was taken with the aid of an electron-beam-scanning microscope.



Figure 32. Photograph From Electron-Beam-Scanning Microscope on Test Gear No. 120 (X 1105).

NEW STRENGTH FORMULAS

While gears were being manufactured and tested, an analysis of the existing strength formulas was initiated, and the following positive steps were taken to improve these formulas.

EFFECTIVE FACE WIDTH

Using data generated in a previous experiment, Reference 14, a detailed study of the stress distribution in the root fillet of several model gear teeth was performed. This experiment consisted of mounting five equally spaced strain gages in the root fillet of each model tooth along the length of the tooth. Point loads of equal value were applied successively at a series of equally spaced grid points on the tooth surface - three rows each at a different height above the base of the tooth and eleven points in each row along the length of the tooth. See Figure 33. Strain readings from each gage were recorded for each loading point. Computer programs were established to interpolate between grid points and between strain gages. By selecting a series of discrete, equally spaced points in a straight line on the tooth surface, a second computer program could effectively duplicate the stress distribution produced by any line of contact. By varying the magnitude of the loads at the various points, any load distribution could be simulated. The method assumed that superposition of strains is valid.

Once the strain distribution along the root of the tooth was determined from the data, an exponential curve was fitted to the data. A regression program then determined the coefficients of the exponential equation.

The final formula for effective face width is based on the ratio of the average stress to the maximum stress and can be expressed as follows:

$$\frac{F_e}{F} = \frac{s_{avg}}{s_{max}} \quad (1)$$

where F_e = effective face width

F = actual net face width

s_{avg} = average stress along root of tooth produced by a uniform load distribution along the total length of the tooth at the assumed load height used for s_{max}

σ_{max} = maximum stress along root of tooth produced by assumed tooth loading

Values of effective face width given by this new formula are smaller than the values given by the present AGMA formulas. This results in higher calculated bending stresses. A detailed and complete derivation of the effective face width formulas is contained in Appendix III.

POSITION OF POINT OF LOAD APPLICATION

In previous work, Reference 8, it was concluded that the center of pressure along the instantaneous line of contact on a spiral bevel gear tooth lies at a point offset toward the heel end of the tooth from the center of the line of contact. This conclusion was based on the assumption that the center of pressure lies close to the widest portion of the instantaneous line of contact. An analysis performed by the contractor prior to the initiation of this project showed that the load will be greatest at this widest point along the line of contact, but the center of pressure will lie nearer the center of the line of contact. By replottting available fatigue test data versus the calculated stresses based on a new assumption that the point of load application lies halfway between the center of the line of contact and the widest point, it was demonstrated that a better correlation existed. The width of the scatter band was reduced appreciably. The most important effect was an improved strength balance between gear and mating pinion.

In the present analysis this new assumption, that the point of load application can be considered to be represented by a point load acting halfway between the center of the instantaneous line of contact and the widest point, has been incorporated in the formula for the geometry factor. This results in the value of the correction factor, k (given in the Appendix to the AGMA Strength Standards, References 15 and 16), being doubled or made equal to $\frac{8n + 6.4N}{N-n}$. The correction factor, k , used in the present formulas is the reciprocal of k , and its value is therefore halved or made equal to $\frac{N-n}{8n + 6.4N}$. This value is used in the formulas documented in Appendix V.

LOAD DISTRIBUTION FACTOR

It has long been known that the shift in the tooth contact along the length of a gear tooth will cause the tooth to break at its end even under moderate loads. In this program a study was made of the effect of this contact shift.

When a deflection test is made on a gear mounting, indicators are placed at strategic positions to measure the relative displacements of the gear and mating pinion. Using the formulas derived by Baxter, Reference 13, it is possible to calculate the shift of the tooth contact position along the length of the tooth under any known relative displacements, assuming that the tooth is a rigid body and does not deflect. From the experimental data obtained on a Gleason No. 14 Testing Machine under light loads, measurements were made of the lengthwise shift in the tooth bearing under various displacements. A correlation coefficient between the calculated shift and the measured shift was thereby determined. This correlation coefficient turned out to be unity, indicating the accuracy of the formulas for adjustability.

Using the same basic data given in Reference 14 and the approach used to determine the stress distribution along the tooth given in the Effective Face Width section, it was possible to establish a formula for the load distribution factor. The final formula for load distribution factor is based on the ratio of the maximum stress at the displaced position of the contact pattern to the maximum stress at the central position on the tooth face width. It can be expressed as follows:

$$K_m = \frac{s_{\text{shift}}}{s_{\text{max}}} \quad (2)$$

where K_m = load distribution factor.

s_{shift} = maximum stress along the root of the tooth when the tooth contact pattern has shifted away from its central position on the tooth.

s_{max} = maximum stress along the root of the tooth when the tooth contact pattern is centrally located. This is the same s_{max} referred to in the Effective Face Width section.

The effect of lengthwise tooth curvature (cutter diameter) is reflected in the adjustability coefficients, which are used in the determination of the calculated lengthwise tooth contact shift. In addition, the effect of the lengthwise radius of curvature on tooth contact length is considered. For the first time, the effect of lengthwise tooth curvature on bending stresses is included in the formulas.

It is the difference in lengthwise tooth contact shift between the test gears produced with 7-1/2-inch and 12-inch cutter diameters that

accounts for the difference in fatigue life between the two designs when tested at the same load level, Figure 34. When an S-N diagram is plotted, based on these new formulas, the difference in calculated stress resulting from this new load distribution factor largely compensates for the difference between the two designs, Figure 35.

A detailed and complete derivation of the load distribution factor is contained in Appendix IV.

SIZE FACTOR

The AGMA bevel gear strength formulas contain a size factor that compensates for the size effect of the particular gear. Formerly, this size factor, for convenience, was included in the formula for calculated stress; in the formulas contained herein, the size factor has been included in the formula for working stress. This has the effect of raising the calculated stresses to a value more nearly equal to the true stress level.

This change was made to comply with the requirement that the strength calculations for bevel gear teeth should produce stresses corresponding to the true stresses in the gear material.

It would be well to point out that this change results in certain disadvantages:

1. For the average gear engineer, it increases the hazard of mistakes. At the present time, the calculated bending stress in a bevel gear tooth requires only the multiplication of a strength factor, given on the contractor's dimension sheets for bevel gears, by the torque. This value is then compared with a single value for the allowable stress of the material. With the present change, both a calculated stress and a working stress must be calculated and compared.
2. When fatigue data are plotted to produce an S-N diagram, the plotting of true stress vs gear life no longer has meaning, except when the data are plotted for a single gear design. Frequently, one wishes to plot data obtained from several gear designs of varying sizes. This cannot be done. Since bevel gears are produced in a wider range of diametral pitches than is common with spur and helical gears, this change results in a greater hardship to the bevel gear user.

If one is concerned only with infinite life applications, the use of true stress may have some merit. Otherwise the existing AGMA method modified by the new effective face width, position of the point of load application, and load distribution factor would appear to be more useful.

The new formula for the size factor for bevel gears incorporated in the equation for working stress is given as follows:

$$K_s = 2P_d^{-0.25} \text{ for gears of 16 DP and coarser} \quad (3)$$
$$= 1.0 \text{ for gears of 16 DP and finer}$$

where K_s = size factor

P_d = transverse diametral pitch at outer end of tooth

This formula for size factor gives values twice the magnitude of those given in the AGMA bevel gear strength standards.

In the present AGMA bevel gear strength standards, the allowable stresses have been reduced to a value corresponding with the working stress in a 1-DP gear. This allowable stress is one-half the working stress for a 16-DP gear. The size factor for a 1-DP gear was established as unity. Therefore, the size factor for a 16-DP gear was 0.5.

With this new approach to the use of a size factor, the allowable stress is established on the basis of the strength of the material in a small specimen (R. R. Moore), which corresponds approximately to a 16-DP gear tooth. The size factor for a 16-DP gear is now established as unity. Therefore, the size factor for a 1-DP gear becomes 2.0.

In the plotting of comparative data in the Analysis of Results section, where it is indicated that a size factor has been included in the calculated stress values, the size factor referred to is the one used in the present AGMA bevel gear strength standards and is not the one used here.

FINAL STRENGTH FORMULAS

The final strength formulas are very similar in form to the existing AGMA formulas. The basic equation for the calculated bending stress in the root fillet is given as follows:

$$s_t = \frac{2 T_P K_O}{K_V} \cdot \frac{P_d}{F \cdot d} \cdot \frac{K_m}{J} \quad (4)$$

where s_t = calculated tensile stress in the root of the tooth, psi

T_P = transmitted pinion torque, lb-in.

K_O = overload factor

K_V = dynamic factor

P_d = transverse diametral pitch at outer end of tooth

F = face width, in.

d = pinion outer pitch diameter, in.

K_m = load distribution factor from equation (2)

J = geometry factor

In equation (4), use the face width, load distribution factor, and geometry factor for the member being calculated. The size factor no longer appears in equation (4). However, the load distribution term is evident. The term for effective face width and the change in the position of the point of load application are incorporated in the geometry factor and therefore do not appear directly in equation (4).

The basic equation for the working stress is given as follows:

$$s_w = \frac{s_{at}}{K_T K_R K_s} \quad (5)$$

where s_w = working stress, psi

s_{at} = allowable bending stress, psi. This is the value of allowable stress taken from an S-N diagram based on R. R. Moore tests on a 0.250-inch-diameter specimen, corrected for single-direction bending.

K_T = temperature factor

K_R = factor of safety

K_s = size factor from equation (3)

The calculated bending stress must be equal to, or less than, the working stress.

$$s_t \leq s_w \quad (6)$$

The complete listing of formulas for calculated bending stress and working stress is given in Appendix V.

ANALYSIS OF RESULTS

Using both the new, improved strength formulas developed during this program and the AGMA strength formulas, plots of the results from the dynamic tests and the pulsing tests have been made. These plots include the following:

1. Gear torque vs life in cycles for dynamic tests, Figure 34.
2. Gear torque vs life in cycles for pulsing tests, Figure 36.
3. Calculated bending stress vs life in cycles for dynamic tests using new, improved strength formulas with the size factor omitted, Figure 35.
4. Calculated bending stress vs life in cycles for pulsing tests using new, improved strength formulas with the size factor omitted, Figure 37.
5. Calculated bending stress vs life in cycles for dynamic tests using new, improved strength formulas with the size factor included, Figure 38.
6. Calculated bending stress vs life in cycles for dynamic tests using AGMA strength formulas with the size factor included, Figure 39.
7. Calculated bending stress vs life in cycles for pulsing tests using new, improved strength formulas with the size factor included, Figure 40.
8. Calculated bending stress vs life in cycles for pulsing tests using AGMA strength formulas with the size factor included, Figure 41.

TORQUE VS LIFE DIAGRAMS

Figures 34 and 36 present the test data in graphical form; that is, the test load in gear torque is plotted against the life in cycles. In Figure 34 the data points have been separated into two groups: those representing the 12-inch cutter diameter design and those representing the 7-1/2-inch cutter diameter design. The mean lines for the two groups are also shown. It can be seen from this graph that the 7-1/2-inch cutter diameter design resulted in a substantially increased average life over the

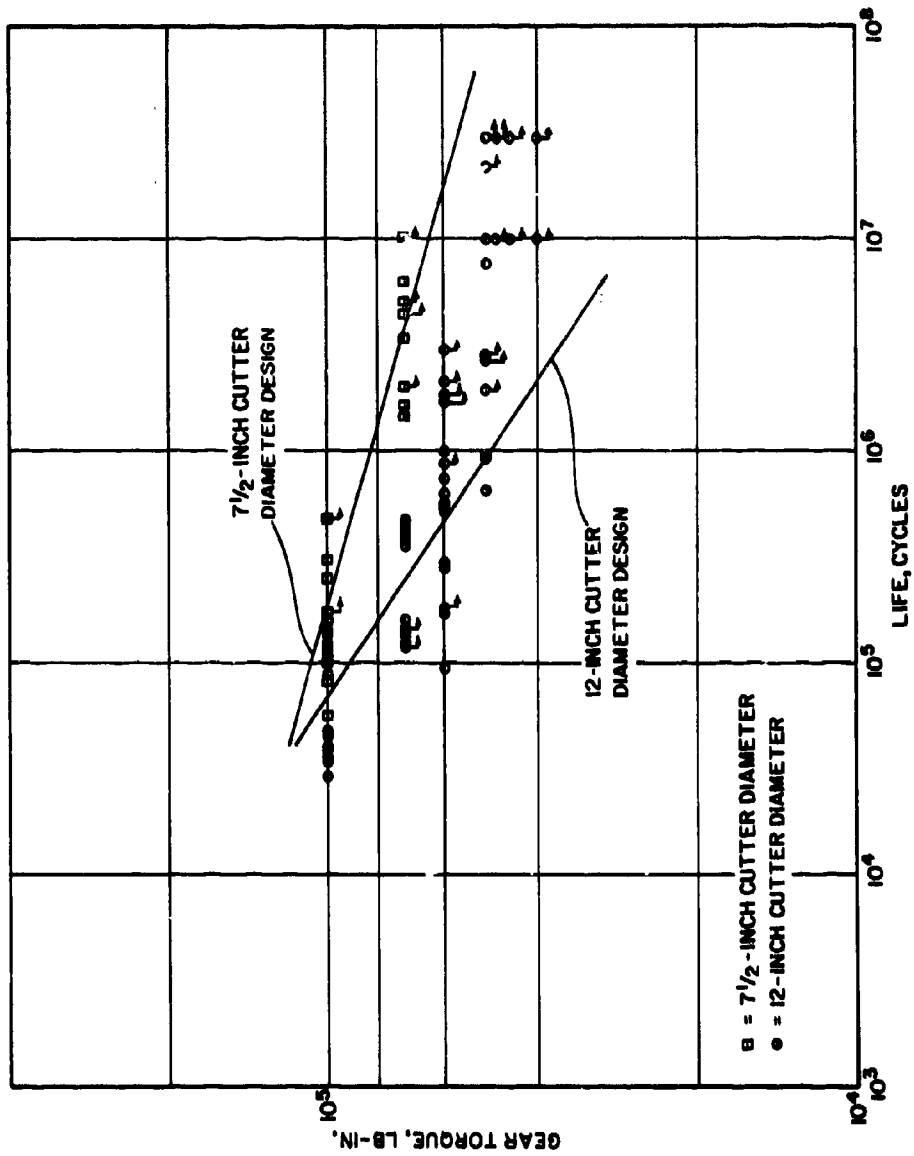


Figure 34. Gear Torque Vs Life in Cycles for Dynamic Tests on 17/51 Test Gears.

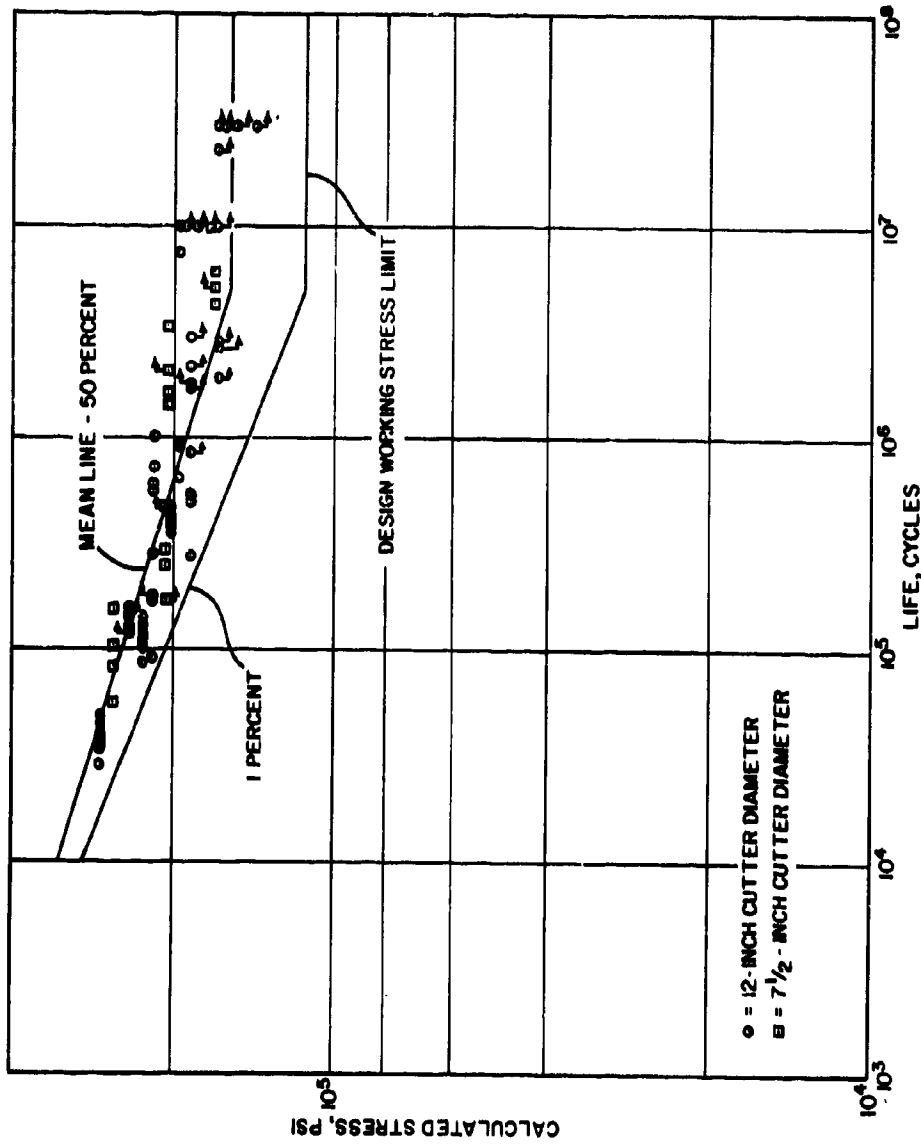


Figure 35. Calculated Bending Stress Vs Life in Cycles for Dynamic Tests on 17/51 Test Gears Using New, Improved Strength Formulas With the Size Factor Omitted.

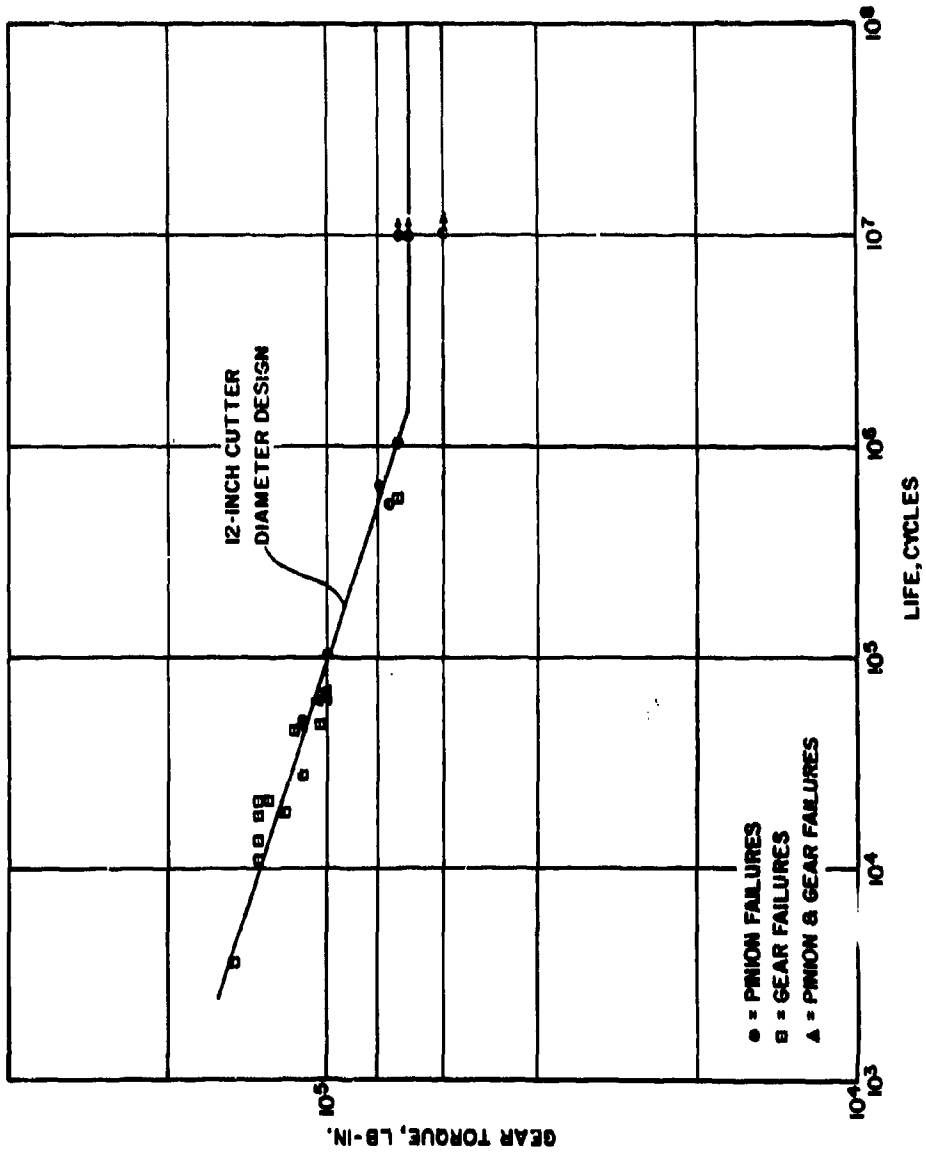


Figure 36. Gear Torque Vs Life in Cycles for Pulsing Tests on 17/51 Test Gears.

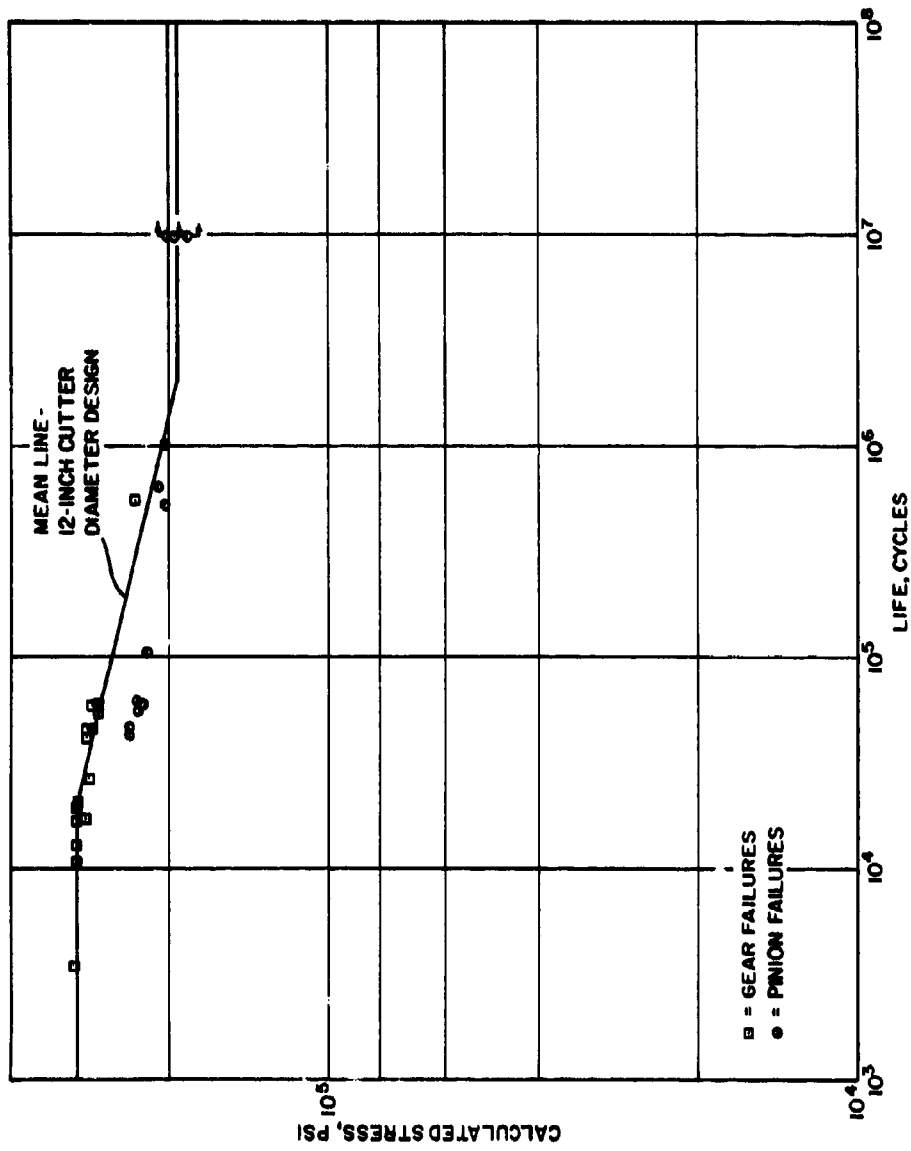


Figure 37. Calculated Bending Stress Vs Life in Cycles for Pulsing Tests on 17/51 Test Gears Using New, Improved Strength Formulas With the Size Factor Omitted.

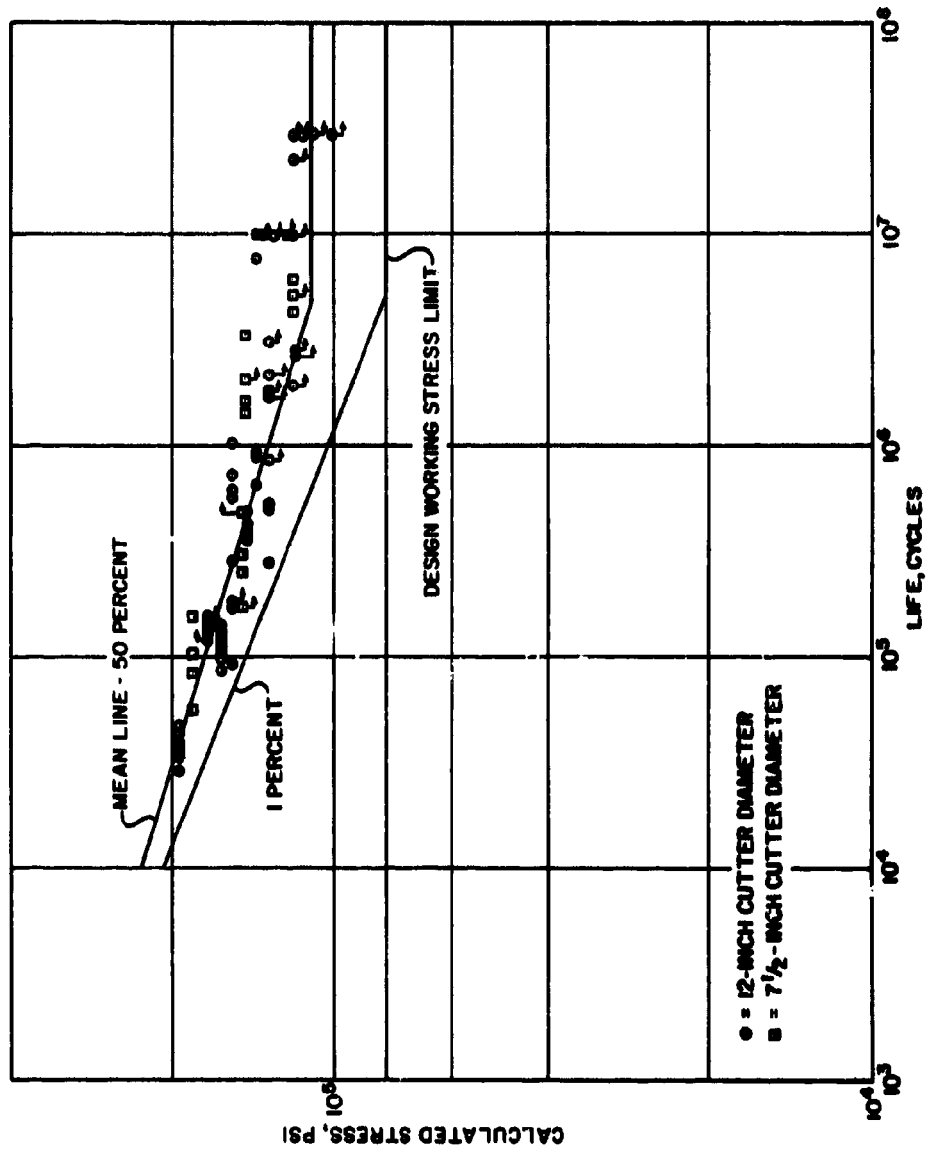


Figure 38. Calculated Bending Stress Vs Life in Cycles for Dynamic Tests on 17/51 Test Gears Using New, Improved Strength Formulas With the Old Size Factor Included.

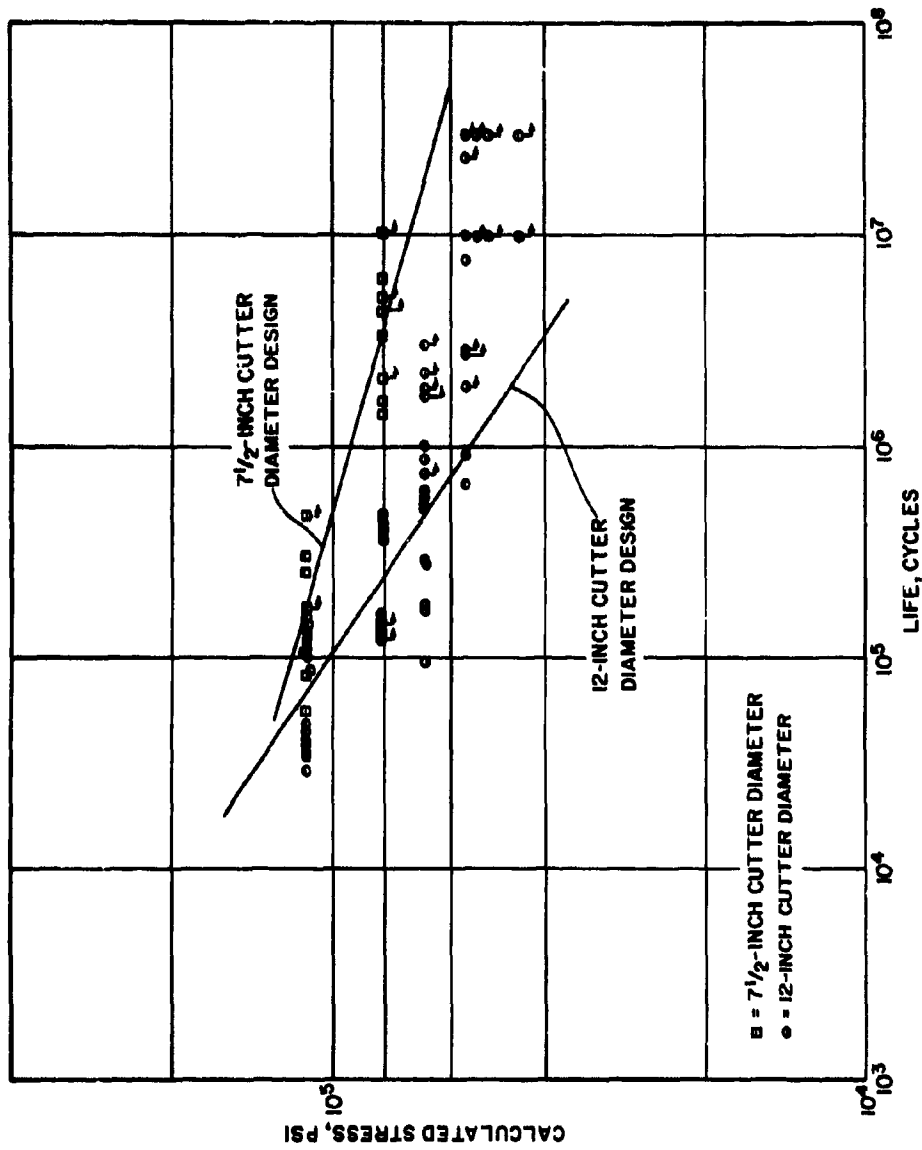


Figure 39. Calculated Bending Stress Vs Life in Cycles for Dynamic Tests on 17/51 Test Gears Using AGMA Strength Formulas With the Old Size Factor Included.

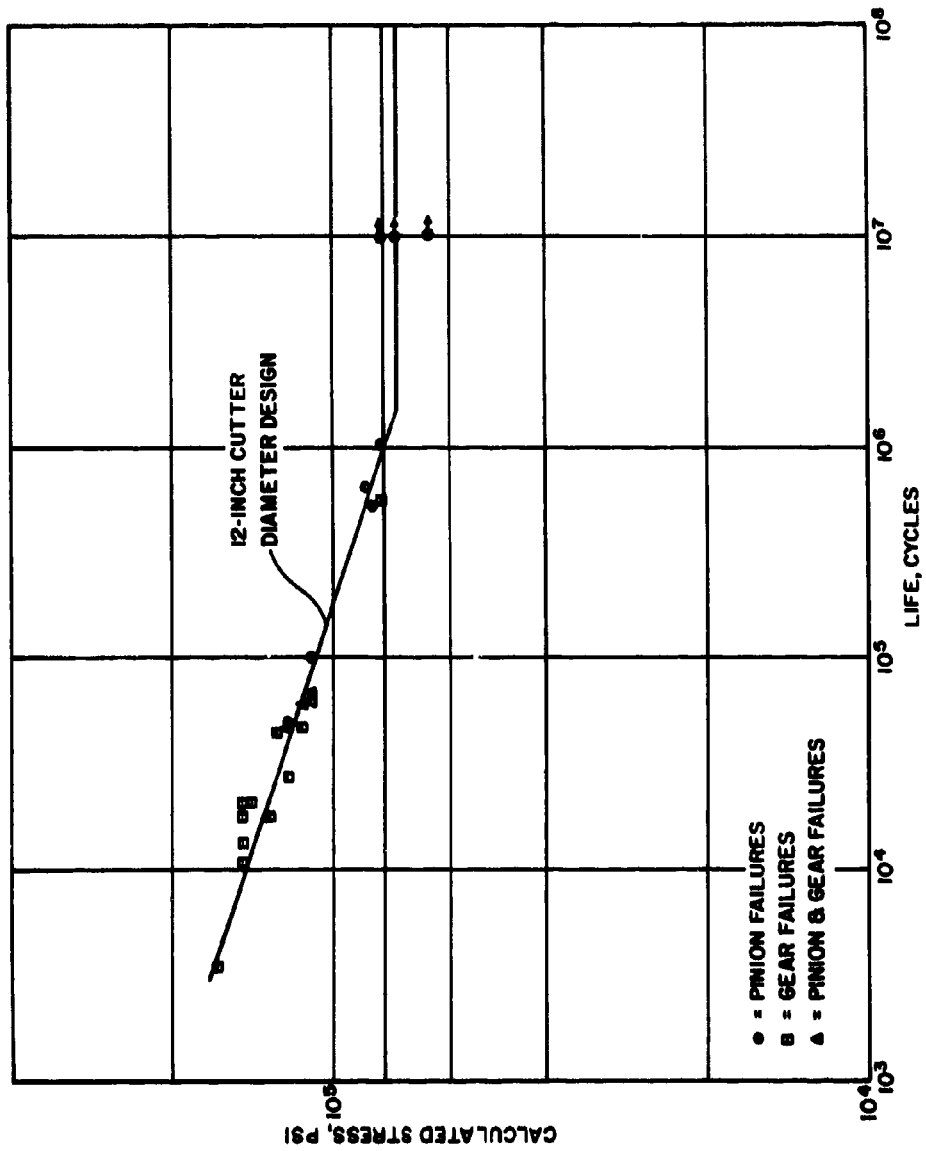


Figure 41. Calculated Bending Stress Vs Life in Cycles for Pulsing Tests on 17/51 Test Gears Using AGMA Strength Formulas With the Old Size Factor Included.

12-inch cutter diameter design. Since only one design (12-inch cutter diameter) was tested on the pulser, only one line representing the mean is shown in Figure 36.

STRESS VS LIFE DIAGRAMS

Figures 35, 38, and 39 present dynamic test data by three S-N diagrams. Figure 35 is a plot of calculated stress by the new, improved method with the size factor omitted vs the life in cycles. Note the compact grouping of the data points, outlining a well-defined slope. Figure 38 is the same plot with the size factor (AGMA method) included in the calculated stress formula. The grouping of the points is the same as that in Figure 35 but at a lower stress level. Figure 39 is a plot of the calculated stress by the AGMA method with the size factor included. There is a much greater scatter of the points on this graph and a less sharply defined slope. In addition, the calculated stresses are much lower than those shown in Figure 38.

Figures 37, 40, and 41 present similar S-N diagrams for the pulsing test results. Figure 37 is a plot of calculated stress by the new, improved method with the size factor omitted vs the life in cycles. Figure 40 is the same plot with the size factor (AGMA method) included in the calculated stress formula. The grouping of the points is the same as that in Figure 37 but at a lower stress level. Figure 41 is a plot of the calculated stress by the AGMA method with the size factor included. The shape of the S-N diagram in this last case differs from that obtained in Figures 37 and 40; there appears to be less scatter of the points. The apparent difference is explained in the next section.

TORQUE VS STRESS

When Figures 34 and 39 for the dynamic tests are compared, it will be seen that the torque and stress data points produce identical patterns. Only the value of the ordinate differs. This is because the stress is proportional to the torque with the AGMA strength formulas. A similar comparison of Figures 34 and 38 shows that the patterns are not identical. This is due to the fact that with the new, improved strength formulas the stress is no longer proportional to the torque. The non-linear increase in the peak root stress is caused by a shift in the contact pattern from the central position lengthwise along the tooth as the load changes. The amount of lengthwise shift is a function of the gear mounting rigidity and the tooth geometry. It can be clearly seen that there is much less scatter among the data points in Figure 38 than in either

Figure 34 or Figure 39. Only one geometric variable affected the test gears; namely, the two cutter diameters. This demonstrates quite conclusively why gear performances cannot be measured by the load alone. This is why the K-factor, commonly used to compare and rate spur and helical gears, is a very inadequate tool for comparing bevel gear designs.

Similarly, the comparison of Figures 36 and 41 for the pulsing tests shows identical patterns for the torque and stress data points. This is for the same reason explained in the preceding paragraph. A comparison of Figures 36 and 40 shows a greater scatter of the data points when the stresses are calculated by the new, improved method. This can be explained primarily by the fact that the mounting displacements were assumed to be the same on the pulser as in the dynamic test boxes. Since no deflection test was performed on the pulser mountings, the true displacements are not known. In addition, every effort was made to maintain the tooth contact in the same position on the tooth for all pulser tests, which would effectively reduce the mounting displacements to zero and would therefore cause the actual stresses to be proportional to the applied torque.

R. R. MOORE ANALYSIS

Ideally, the calculated gear tooth bending stress should correlate directly with the basic strength of the gear material. To provide a basis for this correlation, R. R. Moore tests were performed in order to obtain stress data pertaining to the material. These data in turn were modified to reflect the differences between the R. R. Moore test specimen and the gear tooth and between the R. R. Moore test and the gear tooth action.

Figure 42 provides this basis for reference. It is an R. R. Moore S-N diagram for 9310 vacuum-melt steel (AMS-6265), the material used in the test gears, in which the original test data, Figure 44, have been modified to incorporate the effects of

1. Single-direction bending as experienced by the gear tooth.
2. The difference in surface finish of the gear tooth fillet as compared to the R. R. Moore test specimen.

The effects of temperature, speed, and hardness remained constant for the duration of the R. R. Moore and the gear testing.

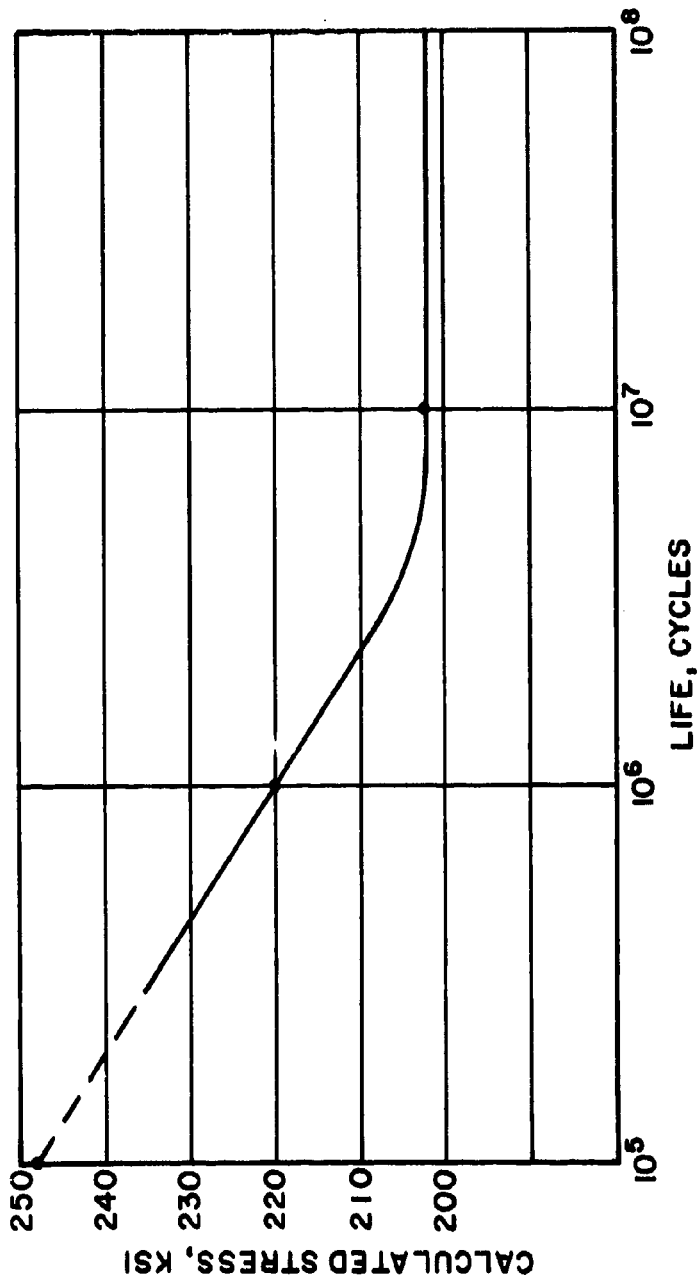


Figure 42. Bending Stress Vs Life in Cycles From the R. R. Moore Tests on AISI 9310 Vacuum-Melt Steel Corrected for Single-Direction Bending.

The true slope of this modified S-N curve is not known because there were no failures below a fatigue life of 3×10^5 cycles, but there are a sufficient number of data points to confidently establish the basic endurance limit of the material.

Effect of Single-Direction Bending

In the R. R. Moore test, the specimens are beams which rotate about their longitudinal axis while subjected to bending in a plane of the axis. Thus, the stress at any point on the surface is completely reversed during each revolution of the beam. This variation of stress is illustrated in Figure 43a. However, the loading on a gear tooth is in a single direction, as illustrated in Figure 43b. To provide the proper basis of comparison, the original R. R. Moore S-N diagram for reversed bending, Figure 44, was adjusted for single-direction bending with the use of the modified Goodman diagram, Figure 45, where the maximum stress, the ordinate, is compared to the mean stress, the abscissa.

A value of 335,000 psi was used as the ultimate strength of the material, Reference 23. This value is based on a case hardness of Rockwell C 60, the condition of the tooth surface in the root fillet where the bending fatigue failures initiated.

The single-direction line in Figure 45 was drawn from the origin with a slope of 2 since the maximum stress is twice the mean stress for gear tooth loading.

The steady-stress line in the same figure was drawn from the origin with a slope of 1 to the ultimate-stress point of 335,000 psi.

The stresses at points X, Y, and Z on the ordinate were obtained from the original R. R. Moore reverse bending curve, Figure 44, which has been repeated as curve C₁ in Figure 46. These are the stress values corresponding to life in cycles of 10^5 (200,000 psi), 10^6 (165,000 psi), and 10^7 (145,000 psi), respectively.

Three straight lines representing life of 10^5 , 10^6 , and 10^7 were then drawn from points X, Y, and Z to the ultimate-stress point (335; 335). The intersection of these cycle lines with the single-direction line establishes points X', Y', and Z' on the ordinate, which were plotted in Figure 46 as curve C₂. This curve represents the R. R. Moore data modified for single-direction bending.

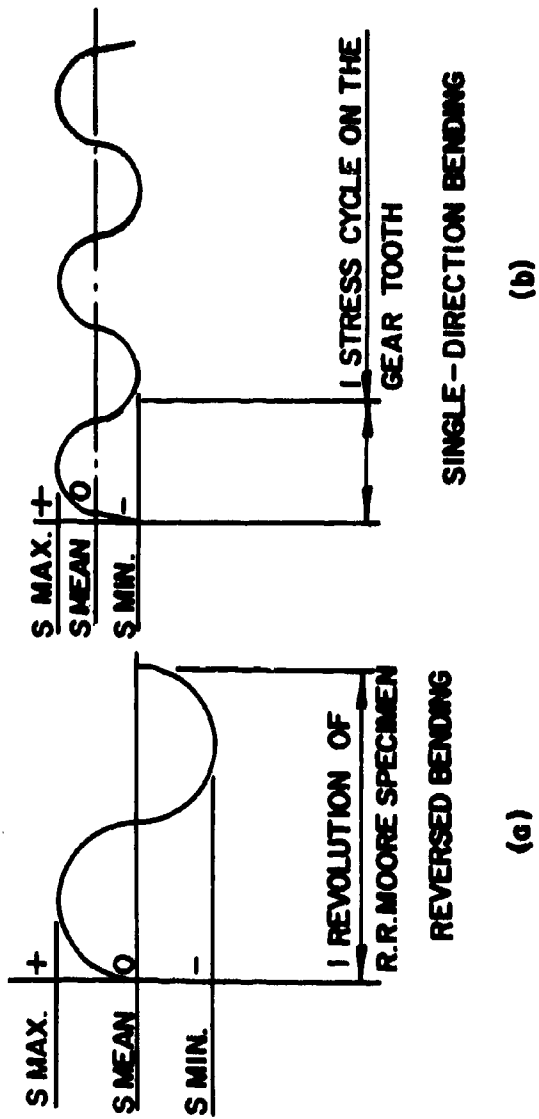


Figure 43. Diagram Showing Reverse Bending (a) and Single-Direction Bending (b).

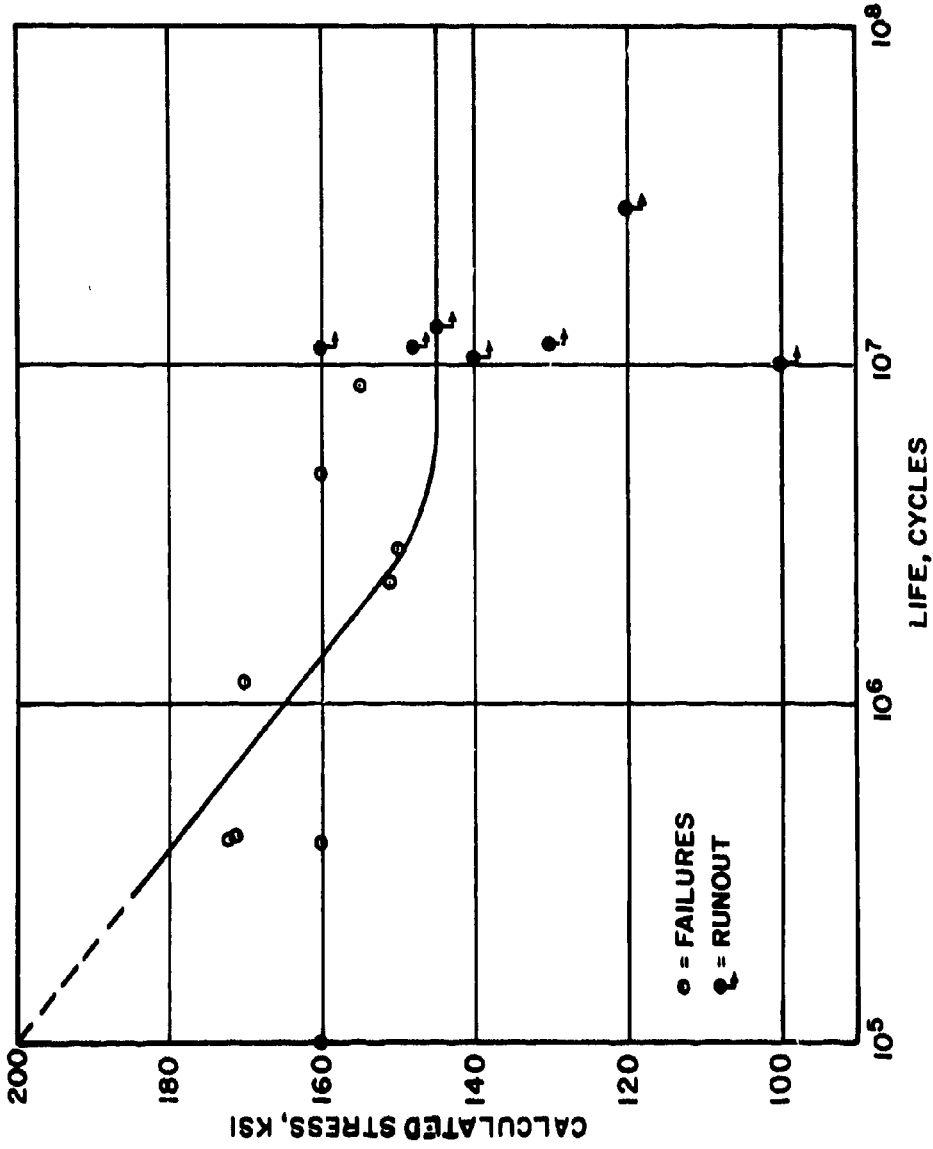


Figure 44. Bending Stress Vs Life in Cycles From R. R. Moore Tests on AISI 9310 Vacuum-Melt Steel Under Reverse Bending on a Polished Specimen.

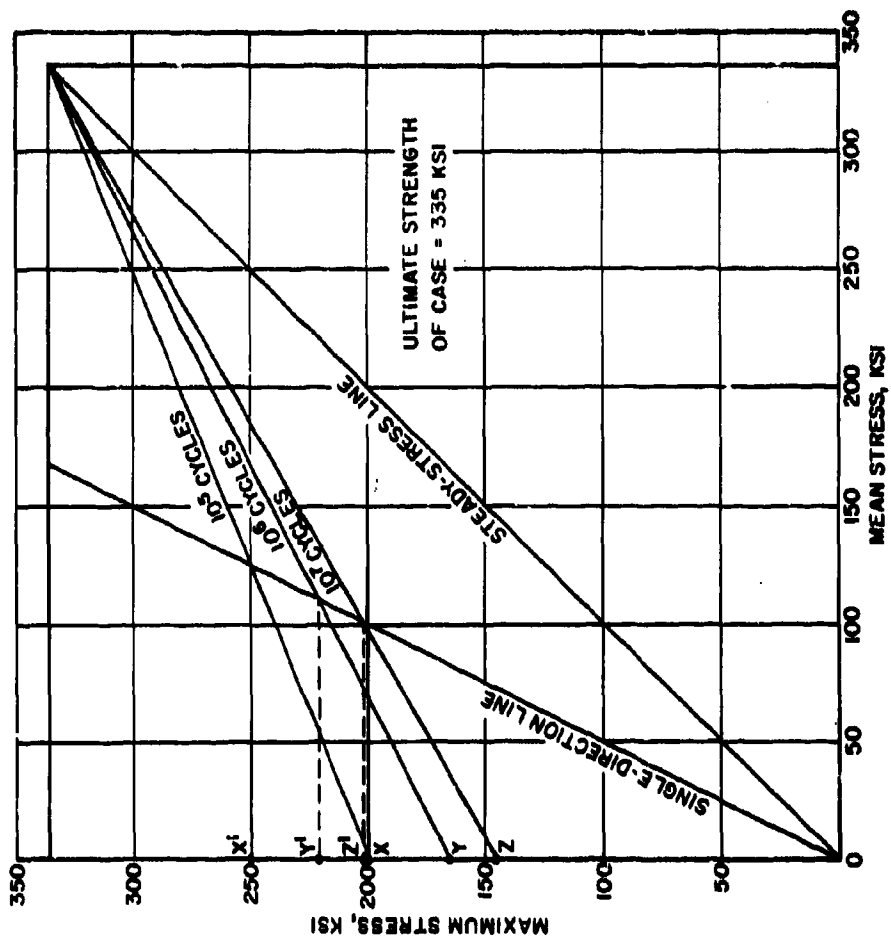


Figure 45. Modified Goodman Diagram Showing Method for Converting From Reverse Bending to Single-Direction Bending.

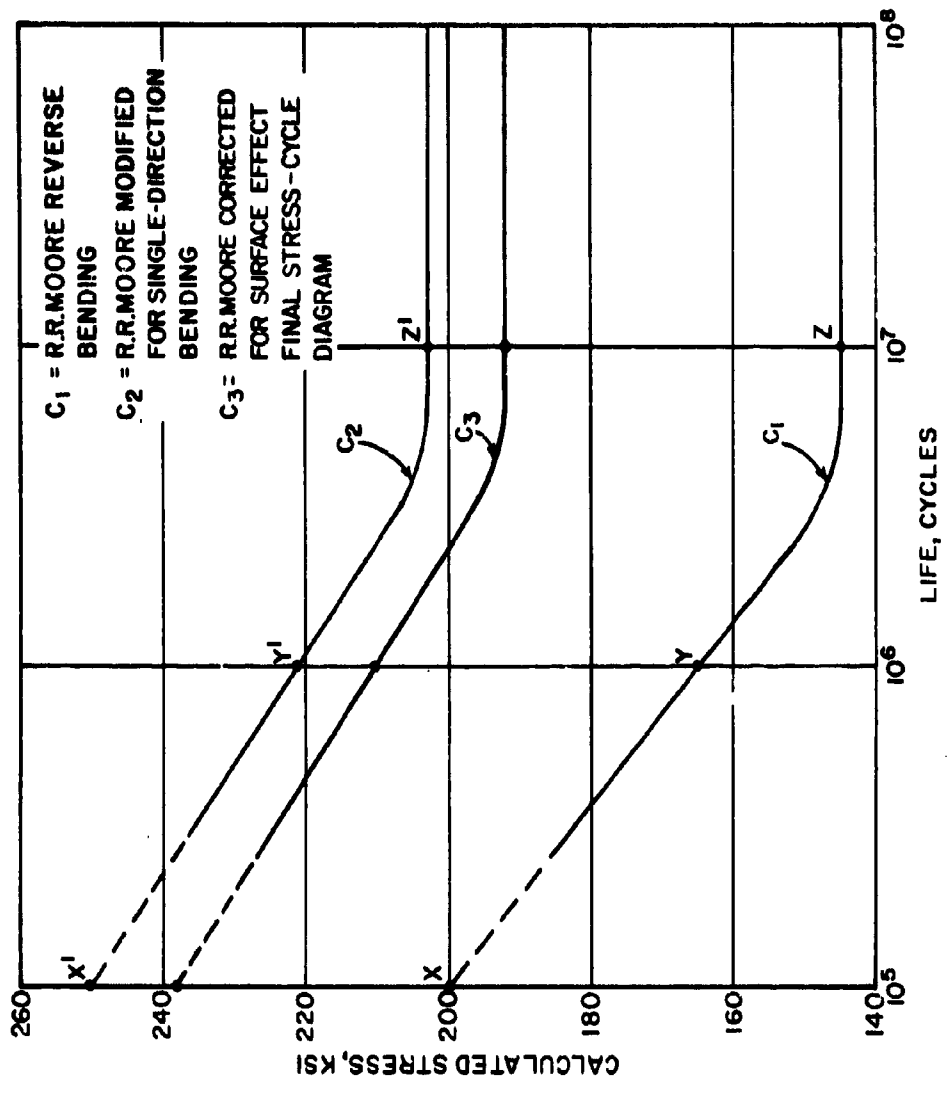


Figure 46. Bending Stress Vs Life in Cycles From the R. R. Moore Analysis.

Surface-Finish Effect

It has been recognized that fatigue life is affected by the surface finish of the stressed area. In this case, the R. R. Moore specimens were polished, whereas the gear tooth surfaces were ground. The allowable stress for a ground surface is estimated to be 95 percent of the allowable stress determined for a polished surface.

Other Effects

While it is recognized that variations in temperature, speed, and hardness have an effect on fatigue life, these factors were closely controlled during the manufacture and the tests and are considered to be constant. Therefore, these factors had no effect on the test data, and their value was set at unity in this analysis.

Final Stress-Cycle Diagram

The resulting R. R. Moore S-N curve is plotted as curve C₃ in Figure 46. It is obtained by applying the surface-finish effect, 0.95, to the allowable stress curve C₂.

Curve C₃ is the final S-N curve and represents the value of mean performance; i. e., for any stress value on this curve, 50% of the parts will have failed at the corresponding life. It is duplicated as Figure 42, the basis of reference of the gear tooth material. From this curve a mean allowable stress for the test material, AISI 9310 vacuum-melt steel (AMS-6265), was established at 192,000 psi.

COMPARISON OF R. R. MOORE AND DYNAMIC TESTS

In Table VIII the mean allowable stress from the R. R. Moore tests is 192,000 psi, Figure 42, and the mean working stress at the endurance limit will also be 192,000 psi. For the dynamic tests, Figure 35, the mean working stress at the endurance limit is 156,000 psi. However, the mean allowable stress for the test gears must be calculated using equation (5). It is rewritten here in a form for direct solution:

$$u_{at} = s_w K_T K_R K_S \quad (5a)$$

where s_w = working stress, psi

K_T = temperature factor

**TABLE VIII. ALLOWABLE STRESS VS WORKING STRESS
FOR AISI 9310 VACUUM-MELT STEEL**

Specimen	Allowable Stress(psi)		Working Stress(psi)	
	Mean	Design Limit	Mean	Design Limit
R. R. Moore*	192,000	160,000	192,000	160,000
Dynamic Test Gears**	221,000	160,000	156,000	115,000
Pulsing Test Gears**	275,000	-	194,000	-

*Mean allowable stress corrected for single-direction bending and surface-finish effects. Values taken from Figure 42.

**Values for working stress taken from Figures 35 and 37.

K_R = factor of safety

K_S = size factor

The temperature factor and factor of safety are both equal to 1.0 for the dynamic tests. The size factor for the test gears from equation (3) is 1.42. Substituting in the above equation,

$$s_{at} = 156,000 (1.0) (1.0) (1.42) = 221,000 \text{ psi mean allowable stress}$$

It will be noted that this value is somewhat above the value obtained from the R. R. Moore tests, but shows reasonable correlation between the new strength formulas and the actual stresses in the gear teeth. The difference may be partially due to the small size of the R. R. Moore specimens.

COMPARISON OF R. R. MOORE AND PULSING TESTS

The mean working stress for the pulsing tests, Figure 37, is 194,000 psi. Since the temperature factor, factor of safety, and size factor for the pulsing tests are identical with the dynamic tests using equation (5a),

$$s_{at} = 194,000 (1.0) (1.0) (1.42) = 275,000 \text{ psi mean allowable stress}$$

It will be noted that this value is approximately 45 percent higher than the R. R. Moore or dynamic test values for mean allowable stress. The explanations for the higher calculated stresses for the pulsing tests are given as follows:

1. The gear and pinion were positioned in the pulser to produce a line of contact between the gear and mating pinion, which was assumed to duplicate the position of the load in the dynamic tests when the root stress would be a maximum. It is probable that the load position selected did not produce the corresponding maximum bending stress in the root of the pulser gears. Thus, the calculated stress was undoubtedly higher than the actual stress.
2. The calculation of bending stress includes a dynamic factor. For both the dynamic tests and the pulsing tests a value of unity was used for the dynamic factor. Although it was assumed that the dynamic effects were negligible on the dynamic tests, this

can be proven only by running more extensive tests on the pulser with the position of the load varied to produce the maximum static root stress in the teeth.

EFFECT OF CUTTER DIAMETER

It was previously pointed out that when running the dynamic tests on the 12-inch and 7-1/2-inch cutter diameter designs, Figure 34, there was a pronounced difference in life between the two designs. With the present AGMA formulas, there is no difference between the stresses for the 12-inch and the 7-1/2-inch cutter diameter designs, Figure 39. But because the life of the 7-1/2-inch design greatly exceeds the life of the 12-inch design, it should be concluded that the stresses in the two designs should not be equal.

Figure 47 is a replot of Figure 35 showing only the comparative tests between the two cutter diameter designs at the two upper load levels. Also shown in Figure 47 are the mean lines for the two designs. It should be apparent that with this new, improved method of stress calculation, the difference in stresses between the 7-1/2-inch and 12-inch cutter diameter designs has resulted in bringing the two mean lines nearly into coincidence. For the first time, the effect of cutter diameter on gear tooth stress has been successfully incorporated in a bevel gear strength formula.

ENDURANCE LIMIT FOR AISI 9310 VACUUM-MELT STEEL

From Table VIII it can be seen that the mean working stress for the dynamic test gears is 156,000 psi. From Figure 35 a design working stress of 115,000 psi has been established. It is now necessary to relate this design working stress to a design allowable stress. The same procedure that was used to relate the mean working stress to the mean allowable stress can be used. Again, equation (5a) will be used with the temperature factor and factor of safety equal to 1.0, and the size factor equal to 1.42. Then,

$$s_{at} = 115,000 (1.0) (1.0) (1.42) = 163,000 \text{ psi design allowable stress}$$

In Table VIII this value has been rounded to 160,000 psi. This, then, is the endurance limit for AISI 9310 vacuum-melt steel.

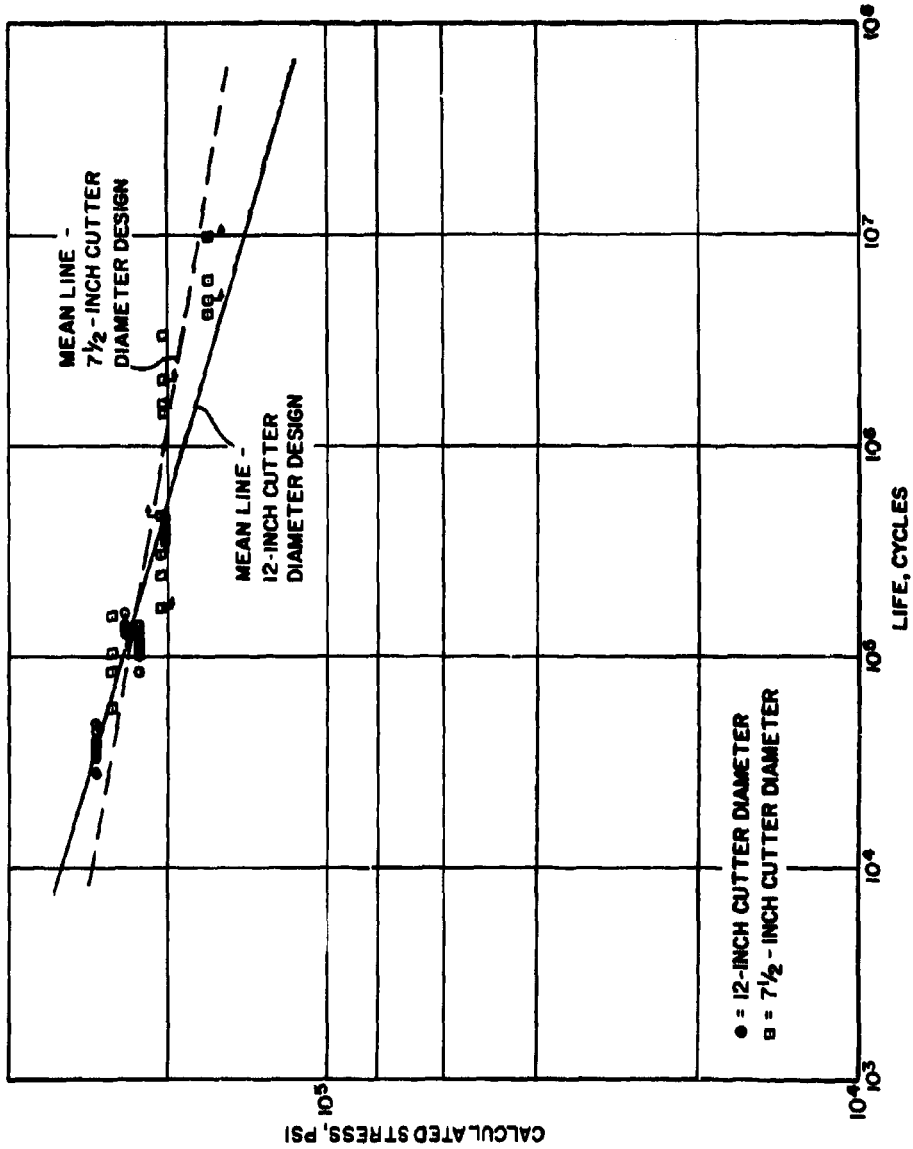


Figure 47. Comparison of the 7-1/2-Inch and 12-Inch Cutter Diameter Gear Designs at Load Levels I and II, as in Figure 35.

FATIGUE TEST DATA FROM PAST DYNAMIC TESTS

Dynamic fatigue test data accumulated by the contractor prior to the initiation of this project are plotted in Figure 48 using the new, improved strength formulas. Figure 49 shows a plot of the same data using the AGMA strength formulas. In both cases the scatter of points is considerable. There appears to be little choice between the two methods.

There is one fairly apparent reason for the wide scatter shown by the new formulas using these previous data. These formulas are based on a reasonably precise knowledge of the gear displacements under load. These gear displacement data were not available for these earlier tests. Therefore, the displacements were based on the approximate formulas contained in the computer program. Also, less attention was paid to control of variables in many of the prior tests. For these reasons, these data have limited usefulness.

ENDURANCE LIMIT FOR AIR-MELT STEEL

The data plotted in Figure 48 are for gears made from air-melt steel. A line representing the design limit for this material is included. The design working stress is approximately 45,000 psi, based on the stresses having been corrected for a 1-DP gear. This means that with the new method, a size factor of 2.0 must be used. Assuming a temperature factor and a factor of safety each equal to 1.0, the design allowable stress can be solved using equation (5a):

$$s_{at} = 45,000 (1.0) (1.0) (2.0) = 90,000 \text{ psi design allowable stress}$$

This, then, is the endurance limit for air-melt steel when used with the new, improved strength formulas. However, as pointed out in a preceding paragraph, the data for air-melt steel are not as well defined, and, therefore, this value of 90,000 psi may be on the low side.

By comparing this value with the value of 160,000 psi obtained for AISI 9310 vacuum-melt steel, it can be seen that the vacuum-melt steel gives a 78 percent increase in strength over the present design limit for normal air-melt gear steels. This is a significant improvement.

SLOPE OF THE S-N DIAGRAMS

In all three series of tests, an attempt was made to determine the slope of the S-N diagrams.

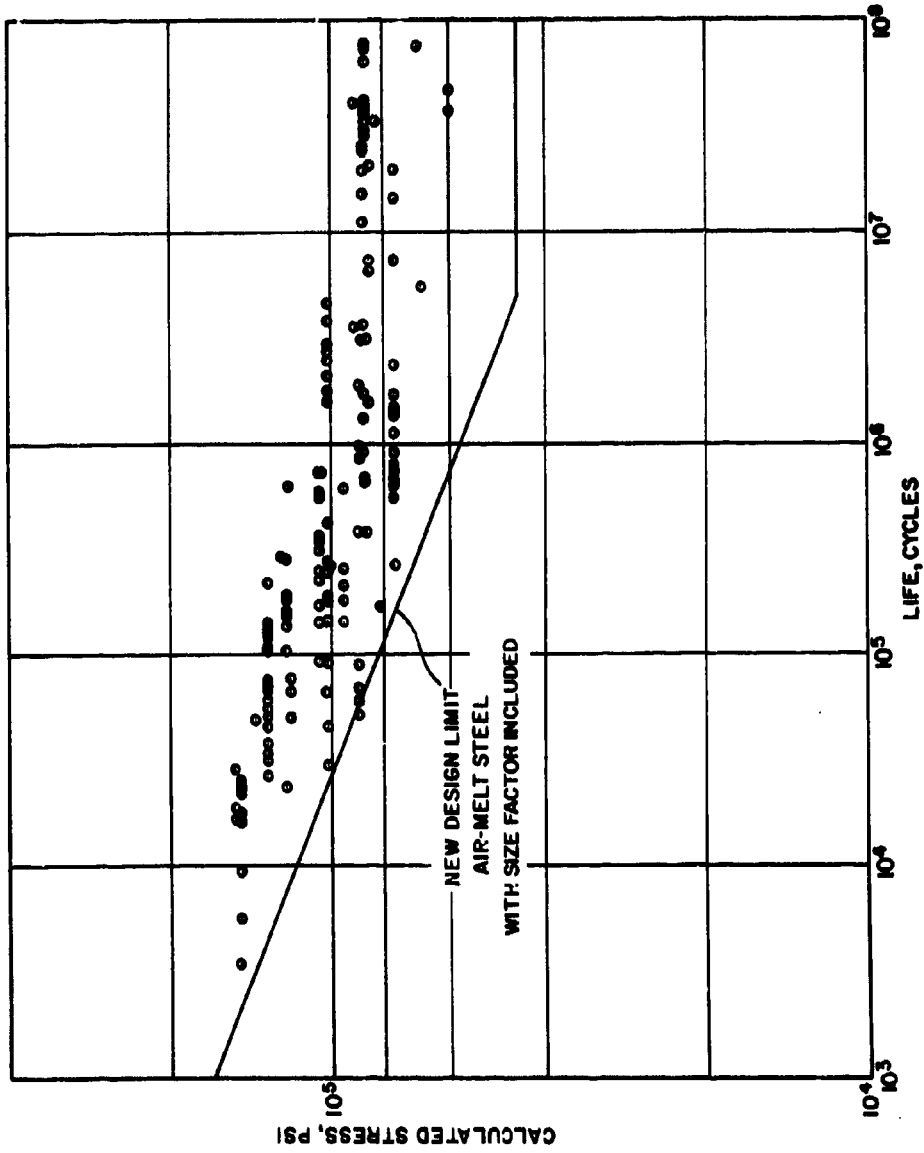


Figure 48. Calculated Bending Stress Vs Life in Cycles for Results of Previous Dynamic Tests Using the New, Improved Strength Formulas With the Old Size Factor Included.

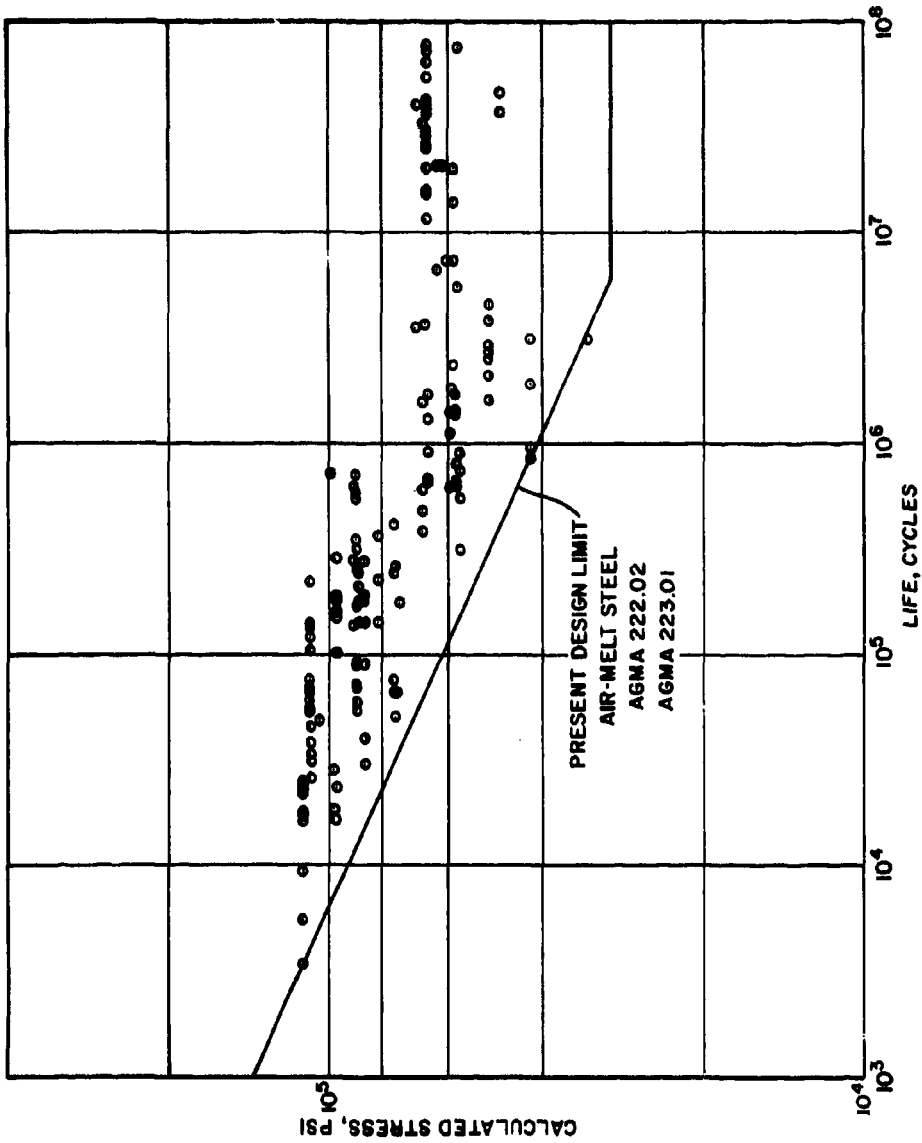


Figure 49. Calculated Bending Stress Vs Life in Cycles for Results of Previous Dynamic Tests Using the AGMA Strength Formulas With the Old Size Factor Included.

For the R. R. Moore specimens it was difficult to obtain a reliable S-N diagram due to the limitations of the test equipment. With the specimen size used for these tests, the peak stress that could be attained was approximately 170,000 psi. This is not too far above the endurance limit of 145,000 psi, Figure 44. For this reason, the portion of the S-N diagram below 3×10^5 cycles cannot be defined from the test data, and the portion between 3×10^5 cycles and 3×10^6 cycles is not well defined from the data because of the relatively wide scatter in the results. Therefore, the slope of the S-N diagram is unknown.

For the dynamic gear tests, Figure 35, the mean slope is shown extending from 10^4 cycles to approximately 5×10^6 cycles. This line has a slope of approximately 8.5. By statistical means, using log-normal, Weibull, and Weibull-hazard techniques, a 1-percent line was established. This line has a slope of approximately 6.6.

For the pulsing gear tests, Figure 37, the mean slope is shown extending from 1.7×10^4 cycles to approximately 10^6 cycles. This line has a slope of approximately 10.3, which is somewhat flatter than the mean slope obtained during the dynamic tests.

PEAK STRESS

Up to this point the emphasis in this analysis has been on the endurance limit for the gear material. However, a look at the peak stress should be taken to determine whether the values are reasonable.

For the R. R. Moore specimens, it was not possible on the existing test equipment to perform tests at the very high stress levels. In fact, very few tests were performed above the endurance limit. For this reason, the value of the peak stress was not obtained.

For the dynamic gear tests, Figure 35, gears were operated at stress levels as high as 275,000 psi. Projecting the line representing the mean slope to a life of 10^4 cycles produces a stress value of 325,000 psi. This is in close agreement with the established value for this material of 335,000 psi, Reference 23.

For the pulsing tests, Figure 37, the plotted points appear to level off at an upper limit of approximately 300,000 psi. This level is reached at a life of approximately 2×10^4 cycles. Agreement between this value for peak stress and the value of 325,000 psi obtained on the dynamic tests is quite reasonable. It might be argued that as the load level increases on the gears, the correlation between the dynamic results and

the pulsing results converges. This is not surprising, since at the higher loads the contact will tend to spread out, thereby tending to equalize the stresses along the tooth root.

An interesting observation can be made concerning the size factor at the peak stress. At the endurance limit, the mean allowable stress for the test gears did not agree with the mean allowable stress for the R. R. Moore tests until the size factor was introduced. However, at the peak stress, the mean allowable stress for both the pulsing tests, Figure 37, and the dynamic tests, Figure 35, was in close agreement with the established value of the material strength without introducing a size factor. Between the endurance limit and the peak stress it appears that there may be a variation in the size factor, which has not been considered in the computer program. Since most designs are based on the endurance limit, this omission in the computer program should not cause any inconvenience.

VALIDATION OF NEW STRENGTH FORMULA

This section of the report has attempted to substantiate the validity of the stress values obtained when using the new, improved strength formulas. It has been shown that

1. Torque vs life is not a satisfactory criterion for design.
2. Since with the AGMA method stress is proportional to torque, the AGMA method is not a completely satisfactory criterion for design.
3. The effect of cutter diameter on gear tooth strength is accounted for by the new, improved formulas for the first time.
4. The stress values resulting from the new formulas are in close agreement with the basic material strength, both at peak loads and at the endurance limit.

COMPUTER PROGRAM

One of the principal purposes of this project was to derive improved formulas for predicting the strength of bevel gears and to furnish a useable computer program which would enable a gear designer to effectively design high-capacity gear sets.

In a previous section of this report, a review has been made of new formulas that have been derived for load distribution factor, effective face width, and size factor. These formulas have been compiled into a computer program that will calculate the stresses in bevel gear teeth.

STRESS FORMULA DOCUMENTATION

The complete set of formulas required for calculating the stresses in a bevel gear tooth comprises a rather lengthy list. These formulas are documented in Appendix V along with a complete list of the letter symbols, FORTRAN symbols, and description of each. All formulas are written in terms of the letter symbols.

Basically the formulas contained in this report include all of the necessary items to calculate the geometry factor and the load distribution factor. These are the two major terms in equation (4) for bending stress. Other terms appearing in this formula are either given or assumed and must be supplied as input to the program. These other terms include the load, the factors for dynamic effects resulting from gear inaccuracies or from external causes, and the dimensions defining the size of the gears.

Finally, the formulas include the complete equations for bending stresses in gear and mating pinion and the equation for working stress.

INPUT-OUTPUT DATA

The input data to the program and the output results from the program are explained in detail in Appendix VI.

Input Data

The input data are contained on six standard 80-column cards. These include the basic design parameters, the tooth proportions, the cutter specifications, the load data and other factors concerning the quality of the gears, the suitability of the gear mountings, and the dynamic effects resulting from the nature of the external loads applied to the gears.

Output Data

The output listing includes all of the input items to the program plus the useful output results from the program. In addition to the calculated bending stresses and working stress, the output includes such items as the geometry factors, the strength factors, the load distribution factors, the contact ratios, the load sharing ratio, and certain additional gear dimensions and (assumed or given) mounting displacements due to deflections under load.

PROGRAM LISTING

The complete FORTRAN IV program listing is given in Appendix VI. This includes the listing of all special subroutines used in the program. It is based on the formulas documented in Appendix V, where an explanation of the FORTRAN symbols is given.

Operating Instructions

Operating instructions include a list of program stops and the possible causes and cures for each.

CONCLUSIONS

This program has resulted in the following conclusions:

1. A new, improved method for the stress determination of bevel gears, which is a modified form of AGMA Standards 222.02 and 223.01, was found to provide better correlation with actual gear tests and with the basic strength of the material. This modified form consists of improved formulas for the effective face width and load distribution factor, and the transfer of the size factor from the equation for calculated stress to the equation for working stress.
2. The basic material strength curve for carburized AMS-6265 was established by R. R. Moore specimens. The strength curve correlates closely with the stresses calculated by the new, improved bending strength formulas for gear teeth when appropriately modified by factors for reverse bending and surface finish.
3. A design S-N curve for AMS-6265 was established based on dynamic fatigue tests on spiral bevel gears. For design purposes, an endurance-limit stress of 160,000 psi was established for this carburized vacuum-melt steel.
4. An improved formula for effective face width was developed, which is based on an extensive previous study of the strain distribution in the root fillet of a gear tooth along its entire length under many different positions and lengths of the line of contact, and under uniform, elliptical, and parabolic load distributions.
5. The correction factor for locating the position of the point of load application has been modified to place the load nearer the center of the instantaneous line of contact. This change results in increased accuracy of the resulting stresses and in an improved strength balance between gear and mating pinion.
6. An improved formula for the load distribution factor was derived based on theoretical and experimental studies of the behavior of root fillet stresses under various concentrations of load. The effect of tooth contact shift on a bevel

gear tooth as a result of mounting deflections is of vital importance on high-capacity gearing.

7. A new formula for size factor has been introduced in the equation for working stress. This is theoretically where the size factor should appear in the design formulas rather than in the equation for calculated stress.
8. The most significant finding resulting from this program is the pronounced effect of lengthwise tooth curvature (cutter diameter) on gear tooth strength. This effect is introduced into the gear tooth strength formulas through the adjustability coefficients, which are used in determining the load distribution factor. A cutter diameter approximately equal to twice the outer cone distance times the sine of the spiral angle was found to produce a significant improvement over the "standard" cutter diameter, which is approximately equal to twice the outer cone distance.
9. A workable computer program is included for the use of the gear designer. This will provide pertinent gear design information for intelligently selecting the correct bevel gears for a given application.

LITERATURE CITED

1. Lewis, Willfred, INVESTIGATIONS OF STRENGTH OF GEAR TEETH, Proceedings of Engineers' Club of Philadelphia, Vol. 10, January 1893.
2. McMullen, F. E., and Durkan, T. M., THE GLEASON WORKS SYSTEM OF BEVEL GEARS, Machinery, June 1922.
3. THE INFLUENCE OF ELASTICITY ON GEAR-TOOTH LOADS, Progress Report No. 6 of the ASME Special Research Committee on Strength of Gear Teeth, Mechanical Engineering, August 1927.
4. Almen, J. O., FACTORS INFLUENCING DURABILITY OF SPIRAL-BEVEL GEARS FOR AUTOMOBILES, Automotive Industries, Vol. 73, November 16 and 23, 1935.
5. Almen, J. O., and Straub, J. C., FACTORS INFLUENCING THE DURABILITY OF AUTOMOBILE TRANSMISSION GEARS-PART 2, Automotive Industries, October 9, 1937.
6. Candee, Allan H., GEOMETRIC DETERMINATION OF TOOTH FORM FACTOR, AGMA Paper, October 1941.
7. Dolan, T. J., and Broghamer, E. L., A PHOTOELASTIC STUDY OF STRESSES IN GEAR TOOTH FILLETS, University of Illinois Experiment Station Bulletin, No. 335, 1942.
8. Coleman, W., IMPROVED METHOD FOR ESTIMATING THE FATIGUE LIFE OF BEVEL AND HYPOID GEARS, SAE Quarterly Transactions, Vol. 2, No. 6, April 1952.
9. Wellauer, E. J., and Seireg, A., BENDING STRENGTH OF GEAR TEETH BY CANTILEVER-PLATE THEORY, Journal of Engineering for Industry, Vol. 82, No. 3, August 1960.
10. AGMA STANDARD FOR RATING THE STRENGTH OF HELICAL AND HERRINGBONE GEAR TEETH, AGMA 221.02, September 1963.
11. Kelley, B. W., and Pedersen, R., THE BEAM STRENGTH OF MODERN GEAR-TOOTH DESIGN, SAE Transactions, Vol. 66, 1958.

12. Baxter, M. L., BASIC GEOMETRY AND TOOTH CONTACT OF HYPOID GEARS, Industrial Mathematics, Vol. 11, Part 2, 1961.
13. Baxter, M. L., EFFECT OF MISALIGNMENT ON TOOTH ACTION OF BEVEL AND HYPOID GEARS, ASME Paper 61-MD-20, May 1961.
14. Hoogenboom, L., EXPERIMENTAL STRESS ANALYSIS OF HYPOID GEAR TOOTH MODELS, MTI-66TR58, November 1966 (unpublished).
15. AGMA STANDARD FOR RATING THE STRENGTH OF STRAIGHT BEVEL AND ZEROL BEVEL GEAR TEETH, AGMA 222.02, January 1964.
16. AGMA STANDARD FOR RATING THE STRENGTH OF SPIRAL BEVEL GEAR TEETH, AGMA 223.01, January 1964.
17. TRAFÄHIGKEITSBERECHNUNG VON STIRN-UND KEGELRÄEDERN MIT AUSSENVERZÄHNUNG, DIN3990, May 1963.
18. BEVEL GEARS (MACHINE CUT), British Standard 545:1949.
19. AGMA STANDARD SYSTEM FOR SPIRAL BEVEL GEARS, AGMA 209.03, May 1964.
20. AGMA STANDARD FOR SURFACE DURABILITY (PITTING) FORMULAS FOR SPIRAL BEVEL GEAR TEETH, AGMA 216.01, January 1964.
21. AGMA DESIGN MANUAL FOR BEVEL GEARS, AGMA 330.01, August 1965.
22. AGMA GEAR CLASSIFICATION MANUAL, AGMA 390.02, September 1964.
23. METALS HANDBOOK, American Society for Metals, Vol. 1, 8th Edition, 1964.

APPENDIX I

GEAR MANUFACTURING DATA

Table IX Summary of Calculated Tooth Stresses for Pulser Gears

Table X Heat-Treatment Batch Groupings

Table XI Inspection Record of Pinions

Table XII Inspection Record of Gears

Table XIII Raw Material Examination Records

Table XIV Inspection Records for R. R. Moore Fatigue Specimens

Pinion Drawing for 7-1/2-Inch Cutter Diameter Test Gearset

Pinion Drawing for 12-Inch Cutter Diameter Test Gearset

Pinion Drawing for 12-Inch Cutter Diameter Pulser Gearset

Gear Drawing for 7-1/2-Inch Cutter Diameter Test Gearset

Gear Drawing for 12-Inch Cutter Diameter Test Gearset

Test Gear Routing Sheets

Test Pinion Routing Sheets

Ground Spiral Bevel Summary for 7-1/2-Inch Cutter Diameter Test Gears

Ground Spiral Bevel Summary for 12-Inch Cutter Diameter Test Gears

Drawing for R. R. Moore Test Specimens

R. R. Moore Specimen Routing Sheet

**TABLE IX. SUMMARY OF CALCULATED TOOTH STRESSES*
FOR PULSER GEARS**

Based on Static Loading
Dimension Sheet No. 139.887AB (Fig. 1)

Test Number	Member	Torque (in. -lb)	Calculated Bending Stress (psi)	Calculated Compressive Stress (psi)
4	Pinion	20,000	66,000	316,000
	Gear	60,000	66,100	-
5	Pinion	23,000	75,900	339,100
	Gear	69,000	76,000	-
6, 8	Pinion	24,500	80,800	349,800
	Gear	73,500	81,000	-
24	Pinion	25,500	84,100	356,900
	Gear	76,500	84,300	-
23	Pinion	26,500	87,400	363,900
	Gear	79,500	87,600	-
3	Pinion	26,700	88,000	365,000
	Gear	80,000	88,100	-
9	Pinion	33,300	109,900	407,900
	Gear	99,900	110,100	-
1, 2	Pinion	33,300	110,000	408,000
	Gear	100,000	110,200	-
10, 11	Pinion	34,500	113,800	415,300
	Gear	103,500	114,100	-
12, 13, 14	Pinion	37,000	122,100	430,000
	Gear	111,000	122,300	-
15	Pinion	38,500	127,000	438,500
	Gear	115,500	127,300	-
16	Pinion	40,000	132,000	447,000
	Gear	120,000	132,200	-
19	Pinion	43,000	141,900	463,500
	Gear	129,000	142,200	-
17, 18, 20, 22	Pinion	45,000	148,500	474,000
	Gear	135,000	148,800	-
21	Pinion	50,000	165,000	499,700
	Gear	150,000	165,300	-

*Calculated stresses in above table are based on present AGMA formulas.

TABLE X. HEAT-TREATMENT BATCH GROUPING

	Carburizing Group	Quenching Group	Serial Number
Gears	I	A	108 - 110 126, 127 130 - 132, 134 - 136
		B	103 - 107 161, 169 170, 171, 178
	II	A	119 - 132 137, 139 141, 144-147
		B	112, 114, 115, 117, 118 165 172, 173, 179, 180
Pinions	III	A	1, 3, 4, 6 - 10, 12 14, 15, 17 - 22 61, 62 69 - 73
	IV	B	26, 27, 30 - 32, 34 - 37, 39, 41, 44 - 47 65 78 - 80

TABLE XI. INSPECTION RECORD

Load Level	Part Number	Serial Number	Pitch Variation		Eccentricity (Runout)		Fillet Radius		
			Convex Side	Concave Side	Convex Side	Concave Side	Convex Side	Concave Side	
I	139887-P	8	.00015	.00013	.0006	.0006	.050	.040	
		12	.00011	.00011	.0006	.0006	.050	.040	
		3	.00038	.00010	.0005	.0008	.045	.040	
		21	.00015	.00005	.0005	.0009	.040	.040	
		34	.00019	.00009	.0007	.0009	.050	.040	
		26	.00015	.00010	.0005	.0004	.045	.040	
		37	.00010	.00013	.0010	.0006	.040	.040	
		41	.00015	.00008	.0006	.0006	.045	.040	
	139898-P	72	.00012	.00018	.0005	.0005	.040	.040	
		78	.00010	.00014	.0005	.0006	.045	.040	
		79	.00012	.00015	.0005	.0006	.045	.040	
		71	.00017	.00011	.0005	.0006	.040	.040	
	II	139887-P	6	.00011	.00012	.0003	.0006	.050	.040
			9	.00019	.00010	.0005	.0007	.040	.040
35			.00008	.00014	.0006	.0008	.050	.040	
17			.00013	.00007	.0010	.0007	.045	.040	
20			.00018	.00009	.0006	.0006	.040	.040	
27			.00006	.00009	.0006	.0007	.045	.040	
46			.00025	.00008	.0003	.0004	.050	.040	
45			.00013	.00014	.0004	.0006	.050	.040	
139898-P		69	.00015	.00017	.0004	.0005	.040	.040	
		70	.00012	.00005	.0006	.0005	.040	.040	
		73	.00011	.00016	.0007	.0006	.040	.040	
		80	.00010	.00016	.0005	.0004	.040	.040	

A

INSPECTION RECORD OF PINIONS

Quantity)	Fillet Radius		Bottom Grind Stock by Blank Checker			Tooth Thickness at Midface			Grind Stock on Each Side of Tooth	
			Depth Check		Total Grind Stock	Before Grind	After Grind Convex Side	After Grind Concave Side	Convex Side	Concave Side
	Convex Side	Concave Side	Before Grind	After Grind						
.0006	.050	.040	+.001	-.003	.004	.373	.368	.362	.005	.006
.0006	.050	.040	+.002	-.003	.005	.369	.365	.361	.004	.004
.0008	.045	.040	+.002	.000	.002	.376	.364	.360	.012	.004
.0009	.040	.040	+.004	-.003	.007	.374	.365	.362	.009	.003
.0009	.050	.040	+.003	+.002	.001	.372	.365	.363	.007	.002
.0004	.045	.035	+.002	+.001	.001	.373	.364	.362	.009	.002
.0006	.040	.040	+.005	.000	.005	.372	.367	.363	.005	.004
.0006	.045	.040	+.003	.000	.003	.372	.365	.363	.007	.002
.0005	.040	.040	+.004	.000	.004	.379	.368	.361	.011	.007
.0006	.045	.045	+.003	.000	.003	.379	.370	.360	.009	.010
.0006	.045	.040	+.003	-.001	.004	.380	.367	.362	.013	.005
.0006	.040	.040	+.005	+.001	.004	.378	.369	.358	.009	.011
.0006	.050	.040	.000	-.003	.003	.372	.366	.363	.006	.003
.0007	.040	.040	+.002	.000	.002	.372	.368	.362	.004	.006
.0008	.050	.030	+.001	.000	.001	.372	.366	.364	.006	.002
.0007	.045	.040	+.001	.000	.001	.373	.367	.363	.006	.004
.0006	.040	.040	+.001	-.001	.002	.373	.366	.362	.007	.004
.0007	.045	.040	+.003	.000	.003	.373	.363	.360	.010	.003
.0004	.050	.040	+.001	+.001	.000	.373	.366	.366	.007	.000
.0006	.050	.040	+.002	.000	.002	.375	.366	.364	.009	.002
.0005	.040	.040	+.004	.000	.004	.378	.367	.360	.011	.007
.0005	.040	.045	+.004	.000	.004	.379	.369	.360	.010	.009
.0006	.040	.040	+.006	-.001	.007	.379	.369	.360	.010	.009
.0004	.040	.040	+.005	-.001	.006	.379	.367	.360	.012	.007

B

TABLE XI - Continued

Load Level	Part Number	Serial Number	Pitch Variation		Eccentricity (Runout)		Fillet Radius	
			Convex Side	Concave Side	Convex Side	Concave Side	Convex Side	Concave Side
III	139887-P	7	.00011	.00012	.0005	.0008	.040	.040
		31	.00005	.00009	.0004	.0007	.040	.040
		18	.00012	.00007	.0008	.0008	.045	.045
		22	.00031	.00012	.0005	.0005	.045	.045
		36	.00010	.00008	.0005	.0008	.040	.040
		32	.00006	.00012	.0005	.0010	.050	.050
		39	.00012	.00009	.0005	.0008	.050	.050
47	.00017	.00010	.0005	.0008	.050	.050		
IV	139887-P	1	.00011	.00010	.0004	.0006	.050	.050
		19	.00008	.00015	.0006	.0007	.050	.050
		4	.00025	.00010	.0006	.0010	.050	.050
		10	.00038	.00007	.0006	.0007	.040	.040
		14	.00010	.00010	.0007	.0010	.045	.045
		15	.00016	.00008	.0004	.0006	.045	.045
		30	.00024	.00014	.0007	.0010	.040	.040
44	.00015	.00009	.0005	.0004	.045	.045		
Pulser	139887-PP	61	.00011	.00012	.0006	.0007	.050	.050
		62	.00013	.00006	.0005	.0004	.050	.050
		65	.00012	.00005	.0006	.0005	.050	.050

All measurements in inches.
 Part Numbers 139887-P and 139887-PP (12" DC)
 Part Number 139898-P (7.5" DC)

TABLE XI - Continued

Quantity (Concave Side)	Fillet Radius Convex Side Concave Side		Bottom Grind Stock by Blank Checker			Tooth Thickness at Midface			Grind Stock on Each Side of Tooth	
			Depth Check Before Grind	After Grind	Total Grind Stock	Before Grind	After Grind Convex Side	After Grind Concave Side	Convex Side	Concave Side
0008	.040	.040	+.002	+.001	.001	.374	.368	.363	.006	.005
0007	.040	.040	+.004	-.001	.005	.372	.365	.364	.007	.001
0008	.045	.040	+.004	-.004	.008	.374	.364	.360	.010	.004
0008	.045	.040	+.003	+.001	.002	.374	.368	.365	.006	.003
0008	.040	.040	.000	.000	.000	.374	.368	.363	.006	.005
0010	.050	.040	+.002	+.001	.001	.370	.362	.362	.008	.000
0008	.050	.040	.000	.000	.000	.373	.368	.363	.005	.005
0008	.050	.040	+.001	+.001	.000	.373	.365	.362	.008	.003
0006	.050	.035	+.001	-.003	.004	.371	.367	.363	.004	.004
0007	.050	.040	+.003	-.002	.005	.371	.367	.362	.006	.005
0010	.050	.040	+.003	-.001	.004	.375	.365	.362	.010	.003
0007	.040	.040	+.003	+.001	.002	.374	.365	.362	.009	.003
0010	.045	.040	+.001	-.005	.006	.373	.365	.360	.008	.005
0006	.045	.040	+.003	+.002	.001	.375	.368	.364	.007	.004
0010	.040	.040	+.001	.000	.001	.372	.365	.362	.007	.003
0004	.045	.040	+.001	+.001	.000	.373	.364	.362	.009	.002
0007	.050	.040	+.003	-.003	.006	.369	.365	.363	.004	.002
0004	.050	.040	+.004	-.003	.007	.370	.366	.363	.004	.003
0005	.050	.040	+.003	-.002	.005	.369	.366	.363	.003	.003

B

TABLE XII. INSPECTION RECORD

Load Level	Part Number	Serial Number	Pitch Variation		Eccentricity (Runout)	Fillet Radii		
			Concave Side	Convex Side		Concave Side	Convex Side	
I	139887-G	108	.00018	.00011	.0006	.080		
		112	.00011	.00011	.0010	.080		
		103	.00016	.00011	.0005	.080		
		121	.00006	.00018	.0006	.080		
		134	.00011	.00012	.0007	.085		
		126	.00016	.00014	.0006	.080		
		137	.00015	.00017	.0005	.080		
		141	.00018	.00016	.0004	.080		
	139898-G	172	.00020	.00020	.0005	.080		
		178	.00016	.00020	.0005	.080		
		179	.00020	.00015	.0003	.080		
		171	.00025	.00018	.0005	.075		
	II	139887-G	106	.00012	.00015	.0005	.080	
			109	.00012	.00005	.0005	.080	
135			.00017	.00013	.0006	.080		
117			.00017	.00005	.0007	.080		
120			.00013	.00014	.0007	.085		
127			.00024	.00016	.0005	.085		
146			.00018	.00017	.0006	.080		
145			.00012	.00013	.0005	.080		
139898-G		169	.00020	.00021	.0007	.080		
		170	.00011	.00020	.0007	.080		
		173	.00020	.00023	.0007	.080		
		180	.00021	.00017	.0006	.075		

A

INSPECTION RECORD OF GEARS

Electricity (out)	Fillet Radius		Bottom Grind Stock by Blank Checker			Tooth Thickness at Midface		Grind Stock Total for Both Sides
	Concave Side	Convex Side	Depth Check		Total Grind Stock	Before Grind	After Grind	
			Before Grind	After Grind				
006	.080	.080	+.004	-.002	.006	.205	.191	.014
010	.080	.080	+.005	+.001	.004	.205	.190	.015
005	.080	.085	+.004	-.003	.007	.206	.192	.014
006	.080	.080	+.005	.000	.005	.205	.192	.013
007	.085	.085	+.003	-.003	.006	.203	.190	.013
006	.080	.080	+.003	-.004	.007	.203	.189	.014
005	.080	.080	+.004	-.001	.005	.205	.190	.015
004	.080	.080	+.004	-.003	.007	.201	.188	.013
005	.080	.080	+.008	+.001	.007	.203	.189	.014
005	.080	.080	+.010	+.001	.009	.204	.191	.013
003	.080	.080	+.008	+.001	.007	.204	.188	.016
005	.075	.075	+.008	+.005	.003	.204	.190	.014
005	.080	.080	+.005	-.003	.008	.202	.188	.014
005	.080	.085	+.004	-.003	.007	.204	.190	.014
006	.080	.085	+.002	-.004	.006	.203	.190	.013
007	.080	.080	+.005	.000	.005	.205	.190	.015
007	.085	.085	+.006	-.003	.009	.205	.189	.016
005	.085	.085	+.003	-.001	.004	.206	.190	.016
006	.080	.080	+.005	-.002	.007	.205	.190	.015
005	.080	.085	+.007	-.002	.009	.205	.188	.017
007	.080	.080	+.008	+.003	.005	.205	.191	.014
007	.080	.080	+.010	+.001	.009	.204	.190	.014
007	.080	.080	+.008	+.002	.006	.205	.191	.014
006	.075	.080	+.008	+.001	.007	.205	.191	.014

B

TABLE XII - Continue

Load Level	Part Number	Serial Number	Pitch Variation		Eccentricity (Runout)	Fillet Radii	
			Concave Side	Convex Side		Concave Side	Convex Side
III	139887-G	107	.00012	.00010	.0006	.085	.085
		131	.00023	.00013	.0003	.085	.085
		118	.00018	.00009	.0005	.085	.085
		122	.00015	.00012	.0006	.080	.080
		136	.00020	.00016	.0004	.085	.085
		132	.00021	.00011	.0006	.080	.080
		139	.00012	.00013	.0008	.085	.085
		147	.00012	.00009	.0006	.080	.080
		104	.00015	.00012	.0005	.080	.080
IV	139887-G	105	.00029	.00011	.0006	.085	.085
		119	.00013	.00000	.0005	.085	.085
		110	.00010	.00016	.0005	.085	.085
		114	.00012	.00011	.0007	.085	.085
		115	.00017	.00010	.0005	.080	.080
		130	.00010	.00007	.0006	.085	.085
		144	.00020	.00020	.0006	.080	.080
Pulser	139887-G	161	.00020	.00020	.0005	.085	.085
		165	.00014	.00007	.0005	.085	.085

All measurements in inches.

Part Number 139887-G (12" DC)

Part Number 139898-G (7.5" DC)

A

TABLE XII - Continued

City	Fillet Radius		Bottom Grind Stock by Blank Checker			Tooth Thickness at Midface		Grind Stock Total for Both Sides
	Concave Side	Convex Side	Depth Check		Total Grind Stock	Before Grind	After Grind	
			Before Grind	After Grind				
	.085	.080	+.004	-.002	.006	.203	.190	.013
	.085	.080	+.002	-.003	.005	.203	.188	.015
	.085	.080	+.004	-.002	.006	.201	.190	.011
	.080	.080	+.003	-.001	.004	.205	.192	.013
	.085	.080	+.001	-.003	.004	.202	.190	.012
	.080	.080	+.003	-.001	.004	.203	.190	.013
	.085	.085	+.006	-.003	.009	.205	.188	.017
	.080	.080	+.006	.000	.006	.205	.190	.015
	.080	.080	+.004	-.002	.006	.205	.191	.014
	.085	.080	+.004	.000	.004	.204	.190	.014
	.085	.080	+.005	-.003	.008	.202	.190	.012
	.085	.085	+.004	-.002	.006	.204	.191	.013
	.085	.085	+.006	-.003	.009	.204	.187	.017
	.080	.085	+.005	-.003	.008	.203	.191	.012
	.085	.085	+.003	-.003	.006	.203	.189	.014
	.080	.080	+.006	.000	.006	.204	.191	.013
	.085	.085	+.003	.000	.003	.203	.190	.013
	.085	.080	+.005	.000	.005	.205	.189	.016

B

TABLE XIII. RAW MATERIAL EXAMINATION RECORDS

		<u>Pinions</u>							
Material Specification	AMS-6265B (AISI 9310-CVM)								
Suppliers Heat No.	23138								
Material Size	90 Weldless Hammered Stem Forgings								
Chemical Analysis									
	C	Mn	P	S	Si	Cr	Ni	Mo	
	.09	.75	.010	0.006	.28	1.35	3.34	.11	
Hardness	BHN 196-228								
Grain Size	6 - 8								
Forging Lines	O.K.								
Hardenability	1/38 6/37								
Jerkontoret (JK) rating									
Inclusion Type	A		B		C		D		
Inclusion Size	Thin	Thick	Thin	Thick	Thin	Thick	Thin	Thick	
	0	0	0	0	0	0	1	0	
Inclusion Content	Material conforms to AMS 2300 Magnaflux F-O, S-O								
		<u>Gears</u>							
Material Specification	AMS-6265B (AISI 9310-CVM)								
Suppliers Heat No.	23138								
Material Size	90 12-5/8" OD x 8" ID x 1-7/8" thick rings								
Chemical Analysis									
	C	Mn	P	S	Si	Cr	Ni	Mo	
	.08	.66	.007	.006	.30	1.34	3.42	.13	
Hardness	BHN 196-217								
Grain Size	6-8								
Forging Lines	O.K.								
Hardenability	1/39 6/38 Quenched from 1500°F								
Jerkontoret (JK) rating									
Inclusion Type	A		B		C		D		
Inclusion Size	Thin	Thick	Thin	Thick	Thin	Thick	Thin	Thick	
	0	0	0	0	0	0	1	0	
Inclusion Content	Magnaflux F-O, S-O								

TABLE XIV. INSPECTION RECORDS FOR
R. R. MOORE FATIGUE SPECIMENS*

Serial Number	Support Bearing Diameters**		Gage Section		
	Right End	Left End	Middle Diameter**	Deviation From 5" Radius**	Surface Finish (rms)
10	.4796	.4793	.2060	+.0010	1.5
12	.4798	.4793	.2071	+.0010	1.5
14	.4796	.4795	.2080	+.0015	2.0-2.5
8	.4797	.4797	.2085	+.0010	1.0-1.5
1	.4797	.4790	.2084	+.0010	1.0
5	.4797	.4796	.2085	+.0015	1.0-1.5
15	.4790	.4790	.2084	+.0010	1.0-1.5
13	.4800	.4795	.2085	+.0010	1.5-2.0
2	.4798	.4795	.2085	+.0010	1.0-1.5
4	.4795	.4793	.2085	+.0010	1.0
3	.4790	.4790	.2076	+.0010	1.0-1.5
11	.4800	.4795	.2085	+.0015	1.5
16	.4790	.4790	.2090	+.0010	1.0-1.5
6	.4810	.4796	.2085	+.0010	1.0-1.5
9	.4794	.4793	.2085	+.0010	1.0-1.5
7	.4797	.4792	.2084	+.0010	1.0-1.5

*Part Number FESP-1
**Dimensions in inches

GROUND SPIRAL BEVEL PINION

INSPECTION DATA
 AGMA QUALITY NO. _____ 13
 RUNOUT TOLERANCE _____ .0007
 PITCH TOLERANCE _____ .0002
 NORMAL CHORDAL ADDENDUM (MEAN) _____ .261
 NORMAL CHORDAL TOOTH THICKNESS (MEAN) _____ .356-.361
 NORMAL BACKLASH AT TIGHTEST POINT OF MESH AT SPECIFIED MOUNTING DISTANCE _____ .006-.008
 WHOLE DEPTH _____ .421-.424

AIRCRAFT QUALITY
 100% INSPECTION REQ'D

DIAMETERS "A" AND "E" MUST BE CONCENTRIC WITH EACH OTHER WITHIN .0002 T.I.R.
 SURFACES "X" AND "Y" MUST BE PAIR WITH EACH OTHER WITHIN .0002 SQUARE WITH DIAMETERS "A" AND "E" WITHIN .0002

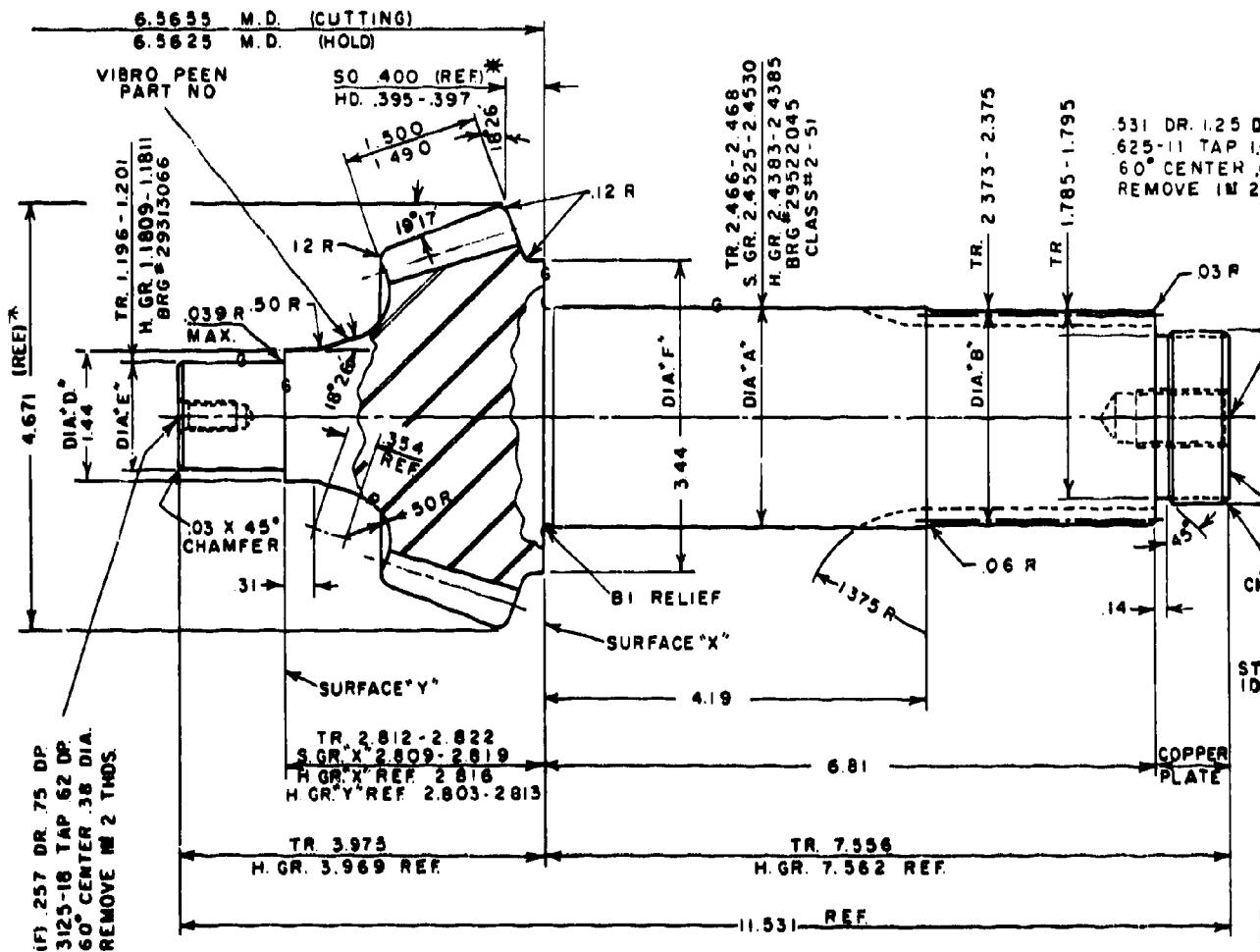


Figure 50. Pinion Drawing for 7-1/2-Inch Cutter Diameter Test Gear Set.

DN

AIRCRAFT QUALITY
100% INSPECTION REQ'D

AND "E" MUST BE
WITH EACH OTHER
T.I.R.

AND "Y" MUST BE PARALLEL
OTHER WITHIN .0002" AND
DIAMETERS "A" AND "E"

BEVEL GEAR DATA

NUMBER OF TEETH _____ 17
 PITCH (DP) _____ (REF) 4.080
 PITCH DIAMETER (THEORETICAL) _____ 4.167
 PITCH ANGLE _____ (REF) 18° 26'
 SHAFT ANGLE _____ - 90°
 PRESSURE ANGLE _____ (REF) 20°
 SPIRAL ANGLE _____ (REF) 35°
 HAND OF SPIRAL _____ L.H.
 DRIVER OR DRIVEN _____ DRIVER
 DIRECTION OF ROTATION _____ C.W.

TOOTH FILLET CURVE _____ .040 MIN. RAD
 PART NO. OF MATE _____ 139898-G
 NUMBER OF TEETH IN MATE _____ 51
 SUMMARY NO. _____ (71 Dg) 139.898

MATERIAL: AMS 6265 B
 COPPER PLATE THDS. AS SHOWN
 CASE .045-.055 EFFECTIVE-ROOT
 REHEAT 1550°F
 DRAW 350°F
 CORE HARDNESS R_c 34-38
 CASE HARDNESS R_c 60 MIN.
 TEST PIECES REQ'D
 FORGINGS TO TEST BRIN. 228 MAX.
 STRESS RELIEVE AT 325°F AFTER
 FINISH GRINDING TEETH

EXTERNAL SPLINE DATA

FILLET ROOT _____ SIDE-FIT
 NO. OF TEETH _____ 18
 PITCH _____ (REF) 8/16
 PITCH DIAMETER (THEO) _____ 2.250
 PRESSURE ANGLE (REF) _____ 30° INV.
 MEASURING PIN DIA. _____ 2.40
 DIM. OVER 2 PINS. _____ 2.616-2.619
 HOB NO. _____ HB 552-1

NOTES ON MACHINING

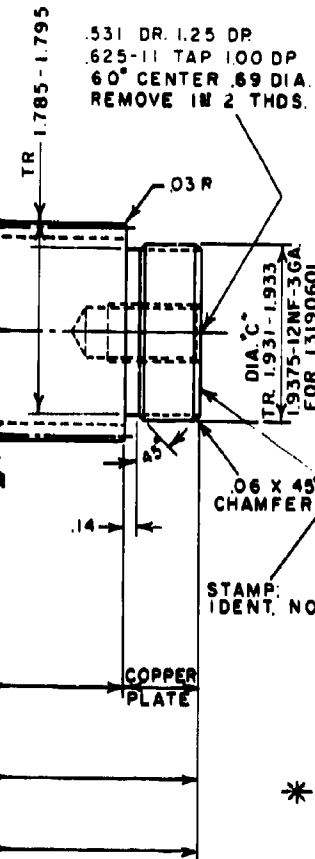
1. LIMITS ON FINISH DIMENSIONS ARE .010 INCH UNLESS OTHERWISE SPECIFIED
2. BREAK ALL SHARP CORNERS
3. ROUND ALL TOOTH EDGES
4. ROUND ALL KEYWAY AND SPLINE ENDS

BLACK OXIDE COAT PER AMS 2485 D

PART NO. 139898-P

* MANUFACTURE AND INSPECT TO STD. BLANK TOLERANCES FOR GLEASON BLANK CHECKER

MAGNAFLUX INSPECT
NITAL ETCH



B

GROUND SPIRAL BEVEL PINION

AGMA QUALITY NO. _____ 13
 RUNOUT TOLERANCE _____ .0007
 PITCH TOLERANCE _____ .0002
 NORMAL CHORDAL ADDENDUM (MEAN) _____ .260
 NORMAL CHORDAL TOOTH THICKNESS (MEAN) _____ .356-.361
 NORMAL BACKLASH AT TIGHTEST POINT OF MESH AT SPECIFIED MOUNTING DISTANCE _____ .006-.008
 WHOLE DEPTH _____ .463-.466

AIRCRAFT QUALITY
 100% INSPECTION REQD

DIAMETERS "A" AND "E" MUST BE CONCENTRIC WITH EACH OTHER WITHIN .002 T.I.R.
 SURFACES "X" AND "Y" MUST BE PARALLEL WITH EACH OTHER WITHIN .0002 ANGLE SQUARE WITH DIAMETERS "A" AND "E" WITHIN .0002

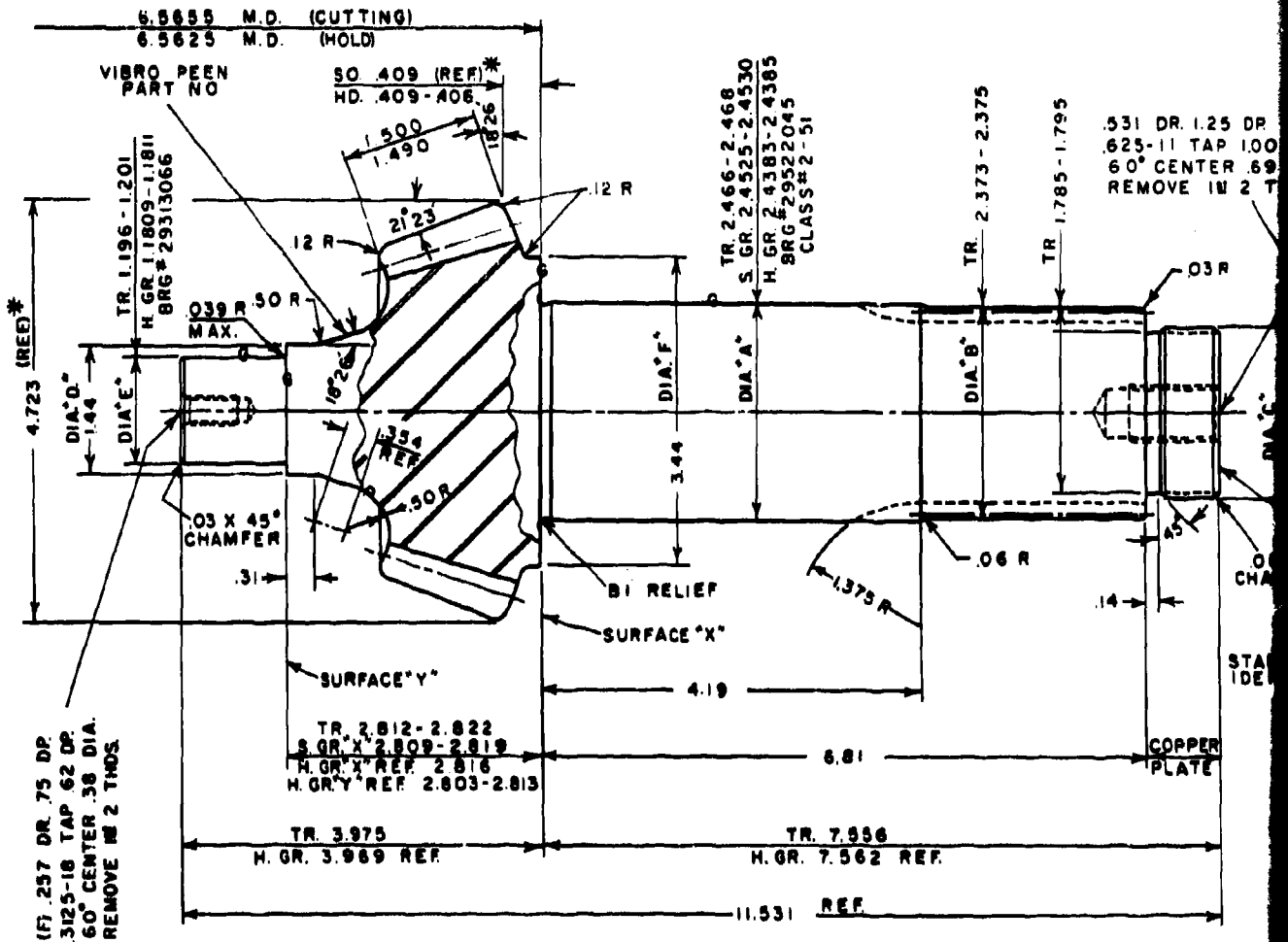


Figure 51. Pinion Drawing for 12-Inch Cutter Diameter Test Gear Set.

A

ION

AIRCRAFT QUALITY
100% INSPECTION REQ'D

"A" AND "E" MUST BE
WITH EACH OTHER
0.02 T.I.R.
"B" AND "Y" MUST BE PARALLEL
OTHER WITHIN .0002" AND
TH DIAMETERS "A" AND "E"
0.02

BEVEL GEAR DATA

NUMBER OF TEETH _____ 17
 PITCH (DP) _____ (REF) 4.080
 PITCH DIAMETER (THEORETICAL) 4.167
 PITCH ANGLE _____ (REF) 18° 26'
 SHAFT ANGLE _____ 90° 00'
 PRESSURE ANGLE _____ (REF) 20°
 SPIRAL ANGLE _____ (REF) 35°
 HAND OF SPIRAL _____ L.H.
 DRIVER OR DRIVEN _____ DRIVER
 DIRECTION OF ROTATION _____ C.W.

TOOTH FILLET CURVE _____ 040 MIN. RAD.
 PART NO. OF MATE _____ 139887-G
 NUMBER OF TEETH IN MATE _____ 51
 SUMMARY NO. _____ (120c) 139.887
 MATERIAL: AMS 6265 B
 COPPER PLATE THDS AS SHOWN
 CASE .045-.055 EFFECTIVE-ROOT
 REHEAT 1550°F
 DRAW 350°F
 CORE HARDNESS Rc 34-38
 CASE HARDNESS Rc 60 MIN.
 TEST PIECES REQ'D
 FORGINGS TO TEST BRIN 228 MAX.
 STRESS RELIEVE AT 325°F AFTER
 FINISH GRINDING TEETH

EXTERNAL SPLINE DATA

FILLET ROOT _____ SIDE-FIT
 NO OF TEETH _____ 18
 PITCH _____ (REF) 8/16
 PITCH DIAMETER (THEO) 2.250
 PRESSURE ANGLE (REF) 30° INV.
 MEASURING PIN, DIA. _____ 240
 DIM. OVER 2 PINS. _____ 2.616-2.619
 HOB NO. _____ HB 552-1

NOTES ON MACHINING

- LIMITS ON FINISH DIMENSIONS ARE .010 INCH UNLESS OTHERWISE SPECIFIED
- BREAK ALL SHARP CORNERS
- ROUND ALL TOOTH EDGES
- ROUND ALL KEYWAY AND SPLINE ENDS

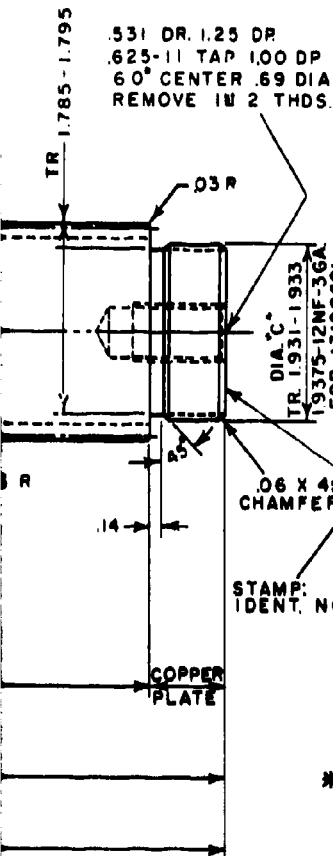
BLACK OXIDE COAT PER AMS 2485 D

PART NO. 139887-P

* MANUFACTURE AND INSPECT TO STD BLANK TOLERANCES FOR GLEASON BLANK CHECKER

MAGNAFLUX INSPECT

NITAL ETCH



B

GROUND SPIRAL BEVEL PINION
(PULSER TEST)

13
0007
0002
MEAN) 250
CKNESS(MEAN) .356 - .361
TEST
MED
.006-.008
.463-.466

AIRCRAFT QUALITY
100% INSPECTION REQ'D

DIAMETERS 'A' AND 'E' MUST BE CONCENTRIC WITH EACH OTHER WITHIN .0002 T.I.R.
SURFACES 'X' AND 'Y' MUST BE PARALLEL WITH EACH OTHER WITHIN .0002 AND SQUARE WITH DIAMETERS 'A' AND 'E' WITHIN .0002

BEVEL GEAR DATA
NUMBER OF TEETH 17
PITCH (DP) (REF) 4.080
PITCH DIAMETER (THEORETICAL) 4.167
PITCH ANGLE (REF) 18°26'
SHAFT ANGLE 90°
PRESSURE ANGLE (REF) 20°
SPIRAL ANGLE (REF) 35°
HAND OF SPIRAL L.H.
DRIVER OR DRIVEN DRIVER
DIRECTION OF ROTATION C.W.

TOOTH FILLET CURVE 0.040 MIN. RAD.
PART NO. OF MATE 139887-G
NUMBER OF TEETH IN MATE 51
SUMMARY NO. (12Dg) 139.887
MATERIAL: AMS 6265 B
COPPER PLATE THDS. AS SHOWN
CASE .045-.055 EFFECTIVE-ROOT
REHEAT 1550°F
DRAW 350°F
CORE HARDNESS R_c 34-38
CASE HARDNESS R_c 60 MIN.
TEST PIECES REQ'D
FORGINGS TO TEST BRIN. 228 MAX.
STRESS RELIEVE AT 325°F AFTER FINISH GRINDING TEETH

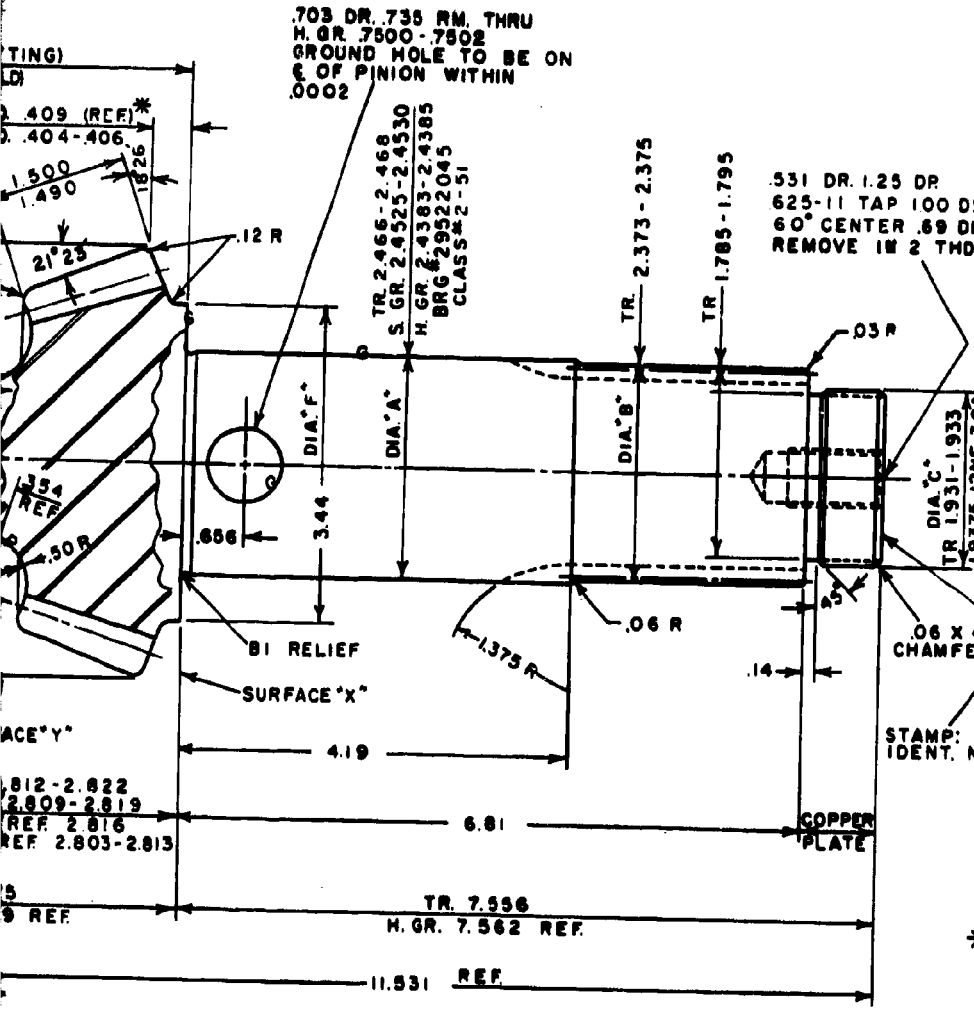
EXTERNAL SPLINE DATA
FILLET ROOT SIDE-FIT
NO. OF TEETH 18
PITCH (REF) 8/16
PITCH DIAMETER (THEQ) 2.250
PRESSURE ANGLE (REF) 30° INV.
MEASURING PIN DIA. 240
DIM. OVER 2 PINS. 2.616-2.619
HOB NO. HB 552-1

NOTES ON MACHINING
1. LIMITS ON FINISH DIMENSIONS ARE .010 INCH UNLESS OTHERWISE SPECIFIED
2. BREAK ALL SHARP CORNERS
3. ROUND ALL TOOTH EDGES
4. ROUND ALL KEYWAY AND SPLINE ENDS

BLACK OXIDE COAT PER AMS 2485 D

PART NO. 139887-PP

* MANUFACTURE AND INSPECT TO STD. BLANK TOLERANCES FOR GLEASON BLANK CHECKER
MAGNAFLUX INSPECT
NITAL ETCH



2. Pinion Drawing for 12-Inch Cutter Diameter Pulser Gear Set.

L

GROUND SPIRAL BEVEL GEAR

AGMA QUALITY NO. _____ 13
 RUNOUT TOLERANCE _____ .0009
 PITCH TOLERANCE _____ .0002
 NORMAL CHORDAL ADDENDUM (MEAN) _____ .105
 NORMAL CHORDAL TOOTH THICKNESS (MEAN) _____ .186 - .191
 NORMAL BACKLASH AT TIGHTEST _____
 POINT OF MESH AT SPECIFIED _____
 MOUNTING DISTANCE _____ .006 - .008
 WHOLE DEPTH _____ .421 - .424

AIRCRAFT QUALITY
 100% INSPECTION REQ'D

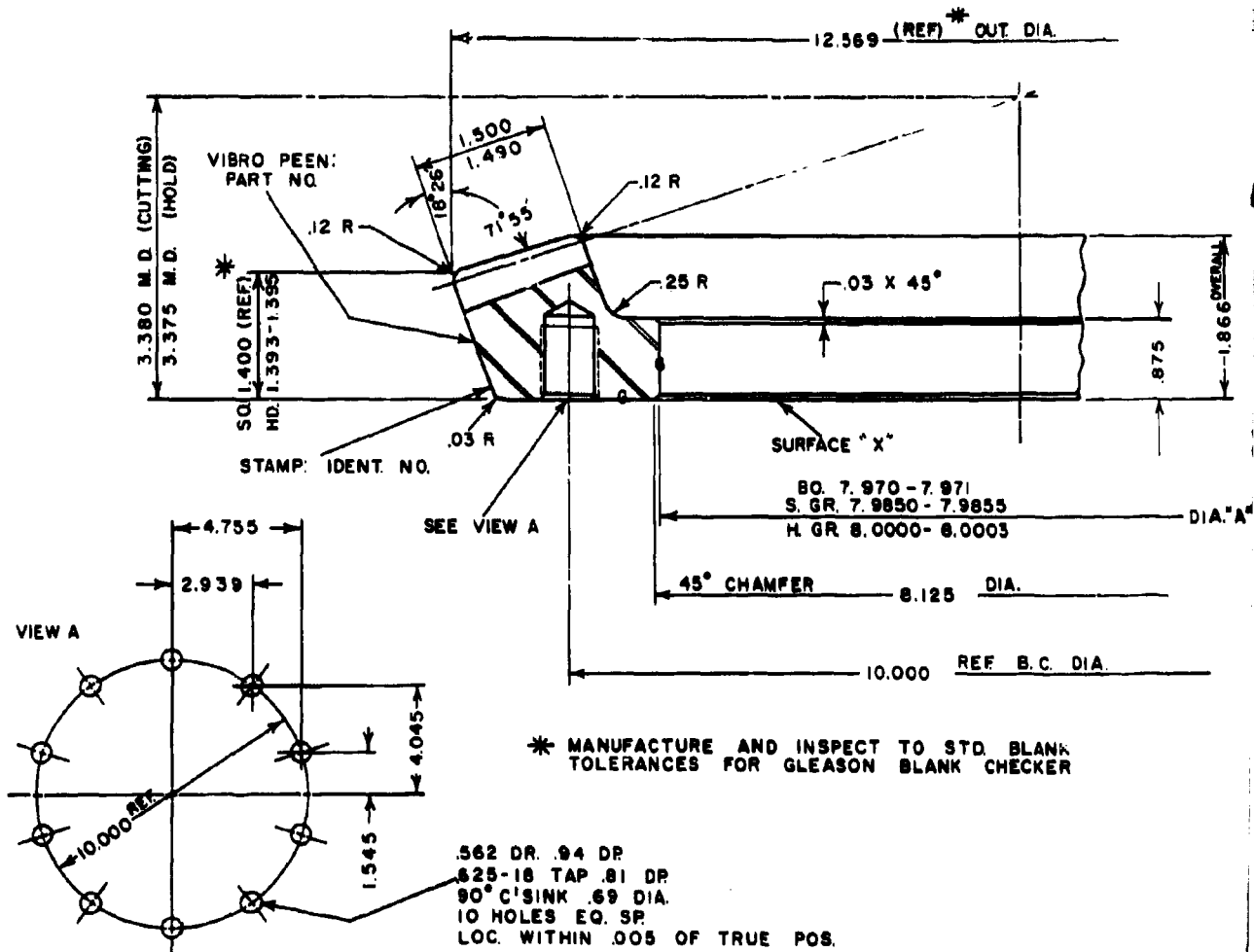


Figure 53. Gear Drawing for 7-1/2-Inch
 Cutter Diameter Test Gear Set.

A

GROUND SPIRAL BEVEL GEAR

AIRCRAFT QUALITY
100% INSPECTION REQ'D

13
0009
0002
105
MEAN .186-.191

006-.008
421-424

BEVEL GEAR DATA
NUMBER OF TEETH _____ 51
PITCH (D.P.) _____ (REF) 4.080
PITCH DIAMETER (THEORETICAL) 12.500
PITCH ANGLE _____ (REF) 71° 34'
SHAFT ANGLE _____ 90° 00'
PRESSURE ANGLE (REF) _____ 20°
SPIRAL ANGLE (REF) _____ 35°
HAND OF SPIRAL _____ R.H.
DRIVER OR DRIVEN _____ DRIVEN
DIRECTION OF ROTATION _____ C.C.W.

TOOTH FILLET CURVE _____ 060 MIN. RAD.
PART NO. OF MATE _____ 139898-P
NUMBER OF TEETH IN MATE _____ 17
SUMMARY NO. (7 1/2 Dc) _____ 139.698

MATERIAL: AMS 6265 B
CASE: .045-.055 EFFECTIVE-ROOT
REHEAT 1550°F
DRAW 350°F
CORE HARDNESS R_c 34-38
CASE HARDNESS R_c 60 MIN.
TEST PIECES REQ'D
FORGINGS TO TEST BRIN. 228 MAX.
STRESS RELIEVE AT 325°F AFTER
FINISH GRINDING TEETH

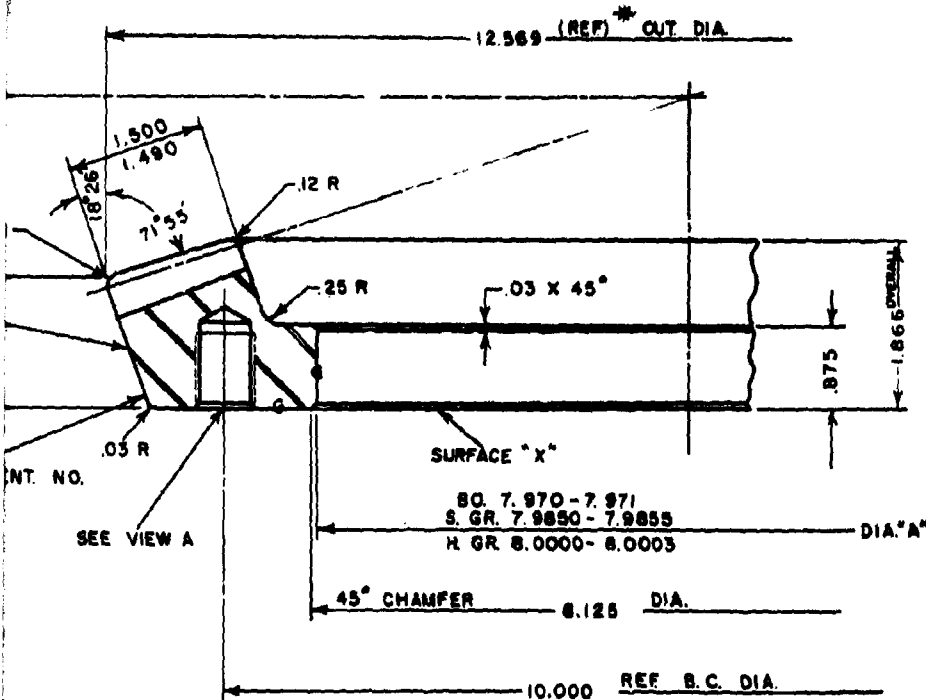
SURFACE "X" MUST BE SQUARE
WITH DIA. "A" WITHIN .0002 T.I.R.

MAGNAFLUX INSPECT

NITAL ETCH

NOTES ON MACHINING
1. LIMITS ON FINISH DIMENSIONS ARE
.010 INCH UNLESS OTHERWISE
SPECIFIED
2. BREAK ALL SHARP CORNERS
3. ROUND ALL TOOTH EDGES
4. ROUND ALL KEYWAY AND SPLINE ENDS
BLACK OXIDE COAT PER AMS 2485 D

PART NO. 139898-G



* MANUFACTURE AND INSPECT TO STD. BLANK
TOLERANCES FOR GLEASON BLANK CHECKER

.562 DR. .94 DR
.825-18 TAP .81 DP
90° C'SINK .69 DIA.
10 HOLES EQ. SP
LOC. WITHIN .005 OF TRUE POS.

3. Gear Drawing for 7-1/2-Inch
Cutter Diameter Test Gear Set.

D

GROUND SPIRAL BEVEL GEAR

INSPECTION DATA
 AGMA QUALITY NO. _____ 13
 RUNOUT TOLERANCE _____ .0008
 PITCH TOLERANCE _____ .0002
 NORMAL CHORDAL ADDENDUM (MEAN) _____ .104
 NORMAL CHORDAL TOOTH THICKNESS (MEAN) _____ .187-.192
 NORMAL BACKLASH AT TIGHTEST POINT OF MESH AT SPECIFIED MOUNTING DISTANCE _____ .008-.008
 WHOLE DEPTH _____ .463-.466

AIRCRAFT QUALITY
100% INSPECTION REQ'D

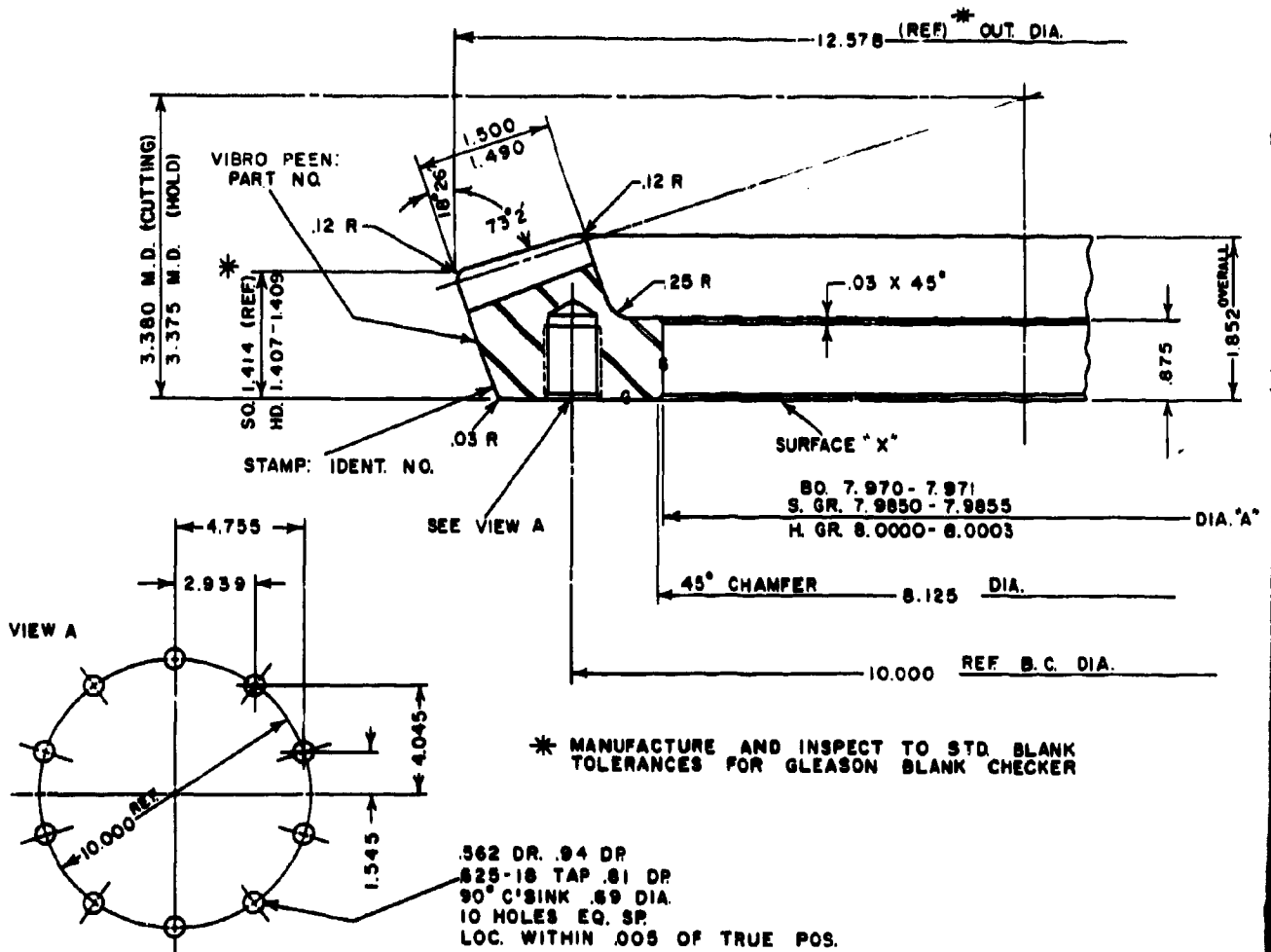


Figure 54. Gear Drawing for 12-Inch Cutter Diameter Test Gear Set.

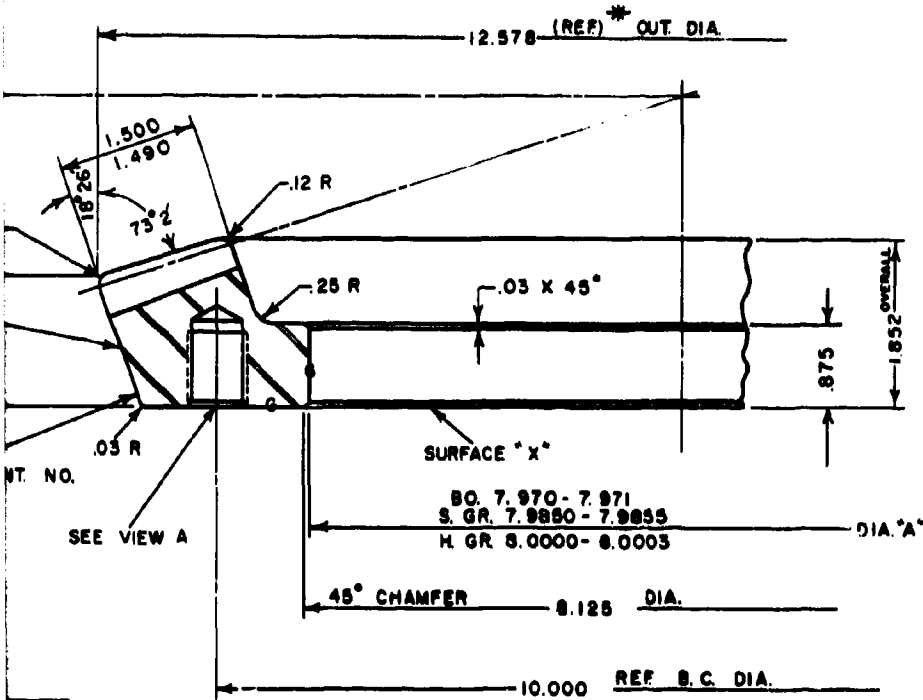
A

GROUND SPIRAL BEVEL GEAR

AIRCRAFT QUALITY
100% INSPECTION REQ'D

13
0009
0002
104
(MEAN) .187 - .192

.006 - .008
463 - 466



* MANUFACTURE AND INSPECT TO STD. BLANK TOLERANCES FOR GLEASON BLANK CHECKER

.562 DR. .94 DR
.825-18 TAP .81 DP
90° C'SINK .69 DIA.
10 HOLES EQ. SP.
LOC. WITHIN .005 OF TRUE POS.

BEVEL GEAR DATA
NUMBER OF TEETH _____ 51
PITCH (DP) _____ (REF) 4.080
PITCH DIAMETER (THEORETICAL) 12.500
PITCH ANGLE _____ (REF) 71° 34'
SHAFT ANGLE _____ 90° 30'
PRESSURE ANGLE _____ (REF) 20°
SPIRAL ANGLE _____ (REF) 35°
HAND OF SPIRAL _____ R.H.
DRIVER OR DRIVEN _____ DRIVEN
DIRECTION OF ROTATION _____ C.C.W.

TOOTH FILLET CURVE _____ D80 MIN. RAD.
PART NO. OF MATE _____ 139 887-
NUMBER OF TEETH IN MATE _____ 17
SUMMARY NO. _____ (12 Ds) 139.887

MATERIAL: AMS 6265 B
CASE .045-.055 EFFECTIVE-ROOT
REHEAT 1550°F
DRAW 350°F
CORE HARDNESS R_c 34-38
CASE HARDNESS R_c 60 MIN.
TEST PIECES REQ'D
FORGINGS TO TEST BRIN. 228 MAX.
STRESS RELIEVE AT 325°F AFTER
FINISH GRINDING TEETH

SURFACE *X* MUST BE SQUARE WITH DIA. *A* WITHIN .002 T.I.R.

MAGNAFLUX INSPECT

NITAL ETCH

- NOTES ON MACHINING
1. LIMITS ON FINISH DIMENSIONS ARE .010 INCH UNLESS OTHERWISE SPECIFIED
 2. BREAK ALL SHARP CORNERS
 3. ROUND ALL TOOTH EDGES
 4. ROUND ALL KEYWAY AND SPLINE ENDS

BLACK OXIDE COAT PER AMS 2485 D

PART NO. 139887-G

B

SHEET 1 OF 3

OPERATION SHEET METHODS MUST INITIAL ALL EXCEPTIONS

ORDER NO

PART NAME GEAR, GROUND SPIRAL BEVEL CUSTOMER FORT EUSTIS-DAAJ02-68-C-0032

PART NO 139

METHODS 3-27-68 N. G. TIME STUDY MAJOR PART SIMILAR PART ASS. PART NO

DEPT.	MACH. CLASS	OPER.	NAME OF OPERATION	TOOL NO.	NAME OF TOOL	CK	SET U
			AMS 6265B PURCHASED FORGINGS				
89	12B	005	MEASURE FORGING ROUGH ANGLES AND FRONT				
89	12B	010	ROUGH & FINISH TURN BORE AND BACK				
89	3	015	TURN SPOTS ON O. D. & FRONT	F24508DF F122522	SPLIT RING BUSHING		
52	34P	020	DRILL, TAP & CO'SINK HOLES		TAPE		
52		023	GREEN BOTTOM TAP HOLES	11518	TAP		
88	17	025	SPOT FRONT & GRIND BACK TO CLEAN				
89	21	030	SOFT GRIND BORE				
89	3	035	DEPT. 89 TO INSPECT FIRST PIECE - SEE OPER. 040 FINISH TURN BACK ANGLE, FACE ANGLE AND RADIUS O. D.	F12252AH F12252	BUSHING ARBOR		
89		040	INSPECT DIMENSIONS TURNED IN OPER. 035 ON FIRST PIECE BEFORE OTHERS ARE TURNED				
89	3	045	DEPT. 89 TO INSPECT FIRST PIECE - SEE OPER. 050 FINISH TURN FRONT ANGLE, FRONT AND RADIUS.				
89		050	INSPECT DIMENSIONS TURNED IN OPER. 045 ON FIRST PIECE BEFORE OTHERS ARE TURNED.				

PD 1181-1BM

Figure 55. Test Gear Routing Sheets.

OPERATION SHEET

METHODS MUST INITIAL ALL EXCEPTIONS

ORDER NO.	QUANTITY

PART NAME GEAR, GROUND SPIRAL BEVEL CUSTOMER FORT EUSTIS-DAAJ02-68-C 8032

PART NO. 139898G	PART NO.

METHODS 3-27-68 N. G.	TIME STUDY	MAJOR PART	SIMILAR PART

TIME ESTIMATE

DEPT	MACH. CLASS	OPER.	NAME OF OPERATION	TOOL NO.	NAME OF TOOL	CK	STD. TIME		TIME ESTIMATE
							SET UP	PER PC.	
26	21	115	DEPT. 89 TO INSPECT FIRST PIECE - SEE OPER. 120 GRIND BORE	F24000 N. H.	PITCH LINE CHUCK				
89		120	INSPECT BORE GROUND IN OPER. 115 ON FIRST PIECE BEFORE OTHERS ARE GROUND						
89	A4B	125	NITAL ETCH GROUND SURFACES (2 MIN. ONLY)						
89	92A	130	MAGNAFLUX INSPECT						
89		135	INSPECT BORE AND BACK						
89	60C	140	GRIND TEETH - M. D. HELD	F24000 N. E. F24000 NE-	BALL SLEEVE BALL SLEEVE	ARBOR			
89		145	ROUND ALL SHARP EDGES						
89	72A	150	TEST & INSPECT - M. D. HELD	F24000 NF F24000 NE-	BALL SLEEVE BALL SLEEVE	ARBOR			
89	A4h	155	NITAL ETCH TEETH ONLY. PROTECT REST OF PIECE						
89	92A	160	MAGNAFLUX INSPECT						
64	C85	162	STRESS RELIEVE						
89		165	VIBRO PEEN AS SHOWN						
90	B36	170	BLACK OXIDE COAT PER AMS 2485D						
89			DELIVER TO TEST CENTER						

D

SHEET 1 OF 4

OPERATION SHEET METHODS MUST INITIAL ALL EXCEPTIONS

ORDER NO

PART NAME PINION, GROUND SPIRAL BEVEL CUSTOMER FORT EUSTIS-DAAJ02-68-C-00

PART NO

METHODS 3-27-68 N.G. TIME STUDY MAJOR PART SIMILAR PART ASS PART NO

DEPT.	MACH. CLASS	OPER.	NAME OF OPERATION	TOOL NO.	NAME OF TOOL	CX	SE
			AMS 6265B PURCHASED FORGINGS				
89	11B	005	MEASURE FORGING FACE END, ROUGH & FINISH TURN DIAMS. C, B, A AND SHOULDER X, ROUGH DIAM. F, BACK ANGLE AND FACE ANGLE. CHECK, CHAMFER, DRILL, TAP & CENTER				
89	11B	010	FACE FRONT TO LENGTH, ROUGH AND FINISH TURN DIAM. E AND SURFACE Y. ROUGH FRONT ANGLE AND HUB D. DRILL, TAP & CENTER.	F24615 AC	FORM TOOL		
89		015	STAMP IDENTIFICATION NO. SEE ORDER FOR NO'S.				
89	33L	020	LAP CENTERS				
89	16	025	DEPT. 89 TO INSPECT FIRST PIECE-SEE OPER. 030 SOFT GRIND DIAM. A AND GRIND SURFACE X TO LENGTH				
89		030	INSPECT DIMENSIONS GROUND IN OPER. 025 ON FIRST PIECE BEFORE OTHERS ARE GROUND.				
89	3	035	DEPT. 89 TO INSPECT FIRST PIECE -SEE OPER. 040 FINISH TURN FACE ANGLE, BACK ANGLE, DIAM. F AND RADIUS.				
89		040	INSPECT DIMENSIONS TURNED IN OPER. 035 ON FIRST PIECE BEFORE OTHERS ARE TURNED.				
89	3	050	DEPT. 89 TO INSPECT FIRST PIECE-SEE OPER. 055 FINISH TURN FRONT ANGLE AND HUB, D	F24615AC	FORM TOOL		

PD 1181-104

Figure 56. Test Pinion Routing Sheets.

A

OPERATION SHEET

METHODS MUST INITIAL ALL EXCEPTIONS

ON, GROUND SPIRAL BEVEL CUSTOMER FORT EUSTIS-DAAJ02-68-C-0032

ORDER NO. QUANTITY

PART NO. 139887P

STUDY MAJOR PART SIMILAR PART

ASS.

PART NO. 139898P

NAME OF OPERATION	TOOL NO.	NAME OF TOOL	CK	STD. TIME		TIME ESTIMATE
				SETUP	PER PC.	
INSPECT DIAMS. A & E FOR SIZE AND CONCENTRICITY SURFACES Y & Y FOR RUNOUT AND LENGTH AND BEARING						
GRIND TEETH (BOTTOM SIDE) M. D. HELD	F1936JH F1936JH-1	BALL SLEEVE CHUCK BALL SLEEVE				
GRIND TEETH (TOP SIDE) M. D. HELD						
ROUND ALL SHARP EDGES						
TEST & INSPECT - M. D. HELD SEE MEMO BY W. COLEMAN	F1936J F1936JH-1	BALL SLEEVE CHUCK BALL SLEEVE				
NITAL ETCH TEETH ONLY. PROTECT REST OF PIECE						
MAGNAFLUX INSPECT						
STRESS RELIEVE						
VIBRO PEEN AS SHOWN						
BLACK OXIDE COAT PER AMS 2485D ALL OVER EXCEPT THDS.						
DELIVER TO TEST CENTER						

E

CUSTOMER - PORT EUSTIS - DAAJ02-60-C-0032

	PIG ON	GEAR
NUMBER OF TEETH	17	51
DIAMETRAL PITCH	1.000	1.000
FACE WIDTH	20° 0'	90° 0'
PRESSURE ANGLE	20° 0'	20° 0'
SHAFT ANGLE	90° 0'	90° 0'
OUTER CONE DISTANCE	6.800	6.800
WORKING DEPTH	.276	.276
WHOLE DEPTH	.421	.421
ADDENDUM	.200	.200
OUTSIDE DIAMETER	6.600	12.600
PART NUMBER	139070-P	139080-G

	PIG ON	GEAR
PITCH ANGLE TO CROWN	6.166°	1.000°
PITCH ANGLE	10° 20'	71° 36'
FACE ANGLE OF BLANK	10° 17'	71° 35'
ROOT ANGLE	10° 5'	70° 45'
SPIRAL ANGLE	20° 0'	20° 0'
HAND OF SPIRAL	LH	RH
CUTTING METHOD	FIXED SETTING	SPREAD BLADE
BACKLASH	MIN	.000" MAX
DRIVING MEMBER	PIG	
DIRECTION OF ROTATION	REV	
MOUNTING DISTANCE (HORN)	6.9625	3.375
MOUNTING DISTANCE (CUTTING)	6.9625	3.300
MOUNTING DISTANCE (GRINDING)	6.9625	3.375

FINISHED TOOTH SIZES (AT NEAR)

NORMAL CHORDAL ADDENDUM	.201	.199
NORMAL CHORDAL THICKNESS-CUT	.371	.369
NORM CHORDAL THICKNESS-GRIND	.361	.359
WHOLE DEPTH AT LARGE END-PIG	.417	.417
WHOLE DEPTH AT LARGE END-GRIND	.421	.421

DEPTH CHECKING DATA - NO. 13 BLANK CHECKER

CHECKING DIAMETER	1.704	10.000
BACKING	NO - 0.166" MD - 2.132"	

RELEASED BY: DATE 01/09/60

GEAR ROUGH AND SEMI-FINISH - NO. 116 GENERATOR

MACHINE ROOT ANGLE	70° 43'
MACHINE CENTER TO BACK	STANDARD
SLIDING BASE	ADV .210"
BLANK OFFSET	0.000"
ECCENTRIC ANGLE	00° 51'
CHARLE ANGLE	10° 1'
SHIVEL ANGLE	00° 0'
CUTTER SPINDLE ROTATION ANG	00° 0'
CRABLE TEST ROLL	20° 0'
WORK TEST ROLL	31° 37'
DECIMAL RATIO	1.0700
NC/DO RATIO GEARS	.0071 R 00/07

GEAR-ROUNDED NO ROLL PRIOR TO SEMI-FINISH
SEE SHOP SHEET

CUTTER SPECIFICATIONS - GEAR ROUGH AND SEMI-FINISH

DIAMETER	1.000"
PRESSURE ANGLE	20° 0'
CUTTER NUMBER	2.000
POINT WIDTH	.140"
BLADE EDGE RADIUS	.000"
BLANK LETTER	
TYPE OF CUTTER	
CUTTER BLADES	STD DEPTH

PIGON SETTINGS

SIDE OF TOOTH	CONCAVE-G.O.B.	CONVEX-I.S.B.
	ROUGH AND SEMI-FINISH	SEMI-FINISH

CUTTER SPECIFICATIONS

AVERAGE DIAMETER	6.960
POINT DIAMETER	7.034
PRESSURE ANGLE	20° 0'
CUTTER NUMBER	.000
POINT WIDTH	.200
BLANK LETTER	0
BLANK EDGE RADIUS	.000
TOPPER LETTER	
CUTTER BLADES	STD DEPTH

MACHINE SETTINGS - NO. 116 GENERATOR

MACHINE ROOT ANGLE	10° 5'	100° 3'
MACHINE CENTER TO BACK	ADV .255" WITH .300"	
SLIDING BASE	ADV .033" ADV .205"	
BLANK OFFSET	UP .110" DOWN .120"	
ECCENTRIC ANGLE	00° 0'	70° 0'
CHARLE ANGLE	00° 00'	00° 40'
SHIVEL ANGLE	00° 0'	00° 0'
CUTTER SPINDLE ROTATION ANG	00° 0'	00° 0'
CRABLE TEST ROLL	20° 0'	20° 0'
WORK TEST ROLL	37° 20'	00° 30'
DECIMAL RATIO	.0700	1.1100
NC/DO RATIO GEARS	.0070 R 00/00	00/00 R 70/70
ROLLER ECCENTRICITY	.032"	
ROLLER ANGLE	200° 0'	000° 0'
ROLLER GEARS	00/00 R 70/70	00/00 R 70/70

PROPORTIONAL CUTTING CHANGES - NO. 116 GENERATOR

SIDE OF TOOTH	CONCAVE-G.O.B.	CONVEX-I.S.B.
	BIAS CHANGE - 60° BIAS OUT	
MACHINE CENTER TO BACK	ADV .007" WITH .007"	
SLIDING BASE	WITH .000" ADV .030"	
ECCENTRIC ANGLE	DEC 10° 1' INC 1° 10'	
CHARLE ANGLE	INC 00° 10' DEC 00° 3'	
WORK TEST ROLL	DEC 10° 0' INC 1° 0'	
DECIMAL RATIO	DEC .0170 INC .0170	
	PROFILE CURVATURE CHANGE - 0.100" PROFILE BUT	
BLANK OFFSET	UP .100" DOWN .100"	
ECCENTRIC ANGLE	DEC 10° 0' INC 10° 0'	
CHARLE ANGLE	DEC 10° 20' INC 1° 25'	
WORK TEST ROLL	DEC 00° 40' INC 00° 45'	
DECIMAL RATIO	DEC .0130 INC .0127	
	LENGTHWISE CURVATURE CHANGE - 0.100" INCREASE IN LENGTH	
ECCENTRIC ANGLE	DEC 00° 5' INC 00° 3'	
CHARLE ANGLE	DEC 00° 40' INC 00° 35'	
CUTTER DIAMETER	DEC 0.100" INC 0.100"	
	SPIRAL ANGLE CHANGE - 0.100" OFF THE TOE	
ECCENTRIC ANGLE	DEC 1° 1' INC 1° 0'	
CHARLE ANGLE	DEC 0° 25' INC 0° 27'	

TEST MACHINE DATA

V AND H CHECK	
CONCAVE G.O.B	CONVEX I.S.B
TOE WHEEL TOTAL TOE WHEEL TOTAL	
VERTICAL ONLY	+0 -0 17 -4 +15 19

CUSTOMER - PORT EUSTIS

NO. 137 GEAR

SIDE OF TOOTH	
DIAMETER	
OUTSIDE WHEEL PRESS	
INSIDE WHEEL PRESS	
POINT WIDTH	
WHEEL EDGE RADIUS	

MACHINE ROOT ANGLE	
MACHINE CENTER TO	
BLANK OFFSET	
BLANK LETTER	
CHARLE ANGLE	
ECCENTRIC ANGLE	
CONCAVE G.O.B	
GENERATING CAP ROL	
INDEX INTERVAL	
INDEX DEPTH	

GRINDER DR	
GRINDER BACK ANGLE	
OUTSIDE PRESSURE	
SIDE DRESSER RADI	
OUTSIDE DRESSER AN	
OUTSIDE DIAMOND BE	
OUTSIDE DIAMOND BE	
OUTSIDE DIAMOND BE	
INSIDE DRESSER AN	
INSIDE DIAMOND BE	
INSIDE DIAMOND BE	
INSIDE DIAMOND BE	
SIDE DRESSER AXIAL	
SIDE DRESSER OFFSE	
RADIUS CAN NUMBER	
SWING ANGLE	
END DIAMOND HORN	
END DIAMOND HORN	
END DIAMOND SETTING	
END DRESSER RADI	

GRINDER DR	
GRINDER BACK ANGLE	
OUTSIDE PRESSURE	
SIDE DRESSER RADI	
OUTSIDE DRESSER AN	
OUTSIDE DIAMOND BE	
OUTSIDE DIAMOND BE	
OUTSIDE DIAMOND BE	
INSIDE DRESSER AN	
INSIDE DIAMOND BE	
INSIDE DIAMOND BE	
INSIDE DIAMOND BE	
SIDE DRESSER AXIAL	
SIDE DRESSER OFFSE	
RADIUS CAN NUMBER	
SWING ANGLE	
END DIAMOND HORN	
END DIAMOND HORN	
END DIAMOND SETTING	
END DRESSER RADI	

GRINDER DR	
GRINDER BACK ANGLE	
OUTSIDE PRESSURE	
SIDE DRESSER RADI	
OUTSIDE DRESSER AN	
OUTSIDE DIAMOND BE	
OUTSIDE DIAMOND BE	
OUTSIDE DIAMOND BE	
INSIDE DRESSER AN	
INSIDE DIAMOND BE	
INSIDE DIAMOND BE	
INSIDE DIAMOND BE	
SIDE DRESSER AXIAL	
SIDE DRESSER OFFSE	
RADIUS CAN NUMBER	
SWING ANGLE	
END DIAMOND HORN	
END DIAMOND HORN	
END DIAMOND SETTING	
END DRESSER RADI	

GRINDER DR	
GRINDER BACK ANGLE	
OUTSIDE PRESSURE	
SIDE DRESSER RADI	
OUTSIDE DRESSER AN	
OUTSIDE DIAMOND BE	
OUTSIDE DIAMOND BE	
OUTSIDE DIAMOND BE	
INSIDE DRESSER AN	
INSIDE DIAMOND BE	
INSIDE DIAMOND BE	
INSIDE DIAMOND BE	
SIDE DRESSER AXIAL	
SIDE DRESSER OFFSE	
RADIUS CAN NUMBER	
SWING ANGLE	
END DIAMOND HORN	
END DIAMOND HORN	
END DIAMOND SETTING	
END DRESSER RADI	

GRINDER DR	
GRINDER BACK ANGLE	
OUTSIDE PRESSURE	
SIDE DRESSER RADI	
OUTSIDE DRESSER AN	
OUTSIDE DIAMOND BE	
OUTSIDE DIAMOND BE	
OUTSIDE DIAMOND BE	
INSIDE DRESSER AN	
INSIDE DIAMOND BE	
INSIDE DIAMOND BE	
INSIDE DIAMOND BE	
SIDE DRESSER AXIAL	
SIDE DRESSER OFFSE	
RADIUS CAN NUMBER	
SWING ANGLE	
END DIAMOND HORN	
END DIAMOND HORN	
END DIAMOND SETTING	
END DRESSER RADI	

GRINDER DR	
GRINDER BACK ANGLE	
OUTSIDE PRESSURE	
SIDE DRESSER RADI	
OUTSIDE DRESSER AN	
OUTSIDE DIAMOND BE	
OUTSIDE DIAMOND BE	
OUTSIDE DIAMOND BE	
INSIDE DRESSER AN	
INSIDE DIAMOND BE	
INSIDE DIAMOND BE	
INSIDE DIAMOND BE	
SIDE DRESSER AXIAL	
SIDE DRESSER OFFSE	
RADIUS CAN NUMBER	
SWING ANGLE	
END DIAMOND HORN	
END DIAMOND HORN	
END DIAMOND SETTING	
END DRESSER RADI	

GRINDER DR	
GRINDER BACK ANGLE	
OUTSIDE PRESSURE	
SIDE DRESSER RADI	
OUTSIDE DRESSER AN	
OUTSIDE DIAMOND BE	
OUTSIDE DIAMOND BE	
OUTSIDE DIAMOND BE	
INSIDE DRESSER AN	
INSIDE DIAMOND BE	
INSIDE DIAMOND BE	
INSIDE DIAMOND BE	
SIDE DRESSER AXIAL	
SIDE DRESSER OFFSE	
RADIUS CAN NUMBER	
SWING ANGLE	
END DIAMOND HORN	
END DIAMOND HORN	
END DIAMOND SETTING	
END DRESSER RADI	

GRINDER DR	
GRINDER BACK ANGLE	
OUTSIDE PRESSURE	
SIDE DRESSER RADI	
OUTSIDE DRESSER AN	
OUTSIDE DIAMOND BE	
OUTSIDE DIAMOND BE	
OUTSIDE DIAMOND BE	
INSIDE DRESSER AN	
INSIDE DIAMOND BE	
INSIDE DIAMOND BE	
INSIDE DIAMOND BE	
SIDE DRESSER AXIAL	
SIDE DRESSER OFFSE	
RADIUS CAN NUMBER	
SWING ANGLE	
END DIAMOND HORN	
END DIAMOND HORN	
END DIAMOND SETTING	
END DRESSER RADI	

Figure 57. Ground Spiral Bevel Summary for 7-1/2-Inch Cutter Diameter Test Gears.

A

BLANK PAGE

CUSTOMER - FORT EUSTIS - DAAJ02-68-C-0032

CUSTOMER - FORT EUSTIS - DAAJ02-68-C-0032

PINION		GEAR	
NUMBER OF TEETH	17	51	
DIAMETRAL PITCH	4.000		
FACE WIDTH	1.500		
PRESSURE ANGLE	20° 0'		
SHAFT ANGLE	90° 0'		
OUTER GEAR DISTANCE		6.500	
WORM DEPTH		0.170	
WHEEL DEPTH	0.030	0.060	
ADDENDUM	0.250	0.250	
OUTSIDE DIAMETER	6.750	12.570	
PART NUMBER	150007-0	150007-6	
	150007-00		

PINION		GEAR	
PITCH AREA TO CROWN	6.197	1.960	
PITCH ANGLE	18° 26'	7° 36'	
FACE ANGLE OF BLANK	21° 25'	7° 2'	
ROOT ANGLE	18° 50'	6° 37'	
SPIRAL ANGLE	33° 0'	13° 0'	
HAND OF SPIRAL	LN	RH	
CUTTING METHOD	FINED SETTING	SPREAD BLADE	
BACKLASH	MIN	0.000	MAX 0.000
DRIVING MEMBER	PIN		
DIRECTION OF ROTATION	REV		
MOUNTING DISTANCE	6.9825	2.375	
MOUNTING DISTANCE (CUTTING)	6.9825	2.380	
MOUNTING DISTANCE (GRINDING)	6.9825	2.375	

NO. 157 GRINDER SETTINGS - GEAR

GRINDER WHEEL SPECIFICATIONS	
SIDE OF TOOTH	RCH
DIAMETER	12.000
OUTSIDE WHEEL PRESSURE ANGLE	18° 26'
INSIDE WHEEL PRESSURE ANGLE	21° 40'
POINT WIDTH	0.150
WHEEL EDGE RADIUS	0.360
MACHINE SETTINGS	
MACHINE ROOT ANGLE	60° 37'
MACHINE CENTER TO BACK	0.015
SLIDING BASE	10.000
BLANK OFFSET	12.000
CAM SETTING	4.956
CRADLE ANGLE	80° 19'
ECCENTRIC ANGLE	0° 2'
CAM GUIDE ANGLE	0° 0'
FEED CAM SETTING	0° 0'
OPERATING CAM NUMBER	462027
INDEX INTERVAL	10
INDEX GEAR	30/90 = 30/90
GRINDER DRESSER SETTINGS - GEAR	
DRESSER BLOCK ANGLE	60° 0'
OUTSIDE PRESSURE ANGLE	18° 26'
SIDE DRESSER RADIAL	6.142
OUTSIDE DRESSER ARM	43021921
OUTSIDE DIAMOND HLD HOLDER	43022380
OUTSIDE DIAMOND HLD EXTENSION	43022620
OUTSIDE DIAMOND SETTING	0.000
INSIDE DRESSER ARM	43021921
INSIDE DIAMOND HLD HOLDER	43022370
INSIDE DIAMOND HLD EXTENSION	43022620
INSIDE DIAMOND SETTING	0.000
SIDE DRESSER ARM	0.000
SIDE DRESSER OFFSET	0.000
RADIUS CAM NUMBER	43020209
MIN ANGLE	10° 20'
END DIAMOND HLD HOLDER	43022380
END DIAMOND HLD EXTENSION	43022620
END DIAMOND SETTING	0.000
END DRESSER RADIAL	6.025

RELEASED BY - DATE 11/06/68

FINISHED TOOTH SIZES (AT MEAN)	
NORMAL CHORDAL ADDENDUM	0.200
NORMAL CHORDAL THICKNESS-CUT	0.372
NORM CHORDAL THICKNESS-GRIND	0.261
WHEEL DEPTH-CUT (AT LARGE END)	0.050
WHEEL DEPTH-GRIND (AT LARGE END)	0.030

DEPTH CHECKING DATA - NO. 15 BLANK CHECKER	
CHECKING DIAMETER	1.750
BACKING	0.197

GEAR ROUGH AND SEMI-FINISH - NO. 116 GENERATOR	
MACHINE ROOT ANGLE	60° 37'
MACHINE CENTER TO BACK	STANDARD
SLIDING BASE	0.000
BLANK OFFSET	0.000
ECCENTRIC ANGLE	77° 21'
CRADLE ANGLE	90° 26'
SWIVEL ANGLE	0° 0'
CUTTER SPINDLE ROTATION ANG	0° 0'
WHEEL TEST ROLL	30° 0'
WORM TEST ROLL	33° 35'
DECIMAL RATIO	1.0757
WORM RATIO GEAR	52/48 = 70/56
TOTAL CRADLE (UP ROLL)	53.50

CUTTER SPECIFICATIONS - GEAR ROUGH AND SEMI-FINISH	
DIAMETER	12.000
PRESSURE ANGLE	20° 0'
CUTTER NUMBER	16.000
POINT WIDTH	0.140
BLADE EDGE RADIUS	0.000
BLADE LETTER	0
TYPE OF CUTTER	
CUTTER BLADES	STD DEPTH

PINION SETTINGS		CONCAVE-0.8 CONVER-1.0	
ROUGH AND SEMI-FINISH		SEMI-FINISH	
AVERAGE DIAMETER	11.740		
POINT DIAMETER		12.270	
PRESSURE ANGLE	20° 0'	20° 0'	
CUTTER NUMBER	12.000	12.000	
POINT WIDTH	0.000		
BLADE LETTER	0		
BLADE EDGE RADIUS	0.000	0.000	
CUTTER BLADES	STD DEPTH		
MACHINE SETTINGS - NO. 116 GENERATOR			
MACHINE ROOT ANGLE	10° 30'	16° 50'	
MACHINE CENTER TO BACK	0.000	0.020	
SLIDING BASE	ADV	0.000	0.100
BLANK OFFSET	DOWN	0.200	UP
ECCENTRIC ANGLE	00° 40'	74° 10'	
CRADLE ANGLE	116° 12'	115° 15'	
SWIVEL ANGLE	0° 0'	0° 0'	
CUTTER SPINDLE ROTATION ANG	0° 0'	0° 0'	
WHEEL TEST ROLL	20° 0'	20° 0'	
WORM TEST ROLL	40° 22'	63° 10'	
DECIMAL RATIO	1.0757	1.0700	
WORM RATIO GEAR	52/70 = 56/70	52/48 = 67/53	
ROLLER ECCENTRICITY	0.340	0.400	
ROLLER ANGLE	53° 45'	115° 15'	
ROLLER GEAR	60/90 = 70/70	60/60 = 70/70	
VPM CHECK SOFT GEAR			
CONCAVE	TOE	HEEL	TOTAL
	V	-10	+30
	H	-10	+22

PROPORTIONAL CUTTING CHANGES - NO. 116 GENERATOR	
SIDE OF TOOTH	CONCAVE-0.8 CONVER-1.0
BLANK OFFSET - 0.000	
MACHINE CENTER TO BACK	ADV 0.000
SLIDING BASE	WITH 0.020
ECCENTRIC ANGLE	DEC 0° 30'
CRADLE ANGLE	INC 0° 30'
WORM TEST ROLL	DEC 1° 0'
DECIMAL RATIO	DEC 0.170
PROFILE CURVATURE CHANGE - 0.100	
BLANK OFFSET	UP 0.100
ECCENTRIC ANGLE	DEC 1° 30'
CRADLE ANGLE	DEC 1° 11'
WORM TEST ROLL	DEC 0° 40'
DECIMAL RATIO	DEC 0.120
LENGTHWISE CURVATURE CHANGE - 0.100	
ECCENTRIC ANGLE	DEC 0° 27'
CRADLE ANGLE	DEC 0° 20'
CUTTER DIAMETER	DEC 0.100
SPIRAL ANGLE CHANGE - 0.100	
ECCENTRIC ANGLE	DEC 1° 36'
CRADLE ANGLE	DEC 0° 19'

ADDITIONAL MACHINE EQUIPMENT

SPINDLE PULLY NUMBER	NO. PINION TO GEAR
46030405	46030406
46030406	46030407
46030407	46030408
WHEEL INSIDE DIAMETER	11" 11 1/2" 11 1/4"
WHEEL OUTSIDE DIAMETER	13 3/4" 12 3/4" 12 3/4"
WHEEL GRINDING OR EQUIVALENT	0420-17-120
WHEEL ADAPTER	04-100
WHEEL GUARD	04-100
WHEEL ROTATION	HEEL TO TOE
WHEEL FEED CAM	43020209
VARIABLE STOP DRUM	43020209
WHEEL FEED FOR DRESSING	0.005
MACHINE FEED SEC/100TH	3.75

GRINDING SURFACE		ROUGH	FINISH
SIDE DRESSER ARM	0	16	
END DRESSER ARM	0	0	
DRESS ROLL	10, 7, 4	START ON NO. 10	

FEED CAM THRU 0.000" SLIDING BASE IS WITH 0.020" TO BE 0.000" WITH THIS SUMMARY, MACH. GEN. NO. 7976

DEVELOPED SETTINGS - UNCOMPILED FOR PRODUCTION
CUSTOMER ORDER NO SALES ORDER NO NO UP SETS DATE
DAAJ02-68-C-0032 20202

Figure 58. Ground Spiral Bevel Summary for 12-Inch Cutter Diameter Test Gears.

A

CUSTOMER - PORT CUSTIS - 2AAJ02-08-C-0032

NO. 127 GRINDER SETTINGS - GEAR GRINDER WHEEL SPECIFICATIONS

Table with 2 columns: Parameter and Value. Includes items like DIAMETER, PITCH ANGLE, PITCH AREA TO CROWN, etc.

NO. 27 GRINDER SETTINGS - PINION GRINDER WHEEL SPECIFICATIONS

Table with 2 columns: Parameter and Value. Includes items like DIAMETER, PITCH ANGLE, PITCH AREA TO CROWN, etc.

ADDITIONAL MACHINE EQUIPMENT

Table with 2 columns: Equipment Name and Quantity/Spec. Includes items like SPINDLE PULLEY NUMBER, MOTOR PULLEY NUMBER, etc.

Table with 2 columns: Parameter and Value. Includes items like RATIO IN SEQUENCE, SIDE DRESSER ANGLE, etc.

DEVELOPED SETTINGS - UNCONFIRMED FOR PRODUCTION

CUSTOMER'S ORDER NO. SALES ORDER NO. NO. OF SETS DATE

PROPORTIONAL GRINDING CHANGES - NO. 27 GRINDER

Table with 2 columns: Parameter and Value. Includes items like MACHINE CENTER TO BACK, SLIDING BASE, etc.

Table with 2 columns: Parameter and Value. Includes items like ECCENTRIC ANGLE, CRABLE ANGLE, etc.

Table with 2 columns: Parameter and Value. Includes items like LENGTHWISE CURVATURE CHANGE, ECCENTRIC ANGLE, etc.

Table with 2 columns: Parameter and Value. Includes items like MACHINE CENTER TO BACK, SLIDING BASE, etc.

Table with 2 columns: Parameter and Value. Includes items like BLANK OFFSET, ECCENTRIC ANGLE, etc.

Table with 2 columns: Parameter and Value. Includes items like V, H, etc.

Table with 2 columns: Parameter and Value. Includes items like PITCH AREA TO CROWN, PITCH ANGLE, etc.

Table with 2 columns: Parameter and Value. Includes items like FINISHED TOOTH SIZE AT MESH, NORMAL CHORDAL ADDENDUM, etc.

Table with 2 columns: Parameter and Value. Includes items like DEPTH CHECKING DATA - NO. 15 BLANK CHECKER, CHECKING DIAMETER, etc.

Table with 2 columns: Parameter and Value. Includes items like CUTTER SPECIFICATIONS - GEAR ROUGH AND SEMI-PINION, DIAMETER, etc.

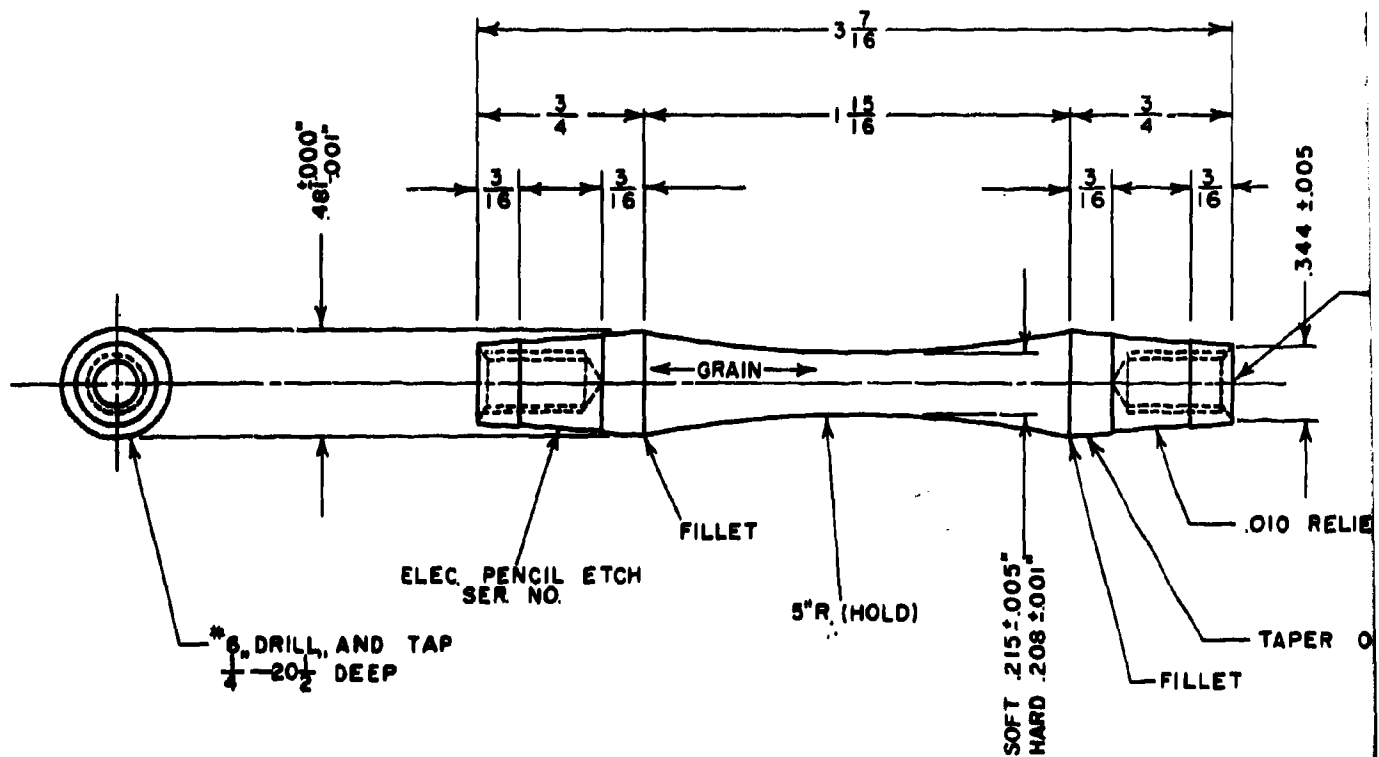
PROPORTIONAL CUTTING CHANGES - NO. 126 GENERATOR

Table with 2 columns: Parameter and Value. Includes items like SIDE OF TOOTH, BIAS CHANGE - ADV BIAS OUT, MACHINE CENTER TO BACK, etc.

58. Ground Spiral Bevel Summary for 12-Inch Cutter Diameter Test Gears.

B

UNNOTCHED ROTATING BEAM SPECIMEN - R. R. MOORE FATIGUE



TOLERANCES UNLESS OTHERWISE SPECIFIED:
 FRACTIONS $\pm \frac{1}{64}$
 DECIMALS $\pm .003$
 ANGLES $1^\circ - 0'$

Figure 59. Drawing for R. R. Moore Test Specimens.

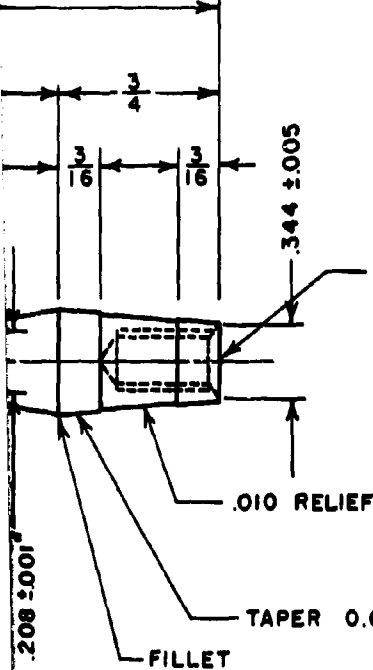
A

R. R. MOORE FATIGUE TEST

INSPECT .215 DIA. AND THDS.
 NON-CASE TAPPED HOLES
 CARB. .030 .040 EFF. CASE
 REHEAT AND QUENCH 1550°F
 DRAW 350°F
 CORE R_e 34-40
 CASE R_e 60⁺

SEND OUT FOR FINAL GRINDING
 AND POLISHING
 INSPECT .481 DIA., .208 DIA., 5 RAD.
 AND SURFACE FINISH
 STRESS RELIEVE AT 325°F
 NITAL ETCH
 BLACK OXIDE COAT PER AMS 2485 D

MATERIAL: AMS 6265 B



CENTER FOR TURNING AND GRINDING

NOTE: FOR SPECIMEN INSPECTION JIG USE 60° INCLUDED ANGLE CENTER WITH MAXIMUM DIAMETER OF CENTER = .344 ± .005 DIAMETER

.010 RELIEF

TAPER 0.625 ± .010 PER FOOT (ON DIAMETER)

FILLET

HARD .208 ± .001

NOTE: UNLESS OTHERWISE SPECIFIED ALL DIMENSIONS ARE IN INCHES

SURFACE FINISH TO BE AS FOLLOW:
 GAGE SECTION .05 TO 2.0 MICROINCHES
 (LONGITUDINALLY POLISHED)
 OTHER SURFACES 16 MICROINCHES OR FINER

B

BLANK PAGE

OPERATION SHEET
METHODS MUST INITIAL ALL EXCEPTIONS

SHEET 1 OF 1 ORDER NO. QUANTITY

PART NAME FATIGUE TEST SPECIMEN CUSTOMER FORT EUSTIS DAAJ02-68-C-0032 PART NO FESP-1
 METROLOG 7-16-68 N.G. FINE STUFF MAJOR PART ASB SIMILAR PART PART NO

DEPT	BACH CLASS	OPER.	NAME OF OPERATION	TOOL NO.	NAME OF TOOL	CK	STD. TIME SET UP PER PC.	TIME ESTIMATE
			CUSTOMERS BLANKS					
90		005	NON-CASE TAPPED HOLES					
64	G15	010	CARBURIZE					
64	J60	015	REHEAT & QUENCH					
64	C85	020	DRAW					
90		025	REMOVE NON-CASE					
89		030	SEND OUT FOR GRINDING & POLISHING SEE ORDER FOR INSTRUCTIONS					
89		035	INSPECT .481 DIAS. AND .208 DIA. FOR SIZE					
16		040	INSPECT 5' RADIUS IN COMPARATOR AND SURFACE FINISH					
64	C85	045	STRESS RELIEVE					
89	A48	050	NITAL ETCH					
89	92A	055	MAGNAFLUX INSPECT					
90		060	BLACK OXIDE COAT PER AMS 2485D					
89		065	SHIP					

Figure 60. R. R. Moore Specimen Routing Sheet.

APPENDIX II

GEAR TESTING DATA

DYNAMIC TESTING MACHINE INSTRUMENTATION

Digital Voltmeter - Hewlett Packard - Model 3439A
Automatic Range Selector - Hewlett Packard - Model 3442A
Rotating Torque Sensor - Lebow Associates, Inc. - Model 1241-101
Temperature Recorder - Taylor Instrument Company - Model 91JF
Temperature Recorder - Minneapolis Honeywell - Model K153X
Vibraswitch - Robertshaw Control Company - Model 66

Function and Purpose of Each Instrument

A digital voltmeter is used to monitor the torque in the system. Direct numerical readout combined with automatic range-changing features permits monitoring the signal of the torque sensors mounted between the cornerboxes and the output shafts of the test gearboxes.

The torque sensors are of the in-line rotating type having a Wheatstone bridge strain gage circuit. Each bridge is connected to slip rings with silver graphite brushes on the shaft, which provide the incoming bridge current and the outgoing strain signal.

A universal multipoint recorder is used to monitor bearing temperatures of the test box. Points are indicated and recorded by a turret wheel mechanism with records identified by various combinations of numbers and symbols.

An air-operated temperature recorder-controller is used to monitor and control the oil temperature in the test box. A preset alarm system shuts off the main drive motor in the event that the test box lubricant temperature exceeds the set point.

The stress-cycle counter consists of a photoelectric cell and a light source which is interrupted through approximately 120 degrees of rotation by a slotted disc. This is used to provide an electrical signal to a two-digit electronic counter which triggers a mechanical counter after each 100 rotations of the gear shaft.

BEVEL GEAR PULSER INSTRUMENTATION

Oscilloscope - Hewlett Packard - Model 140A

Digital Voltmeter - Ballantine - Model 355

Strain Indicator - The Budd Company - Model P-350

TABLE XV. DEFLECTION TEST SUMMARY

Indicator Position	Displacement Unit - Inches											
	12-Inch Cutter Diameter Gear Torque (lb.-in.)				7 1/2-Inch Cutter Diameter Gear Torque (lb.-in.)							
	35, 800	50, 000	71, 600	100, 000	35, 800	50, 000	71, 600	100, 000	100, 000	50, 000	71, 600	100, 000
1	-002	-003	-0045	-006	-0025	-0035	-005	-006	-0025	-0035	-005	-006
1A	-0015	-0025	-004	-005	-002	-0025	-004	-0055	-002	-0025	-004	-0055
1B	-002	-0025	-0035	-0045	-002	-0025	-0035	-004	-002	-0025	-0035	-004
1L	-001	-002	-0025	-003	-002	-0025	-003	-004	-002	-0025	-003	-004
1LA	0	0	-001	0	0	0	0	0	0	0	0	0
1LB	0	-0005	-001	-002	-001	-001	-002	-0025	-001	-001	-002	-0025
1R	0	-001	-001	-002	-001	-001	-002	-0035	-001	-001	-002	-0035
1RA	0	0	0	-002	0	0	-002	+0005	0	+0005	+0005	+0005
2	0	0	0	0	0	0	0	0	0	0	0	0
2L	0	0	0	0	0	0	0	0	0	0	0	0
2LA	+0005	0	0	0	0	0	0	0	0	0	0	0
2LB	0	0	0	0	0	0	0	0	0	0	0	0
2R	0	-0005	-001	-0015	-0005	-001	-0015	-002	-001	-0015	-0015	-002
2RA	0	0	0	-001	0	0	-001	-0005	0	0	0	-0005
3	+002	+003	+004	+005	+002	+0025	+0035	+005	+002	+0035	+0035	+005
3A	+001	+0015	+002	+0035	+0015	+002	+0035	+0045	+0015	+003	+003	+0045
4	+002	+0025	+0035	+005	+0015	+0025	+0035	+0045	+0015	+0025	+003	+0045
4A	+002	+0025	+0035	+004	0	0	+004	+0005	0	+0005	+0005	+0005
5	-001	-001	-001	-001	-0005	-001	-001	-0015	-0005	-0005	-0005	-0005
5A	0	0	0	+001	-0005	-001	+001	0	-0005	0	0	0
5B	0	+003	+005	+007	+0025	+004	+007	+0085	+0025	+006	+0005	+0085
5T	0	0	0	0	0	0	0	+001	0	+0005	+001	+001
6	0	0	-0005	-001	-0005	-001	-001	-0015	-0005	-001	-0015	-002
6A	0	-0005	-001	-001	0	0	-001	0	0	0	0	0

TABLE XV - Continued

Indicator Position	Displacement Unit - Inches											
	12-Inch Cutter Diameter				7 1/2-Inch Cutter Diameter				Gear Torque (lb-in.)			
	35,800	50,000	71,600	100,000	35,800	50,000	71,600	100,000	35,800	50,000	71,600	100,000
7	0	-0005	-001	-0015	-0005	-001	-0015	-002	-0005	-001	-0015	-002
7A	-0005	-001	-001	-0015	0	-0005	-0015	-001	-0005	-0005	-0005	-001
7B	0	0	0	+001	0	0	+0005	+0005	0	+0005	+0005	+0005
8	-001	-001	-0015	-003	-001	-001	-0025	-0025	-001	-001	-002	-0025
8A	-001	-001	-0015	-002	-0005	-001	-0015	-0015	-001	-001	-001	-0015
8B	0	0	0	0	0	+0005	0	0	+0005	+0005	+0005	+001
9	+0015	+0015	+003	+005	+0015	+003	+005	+007	+003	+0045	+0045	+007
9A	0	0	+0005	+001	0	0	+001	+0015	0	+001	+001	+0015
10	+003	+004	+005	+0075	+003	+004	+0075	+007	+003	+0055	+0055	+007
10A	+004	+005	+006	+0085	+003	+004	+0085	+0075	+003	+0055	+0055	+0075
10B	+002	+0025	+004	+005	+0025	+003	+005	+0055	+0025	+004	+004	+0055
10L	+0005	+001	+001	+0015	+0005	+0005	+0015	+001	+0005	+0005	+001	+001
10LA	0	0	-0005	-001	0	0	-001	-001	0	-0005	-0005	-001
10LB	-001	-0015	-002	-0025	-001	-001	-0025	-002	-001	-0015	-0015	-002
10R	+0035	+005	+006	+0085	+003	+004	+0085	+0075	+003	+0055	+0055	+0075
10RA	0	0	+0005	+0005	0	0	+0005	0	0	0	0	0
11	-002	-0025	-004	-005	-0025	-0035	-005	-0055	-0025	-0035	-0045	-0055
11A	0	-0005	-0005	-001	0	0	-001	0	0	0	0	0
13	+001	+0015	+002	+003	+001	+0015	+003	+0025	+001	+0015	+002	+0025
13L	0	0	0	0	0	0	0	0	0	0	0	0
13R	+0035	+0045	+0055	+0075	+003	+004	+0075	+0075	+003	+004	+0055	+0075
13RA	0	0	0	0	0	0	0	0	0	0	0	0
15	-0005	-001	-001	-001	-001	-001	-001	-001	-001	-001	-0015	-0015
16	-001	-001	-002	-002	-001	-001	-002	-002	-001	-001	-0015	-0015

TABLE XV - Continued

Indicator Position	Displacement Unit - Inches											
	12-Inch Cutter Diameter						7½-Inch Cutter Diameter					
	Gear Torque		71,600		100,000		Gear Torque		71,600		100,000	
17	-001	-001	-001	-001	-001	-001	-0005	-0005	-001	-001	-001	-001
18	-0015	-002	-002	-003	-003	-0035	-0015	-002	-003	-003	-0035	-0035
19	0	0	0	0	0	0	0	0	0	0	0	0
20	0	0	+0005	+0005	+0005	+0005	0	+0005	+0005	+0005	+001	+001
23	-002	-003	-0045	-0065	-0065	-007	-003	-004	-0055	-007	-0075	-0075
23L	-002	-0035	-005	-006	-006	-0075	-003	-004	-0055	-0075	-0075	-0075
23R	-0025	-0035	-005	-006	-006	-0065	-0025	-0035	-005	-0065	-0065	-0065
24	+003	+004	+006	+008	+008	+008	+003	+0045	+006	+008	+008	+008
24L	+003	+004	+0055	+008	+008	+008	+0025	+004	+005	+007	+007	+007
24R	+0035	+0045	+006	+008	+008	+008	+003	+0045	+006	+0075	+0075	+0075
25	0	0	+0005	+0005	+0005	+0005	+0005	+0005	+001	+001	+001	+001



Figure 61. Deflection Test Gear Tooth Contacts on 12-Inch Cutter Diameter Gear Design - Friction Load at Start of Test on Gear Convex Tooth Surface.



Figure 62. Deflection Test Gear Tooth Contacts on 12-Inch Cutter Diameter Gear Design - Friction Load at Start of Test on Gear Concave Tooth Surface.



Figure 63. Deflection Test Gear Tooth Contacts on 12-Inch Cutter Diameter Gear Design - 35,800 Lb-In. Gear Torque on Gear Convex Tooth Surface.



Figure 64. Deflection Test Gear Tooth Contacts on 12-Inch Cutter Diameter Gear Design - 50,000 Lb-In. Gear Torque on Gear Convex Tooth Surface.



Figure 65. Deflection Test Gear Tooth Contacts on 12-Inch Cutter Diameter Gear Design - 71,600 Lb-In. Gear Torque on Gear Convex Tooth Surface.



Figure 66. Deflection Test Gear Tooth Contacts on 12-Inch Cutter Diameter Gear Design - 100,000 Lb-In. Gear Torque on Gear Convex Tooth Surface.

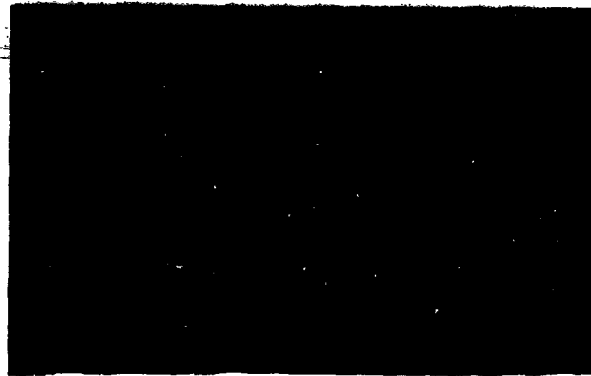


Figure 67. Deflection Test Gear Tooth Contacts on 12-Inch Cutter Diameter Gear Design - Friction Load at End of Test on Gear Convex Tooth Surface.

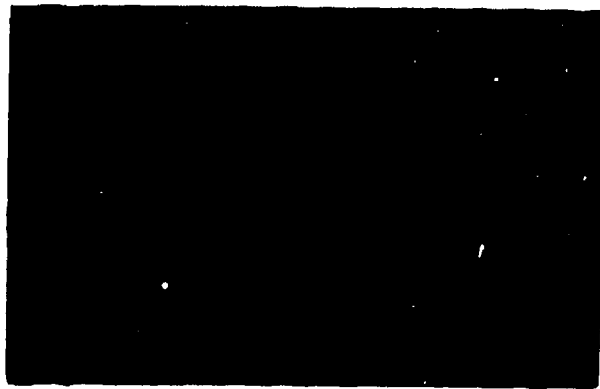


Figure 68. Deflection Test Gear Tooth Contacts on 12-Inch Cutter Diameter Gear Design - Friction Load at End of Test on Gear Concave Tooth Surface.



Figure 69. Deflection Test Gear Tooth Contacts on 7-1/2-Inch Cutter Diameter Gear Design - Friction Load at Start of Test on Gear Convex Tooth Surface.



Figure 70. Deflection Test Gear Tooth Contacts on 7-1/2-Inch Cutter Diameter Gear Design - 35,800 Lb-In. Gear Torque on Gear Convex Tooth Surface.



Figure 71. Deflection Test Gear Tooth Contacts on 7-1/2-Inch Cutter Diameter Gear Design - 50,000 Lb-In. Gear Torque on Gear Convex Tooth Surface.



Figure 72. Deflection Test Gear Tooth Contacts on 7-1/2-Inch Cutter Diameter Gear Design - 71,600 Lb-In. Gear Torque on Gear Convex Tooth Surface.



Figure 73. Deflection Test Gear Tooth Contacts on 7-1/2-Inch Cutter Diameter Gear Design - 100,000 Lb-In. Gear Torque on Gear Convex Tooth Surface.

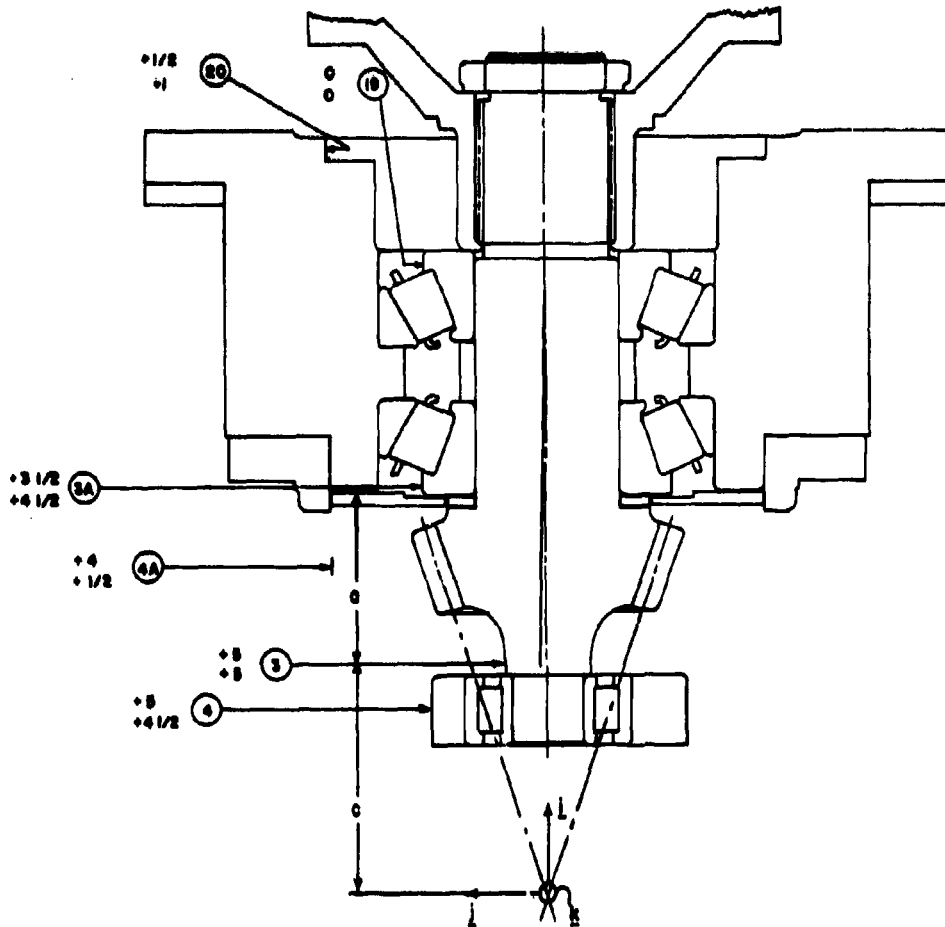


Figure 74. Deflection Test Gear Tooth Contacts on 7-1/2-Inch Cutter Diameter Gear Design - Friction Load at End of Test on Gear Convex Tooth Surface.



Figure 75. Deflection Test Gear Tooth Contacts on 7-1/2-Inch Cutter Diameter Gear Design - Friction Load at End of Test on Gear Concave Tooth Surface.

BLANK PAGE



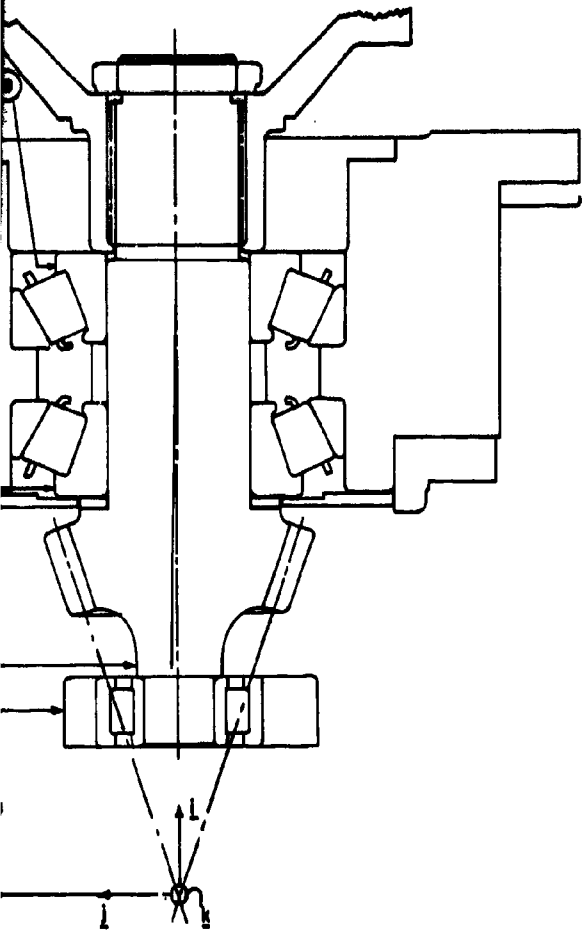
NOTES

- (1) PLUS DEFLECTION IS TO THE RIGHT, MINUS DEFLECTION IS TO THE LEFT.
- (2) INDIVIDUAL INDICATOR VALUES AT 100% LOAD ARE IN THOUSANDTHS OF AN INCH. THE 12" CUT IS FOR THE 7/16" CUT EXCEPT FOR THE 7/16" CUT.
- (3) DEFLECTIONS OF THE PINION SHAFT ARE SHOWN AT A SECTION THROUGH THE SOLID LINE.

(PINION SHAFT HORIZONTAL)

Figure 76. Side Elevation of Pinion Mounted in Test Box Showing Locations of Indicators for Measuring Displacements.

A



NOTES

(1) PLUS DEFLECTION IS TOWARD AN INDICATOR
MINUS DEFLECTION IS AWAY FROM AN INDICATOR.

(2) INDIVIDUAL INDICATOR READINGS GIVEN ARE MAXIMUM
VALUES AT 100% LOAD, AND ARE STATED IN
THOUSANDTHS OF AN INCH. THE UPPER FIGURE
IS FOR THE 12" CUTTER, WHILE THE LOWER
IS FOR THE 7-1/2" CUTTER.

EXAMPLE

③ 5 ← .005 12" CUTTER.
5 ← .005 7-1/2" CUTTER.

(3) DEFLECTIONS OF THE GEAR AND PINION CENTERLINES
ARE SHOWN AT A SCALE OF 100" = .050"
SOLID LINES ——— SHOW DEFLECTION IN 12" CUTTER

(PINION SHAFT HORIZONTAL)

tion of Pinion Mounted in Test Box Showing
of Indicators for Measuring Displacements.

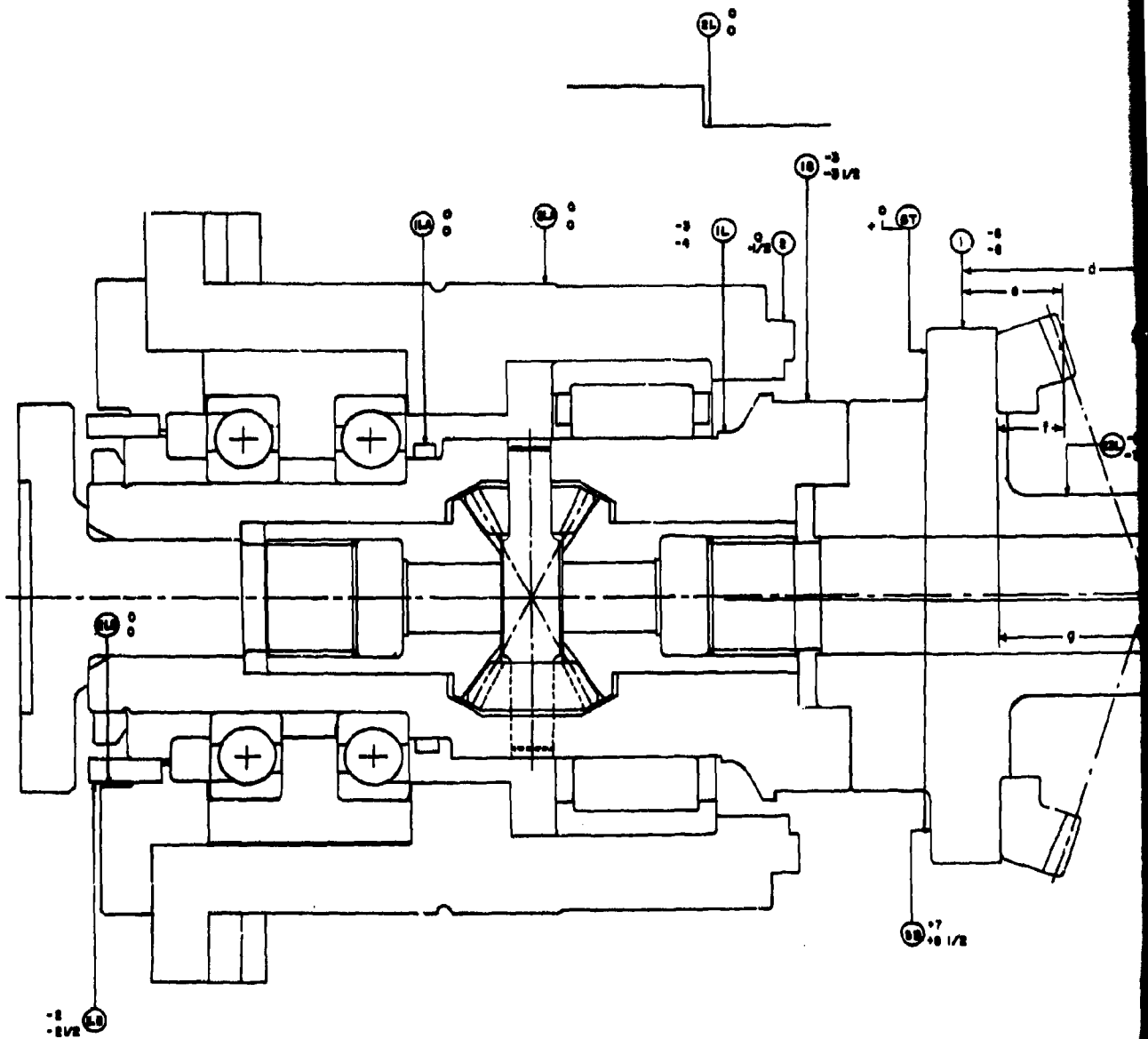


Fig. 77. Front Elevation of Gear Mounted in Test Box Showing Locations of Indicators for Measuring Displacements.

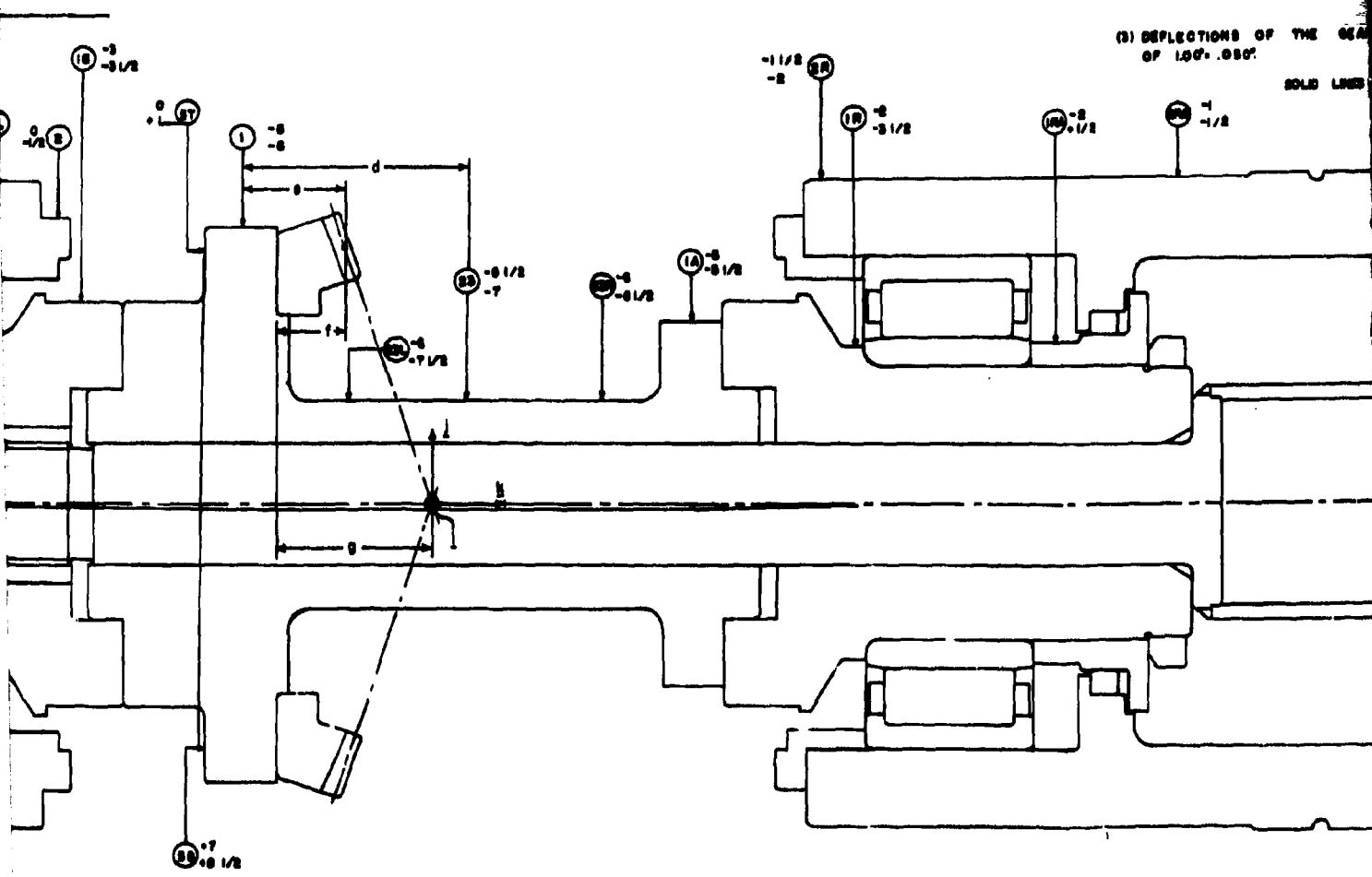
A

NOTES

- (1) PLUS DEFLECTION IS TOWARD MINUS DEFLECTION IS AWAY
- (2) INDIVIDUAL INDICATOR READINGS ARE STATED IN THOUSANDS OF INCHES, WHILE THE

- (3) DEFLECTIONS OF THE GEAR OF 1.00" .050"

SOLID LINE



Showing cements.

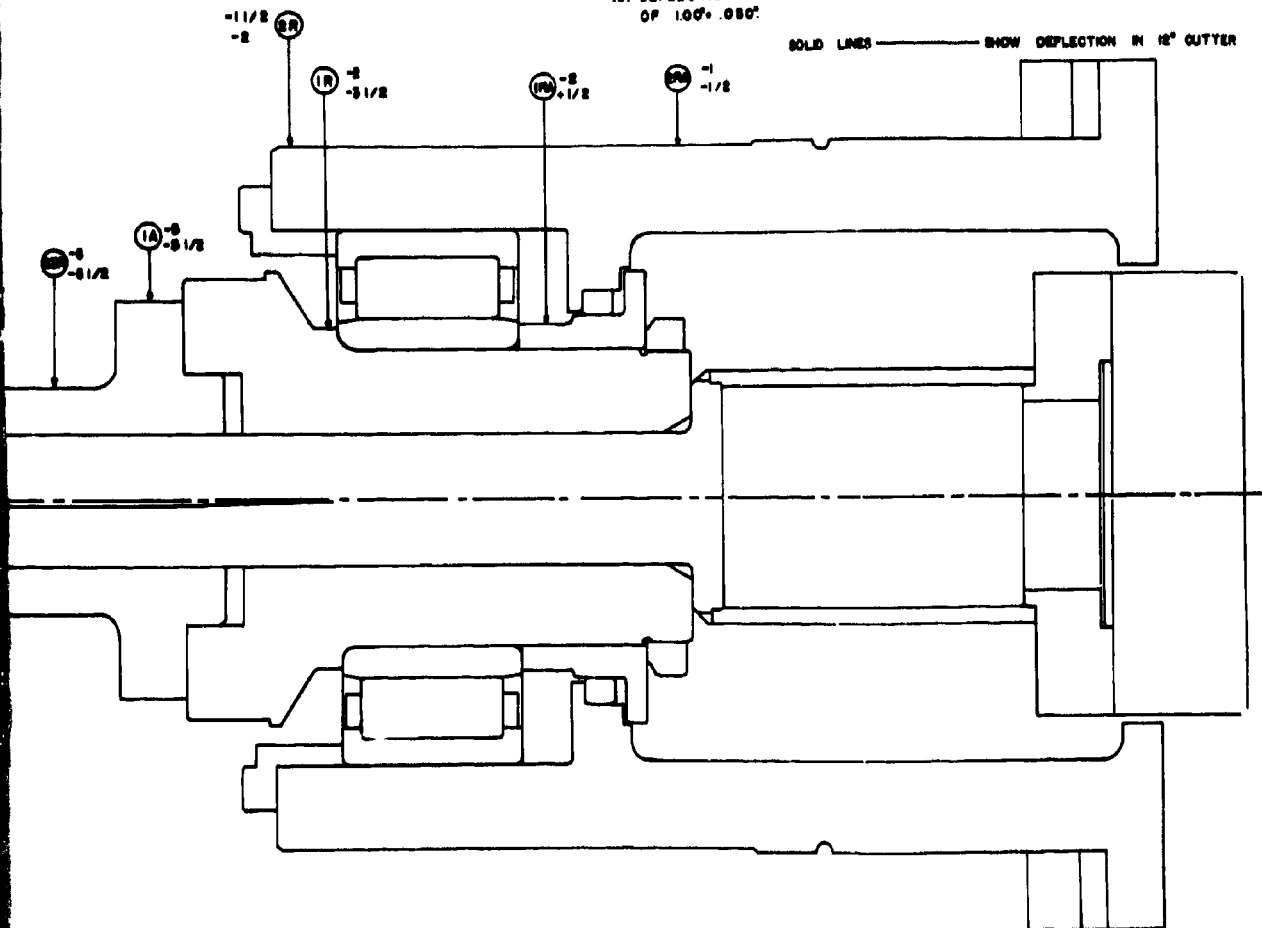
B

NOTES

- (1) PLUS DEFLECTION IS TOWARD AN INDICATOR
MINUS DEFLECTION IS AWAY FROM AN INDICATOR
- (2) INDIVIDUAL INDICATOR READINGS GIVEN ARE MAXIMUM VALUES AT 100% LOAD,
AND ARE STATED IN THOUSANDTHS OF AN INCH. THE UPPER FIGURE IS FOR
12" CUTTER, WHILE THE LOWER IS FOR 7 1/2" CUTTER.

EXAMPLE (1) $\begin{matrix} -6 & \text{---} & .008 & \text{12" CUTTER} \\ -8 & \text{---} & .008 & \text{7 1/2" CUTTER.} \end{matrix}$

- (3) DEFLECTIONS OF THE GEAR CENTERLINES ARE SHOWN AT A SCALE
OF 100 \times .050"



B

C

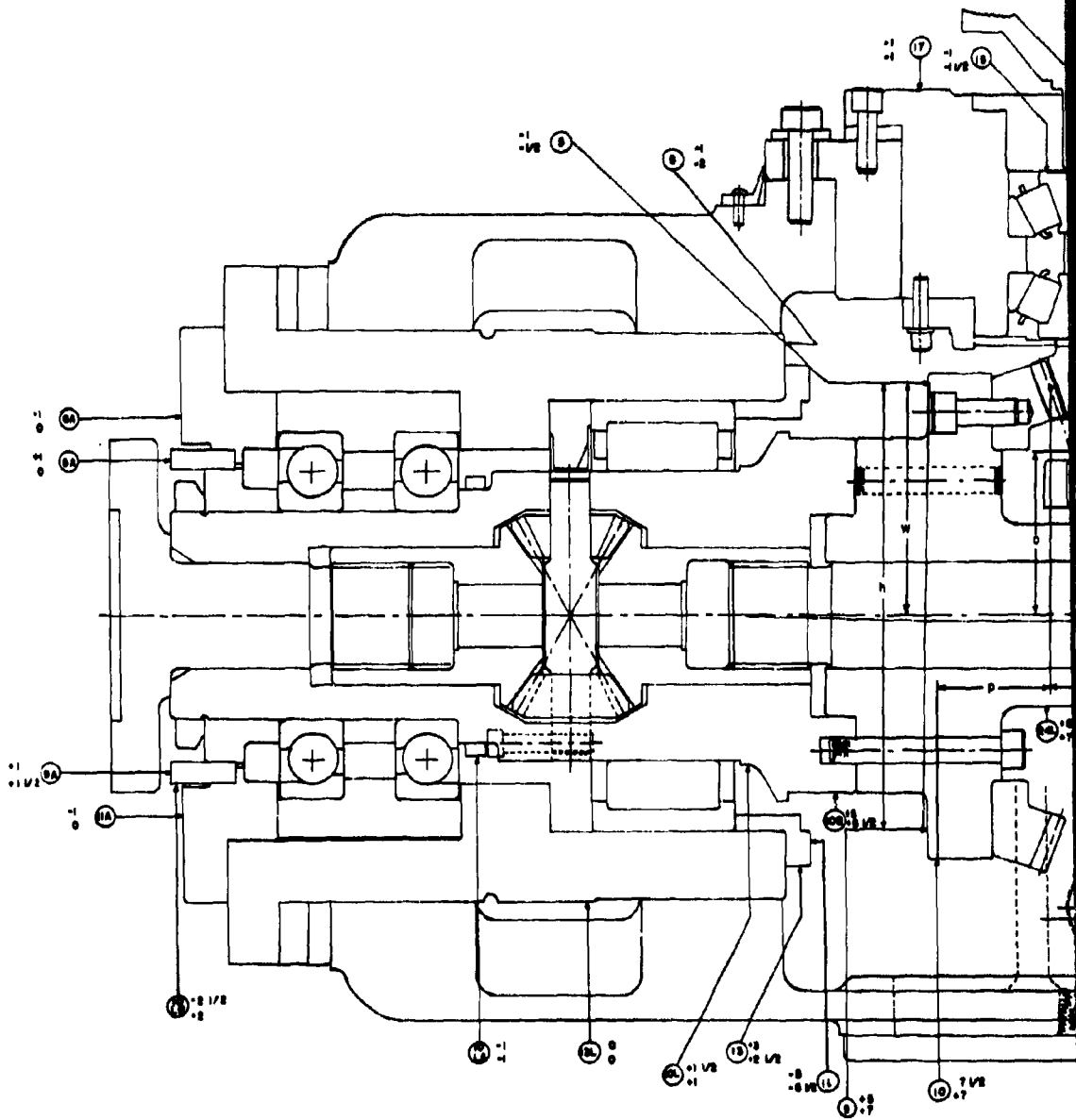


Figure 78. Plan View of Gear and Pinion Mounted in Test Box Showing Locations of Indicators for Measuring Displacements.

A

APPENDIX III

EFFECTIVE FACE WIDTH

This appendix consists of a detailed description of the derivation of the effective face width, F_e . The concept of effective face width has been in use for a number of years and was first introduced for use in bevel gear strength formulas in 1952, Reference B. This concept, as introduced at that time, improved the accuracy of bevel gear strength calculations considerably, and was based on a simplified theory that has since been found to be somewhat inaccurate. The derivation of a new formula for effective face width is outlined below and is based on a thorough strain gage study of gear tooth models.

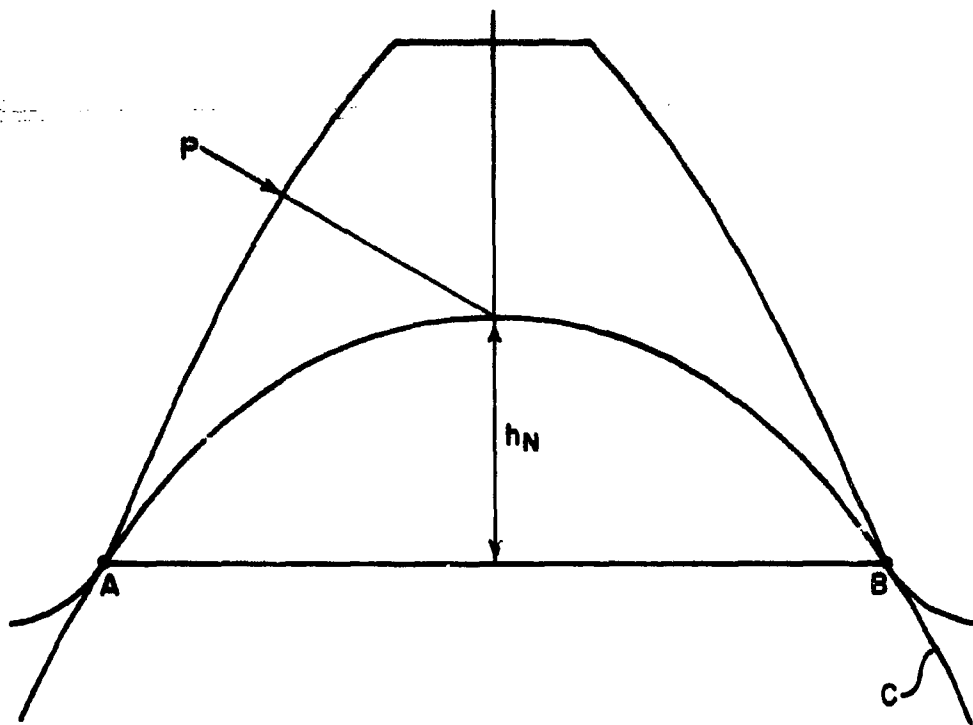
The purpose of the effective face width formula is to account for the following:

1. The fillet stress of a gear tooth is a maximum at a point in the fillet below the instantaneous line of contact and is not uniformly distributed over the tooth, as many calculation methods assume. This becomes obvious in the case of a very long tooth and a relatively short line of contact.
2. The pinion member of a pair is often designed with a longer tooth for increased strength. Calculation procedures assuming concentrated point loads do not provide for this difference in gear and pinion face widths in determining the final stresses.

In the derivation of the formulas for F_e , the following assumptions are made:

1. Calculations are made in a mean section assuming the load at a height h_N above the root of the tooth; see Figure 79.
2. It is generally recognized that for a given line of contact on a crowned gear tooth, the load is not uniformly distributed along the line of contact. In this derivation it is assumed that the load distribution along the line of contact is elliptical. This will result in non-uniform stress along the root of the tooth.

The ratio of the maximum stress to the average stress can be considered as resulting from a reduction in the face width by an amount inversely proportional to the increase in stress. This decreased face width is called the effective face width and is defined as:



- P = APPLIED LOAD
- C = INSCRIBED PARABOLA
- \overline{AB} = ASSUMED WEAKEST SECTION IN ROOT OF TOOTH
- h_N = HEIGHT ALONG TOOTH CENTER LINE FROM THE WEAKEST SECTION TO THE POINT OF LOAD APPLICATION

Figure 79. Mean Section Through Tooth Showing Load Height, h_N .

$$F_e = F(s_{avg}/s_{max}) \quad (1)$$

where F_e = effective face width

F = actual face width

s_{max} = maximum stress along the root of the tooth produced by the assumed tooth loading

s_{avg} = average stress along the root of the tooth produced by a uniform load distribution along the total length of the tooth at the assumed load height used for s_{max} *

DERIVATION

The derivation of the formulas for F_e is based on general formulas for s_{avg} and s_{max} . These stresses are in turn based on calculations that yield the stress distribution in the root of any specified gear tooth. Thus, the derivation amounts to finding for a given tooth the average stress caused by a uniform load across the tooth at height h_N (s_{avg}) and that caused by an elliptical load along a calculated line of contact (s_{max}) also at height h_N .

In 1966, the contractor conducted an experimental investigation to determine the strain distribution in different curved gear tooth models, Reference 14. A certain portion of that work as applied to symmetric teeth is applicable in the derivation of the new effective face width formulas. A brief description of this prior work is included to give the reader a full understanding of how the different stress distributions are determined. In this analysis, stress is assumed to be proportional to strain.

*The actual stress distribution along the root of the tooth resulting from a uniform load distribution closely approximates a uniform stress. However, the departure from uniformity has been considered in arriving at the final formulas.

Strain Distributions in Curved Gear Tooth Models

Experimental Data

Five equally spaced strain gages were mounted lengthwise along the fillets on both sides of the teeth on each of three aluminum gear tooth models. Considerable attention was given to mounting these gages at equal heights above the tooth root. The geometric configurations of the tooth models chosen for this analysis are shown in Table XVIII.

Model Part Number	Pressure Angle (deg)	Nominal Cutter Diameter (in.)
1	20	8.00
2	15	8.00
3	25	8.00

Equal point loads were successively applied normal to the tooth surface on both sides of each tooth at 33 separate locations. The loading matrix, shown in Figure 33, consisted of 3 rows of 11 equally spaced points. For each point load, the 5 tensile strains were recorded. The strain data were refined to minimize any experimental error. It was intended in this analysis to simulate a contact line on the model tooth by a series of point loads along that line.

Data Analysis Program

A computer program was written for the purpose of analyzing the experimental data. The strain gage data for a specified (convex or concave) side of a tooth, which were used as input to the program, determine a set of five strain readings for any contact line on that tooth by superposition of a specified number of uniformly spaced point loads.

Input items include:

1. Strain data in the form of a 33 x 5 matrix; i. e., 33 load points and 5 strain gage readings for each load point
2. Coordinates of the end points of the desired contact line
3. Type of load distribution along the contact line (uniform, elliptical, parabolic)
4. Number of uniformly spaced discrete point loads used to simulate the line load
5. Coordinates of matrix loading points
6. Coordinates of strain gages

Although it is possible to use any number of point loads to simulate a line load, it was found here that 11 points were sufficient to represent any line within the degree of accuracy commensurate with the experimental data. The location of these uniformly spaced points is calculated automatically by the program. For the points not part of the original loading matrix, a second-order interpolation procedure was included to calculate the corresponding strains at each of the gages.

Exponential Curve Fit

It was established for these models that the lengthwise stress distribution in the root of the teeth due to both uniform and elliptical loads can be described by the following equation:

$$Y = A \exp B(x+C)^2 \quad (7)$$

where

Y = the stress

A, B, and C = parameters describing the gear tooth geometry, load line geometry, and the load distribution

x = the lengthwise position along the tooth

Note: All models were of the same length.

For each of the contact lines applied to these models, A, B, and C can be calculated by the computer program to yield a specific equation $Y = A_1 \exp(B_1(x+C_1)^2)$. A_1 , B_1 , and C_1 were found in practice by fitting a power equation through the logarithms of the three highest of the five resulting strain readings. A computer program with a curve-fitting routine was available for power series but not for logarithmic expressions. It is of interest to note that this equation can be modified to fit a gear tooth of any length, provided A_1 , B_1 , and C_1 can be calculated, by nondimensionalizing the variable x by a scaling factor that is a function of the face width F . The length of the test models was 2.94 inches.*

$$\text{Thus, } Y = A \exp B(x \frac{F}{2.94 \cos \psi} + C)^2 \quad (8)$$

is obtained as the equation that describes the resulting stress distribution on any tooth due to either a uniform or an elliptical load distribution.

In practice, the parameters A_1 , B_1 , and C_1 are found by the same procedure that was used to find them for the test models. The mathematical steps involved are outlined below:

Upon taking logarithms of both sides of equation (8), the following equation is obtained:

$$\begin{aligned} \ln Y &= \ln A_1 + B_1 (x \frac{F}{2.94 \cos \psi} + C_1)^2 \quad (9) \\ &= (\ln A_1 + B_1 C_1^2) + 2C_1 B_1 \frac{F}{2.94 \cos \psi} x + B_1 \frac{F^2}{(2.94 \cos \psi)^2} x^2 \end{aligned}$$

or in general,

$$\ln Y = W_1 + W_2 x + W_3 x^2 \quad (10)$$

where the W_1 's are constants for a particular set of A_1 , B_1 , and C_1 . Upon back substitution, A_1 , B_1 , and C_1 can be solved in terms of the W_1 's as follows:

$$A_1 = \exp (W_1 - W_2^2/4W_3) \quad (11)$$

*The distance between the center of the strain gage on the far left and the center of the one on the far right was 2.72 inches.

$$B_i = W_3 \frac{(2.94 \cos \psi)^2}{F^2} \quad (12)$$

$$C_i = (W_2 F) / (2 W_3 2.94 \cos \psi) \quad (13)$$

Thus, knowing the W_i 's for a given line of contact for a given model, A_i , B_i , and C_i can be determined.

Calculation of W_i

As a first step, it is necessary to determine the values of W_i for selected contact lines with uniform as well as elliptical load distributions on the gear tooth models. To differentiate between the values of W_i for the two load distributions, the following change is made:

1. For uniform loads, W_i will be referred to as U_i .
2. For elliptical loads, W_i will be referred to as V_i .

Calculation of U_i (s_{avg}) for Uniform Loads

Three lines of contact were chosen and analyzed on both the convex and concave surfaces of each of the three models using the data analysis program to simulate the loading. The locations of the three lines of contact in the axial plane on each of the three models are shown in Figure 80. The data analysis program yielded for each line of contact a set of five strain readings and a set of coefficients U_1 , U_2 , and U_3 of an exponential equation, which defines a curve closely approximating the strain distribution along the tooth root. The values obtained for U_i for the 18 load lines are given in Table XIX.

Calculation of V_i (s_{max}) for Elliptical Loads

Fifteen contact lines were chosen and analyzed on both the convex and concave surfaces of each of the three models using the data analysis program to simulate the loading, Figure 81. These contact lines varied in:

1. Length (l_1) in the tangent plane.
2. Angle of inclination (w) of contact line with respect to pitch line in the tangent plane.

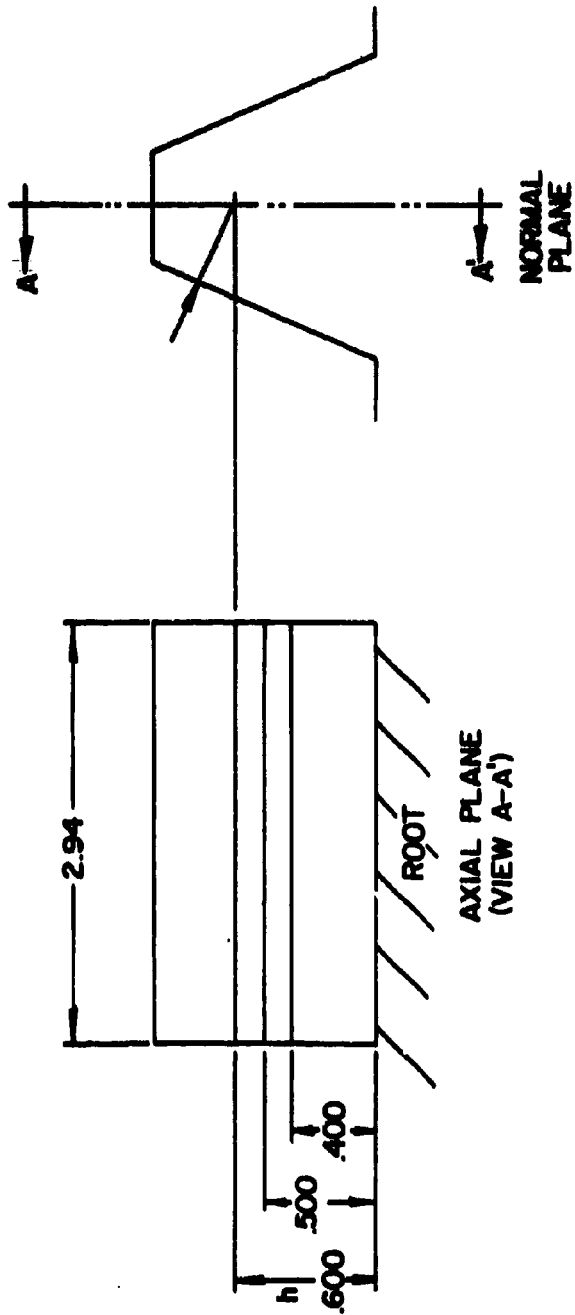


Figure 80. Location of Contact Lines on Tooth Models for Uniform Loading.

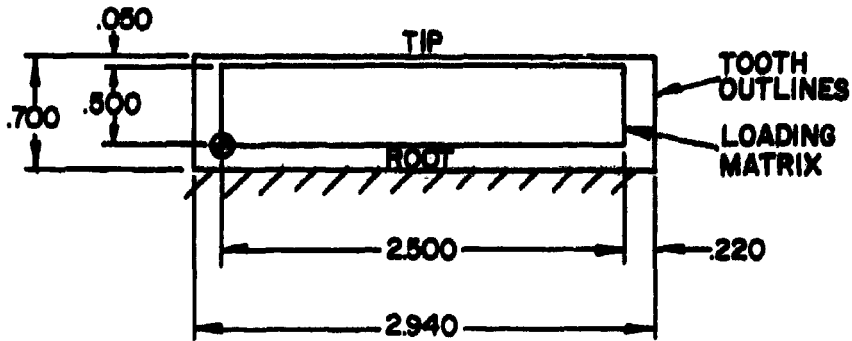
TABLE XIX. U_i AS CALCULATED FROM THE DATA ANALYSIS PROGRAM

Surface	(deg)	h (in.)	U_1	U_2	U_3
<u>Convex</u>	15	0.4	4.25	0.470	-0.176
	15	0.5	4.44	0.487	-0.182
	15	0.6	4.66	0.411	-0.153
	20	0.4	4.05	0.465	-0.171
	20	0.5	4.17	0.626	-0.230
	20	0.6	4.34	0.631	-0.232
	25	0.4	3.61	0.654	-0.236
	25	0.5	3.90	0.680	-0.246
	25	0.6	4.14	0.592	-0.218
<u>Concave</u>	15	0.4	4.33	0.264	-0.0972
	15	0.5	4.54	0.239	-0.0904
	15	0.6	4.70	0.233	-0.0855

TABLE XIX - Continued

Surface	(deg)	^h (in.)	U ₁	U ₂	U ₃
	20	0.4	3.89	0.712	-0.262
	20	0.5	4.13	0.666	-0.248
	20	0.6	4.29	0.670	-0.249
	25	0.4	4.35	-0.265	0.0976
	25	0.5	4.57	-0.291	0.107

LOCATION OF CONTACT LINES
 ELLIPTICAL LOADS
 (ALL DIMENSIONS IN AXIAL PLANE OF TOOTH)



⊙ = ORIGIN OF LOADING MATRIX AT THIS POINT $x_L = y_L = 0$

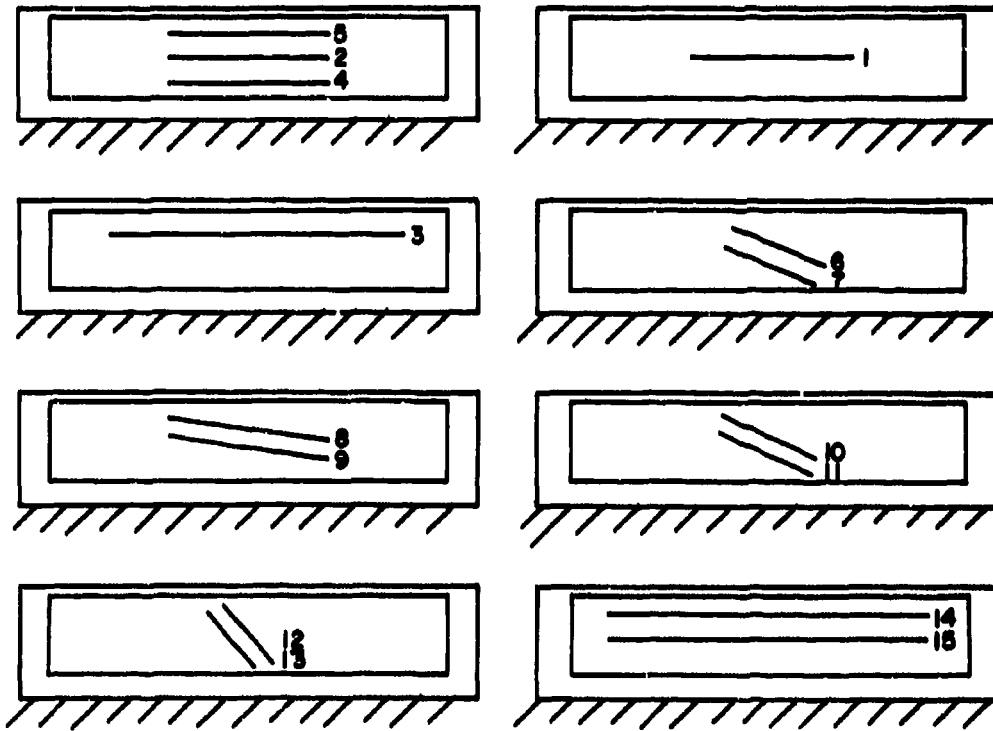


Figure 81. Sketch Showing Location of 15 Contact Lines Used in the Analysis for Effective Face Width.

3. Load height on the tooth (h_N) in the axial plane.

Their exact locations on the tooth are listed in Table XX.

For each line of contact, the data analysis program yielded a set of five strain readings and also the three coefficients V_1 , V_2 , and V_3 of an exponential equation, which defines a curve closely approximating the strain distribution along the tooth root.

An example of a strain distribution obtained in this way is given in Figure 82 for line No. 2, on the concave surface of model No. 1 (20° pressure angle). The values obtained for V_1 for the 90 load lines are shown in Table XXI.

Regression Analysis

From the calculated values of U_1 (Table XIX) and V_1 (Table XXI), general formulas for these parameters can be derived through multiple regression analysis.

Formulas for U_1

Each set of U_1 , U_2 , and U_3 values is used to describe s_{avg} , the stress distribution in the tooth root due to a uniform load distribution across the entire tooth length. The geometrical variables found to have a significant effect on U_1 are:

1. h_N = height along tooth centerline from the weakest section in the root of the tooth to the point of load application.
2. ϕ = normal pressure angle.
3. r_c = cutter radius.

The height h_N is nondimensionalized by dividing by h_t the total tooth height in the axial plane, and the cutter radius is nondimensionalized by dividing by $F/2 \cos \psi$. The latter results in the nondimensional variable $\beta = F/2r_c \cos \psi$. The values of two of the geometrical variables for the nine selected lines of contact are given in Table XXII. The value of β remained constant for the nine lines. The values of the geometrical variables and the corresponding values of U_1 serve as input to a multiple regression program. The final form of the equation of U_1 is:

**TABLE XX. COORDINATES OF CONTACT LINES
IN THE AXIAL PLANE**

Line No.	Left Coordinate*		Right Coordinate*	
	X _L	Y _L	X _R	Y _R
1	1.000	0.350	1.500	0.350
2	0.800	0.350	1.700	0.350
3	0.600	0.350	1.900	0.350
4	0.800	0.250	1.700	0.250
5	0.800	0.450	1.700	0.450
6	1.014	0.433	1.486	0.267
7	1.014	0.333	1.486	0.167
8	0.826	0.500	1.674	0.200
9	0.826	0.400	1.674	0.100
10	1.050	0.500	1.450	0.200
11	1.050	0.400	1.450	0.100
12	1.150	0.500	1.350	0.200
13	1.150	0.400	1.350	0.100
14	0.300	0.350	2.200	0.350
15	0.300	0.250	2.200	0.250

*Coordinates are given in the direction facing the surface of the tooth under study and with respect to the origin of the loading matrix shown in Figure 81.

TABLE XXI. V_i AS CALCULATED FROM THE DATA ANALYSIS PROGRAM

Surface	(deg)	Contact Line No.	V_1	V_2	V_3
<u>Convex</u>	15	1	2.22	4.70	-1.73
	15	2	2.61	4.01	-1.48
	15	3	2.99	3.31	-1.22
	15	4	2.28	4.22	-1.55
	15	5	2.86	3.87	-1.43
	15	6	2.24	4.70	-1.75
	15	7	1.90	4.95	-1.84
	15	8	2.66	4.05	-1.52
	15	9	2.35	4.26	-1.61
	15	10	2.20	4.81	-1.80
	15	11	1.83	5.10	-1.90
	15	12	2.05	5.05	-1.88
	15	13	1.63	5.41	-2.00

TABLE XXI - Continued

Surface	(deg)	Contact Line No.	V ₁	V ₂	V ₃
<u>Convex</u>	15	14	3.66	2.10	-0.775
	15	15	3.47	2.08	-0.769
	20	1	1.60	5.38	-1.97
	20	2	2.04	4.60	-1.69
	20	3	2.46	3.90	-1.44
	20	4	1.67	4.86	-1.78
	20	5	2.31	4.46	-1.64
	20	6	1.60	5.42	-2.00
	20	7	1.21	5.72	-2.11
	20	8	2.11	4.62	-1.73
	20	9	1.78	4.84	-1.82
	20	10	1.53	5.52	-2.07
	20	11	1.10	5.94	-2.20

TABLE XXI - Continued

Surface	(deg)	Contact Line No.	V ₁	V ₂	V ₃
<u>Convex</u>	20	12	1.31	5.92	-2.18
	20	13	0.850	6.32	-2.32
	20	14	3.18	2.62	-0.962
	20	15	3.01	2.57	-0.943
	25	1	1.18	5.70	-2.08
	25	2	1.72	4.81	-1.76
	25	3	2.26	3.87	-1.42
	25	4	1.35	5.05	-1.84
	25	5	2.00	4.68	-1.72
	25	6	1.23	5.69	-2.09
	25	7	0.706	6.16	-2.26
	25	8	1.78	4.86	-1.83
	25	9	1.47	5.06	-1.91

TABLE XXI - Continued

Surface	(deg)	Contact Line No.	V ₁	V ₂	V ₃
<u>Convex</u>	25	10	1.16	5.83	-2.15
	25	11	0.660	6.30	-2.32
	25	12	0.937	6.15	-2.25
	25	13	0.402	6.65	-2.42
	25	14	3.02	2.49	-0.911
	25	15	2.89	2.35	-0.859
<u>Concave</u>	15	1	1.53	5.74	-2.11
	15	2	2.05	4.86	-1.73
	15	3	2.60	3.89	-1.43
	15	4	1.65	5.20	-1.91
	15	5	2.32	4.64	-1.71
	15	6	1.56	5.73	-2.12
	15	7	1.16	6.10	-2.26

TABLE XXI - Continued

Surface	(deg)	Contact Line No.	V1	V2	V3
<u>Concave</u>	15	8	2.08	4.90	-1.83
	15	9	1.73	5.21	-1.96
	15	10	1.50	5.86	-2.17
	15	11	1.08	6.26	-2.32
	15	12	1.32	6.14	-2.27
	15	13	0.864	6.59	-2.44
	15	14	3.49	2.31	-0.849
	15	15	3.25	2.39	-0.877
	20	1	0.703	6.84	-2.51
	20	2	1.26	5.88	-2.16
	20	3	1.92	4.76	-1.75
	20	4	0.909	6.14	-2.26
	20	5	1.60	5.61	-2.06

TABLE XXI - Continued

Surface	(deg)	Contact Line No.	V ₁	V ₂	V ₃
Concave	20	6	0.703	6.88	-2.54
	20	7	0.339	7.18	-2.65
	20	8	1.35	5.89	-2.21
	20	9	1.03	6.11	-2.29
	20	10	0.629	7.03	-2.61
	20	11	0.318	7.26	-2.70
	20	12	0.423	7.33	-2.71
	20	13	0.0890	7.58	-2.80
	20	14	2.95	2.95	-1.09
	20	15	2.71	3.02	-1.11
	25	1	0.915	6.27	-2.30
	25	2	1.56	5.19	-1.91
	25	3	2.23	4.04	-1.48

TABLE XXI - Continued

Surface	(deg)	Contact Line No.	V_1	V_2	V_3
<u>Concave</u>	25	4	1.15	5.56	-2.05
	25	5	1.80	5.04	-1.85
	25	6	0.914	6.31	-2.33
	25	7	0.475	6.75	-2.50
	25	8	1.60	5.26	-1.98
	25	9	1.21	5.64	-2.13
	25	10	0.829	6.49	-2.41
	25	11	0.393	6.93	-2.58
	25	12	0.598	6.83	-2.53
	25	13	0.113	7.34	-2.71
	25	14	3.24	2.26	-0.832
	25	15	3.00	2.36	-0.866

TABLE XXII. GEOMETRIC VARIABLES FOR U_1

Model No. *	Load Height From the Root of the Tooth (in.)	$X_1 = \frac{h_N}{ht}$ **	$X_2 = \phi$ (rad)
2	0.4	0.429	0.262
	0.5	0.566	0.262
	0.6	0.720	0.262
1	0.4	0.403	0.349
	0.5	0.563	0.349
	0.6	0.723	0.349
3	0.4	0.376	0.436
	0.5	0.550	0.436
	0.6	0.726	0.436

*For models 1, 2, and 3, ϕ equals 20°, 15°, and 25°, respectively.

**Each value of h_N is determined from a normal view layout at the mean section of the tooth.

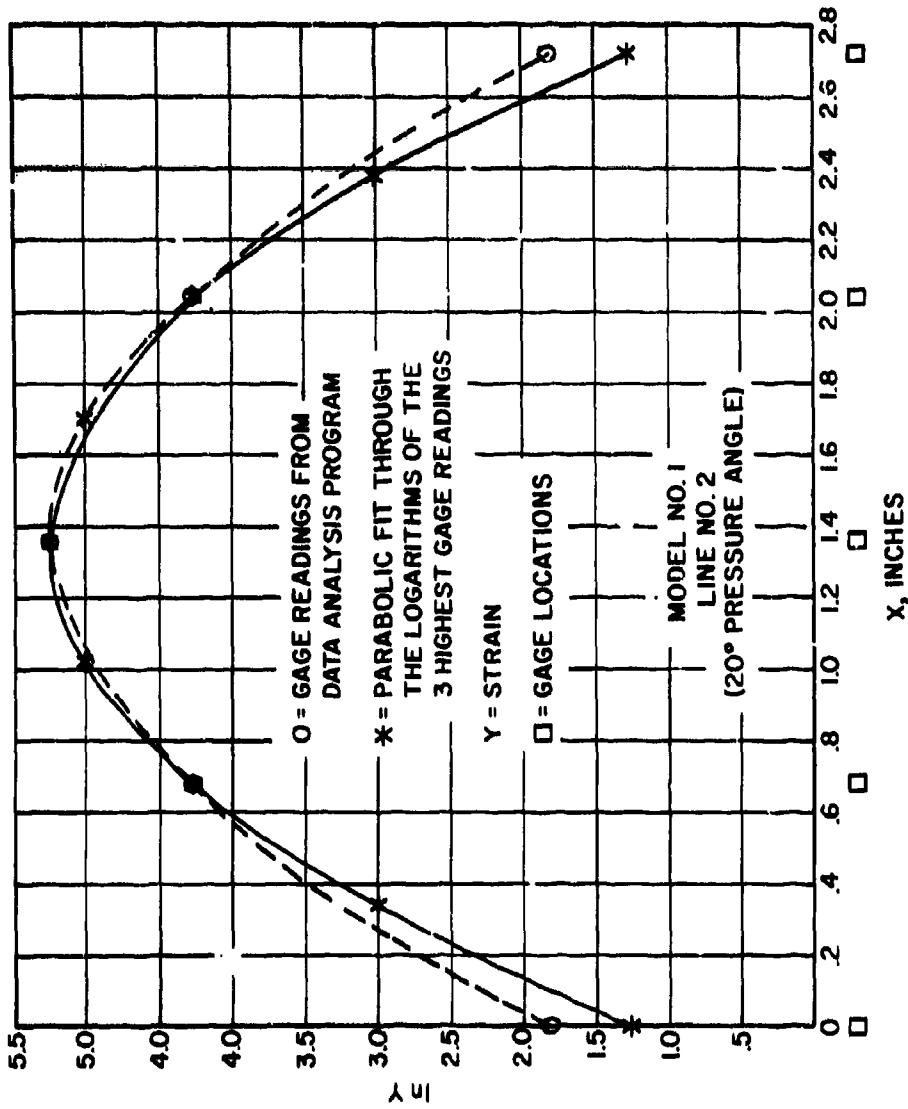


Figure 82. Curve Fit for Strain Distribution Along the Tooth Root on the Tooth Models.

$$\begin{aligned}
 U_1 = & (C_1 \pm C_2 \beta) + (C_3 \pm C_4 \beta) \left(\frac{h_N}{h_t} \right) + (C_5 \pm C_6 \beta) (\phi) \\
 & + (C_7 \pm C_8 \beta) \left(\frac{h_N}{h_t} \right)^2 + (C_9 \pm C_{10} \beta) (\phi)^2
 \end{aligned} \quad (14)$$

where C_1 through C_{10} are determined from the regression coefficients from the computer program.

The upper sign is for the concave surface, and the lower sign is for the mating convex surface.

The final formulas for U_1 are:

$$\begin{aligned}
 U_1 = & (7.29 \pm 7.21 \beta) + (1.48 \pm 2.60 \beta) \left(\frac{h_N}{h_t} \right) \\
 & - (20.9 \pm 50.2 \beta) \phi - (0.273 \pm 2.36 \beta) \left(\frac{h_N}{h_t} \right)^2 \\
 & + (28.0 \pm 78.3 \beta) \phi^2
 \end{aligned} \quad (15)$$

$$\begin{aligned}
 U_2 = & - (5.01 \pm 11.2 \beta) + (0.800 \mp 4.60 \beta) \left(\frac{h_N}{h_t} \right) \\
 & + (32.0 \pm 77.8 \beta) \phi - (0.717 \mp 3.98 \beta) \left(\frac{h_N}{h_t} \right)^2 \\
 & - (47.1 \pm 120 \beta) \phi^2
 \end{aligned} \quad (16)$$

$$\begin{aligned}
 U_3 = & (1.85 \pm 4.19 \beta) - (0.321 \mp 1.61 \beta) \left(\frac{h_N}{h_t} \right) \\
 & - (11.8 \pm 28.8 \beta) \phi + (0.284 \mp 1.39 \beta) \left(\frac{h_N}{h_t} \right)^2 \\
 & + (17.4 \pm 44.4 \beta) \phi^2
 \end{aligned} \quad (17)$$

The formulas for U_1 , U_2 , and U_3 are included in the computer program. For straight bevels $\beta = 0$, U_1 , U_2 , and U_3 are the same for both the gear and mating pinion surfaces.

Formulas for V_1

Each set of V_1 , V_2 , and V_3 values is used to describe the stress distribution in the tooth root due to an elliptical load distribution along the instantaneous line of contact. The following geometrical variables found to have a significant effect on V_1 are:

1. h_N = height along tooth centerline from the weakest section in the root of the tooth to the point of load application.
2. F_K = projected length of the line of contact in the lengthwise direction of the tooth.
3. w = angle of inclination of the line of contact with respect to the pitch line measured in the tangent plane.
4. ϕ = normal pressure angle.
5. r_c = cutter radius.

The variables h_N and F_K were made nondimensional by dividing them by h_t and F_R , respectively; h_t is the total tooth height in the axial plane, and F_R is the root line face width. The values of these variables are calculated for the 45 lines of contact (15 lines on each of the three models). See Table XXIII. The value of β remained constant for all lines of contact.

The final formulas for V_1 are:

$$\begin{aligned} V_1 = & (5.27 \pm 5.80 \beta) + (1.90 \pm 0.530 \beta) \left(\frac{h_N}{h_t} \right) \\ & + (4.07 \pm 1.84 \beta) \left(\frac{F_K}{F_R} \right) - (0.117 \mp 0.179 \beta) w \\ & - (29.6 \pm 48.0 \beta) \phi + (36.7 \pm 73.0 \beta) \phi^2 \end{aligned} \quad (18)$$

$$\begin{aligned} V_2 = & - (1.00 \pm 7.48 \beta) - (1.51 \pm 0.570 \beta) \left(\frac{h_N}{h_t} \right) \\ & - (7.28 \pm 2.60 \beta) \left(\frac{F_K}{F_R} \right) + (0.173 \mp 0.155 \beta) w \\ & + (49.7 \pm 61.8 \beta) \phi - (66.1 \pm 93.5 \beta) \phi^2 \end{aligned} \quad (19)$$

TABLE XXIII. GEOMETRIC VARIABLES FOR V_1

Model No. #	Contact Line No.	$X_1 = \frac{hN}{h_t}^{**}$	$X_2 = \frac{FK}{FR}$	$X_3 = W$ (rad)	$X_4 = \phi$ (rad)
2	1	0.566	0.170	0.0	0.262
	2	0.566	0.306	0.0	0.262
	3	0.566	0.442	0.0	0.262
	4	0.429	0.306	0.0	0.262
	5	0.720	0.306	0.0	0.262
	6	0.566	0.171	0.349	0.262
	7	0.429	0.171	0.349	0.262
	8	0.566	0.307	0.351	0.262
	9	0.429	0.307	0.351	0.262
	10	0.566	0.172	0.660	0.262
	11	0.429	0.172	0.660	0.262
	12	0.566	0.126	0.999	0.262
	13	0.429	0.126	0.999	0.262
	14	0.566	0.647	0.0	0.262
	15	0.429	0.647	0.0	0.262
1	1	0.563	0.170	0.0	0.349
	2	0.563	0.306	0.0	0.349
	3	0.563	0.442	0.0	0.349
	4	0.403	0.306	0.0	0.349
	5	0.723	0.306	0.0	0.349
	6	0.563	0.171	0.358	0.349
	7	0.403	0.171	0.358	0.349
	8	0.563	0.308	0.360	0.349
	9	0.403	0.308	0.360	0.349
	10	0.563	0.174	0.674	0.349
	11	0.403	0.174	0.674	0.349
	12	0.563	0.128	1.01	0.349
	13	0.403	0.128	1.01	0.349
	14	0.563	0.647	0.0	0.349

TABLE XXIII - Continued

Model No. *	Contact Line No.	$X_1 = \frac{h_N^{**}}{h_t}$	$X_2 = \frac{F_K}{F_R}$	$X_3 = W$ (rad)	$X_4 = \phi$ (rad)
1	15	0.403	0.647	0.0	0.349
3	1	0.550	0.170	0.0	0.436
	2	0.550	0.306	0.0	0.436
	3	0.550	0.442	0.0	0.436
	4	0.376	0.306	0.0	0.436
	5	0.726	0.306	0.0	0.436
	6	0.550	0.172	0.370	0.436
	7	0.376	0.172	0.370	0.436
	8	0.550	0.310	0.372	0.436
	9	0.376	0.310	0.372	0.436
	10	0.550	0.177	0.691	0.436
	11	0.376	0.177	0.691	0.436
	12	0.550	0.131	1.03	0.436
	13	0.376	0.131	1.03	0.436
	14	0.550	0.647	0.0	0.436
	15	0.376	0.647	0.0	0.436

*For models 1, 2, and 3, ϕ equals 20°, 15°, and 25°, respectively.

**Each value of h_N is determined from a normal view layout at the mean section of the tooth.

$$\begin{aligned}
V_3 = & (0.365 \pm 2.97 \beta) + (0.593 \pm 0.294 \beta) \left(\frac{h_N}{n_t} \right) \\
& + (2.69 \pm 1.01 \beta) \left(\frac{F_K}{F_R} \right) - (0.0727 \mp 0.0618 \beta) w \\
& - (18.5 \pm 23.8 \beta) \phi + (24.8 \pm 35.8 \beta) \phi^2
\end{aligned} \tag{20}$$

The upper sign is for the concave surface, and the lower sign is for the mating convex surface. The formulas for V_1 , V_2 , and V_3 are included in the computer program.

Final Formulas for s_{avg} and s_{max}

As stated in an earlier section of this appendix, the stress distributions in the root of the tooth for both the uniform and elliptical loads are described by equation (8),

$$Y = A \exp B \left(x \frac{F}{2.94 \cos \phi} + C \right)^2 \tag{8}$$

and in general by equation (10),

$$\ln Y = W_1 + W_2 x + W_3 x^2 \tag{10}$$

both of which are repeated here for reader convenience. Furthermore, by definition, s_{max} and s_{avg} are the maximum values of their respective distributions and can be obtained by differentiating equation (8) with respect to x . Differentiation yields A as the maximum value of Y . Equation (11) shows the relationship between A and the parameters W_i ; this equation is also repeated here.

$$A = \exp (W_1 - W_2^2 / 4W_3) \tag{11}$$

For s_{avg} , U replaces W ; for s_{max} , V replaces W .

The final expressions for s_{avg} and s_{max} are:

$$s_{avg} = \exp (U_1 - U_2^2 / 4U_3) \tag{22}$$

$$s_{max} = \exp (V_1 - V_2^2 / 4V_3) \tag{23}$$

Both equations are valid for gears as well as for pinions. However, the pinion and gear stresses will be different since the expressions for U_i and V_i are different for concave and mating convex surfaces.

Equations (22) and (23) were verified by comparing the calculated values of stress to those obtained directly from the data analysis program. For uniform loads applied to either concave or convex surfaces, the average absolute error between the stresses is less than 1.0 percent. For elliptical loads applied to concave surfaces, the average absolute error between the maximum stresses is less than 3 percent, and on convex surfaces the average absolute error is 5 percent. This is well within the measuring tolerances of the experiment.

Final Formula for Effective Face Width

The final formula for effective face width is:

$$F_e = F (s_{avg} / s_{max}) \quad (1)$$

In the previous section it was stated that the calculated stresses compared favorably with those obtained experimentally. This comparison also indicates the accuracy of the effective face width formula, since F_e is related to s_{avg} and s_{max} by equation (1). The effect of the new formula for effective face width is to raise the calculated stresses on both gear and pinion to a level approaching the true stresses in the teeth.

APPENDIX IV

LOAD DISTRIBUTION FACTOR

This appendix consists of a detailed description of the derivation of the load distribution factor, K_m . When a gear and mating pinion are loaded, the mounting deflections will create relative displacements of the two members, which will cause the original tooth contact to spread out and shift to a new position on the tooth surfaces. The purpose of the load distribution factor is to account for the increase in the stress due to the lengthwise shift of the tooth contact from the central lengthwise position.

The following derivation results in a formula for the load distribution factor as a function of the concave and convex tooth surfaces. In this program the contacting surface of one member (pinion or gear) is concave, and the contacting surface of the mating member is convex. Therefore, the load distribution factors on gear and mating pinion will generally be unequal.

CONTACT CONDITIONS

The development of the tooth contact on a gear pair, particularly the amount of mismatch (crowning) chosen and the lengthwise location of the contact, has a marked effect on gear tooth strength. Therefore, any set of formulas for calculating gear strength needs to make some basic assumptions about these items.

It is particularly important to consider the shift in tooth contact along the tooth due to mounting deflections as load is applied. It has recently become possible to calculate accurately the rate of this shift as a function of tooth design and the characteristics of the mountings. This makes it possible for the first time to include the effect of lengthwise tooth curvature (cutter diameter) in bevel gear strength formulas.

The basic assumption is that the tooth contact will be developed with the least amount of mismatch that will permit the full range of load, from zero to maximum, without the contact extending over the ends of the teeth.

Figure 83 shows the position of the tooth contact under no load. It has a length L_1 , and the center of pressure is a distance f from the center of the tooth.

Figure 84 shows the position of the tooth contact under peak load. It has a length l_2 , and the center of pressure is assumed to be at the center of the tooth; l_2 will generally be somewhat larger than l_1 because of elastic deformation of the surfaces under load.

Actually, the center of pressure does not necessarily coincide with the center of the tooth contact area. For this reason two coefficients have been introduced to modify the results. The coefficient k_3 permits a modification in the length of the tooth contact pattern under load. When k_3 equals zero, the tooth contact pattern under load will have the same length as the pattern under no load ($l_2 = l_1$). When k_3 equals unity, the tooth contact pattern under peak load T_0 will be equal to the tooth length ($l_2 = F \sec \psi$). Under the test conditions used for this program, a value of k_3 equal to unity best fits the test data and is therefore used in the program.

The second coefficient, k_4 , is the ratio of the load at which the center of contact pressure is located at the lengthwise center of the tooth to the load at which the center of the contact pattern is located at the lengthwise center of the tooth. As stated above, when the tooth contact pattern is located at the center of the tooth, the center of contact pressure does not necessarily lie in the center of the tooth. It is usual practice to develop the tooth contact pattern to be centrally located on the tooth under full load. However, there is evidence from previous tests that the center of pressure will lie toward the inner (toe) end of the tooth. From the present test data it has been determined that this ratio should be approximately 1.25. This means that the peak load T_0 is 25 percent higher than full load. The computer program has incorporated this value of $k_4 = 1.25$.

With further experience these two coefficients may require modification, but the values selected did fit the test data.

Derivation of Equations

Referring to Figures 83 and 84, the following simultaneous equations can be derived:

$$f = 1/2 F \sec \psi - 1/2 l_1 \quad (24)$$

$$f = k_1 r_m \quad (25)$$

$$k_2 = 250 / \sqrt[3]{D} \quad (26)$$

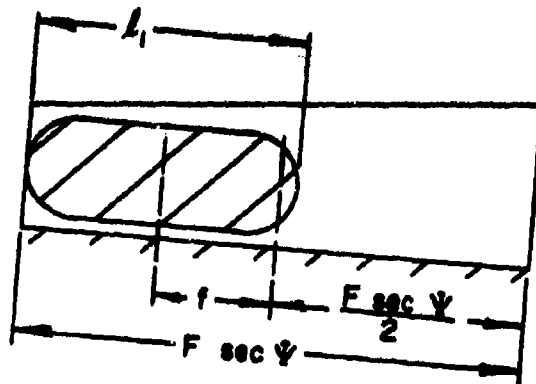


Figure 83. Assumed Position of the Tooth Contact Pattern Under No Load.

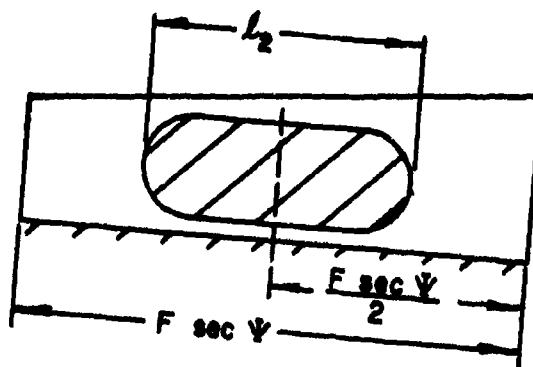


Figure 84. Assumed Position of the Tooth Contact Pattern Under Peak Load.

$$r_m = k_2 l_1^2 \quad (27)$$

where f = shift of contact position under load

l_1 = length of contact under light load

$F \sec \psi$ = tooth length

r_m = mismatch radius of curvature

D = gear pitch diameter

k_1 = calculable factor based on the adjustability coefficients for the particular design, and the mounting characteristics

Equation (24) is apparent from Figure 83.

Equation (25) follows from the definition of adjustability and the factor k_1 .

Equations (26) and (27) are obtained from experience relating the observed length of contact under light load to the mismatch in the gear set and the gear size.

Simultaneous solution of these equations yields the following equation for l_1 :

$$l_1 = \frac{1}{4k_1k_2} \left(\sqrt{1 + 8k_1k_2 F \sec \psi} - 1 \right) \quad (28)$$

It can be demonstrated that for the limiting case of $k_1 = 0$ (no shift of the contact under load), the value of l_1 becomes $F \sec \psi$ as would be expected.

It is convenient to consider the length of contact projected to an axial plane, and B' is the length in this section:

$$B' = l_1 \cos \psi \quad (29)$$

The length of the contact under load (corresponding to the dimension l_2 in Figure 84) may be expected to be larger than the value for light load. Provision is made in the computer program for assuming

a factor k_3 to allow for this effect as follows:

$$B = \left[1 + k_3 \frac{T_G}{T_O} \left(\frac{F}{B'} - 1 \right) \right] B' \quad (30)$$

$$0 \leq k_3 \leq 1.0$$

As mentioned above, a value of $k_3 = 1$ has been tentatively selected for the computer program.

Adjustability Coefficients

The modified adjustability coefficients used in the program are as follows:

$$A_{FP} = \frac{\cos \gamma}{\cos \psi} \left[\cos \phi \left(\frac{\sin \psi}{A} - \frac{1}{r_c} \right) + \tan \gamma \sin \phi \left(\frac{1}{A} - \frac{\sin \psi}{r_c} \right) \right] \quad (31)$$

$$A_{FG} = - \frac{\cos \Gamma}{\cos \psi} \left[\cos \phi \left(\frac{\sin \psi}{A} - \frac{1}{r_c} \right) - \tan \Gamma \sin \phi \left(\frac{1}{A} - \frac{\sin \psi}{r_c} \right) \right] \quad (32)$$

$$A_{FE} = - \frac{1}{A} \frac{\cos \phi}{\sin \Sigma} \quad (33)$$

$$A_{F\alpha} = - \frac{\sin \phi}{\cos \psi \sin \Sigma} \quad (34)$$

where A_{FP} = rate of lengthwise contact shift due to unit displacement in the pinion axial direction

A_{FG} = rate of lengthwise contact shift due to unit displacement in the gear axial direction

A_{FE} = rate of lengthwise contact shift due to unit displacement in the offset direction between the two axes

$A_{F\alpha}$ = rate of lengthwise contact shift due to unit angular change in the shaft angle

γ = pinion pitch angle

Γ = gear pitch angle

ϕ = normal pressure angle

- ψ = mean spiral angle
- Σ = shaft angle
- A = mean cone distance
- r_c = mean cutter radius

Mounting Deflections

The measured displacements obtained from a deflection test on a pair of gears in their mountings must be converted to relative displacements between the gear and mating pinion. The formulas given here apply to the rigid test boxes used for this test program. Other test boxes may be analyzed in a similar manner, but the formulas may require modification to suit the individual case. These formulas are not included in the computer program, since they are not sufficiently general for universal use.

In the following formulas for P, G, E, and α , the circled numbers represent the indicator readings listed in Table XV in Appendix II. The sign convention is shown in Figure 85, and Figures 76, 77, and 78 are the three views of the test box showing the indicator locations. The lowercase letters are the distances illustrated in Figures 76, 77, and 78.

- P = pinion axial displacement, inches; plus (+) means the pinion moves out of mesh.
- G = gear axial displacement, inches; plus (+) means the gear moves out of mesh.
- E = offset displacement, inches; plus (+) means the pinion axis moves down relative to the gear axis when the pinion is to the right of the gear center as an observer looks at the face of the gear.
- α = shaft angle displacement, radians; plus (+) means an increase in the shaft angle.

$$P = P_p + P_G \quad (35)$$

$$P_p = [- \textcircled{25} - \Sigma t]$$

$$P_G = \textcircled{24} - \left[\frac{\textcircled{10} - \textcircled{24}}{p + q} \right] x$$

$$Q = Q_p + Q_G \quad (36)$$

$$Q_p = \textcircled{7} - \Sigma (o)$$

$$Q_G = \textcircled{5} - \xi (w)$$

$$E = E_p + E_G \quad (37)$$

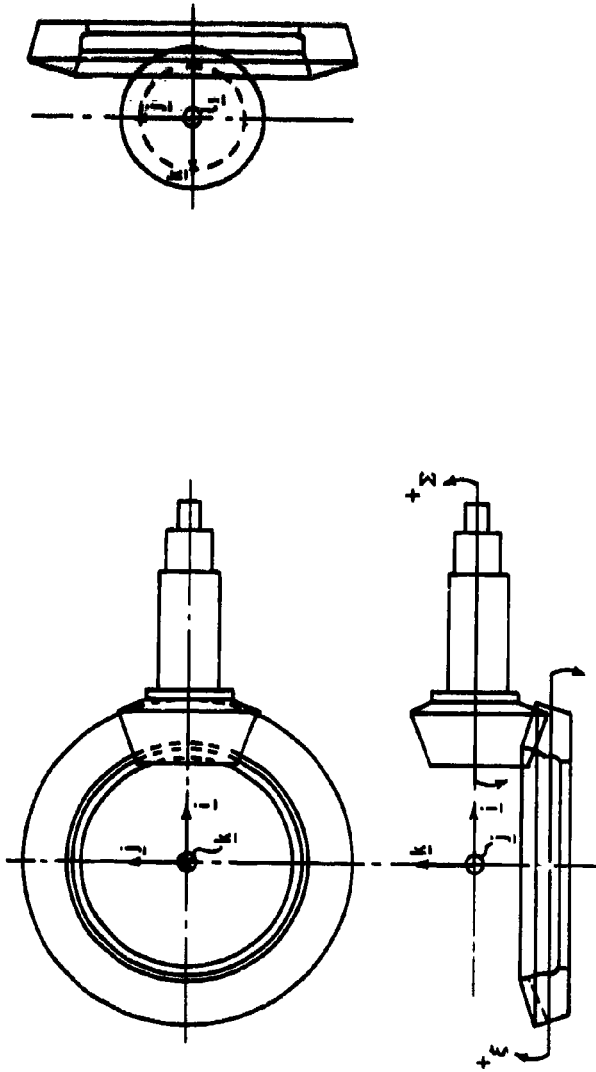
$$E_p = - \left[\frac{\textcircled{3} - \textcircled{3A}}{a} \right] (o) - \textcircled{3}$$

$$E_G = - \left[\frac{\textcircled{1} - \textcircled{28}}{d} \right] (e - f + g) + \textcircled{1}$$

$$a = \xi + \Sigma \quad (38)$$

$$\xi = \frac{\textcircled{5} - \textcircled{9}}{h}$$

$$\Sigma = \frac{\textcircled{7A} - \textcircled{7}}{B}$$



GEAR MOVEMENT

1. GEAR AXIAL (P_g POSITIVE FOR $-k$)
2. GEAR SEPARATION (P_g POSITIVE FOR $-j$)
3. OFFSET (E_g POSITIVE FOR $+j$)
4. ξ , ANGLE OF ROTATION IN k_i PLANE (GEAR AXIAL PLANE)

PINION MOVEMENT

1. PINION AXIAL (P_p POSITIVE FOR $+i$)
2. PINION SEPARATION (P_p POSITIVE FOR $+k$)
3. OFFSET (E_p POSITIVE FOR $-j$)
4. Σ , ANGLE OF ROTATION IN k_i PLANE (GEAR AXIAL PLANE)

Figure 85. Sign Convention Used in Analysis of Deflection Test Results.

INDICATOR LOCATIONS IN TEST BOX

<u>Letter Designation</u>	<u>Distance</u>
a	2.96
c	3.96
d	4.75
e	2.16
f	1.14
g	3.38
h	10.97
m	2.90
o	4.18
p	2.69
q	1.60
t	0.31
w	5.71
x	0.24

The unit vectors \underline{i} , \underline{j} , and \underline{k} are shown in Figure 85. The displacements P, G, E, and α for the four gear torque levels were calculated and are listed in Tables XXIV and XXV. The results for gears produced with both the 7-1/2-inch and 12-inch cutter diameters are included.

When no deflection test data are available to calculate P, G, E, and α , the following approximate formulas were used:

$$\begin{aligned}
 P &= + 0.00000033 T_G && (35) \\
 G &= - 0.00000020 T_G && (36) \\
 E &= - 0.00000033 T_G && (37) \\
 \alpha &= + 0.00000006 T_G && (38)
 \end{aligned}$$

where T_G = gear torque, lb-in.

TABLE XXIV. E, P, G, AND α FOR THE 12-INCH CUTTER DIAMETER DESIGN				
Gear Torque (lb-in.)	Standard Displacements			
	E (in.)	P (in.)	G (in.)	α (rad)
35,800	-0.0053	0.0031	0.0010	-0.00040
50,000	-0.0080	0.0041	0.0005	-0.00040
71,600	-0.0112	0.0056	0.0001	-0.00037
100,000	-0.0135	0.0075	0.0006	-0.00055

TABLE XXV. E, P, G, AND α FOR THE 7-1/2-INCH CUTTER DIAMETER DESIGN				
Gear Torque (lb-in.)	Standard Displacements			
	E (in.)	P (in.)	G (in.)	α (rad)
35,800	-0.0057	0.0024	-0.0007	-0.00001
50,000	0.0072	0.0039	-0.0004	-0.00015
71,600	-0.0097	0.0049	-0.0008	-0.00011
100,000	-0.0126	0.0070	0.0000	-0.00034

These formulas are based on average values of P, G, E, and α , as observed in past deflection tests performed at the contractor's facilities on automotive rear axles, which are typical of most commercial gear-boxes in this size range (7-inch to 9-inch gear diameter), and which are not as rigid as the test boxes used in this program. For other gear designs it would be best to introduce known or assumed values based on some prior experience.

Equation for Contact Shift

The equation for k_1 can now be written

$$k_1 = PA_{FP} + GA_{FG} + EA_{FE} + \alpha A_{F\alpha} \quad (39)$$

This is based on the adjustability coefficients (31) through (34) and the mounting displacements (35) through (38).

The contact shift from the lengthwise center of the tooth at any load level is dependent upon the displacements at that load level. These are given as follows:

$$P_1 = P \frac{T_G - k_4 T_D}{T_D} \quad (40)$$

$$G_1 = G \frac{T_G - k_4 T_D}{T_D} \quad (41)$$

$$E_1 = E \frac{T_G - k_4 T_D}{T_D} \quad (42)$$

$$\alpha_1 = \alpha \frac{T_G - k_4 T_D}{T_D} \quad (43)$$

where T_G = gear torque, lb-in.

T_D = gear torque, lb-in., which produces a central tooth contact pattern - usually full load.

k_4 = ratio coefficient determined previously - assume 1.25.

A new equation for k_1' can now be written.

$$k_1' = P_1 A_{FP} + G_1 A_{FG} + E_1 A_{FE} + a_1 A_{Fa} \quad (44)$$

which is proportional to the contact shift from a central bearing at any specific load T_G .

The shift can be calculated by solving equations (24) through (27) for f and using the coefficient k_1' in place of k_1 . The resulting equation becomes

$$f = \frac{F \sec \psi}{2} - \frac{1}{8k_1' k_2} \left[\sqrt{1 + 8k_1' k_2 F \sec \psi} - 1 \right] \quad (45)$$

The contact shift was checked experimentally on a testing machine under light loads. The gears were displaced in many combinations on this machine, and the contact shift was observed by eye. The correlation proved to be excellent between the calculated shift and the observed shift. A similar correlation under load is shown in Figures 86 and 87.

LOAD DISTRIBUTION FACTOR

The data analysis program, previously described in Appendix III, was used to determine the stress distribution in the root of the tooth as the center of an assumed elliptical load distribution shifts toward the end of the tooth. In this analysis it was assumed that the line of contact on the tooth remained parallel to the pitch line at a constant height above the root of the tooth and that the total load on the line of contact remained constant. The procedure of shifting the line of contact to various lengthwise positions was repeated for both the concave and convex tooth surfaces on three teeth with pressure angles of 15, 20, and 25 degrees. The ratio of the maximum root stress caused by a centrally located contact pattern was found to be nearly identical for the three pressure angles. The resulting factors for the three pressure angles were therefore averaged, and one equation is presented. The general form of this equation for load distribution is:

$$K_m = \frac{s_{\text{shift}}}{s_{\text{max}}} \quad (46)$$

where K = load distribution factor.

s_{shift} = maximum stress along the root of the tooth when the tooth contact pattern has shifted away from its central position on the tooth.

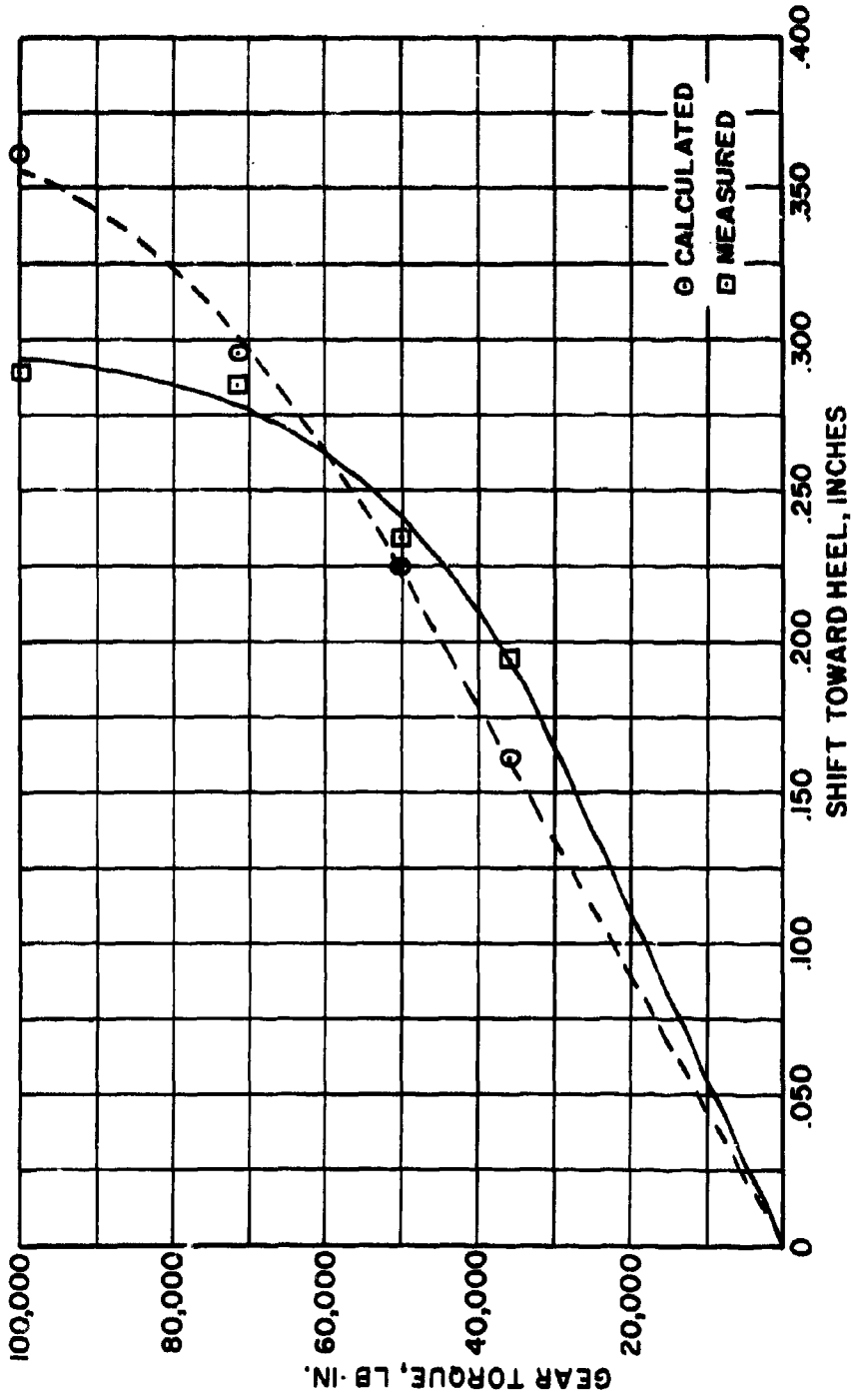


Figure 86. Correlation Between Calculated and Measured Contact Shift, 12-Inch Cutter Diameter Design.

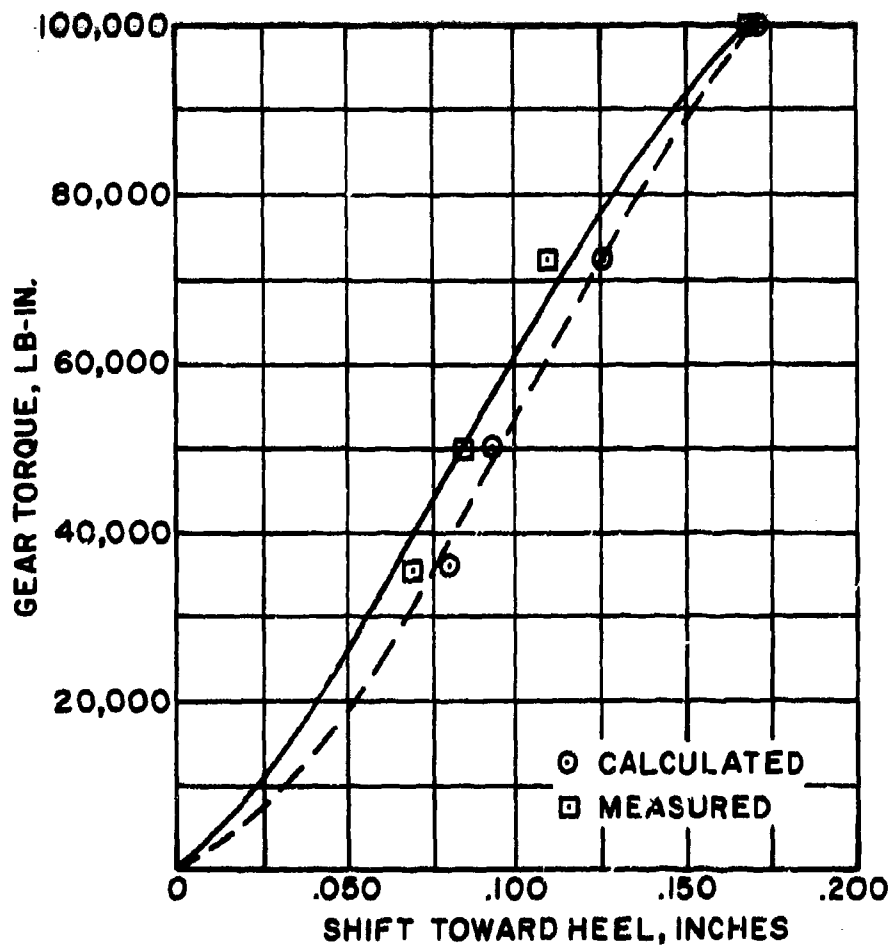


Figure 87. Correlation Between Calculated and Measured Contact Shift, 7-1/2-Inch Cutter Diameter Design.

s_{\max} = maximum stress along the root of the tooth when the tooth contact pressure is centrally located. This is the same s_{\max} referred to in Appendix III on Effective Face Width.

By nondimensionalizing the factors used in this equation, it is possible to develop a general equation from the model tooth data. The tooth length of the model used in this analysis was 2.94 inches, and the lengthwise radius of curvature (cutter radius) was 4 inches. Figure 88 shows the relationship between the face width F and the tooth length for spiral bevel gears. After plotting the nondimensional contact shift, $f/F \sec \psi$, versus the load distribution factor, K_m (Figures 89 and 90), a polynomial of the form $y = A_n x^{2n}$ was fitted to the curve. The resulting polynomial formula for the load distribution factor is:

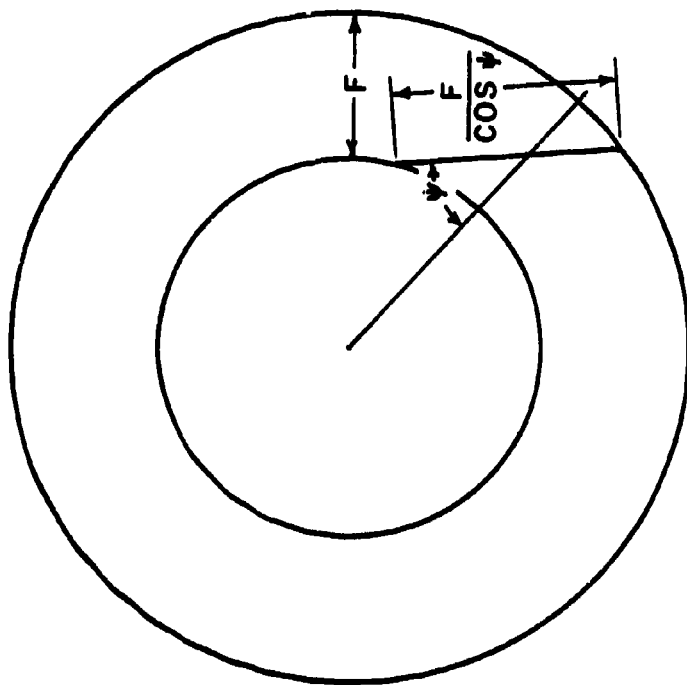
$$K_m = 1.00 + (14.6 \pm 7.6 \beta) X_{FR}^2 - (66.3 \pm 17.7 \beta) X_{FR}^4 + 105 X_{FR}^6 \quad (47)$$

Concave
Convex

where $\beta = \frac{F}{2r_c \cos \psi}$ = nondimensionalized lengthwise radius of curvature

$X_{FR} = \frac{f \cos \psi}{F}$ = nondimensionalized tooth contact shift

The upper sign applies to the concave tooth surface, and the lower sign applies to the convex tooth surface.



F = FACE WIDTH
 $F/\cos \psi$ = TOOTH LENGTH
 ψ = MEAN SPIRAL ANGLE

Figure 88. Relationship Between Face Width and Tooth Length on a Spiral Bevel Gear Tooth.

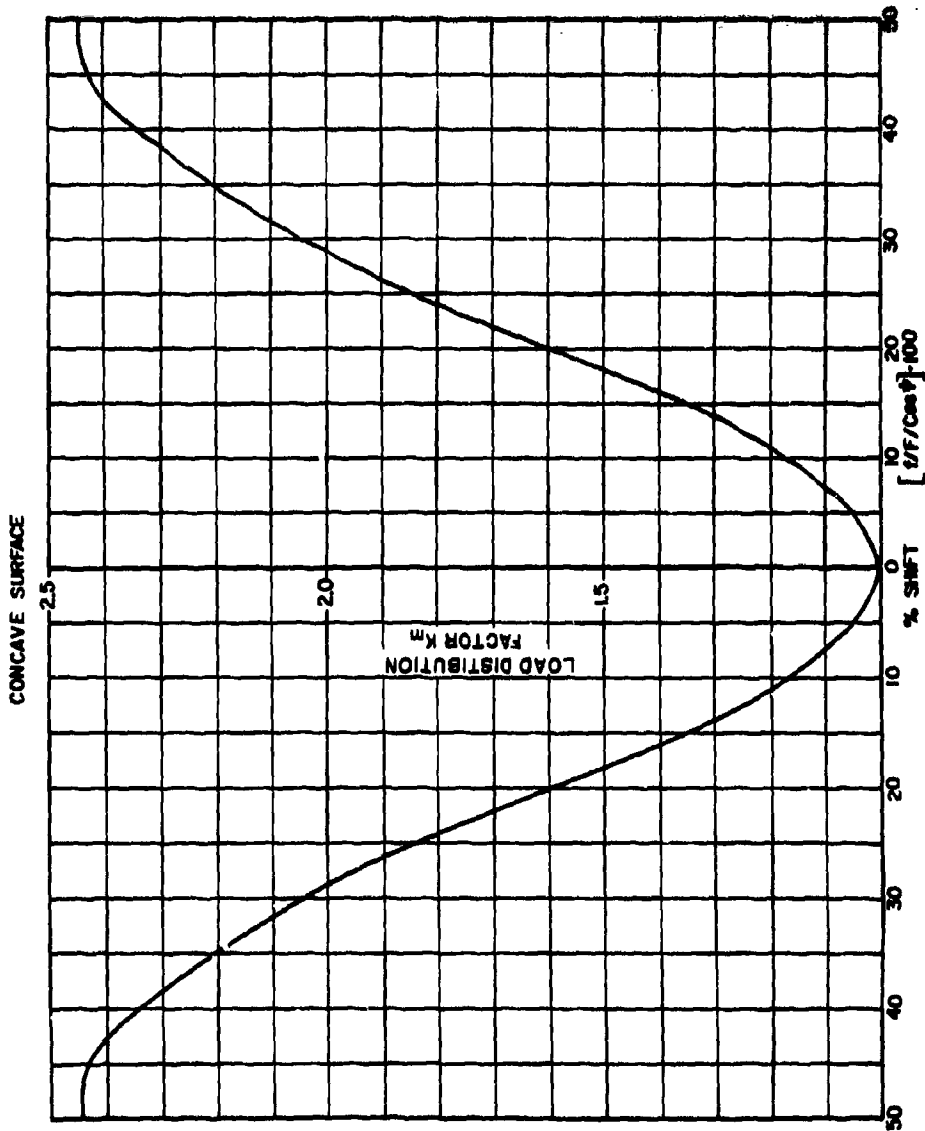


Figure 89. Load Distribution Factor V_s Contact Shift for the Concave Tooth Surface.

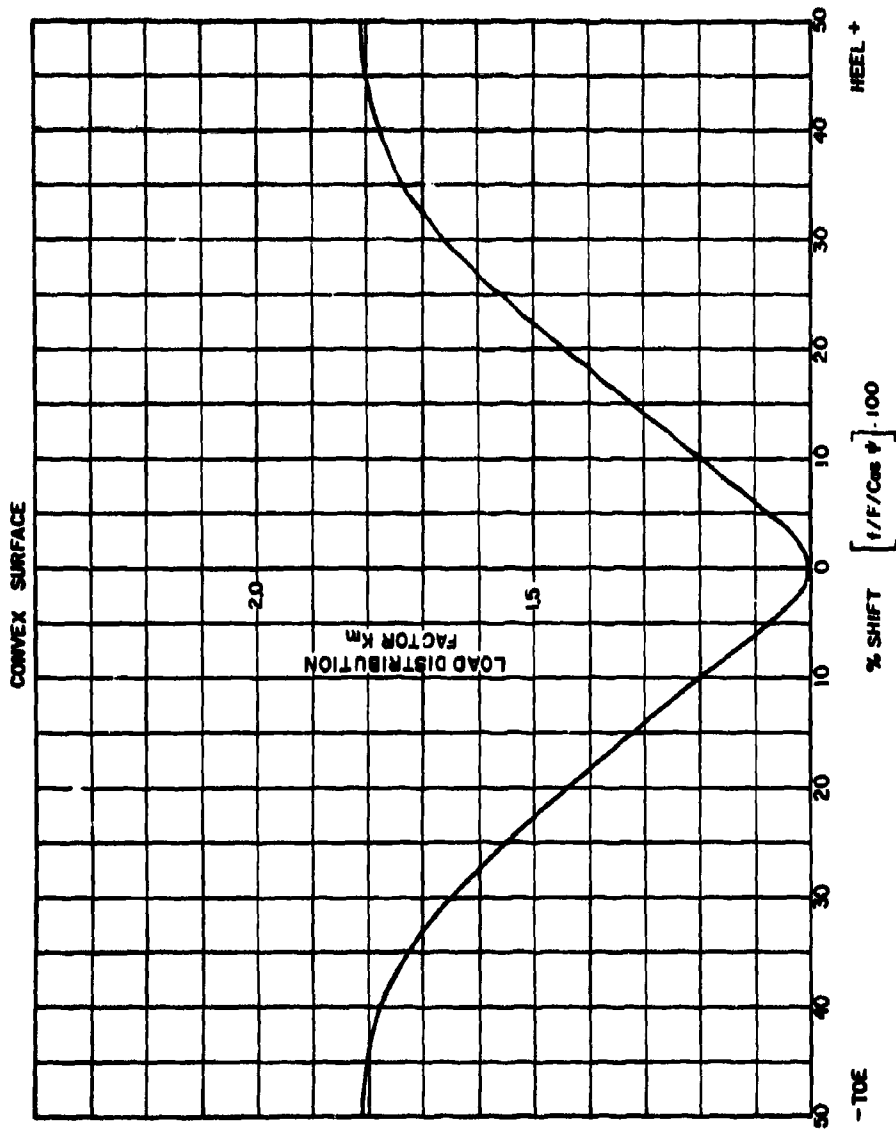


Figure 90. Load Distribution Factor Vs Contact Shift for the Convex Tooth Surface.

APPENDIX V

STRESS FORMULA DOCUMENTATION

This appendix consists of a complete description of the formulas used in the program.

DESCRIPTION OF PROBLEM

Given the details of the tooth design and the cutter specifications, these formulas lead to the calculation of the bending stress in the root fillet of a bevel gear tooth.

Referring to the New Strength Formulas section in the main body of this report, the two major unknown factors in equation (4) for bending stress are the load distribution factor, K_m , and the geometry factor, J . The formulas for these two factors as well as the formulas for the bending stress, s_t , are given for both the gear and the mating pinion. The other factors in equation (4) are either known or assumed.

Also included is the formula for working stress.

METHOD OF SOLUTION

The basic formulas used here are based on those used in the AGMA bevel gear strength standards, References 15 and 16. Modifications have been made in the formulas for effective face width and load distribution factor, as described in detail elsewhere in this report. In addition, the size factor has been removed from the equation for calculated bending stress, and a modified formula for size factor has been incorporated in the equation for working stress.

FORMULA DOCUMENTATION

m_G	$= \frac{N}{n}$	gear ratio
$\tan \gamma$	$= \frac{\sin \Sigma}{m_G + \cos \Sigma}$	γ = pinion pitch angle
Γ	$= \Sigma - \gamma$	gear pitch angle
A_o	$= \frac{D}{2 \sin \Gamma}$	outer cone distance
F_{mn}	$= F_G, F_P, F_{RG}, \text{ or } F_{RP}$	whichever is smallest
F_{mx}	$= F_G, F_P$	whichever is larger
F_{Pmn}	$= F_P \text{ or } F_{RP}$	whichever is smaller
F_{Pmx}	$= F_P \text{ or } F_{RP}$	whichever is larger
F_{Gmn}	$= F_G \text{ or } F_{RG}$	whichever is smaller
F_{Gmx}	$= F_G \text{ or } F_{RG}$	whichever is larger
A	$= A_o - 0.5 F_{mn}$	mean cone distance
p	$= \frac{\pi}{P_d}$	circular pitch
a_{oP}	$= h_k - a_{oG}$	pinion addendum at outer end of tooth
b_{oP}	$= h_{tP} - a_{oP}$	pinion dedendum at outer end of tooth
b_{oG}	$= h_{tG} - a_{oG}$	gear dedendum at outer end of tooth
b_P	$= b_{oP} - 0.5 F_{mn} \tan \delta_P$	mean pinion dedendum
b_G	$= b_{oG} - 0.5 F_{mn} \tan \delta_G$	mean gear dedendum

$$a_p = a_{op} - 0.5 F_{mn} \tan \alpha_p \quad \text{mean pinion addendum}$$

$$a_G = a_{oG} - 0.5 F_{mn} \tan \alpha_G \quad \text{mean gear addendum}$$

$$t_{mP_0} = \frac{(2b_G \tan \phi + W_G)}{\cos \psi} - \frac{A}{A_o} \cdot \frac{B_{mx}}{2 \cos \phi \cos \psi_o} \quad \left. \begin{array}{l} \text{when } W_G \text{ is} \\ \text{given} \end{array} \right\} \text{pinion mean circular} \\ \text{thickness assuming} \\ \text{zero backlash}$$

$$= t_{mP} + \frac{A}{A_o} \cdot \frac{B_{mx}}{2 \cos \phi \cos \psi_o} \quad \text{when } t_{mP} \text{ is given}$$

$$t_{mP} = t_{mP_0} - \frac{A}{A_o} \cdot \frac{B_{mx}}{2 \cos \phi \cos \psi_o} \quad \text{pinion mean circular thickness}$$

$$t_{mG} = \frac{A}{A_o} p - t_{mP} - \frac{A}{A_o} \cdot \frac{B_{mx}}{\cos \phi \cos \psi_o} \quad \text{gear mean circular thickness}$$

$$\left. \begin{array}{l} H_f = 0.3254545 - 0.416695 \phi \\ J_f = 0.3318182 - 0.52087 \phi \\ L_f = 0.2681318 + 0.52087 \phi \end{array} \right\} \text{stress concentration constants } (\phi \text{ in radians)}$$

$$P_m = \frac{A_o}{A} \cdot P_d \quad \text{mean diametral pitch}$$

$$p_n = \frac{\pi \cos \psi}{P_m} \quad \text{mean normal circular pitch}$$

$$p_s = \frac{P_d p_n}{\cos \phi (\cos^2 \psi + \tan^2 \phi)} = \frac{P_N}{\cos^2 \psi_b}$$

$$k_3 = 1.0$$

$$k_4 = 1.25$$

$$T_o = T_G \text{ or } k_4 T_D \quad \text{whichever is larger}$$

$$\left. \begin{array}{l} P = 0.00000033 T_D \\ G = -0.00000020 T_D \\ E = -0.00000033 T_D \\ \alpha = 0.00000006 T_D \end{array} \right\} \text{when not given; otherwise use given values}$$

$$\left. \begin{array}{l} P_1 = 0.00000033 (T_G - k_4 T_D) \\ G_1 = -0.00000020 (T_G - k_4 T_D) \\ E_1 = -0.00000033 (T_G - k_4 T_D) \\ \alpha_1 = 0.00000006 (T_G - k_4 T_D) \end{array} \right\} \text{when } P, G, E, \text{ and } \alpha \text{ are not given}$$

$$P_1 = P \cdot \frac{(T_G - k_4 T_D)}{T_D}$$

$$G_1 = G \cdot \frac{(T_G - k_4 T_D)}{T_D}$$

$$E_1 = E \cdot \frac{(T_G - k_4 T_D)}{T_D}$$

$$\alpha_1 = \alpha \cdot \frac{(T_G - k_4 T_D)}{T_D}$$

$$C_2 = k_3 \frac{T_G}{T_o}$$

when P, G, E, and α are given

$$A_{FP} = \frac{\cos \gamma}{\cos \psi} \left[\cos \phi \left(\frac{\sin \psi}{A} - \frac{1}{r_c} \right) + \tan \gamma \sin \phi \left(\frac{1}{A} - \frac{\sin \psi}{r_c} \right) \right]$$

$$A_{FG} = - \frac{\cos \Gamma}{\cos \psi} \left[\cos \phi \left(\frac{\sin \psi}{A} - \frac{1}{r_c} \right) - \tan \Gamma \sin \phi \left(\frac{1}{A} - \frac{\sin \psi}{r_c} \right) \right]$$

$$A_{FE} = - \frac{1}{A} \cdot \frac{1}{\sin \Sigma} \cos \phi$$

$$A_{F\alpha} = - \frac{\sin \phi}{\cos \psi} \cdot \frac{1}{\sin \Sigma}$$

modified adjustability coefficients

$$k_1 = (P \cdot A_{FP} + G \cdot A_{FG} + E \cdot A_{FE} + \alpha \cdot A_{F\alpha}) k_4$$

$$k_1' = P_1 \cdot A_{FP} + G_1 \cdot A_{FG} + E_1 \cdot A_{FE} + \alpha_1 \cdot A_{F\alpha}$$

$$k_2 = \frac{250}{\sqrt[3]{D}}$$

$$l_1 = \frac{1}{4 |k_1| k_2} \left[\sqrt{1 + \frac{8 |k_1| k_2 F_{mn}}{\cos \psi}} - 1 \right]$$

length of tooth contact at no load in tangent plane (when $k_1 < 0.000G1$, $l_1 = F_{mn}$)

$$A_2 = C_2 \left(\frac{F_{mn}}{l_1 \cos \psi} - 1 \right) + 1$$

$$B = A_2 l_1 \cos \psi$$

length of tooth contact at given load in axial plane

$$m_F = \frac{A_o}{A} \cdot \frac{B \tan \psi}{p}$$

face contact ratio

$$R_{P1} = \frac{n}{2 \cos \gamma} \cdot \frac{A}{A_o}$$

pinion pitch radius in mean transverse section (1 DP)

$R_{G1} = \frac{N}{2 \cos \Gamma} \cdot \frac{A}{A_0}$	gear pitch radius in mean transverse section (1 DP)
$R_{NP1} = \frac{R_{P1}}{\cos^2 \psi}$	pinion pitch radius in mean normal section (1 DP)
$R_{NG1} = \frac{R_{G1}}{\cos^2 \psi}$	gear pitch radius in mean normal section (1 DP)
$R_{bNP1} = R_{NP1} \cos \phi$	pinion base radius in mean normal section (1 DP)
$R_{bNG1} = R_{NG1} \cos \phi$	gear base radius in mean normal section (1 DP)
$a_{P1} = a_P \cdot P_d$	pinion mean addendum (1 DP)
$a_{G1} = a_G \cdot P_d$	gear mean addendum (1 DP)
$b_{P1} = b_P \cdot P_d$	pinion mean dedendum (1 DP)
$b_{G1} = b_G \cdot P_d$	gear mean dedendum (1 DP)
$R_{oNP1} = R_{NP1} + a_{P1}$	pinion outside radius in mean normal section (1 DP)
$R_{oNG1} = R_{NG1} + a_{G1}$	gear outside radius in mean normal section (1 DP)
$Z_1' = R_{oNP1} \sqrt{1 - \left(\frac{R_{bNP1}}{R_{oNP1}}\right)^2} - R_{NP1} \sin \phi$	arc of (approach) recess in mean normal section (1 DP)
$Z_2' = R_{oNG1} \sqrt{1 - \left(\frac{R_{bNG1}}{R_{oNG1}}\right)^2} - R_{NG1} \sin \phi$	arc of (approach) recess in mean normal section (1 DP)
$Z_{N1} = Z_1' + Z_2'$	length of action in normal section (1 DP)
$m_p = \frac{Z_{N1}}{P_2} = m_n \cos^2 \psi_b$	transverse (profile) contact ratio
$m_o = \sqrt{m_p^2 + m_F^2}$	modified contact ratio
$P_N = P_d P_n \cos \phi$	normal base pitch (1 DP)
$k' = \frac{N - n}{8n + 8.4N}$	load position correction factor
$m_n = \frac{Z_{N1}}{P_N}$	normal contact ratio

$$\sin \psi_b = \sin \psi \cos \phi$$

ψ_b = base spiral angle

$$Z_1 = Z_{N1} \cos \psi_b$$

length of action in transverse section (1 DP)

$$F_1 = F_{mn} P_d$$

minimum net face width (1 DP)

$$B_1 = B P_d$$

length of tooth contact area in axial plane (1 DP)

$$\eta = \sqrt{Z_1^2 \cos^2 \psi_b + B_1^2 \sin^2 \psi_b}$$

$$f_{JP} = \left. \begin{aligned} &= P_N - \frac{\eta}{2} \quad \text{when } m_o < 2 \\ &= 0 \quad \text{when } m_o > 2 \end{aligned} \right\} = f_{JG}$$

$$\eta_{JP} = \sqrt{\eta^2 - 4f_{JP}^2}$$

$$\eta_{JG} = \sqrt{\eta^2 - 4f_{JG}^2}$$

$$P_{sP} = \frac{Z_1}{2 \cos \psi_b} + \frac{Z_1^2 f_{JP}}{\eta^2} \pm \frac{B_1 Z_1 \eta_{JP} k' \tan \psi_b}{\eta^2} \quad \begin{array}{l} \text{Concave} \\ \text{Convex} \end{array}$$

$$P_{sG} = \frac{Z_1}{2 \cos \psi_b} + \frac{Z_1^2 f_{JG}}{\eta^2} \pm \frac{B_1 Z_1 \eta_{JG} k' \tan \psi_b}{\eta^2} \quad \begin{array}{l} \text{Concave} \\ \text{Convex} \end{array}$$

$$(\eta_{JP}')^3 = \eta_{JP}^3 + \sum_{k_n=1}^{\alpha} \sqrt{[\eta_{JP}^2 - 4k_n P_N (k_n P_N + 2f_{JP})]^3} + \sum_{k_n=1}^{\beta} \sqrt{[\eta_{JP}^2 - 4k_n P_N (k_n P_N - 2f_{JP})]^3}$$

$$(\eta_{JG}')^3 = \eta_{JG}^3 + \sum_{k_n=1}^{\alpha} \sqrt{[\eta_{JG}^2 - 4k_n P_N (k_n P_N + 2f_{JG})]^3} + \sum_{k_n=1}^{\beta} \sqrt{[\eta_{JG}^2 - 4k_n P_N (k_n P_N - 2f_{JG})]^3}$$

$$\left. \begin{aligned} m_{NP} &= \left(\frac{\eta_{JP}'}{\eta_{JP}} \right)^3 \\ &= 1.0 \text{ when } \eta_{JP} = 0 \\ m_{NG} &= \left(\frac{\eta_{JG}'}{\eta_{JG}} \right)^3 \\ &= 1.0 \text{ when } \eta_{JG} = 0 \end{aligned} \right\}$$

load sharing ratio

$$K_i = \left. \begin{aligned} &= \frac{2.0}{m_n} \text{ when } m_o < 2 \\ &= 1.0 \text{ when } m_o > 2 \end{aligned} \right\} \text{ inertia factor}$$

$$\Sigma R_{N1} = R_{NP1} + R_{NG1}$$

$$\tan \phi_{hP} = \frac{P_{sP} + \Sigma R_{N1} \sin \phi - \sqrt{(R_{oNG1}^2 - R_{bNG1}^2)}}{R_{bNP1}}$$

$$\tan \phi_{hG} = \frac{P_{sG} + \Sigma R_{N1} \sin \phi - \sqrt{(R_{oNP1}^2 - R_{bNP1}^2)}}{R_{bNG1}}$$

$$x_P'' = \frac{B_1 Z_1 \eta_{JP} k' \cos \psi_b \mp B_1^2 f_{JP} \sin \psi_b}{\eta^2} \quad \begin{array}{l} \text{Concave} \\ \text{Convex} \end{array}$$

$$x_G'' = \frac{B_1 Z_1 \eta_{JG} k' \cos \psi_b \mp B_1^2 f_{JG} \sin \psi_b}{\eta^2} \quad \begin{array}{l} \text{Concave} \\ \text{Convex} \end{array}$$

$$F_{KP} = \frac{B_1 Z_1 \eta_{JP} \cos \psi_b}{\eta^2}$$

$$F_{KG} = \frac{B_1 Z_1 \eta_{JG} \cos \psi_b}{\eta^2}$$

$$t_P = t_{mP} \cos \psi \quad \text{pinion mean normal circular thickness}$$

$$t_G = P_n - t_P - \frac{A}{A_o} \cdot \frac{\cos \psi}{\cos \psi_o} \cdot \frac{B_{MX}}{\cos \phi} \quad \text{gear mean normal circular thickness}$$

$$t_{P1} = P_d t_P \quad \text{pinion mean normal circular thickness (1 DP)}$$

$$t_{G1} = P_d t_G \quad \text{gear mean normal circular thickness (1 DP)}$$

$$r_{TP1} = P_d r_{TP} \quad \text{pinion cutter edge radius (1 DP)}$$

$$r_{TG1} = P_d r_{TG} \quad \text{gear cutter edge radius (1 DP)}$$

$$\phi_{LP} = \phi_{hP} - \left(\frac{t_{P1}}{2R_{NP1}} - \text{inv } \phi_{hP} + \text{inv } \phi \right) \quad \text{angle in radians which the normal force makes with a line perpendicular to the tooth center-line}$$

$$\phi_{LG} = \phi_{hG} - \left(\frac{t_{G1}}{2R_{NG1}} - \text{inv } \phi_{hG} + \text{inv } \phi \right) \quad \text{angle in radians which the normal force makes with a line perpendicular to the tooth center-line}$$

$$\Delta R_{NP} = \frac{R_{bNP1}}{\cos \phi_{LP}} - R_{NP1}$$

$$\Delta R_{NG} = \frac{R_{bNG1}}{\cos \phi_{LG}} - R_{NG1}$$

distance from pitch circle to point of load application on tooth centerline

$$x_{P1} = \frac{t_{P1}}{2} + b_{P1} \tan \phi + r_{TP1} (\sec \phi - \tan \phi)$$

$$x_{G1} = \frac{t_{G1}}{2} + b_{G1} \tan \phi + r_{TG1} (\sec \phi - \tan \phi)$$

$$y_{2P} = b_{P1} - r_{TP1}$$

$$y_{2G} = b_{G1} - r_{TG1}$$

$$X_{\theta P} \text{ (first trial)} = x_{P1} + y_{2P}$$

must always be positive

$$\theta_P = \frac{X_{\theta P}}{R_{NP1}}$$

$$x_{2P} = X_{\theta P} - x_{P1}$$

$$z_{1P} = y_{2P} \cos \theta_P - x_{2P} \sin \theta_P$$

$$z_{2P} = y_{2P} \sin \theta_P + x_{2P} \cos \theta_P$$

must always be positive

$$\tan \zeta_P = \frac{z_{1P}}{z_{2P}}$$

ζ_P must be greater than ϕ

$$t_{NP} = X_{\theta P} - R_{NP1} (\theta_P - \sin \theta_P) - r_{TP1} \cos \zeta_P - z_{2P}$$

$$h_{NP} = \Delta R_{NP} + R_{NP1} (1 - \cos \theta_P) + r_{TP1} \sin \zeta_P + z_{1P}$$

$$k_P = \frac{t_{NP} \cot \zeta_P}{h_{NP}}$$

$$k_P' = 2.0$$

k_P must be equal to k_P' to 3 decimal places. If it is not, for second trial make $X_{\theta P}$ equal to $1.1 X_{\theta P}$ (first trial). For subsequent trials, interpolate.

$$X_{\theta G} \text{ (first trial)} = x_{G1} + y_{2G}$$

must always be positive

$$\theta_G = \frac{X_{\theta G}}{R_{NG1}}$$

$$x_{2G} = X_{\theta G} - x_{G1}$$

$$z_{1G} = y_{2G} \cos \theta_G - x_{2G} \sin \theta_G$$

$$z_{2G} = y_{2G} \sin \theta_G + x_{2G} \cos \theta_G$$

must always be positive

$$\tan \zeta_G = \frac{z_{1G}}{z_{2G}}$$

ζ must be greater than ϕ

$$t_{NG} = X_{\theta G} - R_{NG1}(\theta_G - \sin \theta_G) - r_{TG1} \cos \zeta_G - z_{1G}$$

$$h_{NG} = \Delta R_{NG} + R_{NG1}(1 - \cos \theta_G) + t_{TG1} \sin \zeta_G + z_{1G}$$

$$k_G = \frac{t_{NG} \cot \zeta_G}{h_{NG}}$$

$$k_G' = 2.0$$

k_G must be equal to k_G' to 3 decimal places. If it is not, for second trial make $X_{\theta G}$ equal to $1.1X_{\theta G}$ (first trial). For subsequent trials, interpolate.

$$X_{NP} = \frac{t_{NP}^2}{h_{NP}}$$

$$X_{NG} = \frac{t_{NG}^2}{h_{NG}}$$

tooth strength factors

$$F_{RP1} = P_d \cdot F_{RP}$$

pinion root face width (1 DP)

$$F_{RG1} = P_d \cdot F_{RG}$$

gear root face width (1 DP)

$$\tan w = \sin \phi \cdot \tan \psi$$

w = angle of inclination of line of contact with pitch line in tangent plane

$$h_{tP1} = P_d \cdot h_{tP}$$

pinion outer whole depth (1 DP)

$$h_{tG1} = P_d \cdot h_{tG}$$

gear outer whole depth (1 DP)

$$V_{1P} = (5.27 \pm 5.80\beta) + (1.90 \pm 0.530\beta) \left(\frac{h_{NP}}{h_{IP1}} \right) + (4.07 \pm 1.84\beta) \left(\frac{F_{KP}}{F_{RP1}} \right) - (0.117 \mp 0.179\beta) w$$

$$- (29.6 + 4.80\beta)\phi + (36.7 \pm 73.0\beta)\phi^2$$

Concave

Convex

$$V_{2P} = -(1.00 \pm 7.48\beta) - (1.51 \pm 0.570\beta) \left(\frac{h_{NP}}{h_{IP1}} \right) - (7.28 \pm 2.80\beta) \left(\frac{F_{KP}}{F_{RP1}} \right) + (0.178 \mp 0.155\beta) w$$

$$+ (49.7 \pm 61.8\beta)\phi - (66.1 \pm 98.5\beta)\phi^2$$

Concave

Convex

$$V_{3P} = (0.365 \pm 2.87\beta) + (0.598 \pm 0.294\beta) \left(\frac{h_{NP}}{h_{IP1}} \right) + (2.69 \pm 1.01\beta) \left(\frac{F_{KP}}{F_{RP1}} \right) - (0.0727 \mp 0.0618\beta) w$$

$$- (18.5 \pm 23.8\beta)\phi + (24.8 \pm 35.8\beta)\phi^2$$

Concave

Convex

$$s_{maxP} = \phi \left[V_{1P} - \frac{V_{2P}^2}{4V_{3P}} \right]$$

$$U_{1P} = (7.29 \pm 7.21\beta) + (1.48 \pm 2.60\beta) \left(\frac{h_{NP}}{h_{IP1}} \right) - (20.9 \pm 50.2\beta)\phi - (0.273 \pm 2.36\beta) \left(\frac{h_{NP}}{h_{IP1}} \right)^2$$

$$+ (23.0 \pm 78.3\beta)\phi^2$$

Concave

Convex

$$U_{2P} = -(5.01 \pm 11.2\beta) + (0.800 \mp 4.80\beta) \left(\frac{h_{NP}}{h_{IP1}} \right) + (32.0 \pm 77.8\beta)\phi - (0.717 \mp 3.98\beta) \left(\frac{h_{NP}}{h_{IP1}} \right)^2$$

$$- (47.1 \pm 120.0\beta)\phi^2$$

Concave

Convex

$$U_{3P} = (1.85 \pm 4.19\beta) - (0.321 \mp 1.61\beta) \left(\frac{h_{NP}}{h_{IP1}} \right) - (11.8 \pm 28.8\beta)\phi + (0.284 \mp 1.39\beta) \left(\frac{h_{NP}}{h_{IP1}} \right)^2$$

$$+ (17.4 \pm 44.4\beta)\phi^2$$

Concave

Convex

$$s_{avgP} = \phi \left[U_{1P} - \frac{U_{2P}^2}{4U_{3P}} \right]$$

$$F_{eP} = F_P P_d \frac{s_{avgP}}{s_{maxP}}$$

pinion effective face width (1.DP)

$$V_{1G} = (5.27 \pm 5.80\beta) + (1.90 \pm 0.530\beta) \left(\frac{h_{NG}}{h_{IG1}} \right) + (4.07 \pm 1.84\beta) \left(\frac{F_{KG}}{F_{RG1}} \right) - (0.117 \mp 0.179\beta) w$$

$$- (29.6 \pm 48.0\beta)\phi + (36.7 \pm 73.0\beta)\phi^2$$

Concave

Convex

$$V_{2G} = -(1.00 \pm 7.48\beta) - (1.51 \pm 0.570\beta) \left(\frac{h_{NG}}{h_{tG1}} \right) - (7.28 \pm 2.60\beta) \left(\frac{F_{KG}}{F_{RG1}} \right) + (0.173 \mp 0.155\beta) w$$

$$+ (49.7 \pm 61.8\beta) \phi - (66.1 \pm 98.5\beta) \phi^2 \quad \begin{array}{l} \text{Concave} \\ \text{Convex} \end{array}$$

$$V_{1G} = (0.365 \pm 2.87\beta) + (0.598 \pm 0.294\beta) \left(\frac{h_{NG}}{h_{tG1}} \right) + (2.69 \pm 1.01\beta) \left(\frac{F_{KG}}{F_{RG1}} \right) - (0.0787 \mp 0.0618\beta) w$$

$$- (18.5 \pm 23.8\beta) \phi + (24.8 \pm 35.8\beta) \phi^2 \quad \begin{array}{l} \text{Concave} \\ \text{Convex} \end{array}$$

$$s_{maxG} = e \left[V_{1G} - \frac{V_{2G}^2}{4V_{3G}} \right]$$

$$U_{1G} = (7.29 \pm 7.21\beta) + (1.48 \pm 2.60\beta) \left(\frac{h_{NG}}{h_{tG1}} \right) - (20.9 \pm 50.2\beta) \phi - (0.273 \pm 2.36\beta) \left(\frac{h_{NG}}{h_{tG1}} \right)^2$$

$$+ (28.0 \pm 78.3\beta) \phi^2 \quad \begin{array}{l} \text{Concave} \\ \text{Convex} \end{array}$$

$$U_{2G} = -(5.01 \pm 11.2\beta) + (0.800 \mp 4.60\beta) \left(\frac{h_{NG}}{h_{tG1}} \right) + (32.0 \pm 77.8\beta) \phi - (0.717 \pm 3.98\beta) \left(\frac{h_{NG}}{h_{tG1}} \right)^2$$

$$- (47.1 \pm 120.0\beta) \phi^2 \quad \begin{array}{l} \text{Concave} \\ \text{Convex} \end{array}$$

$$U_{3G} = (1.85 \pm 4.19\beta) - (0.321 \mp 1.61\beta) \left(\frac{h_{NG}}{h_{tG1}} \right) - (11.8 \pm 28.8\beta) \phi + (0.284 \mp 1.89\beta) \left(\frac{h_{NG}}{h_{tG1}} \right)^2$$

$$+ (17.4 \pm 44.4\beta) \phi^2 \quad \begin{array}{l} \text{Concave} \\ \text{Convex} \end{array}$$

$$s_{avgG} = e \left[U_{1G} - \frac{U_{2G}^2}{4U_{3G}} \right]$$

$$F_{eG} = F_G P_d \frac{s_{avgG}}{s_{maxG}} \quad \text{gear effective face width (1 DP)}$$

$$r_{fP} = \frac{(y_{2P})^2}{R_{NP1} + b_{P1} - r_{TP1}} + r_{TP1} \quad \text{pinion fillet radius at root circle (1 DP)}$$

$$r_{fG} = \frac{(y_{2G})^2}{R_{NG1} + b_{G1} - r_{TG1}} + r_{TG1} \quad \text{gear fillet radius at root circle (1 DP)}$$

$$\left. \begin{aligned} K_{tP} &= H_t + \left(\frac{2t_{NP}}{r_{tP}} \right)^{J_t} \cdot \left(\frac{2t_{NP}}{h_{NP}} \right)^{L_t} \\ K_{tG} &= H_t + \left(\frac{2t_{NG}}{r_{tG}} \right)^{J_t} \cdot \left(\frac{2t_{NG}}{h_{NG}} \right)^{L_t} \end{aligned} \right\}$$

stress concentration factors per Dolan and Broghamer

$$R_{tP} = R_{P1} \left(1 + \frac{x_P^n}{P_d A} \right) + \Delta R_{NP}$$

$$R_{tG} = R_{G1} \left(1 + \frac{x_G^n}{P_d A} \right) + \Delta R_{NG}$$

$$F_{P1} = P_d F_P$$

pinion face width (1 DP)

$$F_{G1} = P_d F_G$$

gear face width (1 DP)

$$X_P = \frac{2X_{NP} t_{NP}}{3t_{NP} - X_{NP} \tan \phi_{LP}}$$

$$X_G = \frac{2X_{NG} t_{NG}}{3t_{NG} - X_{NG} \tan \phi_{LG}}$$

$$Y_{KP} = \frac{2X_P}{3K_{tP}}$$

$$Y_{KG} = \frac{2X_G}{3K_{tG}}$$

$$J_P = \frac{Y_{KP}}{m_{NP} K_I} \cdot \frac{F_{oP}}{F_{P1}} \cdot \frac{R_{tP}}{R_{P1}} \cdot \frac{1}{m}$$

pinion geometry factor for strength

$$J_G = \frac{Y_{KG}}{m_{NG} K_I} \cdot \frac{F_{oG}}{F_{G1}} \cdot \frac{R_{tG}}{R_{G1}} \cdot \frac{P_d}{P_m}$$

gear geometry factor for strength

$$\left. \begin{aligned} K_s &= 2 \left(\frac{1}{\sqrt{P_d}} \right) && \text{when } P_d \text{ is less than 16} \\ &= 1.0 && \text{when } P_d \text{ is greater than 16} \end{aligned} \right\} \text{size factor}$$

$$Q_P = \frac{2.0 P_d}{F_P \cdot d \cdot J_P}$$

pinion strength factor

$$Q_G = \frac{2.0 P_d}{F_G \cdot D \cdot J_G}$$

gear strength factor

$$f = \frac{|k_1'| F_{mn}}{2k_1' \cos \psi} - \frac{1}{8k_1' k_2} \left[\sqrt{1 + \frac{8|k_1'| k_2 F_{mn}}{\psi}} - 1 \right] \text{tooth bearing shift from center (when } k_1' < 0.00001, f = 0)$$

$$x_{FR} = \frac{f}{\left(\frac{F_{mn}}{\cos \psi} \right)}$$

$$\beta = \frac{F_{mn}}{2r_c \cos \psi}$$

$$K_{mP} = 1.00 + (14.6 \pm 7.6\beta) x_{FR}^2 - (86.3 \pm 17.7\beta) x_{FR}^4 + 105 x_{FR}^6 \begin{matrix} \text{Concave} \\ \text{Convex} \end{matrix}$$

load distribution factors

$$K_{mG} = 1.00 + (14.6 \pm 7.6\beta) x_{FR}^2 - (86.3 \pm 17.7\beta) x_{FR}^4 + 105 x_{FR}^6 \begin{matrix} \text{Concave} \\ \text{Convex} \end{matrix}$$

$$s_{tP} = T_P \cdot Q_P \cdot \frac{K_o K_{mP}}{K_v}$$

pinion bending stress

$$s_{tG} = T_G \cdot Q_G \cdot \frac{K_o K_{mG}}{K_v}$$

gear bending stress

$$K_T = \frac{460 + T_F}{620}$$

temperature factor

$$s_w = \frac{s_{at}}{K_T K_R K_S}$$

working stress

APPENDIX VI

COMPUTER PROGRAM

This appendix consists of a complete description of the computer program and includes the input and output data sheets together with instructions for their use, the source program listing with operating instructions, and a sample problem.

COMPUTER TYPE AND PROGRAM LANGUAGE

The subject program is written in FORTRAN IV language for use on the IBM 7090/7094 Computer. Computer running time is approximately one minute per data set.

PROGRAM DESCRIPTION

The program was written to calculate the bending stresses in a pair of bevel gears given the gear design details, the cutter specifications, the adjustability characteristics, and the load.

Three lists of symbols are included in the report:

1. A list of all input symbols showing the card numbers, column numbers, letter symbols, FORTRAN symbols, and a description of each item.
2. A list of all the symbols used in the program showing the letter symbols, FORTRAN symbols, and a description of each item.
3. A list of all output symbols showing the letter symbols, FORTRAN symbols, and a description of each item.

INPUT INFORMATION

All but the items on card No. 0 and the last three input items on card No. 1 (DRIVE, ROT, and HAND) must be entered in the following manner:

1. Each value must have a decimal point. The decimal point may be placed in any position necessary but must occupy a column on the card.

2. A negative number must be preceded by a minus (-) sign, whereas the plus (+) sign may be omitted from a positive number.
3. All input items except T_D , K_v , K_o , C_2 , T_G , E , P , G , and α may be found on a Gleason dimension sheet.
4. The computer program is written to permit multiple sets of data to be run consecutively. Data card No. 0 precedes the No. 1 data card for the first set of data only. It is not necessary to duplicate card No. 0 for successive sets of data when running multiple sets. It is necessary that a blank card follow the last data card in the last set of data.

INPUT DATA

All data should be placed on 80-column IBM cards. A complete description of each item of input is given on pages 219 through 223, and sample input sheets are included on pages 224 and 225.

PROGRAM LISTING

The complete program listing is given on pages 232 through 243. All special subroutines are included in the listing.

OPERATING INSTRUCTIONS FOR PROGRAM

After all input data are placed properly on standard 80-column IBM cards, the standard procedures for running a program on the IBM 7090 computer should be used.

There are only three subroutines used in this program that are not standard on the IBM 7090. They are PICK, INTP1A, and ANGLE. PICK is the subroutine used for picking a maximum or minimum value from a given set of numbers. INTP1A is used for interpolation in the X_θ loop. ANGLE is used for finding all functions (angle, sin, cos, and tan), given any one function. These subroutines are included as part of the program deck.

List of Stops

There are two program stops that have been introduced. If a stop occurs, the stop number, along with the key values, is printed out.

Stop Number

Description

- | | |
|---|---|
| i | Gear pitch angle Γ greater than or equal to 105° . This may occur if shaft angle is too high. Reduce the shaft angle. |
| 2 | Iteration failed in X_0 loop. This situation will arise if the input data are not reasonable. Check the input cards for accuracy. |

OUTPUT DATA

The output from the program is in the form of a printer listing. Each line of output contains a brief description of the item, its FORTRAN symbol, and its numerical value. The output list is divided into two parts: INPUT and OUTPUT.

On page 244 will be found an explanation of the calculated output values. The letter symbol, the FORTRAN symbol, and a description are given for each item.

All angles given in the output are in degrees. Linear dimensions are in inches. Stresses are given in pounds per square inch. The direction of the bearing shift is dependent upon its algebraic sign: plus means movement toward the outer end of the tooth (heel); minus means movement toward the inner end of the tooth (toe).

SAMPLE PROBLEM

The sample input and output data listed on pages 245 through 248 are for the 17/51 test gear ratio produced with a 12-inch cutter diameter.

INPUT DATA INSTRUCTIONS

<u>Card No.</u>	<u>Columns</u>	<u>Letter Symbol</u>	<u>FORTRAN Symbol</u>	<u>Description</u>
0	1-3	-	T1111	These items are constants used in the program. This card must be the first card of the data. When multiple sets of data are being run, this card has to be included only at the very beginning, and not with every set of data.
	5-8	-	T1112	
	9-10	-	T1113	
	13-15	-	T1114	
1	1-10	n	ZN(1)	Number of teeth in pinion.
	11-20	N	ZN(2)	Number of teeth in gear.
	21-30	P _d	PDIA	Diametral pitch.
	31-40	φ	PHA9	Normal pressure angle - decimal degrees.
	41-50	Σ	SIG9	Shaft angle - decimal degrees.
	51-54	-	DRIVE	Driving member. Enter PIN for pinion, GEAR for gear, or BOTH when either member drives. Must start in column 51.
	61-63	-	ROT	Direction of rotation of driving member (when viewed from back). Enter CW for clockwise, CCW for counterclockwise, or REV when rotation is in either direction. Must start in column 61.

<u>Card No.</u>	<u>Columns</u>	<u>Letter Symbol</u>	<u>FORTRAN Symbol</u>	<u>Description</u>
1	71-72	-	HAND	Pinion hand of spiral. Enter LH for left hand or RH for right hand. Leave blank for straight and Zerol bevels.
2	1-10	F _P	FACE(1)	Pinion pitch line face width.
	11-20	F _G	FACE(2)	Gear pitch line face width.
	21-30	↓	PSM9	Mean spiral angle, decimal degrees. Use zero for straight bevel or Zerol gears.
	31-40	t _{mP}	TMP	Mean pinion circular thickness. Use for spiral bevels only when W _G (fifth item on this card) is not given. For straight bevels only: $t_{mP} = \frac{A}{A_0} \left(t_{oP} - \frac{B_{mx}}{2 \cos \phi} \right)$ <p>where t_{oP} = outer pinion thickness A₀ = outer cone distance A = A₀ - 0.5 F_G</p> t _{oP} and A ₀ are given on Gleason straight bevel gear dimension sheets. F _G is second item on this card. B _{mx} is eighth item on this card. φ is fourth item on card No. 1.
41-50	W _G	WFG	Point width of spread blade gear finishing cutter. Use zero for straight bevels.	

<u>Card No.</u>	<u>Columns</u>	<u>Letter Symbol</u>	<u>FORTRAN Symbol</u>	<u>Description</u>
2	51-60	r_{TP}	REF(1)	Pinion cutter tip edge radius.
	61-70	r_{TG}	REF(2)	Gear cutter tip edge radius.
	71-80	B_{mx}	BMAX	Maximum normal backlash allowance.
3	1-10	h_k	HK	Outer working depth.
	11-20	h_{tP}	HT(1)	Outer pinion whole depth.
	21-30	h_{tG}	HT(2)	Outer gear whole depth.
	31-40	α_P	ADD9(1)	Pinion addendum angle, decimal degrees.
	41-50	α_G	ADD9(2)	Gear addendum angle, decimal degrees.
	51-60	δ_P	DED9(1)	Pinion dedendum angle, decimal degrees.
	61-70	δ_G	DED9(2)	Gear dedendum angle, decimal degrees.
	71-80	a_{oG}	ADO(2)	Gear outer addendum.
4	1-10	FRP	FACR(1)	Pinion root face width; usually equals F_p . This is the face width measured along the root line.
	11-20	FRG	FACR(2)	Gear root face width; usually equals F_g . This is the face width measured along the root line.

<u>Card No.</u>	<u>Columns</u>	<u>Letter Symbol</u>	<u>FORTRAN Symbol</u>	<u>Description</u>
4	21-30	K_o	SKO	Overload factor for strength. This factor takes care of unknown dynamic loads resulting from shock overloads caused by the driving motor or driven machine. References 15 and 16 provide additional information.
	31-40	T_D	CTD	Gear torque, in. -lb (central tooth bearing). This is the torque for which the gear has been designed. Frequently, it is the maximum torque. It is the torque that produces a tooth bearing centrally located on the tooth in the lengthwise direction.
	41-50	K_v	SKV	Dynamic factor for strength. This factor is dependent upon the accuracy of the gears and the operating speed. References 15 and 16 provide additional information.
	51-60	T_G	CTG	Gear torque, in. -lb, for which stress data are required.
	61-70	r_c	RCN	Mean cutter radius. Enter 999999999 for straight bevels.
5	1-10	E	AR(1)	Offset change due to displacement measured at torque level (T_D). If unknown, use zero.

<u>Card No.</u>	<u>Columns</u>	<u>Letter Symbol</u>	<u>FORTTRAN Symbol</u>	<u>Description</u>
5	11-20	P	AR(2)	Pinion axial change due to displacement measured at torque level (T_D). If unknown, use zero.
	21-30	G	AR(3)	Gear axial change due to displacement measured at torque level (T_D). If unknown, use zero.
	31-40	α	AR(4)	Shaft angle change, radians, due to displacement measured at torque level (T_D). If unknown, use zero. Note: E, P, G, and α will be approximated for torque level (T_D) in the program when values of zero are used as input.
	41-50	s_{at}	SAT	Allowable stress for gear material, psi For carburized air-melt steel, use 80,000. For carburized vacuum-melt steel, use 140,000.
	51-60	K_R	SKR	Factor of safety. Use 1 unless extra safety is required.
	61-70	T_F	STF	Operating temperature, degrees Fahrenheit. If unknown, assume 160°F.

CARD
NO. 0

COLUMNS		1	2	3	4	5	6	7	9	9	10
1-10		R	E	V		G	E	A	R	R	H
11-20				C	C	W					
21-30											
31-40											
41-50											
51-60											
61-70											
71-80											

CARD
NO. 1

COLUMNS		1	2	3	4	5	6	7	8	9	10
1 - 10	ZN(1)										
11 - 20	ZN(2)										
21 - 30	PDIA										
31 - 40	PHA9										
41 - 50	SIG9										
51 - 60	DRIVE										
61 - 70	ROT										
71 - 80	HAND										

CARD
NO. 2

COLUMNS		1	2	3	4	5	6	7	8	9	10
1 - 10	FACE(1)										
11 - 20	FACE(2)										
21 - 30	PSM9										
31 - 40	TMP										
41 - 50	WFG										
51 - 60	REF(1)										
61 - 70	REF(2)										
71 - 80	BMAX										

CARD
NO. 3

COLUMNS		1	2	3	4	5	6	7	8	9	10
1 - 10	HK										
11 - 20	HT(1)										
21 - 30	HT(2)										
31 - 40	ADD9(1)										
41 - 50	ADD9(2)										
51 - 60	DED9(1)										
61 - 70	DED9(2)										
71 - 80	ADO(2)										

CARD
NO. 4

COLUMNS		1	2	3	4	5	6	7	8	9	10
1 - 10	FACR(1)										
11 - 20	FACR(2)										
21 - 30	SKO										
31 - 40	CTD										
41 - 50	SKV										
51 - 60	CTG										
61 - 70	RCN										
71 - 80											

CARD
NO. 5

COLUMNS		1	2	3	4	5	6	7	8	9	10
1 - 10	AR(1)										
11 - 20	AR(2)										
21 - 30	AR(3)										
31 - 40	AR(4)										
41 - 50	SAT										
51 - 60	SKR										
61 - 70	STF										
71 - 80											

TABLE XXVI. LIST OF SYMBOLS

FORTRAN SYMBOL	LETTER SYMBOL	DESCRIPTION
AS	A_2	-
ADD9(T)	$\alpha_{(P, G)}$	Addendum angle
ADM(I)	$a_{(P, G)}$	Mean addendum
AD0(I)	$a_o(P, G)$	Outer addendum
AFG	A_{FG}	Gear axial modified adjustability coefficient
AFP	A_{FP}	Pinion axial modified adjustability coefficient
AINCT	w	Angle of inclination of line of contact with pitch line
AM	A	Mean cone distance
A0	A_o	Outer cone distance
AR(1)	E	Offset displacement from no-load position to load CTD (T_D)
AR(2)	P	Pinion axial displacement from no-load position to load CTD (T_D)
AR(3)	G	Gear axial displacement from no-load position to load CTD (T_D)
AR(4)	α	Shaft angle displacement from no-load position to load CTD (T_D)
AR1(1)	E_1	Offset displacement from position corresponding to load which produces a centrally located tooth bearing
AR1(2)	P_1	Pinion axial displacement from position corresponding to load which produces a centrally located tooth bearing
AR1(3)	G_1	Gear axial displacement from position corresponding to load which produces a centrally located tooth bearing
AR1(4)	α_1	Shaft angle displacement from position corresponding to load which produces a centrally located tooth bearing
AR5(1)	A_{FE}	See BFE
AR5(2)	A_{FP}	See AFP
AR5(3)	A_{FG}	See AFG
AR5(4)	$A_{F\alpha}$	See BFALPH
ASK1	-	Absolute value of SK1 (k_1)
ASK1P	-	Absolute value of SK1P (k_1')
B	B	Length of tooth contact area under given load
B1	B_1	Length of tooth contact area under given load (1 DP)
BETA	β	-

TABLE XXVI - Continued

FORTRAN SYMBOL	LETTER SYMBOL	DESCRIPTION
BFALPH	A_{Fa}	Shaft angle adjustability coefficient
BFE	A_{FE}	Offset adjustability coefficient
BMAX	B_{mx}	Maximum normal backlash allowance
CB	C_s	Factor to determine lengthening of tooth contact under load
CR(I)	$R_{1(P, G)}$	Pitch radius in mean transverse section (1 DP)
OTD	T_D	Gear torque for central tooth contact
OTG	T_G	Gear torque
OTP	T_P	Pinion torque
CX	$X_{(P, G)}$	-
DED δ (I)	$\delta_{(P, G)}$	Dedendum angle
DEDM(I)	$b_{(P, G)}$	Mean dedendum
DED \bar{O} (I)	$b_o(P, G)$	Outer dedendum
DIAP(I)	d, D	Outer pitch diameter
DRIVE	-	Driving member
DRN	$\Delta R_{N(P, G)}$	Distance from pitch circle to point of load application measured along tooth centerline
ETA	η	-
ETAJ	$\eta_{J(P, G)}$	-
ETAJP	$\eta_{J(P, G)}$	-
F1	F_1	Minimum face width (1 DP)
FACE(I)	$F_{(P, G)}$	Pitch line face width
FACR(I)	$F_R(P, G)$	Root line face width
FE	$F_e(P, G)$	Effective face width
FJ	$f_{J(P, G)}$	-
FK	$F_K(P, G)$	Projected length of the line of contact within the ellipse of tooth contact in the lengthwise direction of the tooth
FMN	F_{mn}	Minimum face width
FR1	$F_{R1(P, G)}$	Root face width (1 DP)
FX1	f	Lengthwise shift of tooth contact from center under given load

TABLE XXVI - Continued

FORTRAN SYMBOL	LETTER SYMBOL	DESCRIPTION
GAM9(I)	γ, Γ	Pitch angle
HAND	-	Hand of pinion spiral
HK	h_k	Outer working depth
HN	$h_N(P, G)$	Distance along tooth centerline from the weakest section to the point of load application
HT(I)	$h_t(P, G)$	Outer whole depth
HTM1	$h_{t1}(P, G)$	Outer whole depth (1 DP)
P2	P_2	-
P3	$P_3(P, G)$	Distance in mean normal section from beginning of action to point of load application
PCIR	p	Outer circular pitch
PCN	P_N	Normal base pitch (1 DP)
PDIA	P_d	Transverse diametral pitch
PHA9	ϕ	Normal pressure angle
PHA9I	-	Involute function of PHA9 (inv ϕ)
PHIH	$\phi_L(P, G)$	Pressure angle at point of load application
PHIL	$\phi_L(P, G)$	Angle that the normal force makes with a line perpendicular to the tooth centerline
PM	P_m	Mean transverse diametral pitch
PN	P_n	Mean normal circular pitch
PSIB	ψ_b	Base spiral angle
PSM9	ψ	Mean spiral angle
PSO9	ψ_o	Outer spiral angle
Q(I)	$Q(P, G)$	Strength factor
RBN1(I)	$R_{bn1}(P, G)$	Base radius in mean normal section (1 DP)
RCN	r_o	Mean cutter radius
REF(I)	$r_T(P, G)$	Cutter tip edge radius
RF	$r_f(P, G)$	Fillet radius at root circle (1 DP)
RN(I)	$R_1(P, G)$	Pitch radius in mean transverse section (1 DP)

TABLE XXVI - Continued

FORTRAN SYMBOL	LETTER SYMBOL	DESCRIPTION
RN1(I)	$R_{N1}(P, G)$	Pitch radius in mean normal section (1 DP)
RON1(I)	$R_{oN1}(P, G)$	Outside radius in mean normal section (1 DP)
ROT	-	Direction of rotation of driving member as viewed from the back
RT	$R_t(P, G)$	Mean transverse radius to point of load application (1 DP)
RT1(I)	$r_{T1}(P, G)$	Cutter tip edge radius (1 DP)
SA1(I)	$a_1(P, G)$	Mean addendum (1 DP)
SAT	σ_{at}	Allowable stress in gear material
SAVE	$\sigma_{avg}(P, G)$	Average stress
SB1(I)	$b_1(P, G)$	Mean dedendum (1 DP)
SF1(I)	$F_1(P, G)$	Pitch face width (1 DP)
SIG9	Σ	Shaft angle
SJ(I)	$J(P, G)$	Geometry factor for strength
SK	$k(P, G)$	-
SK1	k_1	Coefficient for lengthwise tooth contact shift
SK2	k_2	Coefficient descriptive of lengthwise crowning of the teeth
SK3	k_3	Coefficient descriptive of relative tooth contact length under load and no load
SK4	k_4	Coefficient descriptive of center of contact pressure under load
SK1P	k_1'	Coefficient for lengthwise tooth contact shift
SKF	$K_f(P, G)$	Combined stress concentration and stress correction factor
SKI	K_i	Inertia factor
SKM(I)	$K_m(P, G)$	Load distribution factor
SKN	k_n	Positive integer
SKO	k_o	Overload factor
SKP	k'	Load position correction factor
SKR	K_R	Factor of safety
SKS	K_S	Size factor
SKT	K_T	Temperature factor
SKV	K_v	Dynamic factor

TABLE XXVI - Continued

FORTRAN SYMBOL	LETTER SYMBOL	DESCRIPTION
SL1	i_1	Length of tooth contact area at no load
SMAX	s_{max}	Maximum stress
SMN(I)	m_n	Load sharing ratio
SST(I)	$s_{t(P,G)}$	Bending stress in root fillet
ST(I)	$t_{(P,G)}$	Mean normal circular thickness
ST1(I)	$t_{1(P,G)}$	Mean normal circular thickness (1 DP)
STF	T_F	Operating temperature of gears
SW	s_w	Working stress
SZ1	$z_{1(P,G)}$	-
SZ2	$z_{2(P,G)}$	-
THET	$\theta_{(P,G)}$	-
TMGP	t_{mG}	Gear mean circular thickness (output)
TMP	t_{mP}	Pinion mean circular thickness (input)
TMP0P	t_{mP0}	Pinion mean circular thickness assuming zero backlash
TMPP	t_{mP}^i	Pinion mean circular thickness (output)
TN	$t_{N(P,G)}$	One-half tooth thickness at weakest section
T0	T_0	Peak torque
U1(I)	$U_{1(P,G)}$	-
U2(I)	$U_{2(P,G)}$	-
U3(I)	$U_{3(P,G)}$	-
UHF	H_f	Stress concentration factor constant
UJF	J_f	Stress concentration factor constant
ULF	L_f	Stress concentration factor constant
V1(I)	$V_{1(P,G)}$	-
V2(I)	$V_{2(P,G)}$	-
V3(I)	$V_{3(P,G)}$	-
WFG	W_G	Point width of spread blade gear finishing cutter

TABLE XXVI - Continued

FORTRAN SYMBOL	LETTER SYMBOL	DESCRIPTION
X1	$x_1(P, G)$	-
X2	$x_2(P, G)$	-
XFR	$x_{FR}(P, G)$	-
XMF	m_F	Face contact ratio
XMNR	m_n	Normal contact ratio
XMO	m_o	Modified contact ratio
XMP	m_p	Transverse (profile) contact ratio
XN	$x_N(P, G)$	Tooth strength factor
XNGNP	m_G	Gear ratio
XPP	$x_{(P, G)}$	-
XTHET	$x_{\theta}(P, G)$	-
Y2	$y_2(P, G)$	-
YK	$y_K(P, G)$	Tooth form factor
Z1	Z_1	Length of action in mean transverse section (1 DP)
ZETA	$\zeta_{(P, G)}$	-
ZN(I)	n, N	Number of teeth
ZN1	Z_{N1}	Length of action in mean normal section (1 DP)
ZP (I)	Z_1', Z_2'	Arc of action (approach / recess) in mean normal section (1 DP)

BENDING STRESS CALCULATIONS FOR BEVEL GEARS

PROGRAMMED BY R. TOMASINO

GLEASON WORKS U.S.A.

C C C C C C C C C C C C C C C

```

DIMENSION ZN(2),FACE(2), REF(2),HT(2),ADD9(2),DED9(2),ADO(2)
1)FACR(2),DEDO(2),GAM9(2),ADM(2),DEDM(2),SGAM9(2),CGAM9(2),TGAM9(2)
2)SDED9(2),TDED9(2),TDED9(2),SADD9(2),CADD9(2),TADD9(2),CR(2),RN(2)
3)RBN1(2),SAL(2),SBI(2),ROWN(2),ZP(2),ST(2),SMN(2),RT1(2),SF1(2),Q
4(2),SST(2),ST1(2), SJ(2),DIAP(2),RN1(2),ISST(2),
5ARI(4),AR(4),AR5(4),V1(2),V2(2),V3(2),U1(2),U2(2),U3(2),SKM(2)
READ(5,9920)T1111,T1112,T1113,T1114
9920 FORMAT(4A4)
6 READ (5,9900)ZN(1),ZN(2),PDIA,PHA9 ,SIG9,DRIVE,ROT,HAND
9900 FORMAT(5F10.0,A4,6X,A3,7X,A2)
IF(ZN(1))301,29,301
301 READ(5,9910)FACE(1),FACE(2),PSM9,TMP,WFG,REF(1),REF(2),BMAX,HK,
2,SKO,CTD,SKV,CTG,RCN
9910 FORMAT(8F10.0)
READ(5,303)AR,SAT,SKR,STF
303 FORMAT(8F10.0)
PI=3.1415927
RAD=57.29578
SIDE=1.
IF(ROT-T1111)1,2,1
1 IF(DRIVE-T1112)3,4,3
4 SIDE=-SIDE
3 IF(HAND -T1113)5,306,5

```

22

```

306 SIDE=-SIDE
5 IF(ROT-T1114) 12*7*2
7 SIDE=-SIDE
2 PHA9=PHA9/RAD
PSM9=PSM9/RAD
DO 601 I=1*2
DED9(I)=DED9(I)/RAD
ADD9(I)=ADD9(I)/RAD
CONTINUE
601 CALL ANGLE (PHA9*SPHA9*CPHA9*TPHA9*1)
CTP=CTG*(ZM(1)/ZN(2))
DIAP(1)=ZN(1)/PDIA
DIAP(2)=ZN(2)/PDIA
SIG9=SIG9/RAD
SSIG9= SIN(SIG9)
CSIG9= COS(SIG9)
XNGMP=ZN(2)/ZN(1)
TGAM9(1)=SSIG9/(XNGMP + CSIG9)
CALL ANGLE(GAM9(1)*SGAM9(1)*CGAM9(1)*TGAM9(1)*4)
GAM9(2)=SIG9-GAM9(1)
IF( ABS(GAM9(2))-1.5707963)-0.0087266)196*197*197
196 TGAM9(2) = 10000.0
CGAM9(2) = 0.00001
SGAM9(2) = SIN(GAM9(2))
GO TO 1197
197 CALL ANGLE(GAM9(2)*SGAM9(2)*CGAM9(2)*TGAM9(2)*1)
1197 AO = 0.5*DIAP(2)/SGAM9(2)
AM=AO - 0.5*FACE(2)
PCIR = PI/PDIA
ADO(1)=HK-ADO(2)
CALL ANGLE(PSM9*SPSM9*CPSM9*TPSM9*1)
CALL ANGLE (DED9(1)*SDED9(1)*CDED9(1)*TDED9(1)*1)
CALL ANGLE (DED9(2)*SDED9(2)*CDED9(2)*TDED9(2)*1)
CALL ANGLE(ADD9(1)*SADD9(1)*CADD9(1)*TADD9(1)*1)
CALL ANGLE (ADD9(2)*SADD9(2)*CADD9(2)*TADD9(2)*1)
DO 460 I=1*2
DED0(I)=HT(I)-ADO(I)

```

063
064
065
066
067
068
069
070
071
072
073
074
075
076
077
078
079
080
081
082
083
084
085
086
087
088
089
090
091
092
093
094
095
096
097
098
099

```
460 DEDM(1)=DEDO(1)-.5*FACE(2)*TDED9(1)
    ADM(1)=ADO(1)-.5*FACE(2)*TADD9(1)
    DC = 2.0*RCN
    SPS09=(AM*(DC*SPSM9 -AM) + AO**2.0)/(DC*AO)
    CALL ANGLE (PS09*SPS09*CPS09*TPS09*2)
    TEM=AM/AO
    TEM1=.5*TEM/(CPHA9*CPS09)
    IF (MFG)19*21*19
19  TMP0P=(2.*DEDM(2)*TPHA9+WFG)/CPSM9-TEM1*BMAX
    GO TO 22
21  TMP0P=TMP+TEM1*BMAX
22  TMPP=TMP0P-TEM1*BMAX
    TMGP=TEM*PCIR-TMP-TEM1*2.*BMAX
    TEM=1./TEM
    UMF =.3254545-.416695*PHA9
    UJF =.3318182-.52087*PHA9
    ULF =.2681818+.52087*PHA9
    PM=AO*PDIA/AM
    PN=3.1415926*CPSM9/PM
    P2=PDIA*PN/(CPHA9*(CPSM9**2+TPHA9**2))
    IF( FACE(2)-FACE(1)62*63*63
62  FMX=FACE(1)
    CALL PICK(FACE(2)*FACR(2)*FACR(1)*1*FMN)
    GO TO 64
63  FMX=FACE(2)
    CALL PICK(FACE(1)*FACR(2)*FACR(1)*1*FMN)
64  IF(FACE(1)-FACR(1))65*66*66
65  FPMX=FACR(1)
    FPMN=FACE(1)
    GO TO 67
66  FPMX=FACE(1)
    FPMN=FACR(1)
67  IF(FACE(2)-FACR(2))68*69*69
68  FGMN=FACE(2)
    FGMX=FACR(2)
    GO TO 70
69  FGMN=FACR(2)
```

100
101
102
103
104
105
106
107
108
109
110
111
112
113
114
115
116
117
118
119
120
121
122
123
124
125
126
127
128
129
130
131
132
133
134
135
136

FGMX=FACE(2)
TEM4=CPHA9*((SPSM9/AM)-(1./RCN))
TEM5=CGAM9(1)*SPHA9*((1./AM)-(SPSM9/RCN))
AFP=(CGAM9(1)/CPSM9)* (TEM4+TEM5)
TEM7=CGAM9(2)*SPHA9*((1./AM)-(SPSM9/RCN))
AFG=-((CGAM9(2)/CPSM9)* (TEM4-TEM7))
BFE=(-1./AM)*((1./SSIG9)*CPHA9
BFALPH=- (SPHA9/CPSM9)*((1./SSIG9)
AR5(1)=BFE
AR5(2)=AFP
AR5(3)=AFG
AR5(4)=BFALPH
SK4=1.25
IF(AR(1))4001'4000
4001 AR(1)=-.00000033*CTD
AR(2)=.00000033*CTD
AR(3)=-.00000020*CTD
AR(4)=.00000006*CTD
AR(1)=-.00000033*(CTG-(SK4*CTD))
AR(2)=.00000033*(CTG-(SK4*CTD))
AR(3)=-.00000020*(CTG-(SK4*CTD))
AR(4)=.00000006*(CTG-(SK4*CTD))
4000 IF(CTD-CTG)4003'4003'4004
4003 TO=(SK4*CTG)
IF(AR(1))4006'4005'4006
4004 TO=(SK4*CTD)
IF(AR(1))4006'4005'4006
4005 AR(1)=AR(1)*((CTG-(SK4*CTD))/CTD)
AR(2)=AR(2)*((CTG-(SK4*CTD))/CTD)
AR(3)=AR(3)*((CTG-(SK4*CTD))/CTD)
AR(4)=AR(4)*((CTG-(SK4*CTD))/CTD)
SK3=1.
C2=SK3*(CTG/TO)
4006 SK1=SK9*(AR(1)*AR5(1)+AR(2)*AR5(2)+AR(3)*AR5(3)+AR(4)*AR5(4))
SK2=250./(DIAP(2))*-.3333333333
ASK1=ABS(SK1)
IF(ASK1-.00061)5000'5001'5001

137
138
139
140
141
142
143
144
145
146
147
148
149
150
151
152
153
154
155
156
157
158
159
160
161
162
163
164
165
166
167
168
169
170
171
172
173

```
5000 SL1=FMM  
GO TO 5007  
5001 TEMP10= SORT(1.+(8.*ASK1*SK2+FMM/CPSM9))  
SL1=1./(4.*ASK1*SK2)*(TEMP10-1.)  
5007 A2=C2*(FMM/(SL1*CPSM9)-1.))+1.  
B=A2*SL1*CPSM9  
B1=B*PDIA  
SK1P=AR1(1)*AR5(1)+AR1(2)*AR5(2)+AR1(3)*AR5(3)+AR1(4)*AR5(4)  
ASKIP=ABS(SK1P)  
IF(ASKIP-.00001)5002*5003*5003  
5002 FX1=0.  
GO TO 70  
5003 TEMP11=SGRT(1.+(8.*ASK1P*SK2+FMM/CPSM9))  
FX1=(FMM*ASKIP)/(2.*SK1P*CPSM9)-(1.)/(8.*SK1P*SK2)*(TEMP11-1.)  
70 XMF = (AO/AM)*(B *TPSM9/PCIR)  
CR(1)=.5*ZN(1)/(CGAM9(1)*TEM)  
IF(1.5708-GAM9(2))139*140*140  
139 IF(1.8326-GAM9(2))141*142*142  
141 ISTOP=1  
GO TO 36  
140 CR(2)=.5*ZN(2)/(CGAM9(2)*TEM)  
GO TO 144  
142 CR(2)=10000.  
144 DO 71 I=1,2  
RN1(I)=CR(I)/CPSM9**2  
RBN1(I)=RN1(I)*CPHA9  
SAL(I)=ADM(I)*PDIA  
SBI(I)=DEDM(I)*PDIA  
RON1(I)=RN1(I)+SAL(I)  
71 ZP(I)=RON1(I)* SORT(1.-(RBN1(I)/RON1(I)**2)-RN1(I)*SPHA9  
ZNI=ZP(I)+ZP(2)  
XMP=ZNI/P2  
XMO= SORT(XMP**2+XMF**2)  
PCN=PDIA*PN*CPHA9  
SKP=(ZN(2)-ZN(1))/(8.*ZN(1))+6.4*ZN(2))  
SPSIB=SPSM9*CPHA9  
CALL ANGLE(PSIB*SPSIB*CPISIB*TPSIB*2)
```

```

174 Z1=ZMI*CPSIB
175 F1=FMW*PDIA
176 ETA = SORT((Z1*CPSIB)**2+(B1*SPSIB)**2)
177 DUM=0.
178 K=1
179 ST(1)=TMPP*CPSM9
180 ST(2)=PN-ST(1)-TEM1*BMAX*CPSM9*2.
181 PHA 9]=TPHA9-PHA9
182 DO 226 I=1,2
183 ST1(1)=PDIA*ST(1)
184 GO TO 97
185 ISUB=2
186 SKI=1.
187 FJ=0.
188 GO TO 111
189 I=1
190 IF(XMO-2.199*100*100
191 FJ=PCN-.5*ETA
192 SKI=2./XMO
193 ISUB=2
194 ETAJ= SORT(ETA**2-4.*FJ**2)
195 P3=.5*Z1/CPSIB+(Z1/ETA)**2*FJ +SIDE*B1*Z1*ETAJ*SKP*TPSIB/ETA**2
196 I-DUM
197 ISW2=1
198 COMS=1.
199 ETAJP=ETAJ**3
200 SKN=1.
201 TEM2=(ETAJ**2-4.*SKN*PCN*(SKN*PCN+2.*FJ #COMS))**3
202 IF(TEM2)117,118,118
203 ETAJP=ETAJP+ SORT(TEM2)
204 SKN=SKN+1.
205 GO TO 119
206 GO TO(120,121)*ISW2
207 COMS=-1.
208 ISW2=2
209 GO TO 122
210 SMN(1)=ETAJ**3/ETAJP

```

211
212
213
214
215
216
217
218
219
220
221
222
223
224
225
226
227
228
229
230
231
232
233
234
235
236
237
238
239
240
241
242
243
244
245
246
247

```

TPH IH=(P3+(RN1(I)+RN1(2))*SPHA9- SORT(RN1(ISUB)**2-RN1(ISUB)**2)
1)/RN1(I)
PHIH= ATAN(TPHIH)
FK=B1*Z1*ETA+CPSIB/ETA**2
XPP=FK*SKP-SIDE*B1**2*FJ *SPSIB/ETA**2
PHIL=PHIH-ST1(I)*.5/RN1(I)+TPH IH-PHIH-PHA9I
CALL ANGLE(PHIL'SPHIL'CPHIL'TPHIL'1)
DRN=RN1(I)/CPHIL-RN1(I)
RT1(I)=PDIA*REF(I)
X1=.5*ST1(I)+SB1(I)*TPHA9+RT1(I)*(1./CPHA9-TPHA9)
Y2=SB1(I)-RT1(I)
XTHET=X1+Y2
DO 124 K=1'12
THET=XTHET/RN1(I)
X2=XTHET-X1
CALL ANGLE(THET'STHET'CTHET'TTHET'1)
SZ1=Y2*CTHET-X2*STHET
SZ2=Y2*STHET+X2*CTHET
TZETA=SZ1/SZ2
CALL ANGLE(ZETA'SZETA'CZETA'TZETA'4)
TN=XTHET-RN1(I)*(THET-STHET)-RT1(I)*CZETA-SZ2
HN=DRN+RN1(I)*(1.-CTHET)+RT1(I)*SZETA+SZ1
SK=TN/(HN*TZETA)
ERR=2.-SK
IF( ABS(ERR)-.001)125'124'124
124 CALL INTPIA(XTHET'ERR'K'.005)
ISTOP=2
WRITE (6'06) XTHET'ERR'I
86 FORMAT(1X'2F13.7'15)
GO TO 36
125 XM=TN**2/HN
FRI=PDIA*FACR(I)
AINCT=ATAN(SPHA9*TPSM9)
HTM1=PDIA*HT(I)
BETA=FHN/12.*RCN*CPISM9)
V1(I)=(5.27+SIDE*(5.80*BETA)+(1.90+SIDE*(1.530*BETA))*(HN/HTM1)+(4
1.07+SIDE*(1.84*BETA))*(FK/FRI)-(1.117-SIDE*(.179*BETA))*AINCT-(29.6

```

```

2+SIDE*(48.*BETA))*PHA9+(36.7+SIDE*(73.*BETA))*PHA9**2
V2(I)=(-1.00-SIDE*(7.45*BETA))-((1.51+SIDE*(.570*BETA))*{(HN/HTMI)}-(
17.28+SIDE*(2.60*BETA))*{(FK/FRI)}+(.173-SIDE*(.155*BETA))*AINCT+(49.
27+SIDE*(61.8*BETA))*PHA9-(66.1+SIDE*(93.5*BETA))*PHA9**2
V3(I)=(.365+SIDE*(2.87*BETA))*{(FK/FRI)}-(.593+SIDE*(.294*BETA))*{(HN/HTMI)}+(2
1.69+SIDE*(1.01*BETA))*{(FK/FRI)}-(.0727-SIDE*(.0620*BETA))*AINCT-(18
1.5+SIDE*(23.8*BETA))*PHA9+(24.8+SIDE*(35.8*BETA))*PHA9**2
SMAX=EXP(V1(I))-V2(I)**2/(4.*V3(I))
U1(I)=(7.29+SIDE*(7.21*BETA))*{(1.48+SIDE*(2.60*BETA))*{(HN/HTMI)}+(
120.9-SIDE*(50.2*BETA))*PHA9+(-.273-SIDE*(2.36*BETA))*{(HN/HTMI)**2+
2(28.0+SIDE*(78.3*BETA))*PHA9**2
U2(I)=(-5.01-SIDE*(11.2*BETA))*{(1.800-SIDE*(4.60*BETA))*{(HN/HTMI)}+(
132.0+SIDE*(77.9*BETA))*PHA9+(-.717+SIDE*(3.98*BETA))*{(HN/HTMI)**2+
2(-47.1-SIDE*(120.*BETA))*PHA9**2
U3(I)=(1.85+SIDE*(4.19*BETA))*{(-.321+SIDE*(1.61*BETA))*{(HN/HTMI)}+(
1-11.8-SIDE*(28.9*BETA))*PHA9+(.284-SIDE*(1.39*BETA))*{(HN/HTMI)**2+
2(17.4+SIDE*(44.4*BETA))*PHA9**2
SAVG=EXP(U1(I))-U2(I)**2/(4.*U3(I))
RF=Y2**2/(RN1(I)+SB1(I))-RT1(I)+RT1(I)
SKF=UHF+(2.*TN/RF)**UJF*(2.*TN/HN)**ULF
RT=CR(I)*(1.+XPP/(AM*PDIA))+DRN
SF1(I)=PDIA*FACE(I)
FE=FACE(I)*PDIA*SAVG/SMAX
XFR=FX1/(FMN/CP*SM9)
SKM(I)=1.00+(14.6+SIDE*(7.6*BETA))*XFR**2-(66.3+SIDE*(17.7*BETA))
1*XFR**4+105.*XFR**6
CX=3.*XM*TN/13.*TN-TPHIL*XM
YK=.66666667*CX/SKF
SJC(I)=YK*FE*R*PDIA/(SMN(I)*SKI*SF1(I))*CR(I)*PH
I=I+1
IF(I-2)159*159*568
159 ISUB=1
SIDE=-SIDE
GO TO 111
568 IF(PDIA-16.)179*179*179
179 SKS=2.*1./PDIA**25)
GO TO 180

```

248
249
250
251
252
253
254
255
256
257
258
259
260
261
262
263
264
265
266
267
268
269
270
271
272
273
274
275
276
277
278
279
280
281
282
283
284

285
286
287
288
289
290
291
292
293
294
295
296
297
298
299
300
301
302
303
304
305
306
307
308
309
310
311
312
313
314
315
316
317
318
319
320
321

179 SKS=1.0
180 TEM2=2.*PDIA
Q(1)=TEM2/(FACE(1)*DIAP(1)*SJ(1))
Q(2)=TEM2/(FACE(2)*DIAP(2)*SJ(2))
SST(1)=CTP*Q(1)*SKO*SKM(1)/SKV
SST(2)=CTG*Q(2)*SKO*SKM(2)/SKV
XMR=ZM1/PCN
SKT=(460*STF)/620
SW=SAT/(SKT*SKR*SKS)
PHA9=PHA9*
PSM9=PSM9*
SIG9=SIG9*
DO 168 I=1,2
ADD9(I)=ADD9(I)*
DED9(I)=DED9(I)*
GAM9(I)=GAM9(I)*
ICTP=CTP
ICTG=CTG
ISST(1)=SST(1)
ISST(2)=SST(2)
ISW=SM
ICTD = CTD
ISAT=SAT
WRITE(6,'277)ZN(1)*ZN(2)*PDIA*PHA9*SIG9*DRIVE*ROT*HAND*FACE(1)*FACE
1(2)*PSM9*TMP*WFG*REF(1)*REF(2)*BMAX*HK*HT(1)*HT(2)*ADD9(1)
WRITE(6,'377)ADD9(2)*DED9(1)*DED9(2)*FACR(1)*FACR(2)*SKO*ICT
10*SKV*ICTP*ICTG*RCN*AR(1)*AR(2)*AR(3)*AR(4)*ISAT*SKR*STF
WRITE(6,'378) TMPP*TMGP*GAM9(1)*GAM9(2)*XMP*XMF*XMO*AO*AM*PCI
2R*SMN(1)*SMN(2)*SKI*SJ(1)*SJ(2)
WRITE(6,'477) G(1)*G(2)*ISST(1)*ISST(2)*FX1*ISW
277 FORMAT(20X,'5HINPUT//2X,'25HNUMBER OF TEETH IN PINION,'20X,'5HZN(1)),F1
10.5/2X,'23HNUMBER OF TEETH IN GEAR,'22X,'5HZN(2)',F10.5/2X,'15HDIAMETRA
2L PITCH,' 31X,'4HPDIA',F10.5/2X,'21HNORMAL PRESSURE ANGLE,'25X,'4HPHA9'
3F10.5/2X,'11HSHAFT ANGLE,'35X,'4HSIG9',F10.5/2X,'14HDRVING MEMBER,'31X'
45HDRIVE,'4X,'A4/2X,'21HDIRECTION OF ROTATION,'26X,'3HROT,'4X,'A3/2X,'21HPI
5NION HAND OF SPIRAL,'25X,'4HHAND,'4X,'A2/2X,'17HPINION FACE WIDTH,'26X,'7
1HFACE(1)',F10.5/2X,'15HGEAR FACE WIDTH

1'28X'7HFACE(2)'F10.5/2X'17HMEAN SPIRAL ANGLE'29X'4HPSM9'F10.5/2X'3
 20HPINION MEAN CIRCULAR THICKNESS'17X'3HTMP'F10.5/2X'39HPOINT WIDTH
 3 OF SPREAD BLADE GEAR CUTTER'8X'3HWFG'F10.5/
 32X'28HEDGE RADIUS ON PINION CUTTER
 4 '16X'6HREF(1)'F10.5/2X'26HEDGE RADIUS ON GEAR CUTTER'18X'6HRE
 5F(2)'F10.5/2X'23HMAXIMUM NORMAL BACKLASH'23X'4HBMX'F10.5/2X'35HMO
 6R KING DEPTH AT OUTER END OF TOOTH'13X'2HHK'F10.5/2X'40HPINION WHOL
 7E DEPTH AT OUTER END OF TOOTH'5X'5HHT(1)'F10.5/2X'38HGEAR WHOLE DE
 8PTH AT OUTER END OF TOOTH'7X'5HHT(2)'F10.5/2X'21HPINION ADDENDUM A
 9NGLE'22X'7HADD9(1)'F10.5/
 377 FORMAT(2X'19HGEAR ADDENDUM ANGLE'24X'7HADD9(2)'F10.5/2X'21HPINION
 1DEDENDUM ANGLE'22X'7HDED9(1)'F10.5/2X'19HGEAR DEDENDUM ANGLE'24X'7
 2HDED9(2)'F10.5/2X'35HGEAR ADDENDUM AT OUTER END OF TOOTH'9X'6HADO(1
 3)'F10.5/2X'22HPINION ROOT FACE WIDTH'21X'7HFACR(1)'F10.5/2X'20HGE
 4AR ROOT FACE WIDTH'23X'7HFACR(2)'F10.5/2X'28HVERLOAD FACTOR FOR S
 5TRENGTH'19X'3HSKO'F10.5/2X'31HGEAR TORQUE FOR CENTRAL BEARING'16X'
 6 3HCTD'3X'17 /2X'27HDYNAMIC FACTOR FOR STRENGTH'20X'3HSKV'F10.
 75/2X'13HPINION TORQUE'34X'3HCTP'3X'17 /2X'11HGEAR TORQUE'36X'3HC
 3TG'3X'17 /2X'13HCUTTER RADIUS'34X'3HRCN'F10.5/2X'33HOFFSET CHANG
 1E DUE TO DISPLACEMENT'12X'5SHAR(1)'F10.5/2X'39HPINION AXIAL CHANGE
 1DUE TO DISPLACEMENT'6X'5SHAR(2)'F10.5/2X'37HGEAR AXIAL CHANGE DUE T
 20 DISPLACEMENT'8X'5SHAR(3)'F10.5/2X'38HSHAFT ANGLE CHANGE DUE TO DI
 3SPLACEMENT'7X'5SHAR(4)'F10.5
 3/2X'16HALLOWABLE STRESS'31X'3HSAT'3X'17 /2X'16HFACTOR OF SA
 4FETY'31X'3HSKR'F10.5/2X'21HOPERATING TEMPERATURE'26X'3HSTF'F10.5/
 378 FORMAT(1H5'20X'
 9 6HOUTPUT/2X'30HPINION MEAN CIRCULAR THICKNESS'16X'4HTMPP'F10.
 85/2X'28HGEAR MEAN CIRCULAR THICKNESS'18X'4HTMGP'F10.5/
 1 2X'18HPINION PITCH ANGLE'25X'7HGAM9(1)'F10.5/2X'16HGEAR PIT
 2CH ANGLE'27X'7HGAM9(2)'F10.5/2X'24HTRANSVERSE CONTACT RATIO'23X'3H
 3XMP'F10.5/2X'18HFACE CONTACT RATIO'29X'3HXMF'F10.5/2X'22HMODIFIED
 4CONTACT RATIO'25X'3HXMO'F10.5/2X'19HOUTER CONE DISTANCE'29X'2HAOF
 510.5/2X'18HMEAN CONE DISTANCE'30X'2HAM'F10.5/2X'14HCIRCULAR PITCH'
 632X'4HPCIR'F10.5/2X'25HPINION LOAD SHARING RATIO'19X'6HSMN(1)'F10.
 75/2X'23HGEAR LOAD SHARING RATIO'21X'6HSMN(2)'F10.5/2X'14HINERTIA F
 1ACTOR'33X'3HSKI'F10.5
 I /2X'35HPINION GEOMETRY FACTOR FOR STRENGTH'10X'5HSJ(1)

```

359 9'F10.5/2X'33HGEAR GEOMETRY FACTOR FOR STRENGTH'12X'5HSJ(2)'F10.5 )
360 477 FORMAT(2X'2HPINION STRENGTH FACTOR'24X'4HQ(1)'F10.5/2X'20HGEAR ST
361 LENGTH FACTOR'26X'4HQ(2)'F10.5/2X'24HBENDING STRESS ON PINION'20X'
362 16HSSI(1)'3X'17/2X'22HBENDING STRESS ON GEAR'22X'6HSSI(2)'3X'17/2X'
363 524HLENGTHWISE BEARING SHIFT'23X'3HFX1'F10.5/2X'14HWORKING STRESS'3
364 34X'2HSM'3X'17//////////)
365 GO TO 6
366 WRITE(6,35)I$STOP
367 35 FORMAT(7H STOP 'I2)
368 29 CALL EXIT
369 END
370 SUBROUTINE ANGLE(ANG'XSIN'XCOS'XTAN*K)
371 REVISION - AUGUST 14'1968
372 GO TO(1'3'6'7)'K
373 1 XSIN = SIN(ANG)
374 XCOS = COS(ANG)
375 4 IF(XCOS) 8'9'8
376 9 XTAN = .99999999*(10.0**90)
377 IF(XSIN)14'10'10
378 14 XTAN = -XTAN
379 GO TO 10
380 8 XTAN = XSIN / XCOS
381 10 GO TO (2'5'11'5)'K
382 3 IF(ABS(1.0 - ABS(XSIN)) -.000000001)16'17'17
383 16 XCOS = 0.0
384 GO TO 4
385 17 XCOS = SORT(1.0 - XSIN**2)
386 GO TO 4
387 5 ANG = ATAN(XTAN)
388 2 RETURN
389 6 IF(ABS(1.0 - ABS(XCOS)) -.000000001)19'20'20
390 19 XSIN = 0.0
391 GOTO 4
392 20 XSIN = SORT(1.0 - XCOS**2)
393 GO TO 4
394 7 XCOS = 1.0/SORT(1.0 + XTAN**2)
395 XSIN=XCOS*XTAN

```

```

GO TO 5
11 IF (XCOS) 12,5,5
12 ANG = 3.1415928 + ATAN(X/TAN)
GOTO 2
END
SUBROUTINE INTPI(A,X,I,ASTEP)
IF(I-1)1,1,2
1 DA=ASTEP
3 A=A+DA
XO=X
RETURN
2 DA= X*DA/(XO-X)
GO TO 3
ENC
SUBROUTINE PICK(X1,X2,X3,I,X)
GO TO(1,2),I
1 IF(X1-X2)3,4,4
4 IF(X2-X3)5,6,6
5 X=X2
7 RETURN
6 X=X3
GO TO 7
3 IF(X1-X3)8,6,6
8 X=X1
GO TO 7
2 IF(X1-X2)9,10,10
10 IF(X1-X3)6,8,8
9 IF(X2-X3)6,5,5
END

```

396
397
398
399
400
401
402
403
404
405
406
407
408
409
410
411
412
413
414
415
416
417
418
419
420
421
422
423
424

TABLE XXVII. OUTPUT SYMBOLS

LETTER SYMBOL	FORTRAN SYMBOL	DESCRIPTION
t_{mP}	TMP	Pinion mean circular thickness
t_{mG}	TMG	Gear mean circular thickness
γ	GAM9(1)	Pinion pitch angle
Γ	GAM9(2)	Gear pitch angle
m_p	XMP	Transverse contact ratio
m_F	XMF	Face contact ratio
m_o	XMO	Modified contact ratio
A_o	AO	Outer cone distance
A	AM	Mean cone distance
p	PCIR	Circular pitch
m_{NP}	SMN(1)	Pinion load sharing ratio
m_{NG}	SMN(2)	Gear load sharing ratio
K_i	SKI	Inertia factor
J_P	SJ(1)	Pinion geometry factor for strength
J_G	SJ(2)	Gear geometry factor for strength
Q_P	Q(1)	Pinion strength factor
Q_G	Q(2)	Gear strength factor
σ_{tP}	SST(1)	Bending stress on concave side of pinion tooth
σ_{tG}	SST(2)	Bending stress on convex side of gear tooth
f	FX 1	Lengthwise shift of tooth bearing from center
σ_w	SW	Working stress

CARD
NO. 0

COLUMNS		1	2	3	4	5	6	7	8	9	10
1-10		R	E	V		G	E	A	R	R	H
11-20				C	C	W					
21-30											
31-40											
41-50											
51-60											
61-70											
71-80											

CARD
NO. 1

COLUMNS		1	2	3	4	5	6	7	8	9	10
1 - 10	ZN(1)	1	7	.							
11 - 20	ZN(2)	5	1	.							
21 - 30	PDIA	4	.	0	8	0					
31 - 40	PHA9	2	0	.							
41 - 50	SIG9	9	0	.							
51 - 60	DRIVE	P	I	N							
61 - 70	ROT	R	E	V							
71 - 80	HAND	L	H								

CARD
NO. 2

COLUMNS		1	2	3	4	5	6	7	8	9	10
1 - 10	FACE(1)	1	.	5	0						
11 - 20	FACE(2)	1	.	5	0						
21 - 30	PSM9	3	5	.							
31 - 40	TMP	0	.	0							
41 - 50	WFG	.	1	5	0						
51 - 60	REF(1)	.	0	4	0						
61 - 70	REF(2)	.	0	8	0						
71 - 80	BMAX	.	0	0	8						

CARD
NO. 3

COLUMNS		1	2	3	4	5	6	7	8	9	10
1 - 10	HK	.	3	7	4						
11 - 20	HT(1)	.	4	2	1						
21 - 30	HT(2)	.	4	2	1						
31 - 40	ADD9(1)	.	8	5	0						
41 - 50	ADD9(2)	.	3	5	0						
51 - 60	DED9(1)	.	3	5	0						
61 - 70	DED9(2)	.	8	5	0						
71 - 80	ADO(2)	.	1	0	9						

CARD
NO. 4

COLUMNS		1	2	3	4	5	6	7	8	9	10
1 - 10	FACR(1)	1	.	5	0						
11 - 20	FACR(2)	1	.	5	0						
21 - 30	SKO	1	.	0							
31 - 40	CTD	1	0	0	0	0	0	.			
41 - 50	SKV	1	.	0							
51 - 60	CTG	1	0	0	0	0	0	.			
61 - 70	RCN	6	.	0							
71 - 80											

CARD
NO. 5

COLUMNS		1	2	3	4	5	6	7	8	9	10
1 - 10	AR(1)	-	.	0	1	3	5	0			
11 - 20	AR(2)	.	0	0	7	5	0				
21 - 30	AR(3)	.	0	0	0	6	0				
31 - 40	AR(4)	-	.	0	0	0	5	5			
41 - 50	SAT	1	4	0	0	0	0	.			
51 - 60	SKR	1	.	0							
61 - 70	STF	1	6	0	.						
71 - 80											

INPUT

NUMBER OF TEETH IN PINION	ZN(1)	17.00000
NUMBER OF TEETH IN GEAR	ZN(2)	51.00000
DIAMETRAL PITCH	PDIA	4.08000
NORMAL PRESSURE ANGLE	PHA9	20.00000
SHAFT ANGLE	SIG9	90.00000
DRIVING MEMBER	DRIVE	PIN
DIRECTION OF ROTATION OF DRIVING MEMBER	ROT	REV
PINION HAND OF SPIRAL	HAND	LH
PINION FACE WIDTH	FACE(1)	1.50000
GEAR FACE WIDTH	FACE(2)	1.50000
MEAN SPIRAL ANGLE	PSM9	35.00000
PINION MEAN CIRCULAR THICKNESS	TMP	.00000
POINT WIDTH OF SPREAD BLADE GEAR CUTTER	WFG	.15000
EDGE RADIUS ON PINION CUTTER	REF(1)	.04000
EDGE RADIUS ON GEAR CUTTER	REF(2)	.08000
MAXIMUM NORMAL BACKLASH	BMAX	.00800
WORKING DEPTH AT OUTER END OF TOOTH	HK	.37400
PINION WHOLE DEPTH AT OUTER END OF TOOTH	HT(1)	.42100
GEAR WHOLE DEPTH AT OUTER END OF TOOTH	HT(2)	.42100
PINION ADDENDUM ANGLE	ADD9(1)	.85000
GEAR ADDENDUM ANGLE	ADD9(2)	.35000
PINION DEPENDUM ANGLE	DED9(1)	.35000
GEAR DEPENDUM ANGLE	DED9(2)	.85000
GEAR ADDENDUM AT OUTER END OF TOOTH	ADO(2)	.10900
PINION ROOT FACE WIDTH	FACR(1)	1.50000
GEAR ROOT FACE WIDTH	FACR(2)	1.50000
OVERLOAD FACTOR FOR STRENGTH	SKO	1.00000
GEAR TORQUE FOR CENTRAL BEARING	CTD	100000
DYNAMIC FACTOR FOR STRENGTH	SKV	1.00000
PINION TORQUE	CTP	33333
GEAR TORQUE	CTG	100000
CUTTER RADIUS	RCN	6.00000
OFFSET CHANGE DUE TO DISPLACEMENT	AR(1)	-.01350
PINION AXIAL CHANGE DUE TO DISPLACEMENT	AR(2)	.00750
GEAR AXIAL CHANGE DUE TO DISPLACEMENT	AR(3)	.00060

SHAFT ANGLE CHANGE DUE TO DISPLACEMENT
 ALLOWABLE STRESS
 FACTOR OF SAFETY
 OPERATING TEMPERATURE

AR(4) -0.0055
 SAT 140000
 SKR 1.00000
 STF 160.00000

OUTPUT

PINION MEAN CIRCULAR THICKNESS
 GEAR MEAN CIRCULAR THICKNESS
 PINION PITCH ANGLE
 GEAR PITCH ANGLE
 TRANSVERSE CONTACT RATIO
 FACE CONTACT RATIO
 MODIFIED CONTACT RATIO
 OUTER CONE DISTANCE
 MEAN CONE DISTANCE
 CIRCULAR PITCH
 PINION LOAD SHARING RATIO
 GEAR LOAD SHARING RATIO
 INERTIA FACTOR
 PINION GEOMETRY FACTOR FOR STRENGTH
 GEAR GEOMETRY FACTOR FOR STRENGTH
 PINION STRENGTH FACTOR
 GEAR STRENGTH FACTOR
 BENDING STRESS ON PINION
 BENDING STRESS ON GEAR
 LENGTHWISE BEARING SHIFT
 WORKING STRESS

TMPP 0.44081
 TMGP 0.23185
 GAM9(1) 10.43495
 GAM9(2) 71.56505
 XMP 1.21122
 XMF 1.42369
 XMO 1.86921
 AO 6.58808
 AM 5.83808
 PCIR 0.77000
 SMN(1) 1.00000
 SMN(2) 1.00000
 SKI 1.06997
 SJ(1) 0.20643
 SJ(2) 0.16918
 Q(1) 6.32455
 Q(2) 2.57246
 SST(1) 227153
 SST(2) 274215
 FX1 -0.12982
 SW 99486

APPENDIX VII

COMPARISON OF AGMA AND GERMAN METHODS OF STRENGTH DETERMINATION FOR BEVEL GEARS

SUBJECT

Comparison of bending stress calculations for bevel gears by American Gear Manufacturers Standards AGMA 222.02 and 223.01 and German Standard DIN 3990.

PURPOSE

The purpose of this appendix is to point out the differences between the American (AGMA) and German (DIN) methods for calculating bevel gear stresses and to show which method will produce the most reliable results.

CONCLUSION

The following information was obtained from a careful study of the above two methods:

1. The American (AGMA) Method:
 - a. Has been engineered to give simple design formulas that yield correct values for actual bending stresses and that permit design to maximum capacity of the materials.
 - b. Can balance the strength of gear and mating pinion to give optimum life.
 - c. Can be used to accurately compare two different gear designs.
 - d. Is backed by extensive testing in the laboratory and in the field.
 - e. Is widely used throughout the world.

2. The German (DIN) Method:

- a. Results in stresses which are generally too low when compared with an allowable stress, thus resulting in gears which are too weak.
- b. Indicates that straight bevel gears are much stronger than the corresponding spiral bevel gears, a conclusion that is contrary to established fact.
- c. Is not designed to balance the strength of gear and mating pinion.
- d. Cannot be used to accurately compare two different gear designs.

DISCUSSION

Meaning of Calculated Stresses Versus True Stresses

The ideal method for stress calculation would result in the calculation of the actual stresses existing in a machine structure. However, current design formulas are based on approximations in order to simplify the formulas sufficiently for everyday use. In some methods more attention is given to establishing a correlation between the calculated stresses and the observed measured stresses.

In order to insure a safe working formula for the strength of gear teeth, it is customary to make a chart showing the relationship between the calculated bending stress and the life in stress cycles to failure by fatigue. With sufficient test data it is possible to determine statistically the reliability of a given gear pair under any given load conditions. It should be borne in mind that these calculated bending stresses are not necessarily true stresses, and therefore they cannot be used as a measure of safety when compared with the usually specified allowable stresses resulting from tensile tests on the standard test specimens.

In the AGMA method, for example, a size factor has been included in the formula for calculated stress. This size factor is intended to reflect the effects of specimen size on the allowable working stress. Since the size factor is a function of gear geometry, it has been applied to the calculated stress rather than to the allowable working stress as a matter of convenience. Because this factor has the effect of reducing

the calculated stress as the specimen size is reduced, it is necessary to reduce the values of allowable working stress. This has been done in the AGMA publications.

Because the German standard does not make the distinction between calculated bending stresses and the method for arriving at allowable bending stresses, there is danger that the gear designer will be misguided by the German formula.

Comparison of Specific Results

Tables XXVIII, XXIX, and XXX show comparative results of bending stress calculations by both the AGMA method and the German method.

Tables XXVIII and XXIX show a comparison of selected gear ratios from the AGMA straight bevel gear system and the AGMA spiral bevel gear system. In these two tables the face width was assumed to be equal to three-tenths of the outer cone distance, and the tangential load was given by the following formula:

$$W_t = \frac{9,000 F}{P_d}$$

where W_t = large end of tangential load, pounds

F = face width, inches

P_d = large end of transverse diametral pitch

Comparative Stresses Between AGMA and German Methods

It will be noted in the tabulation for straight bevel gears (Table XXVIII) that for 2.5-DP gears the German calculated pinion stresses average 40 percent less than the AGMA calculated pinion stresses, whereas for 20-DP gears the German values average only 2 percent less than the AGMA values. This difference between the coarse-pitch and fine-pitch gears is the result of the size factor included in the AGMA method.

A similar comparison is shown for spiral bevel gears in Table XXIX. For 2.5-DP gears the German calculated pinion stresses average 10 percent less than the AGMA calculated pinion stresses, whereas for 20-DP gears the German values average 30 percent more than the AGMA values.

**TABLE XXVIII. STRAIGHT BEVEL GEARS
WITH 20° PRESSURE ANGLE**

Gear Com- bination	DP	AGMA Method		German Method		**Stress Ratio	
		Pinion Stress (psi)	Gear Stress (psi)	Pinion Stress (psi)	Gear Stress (psi)	Pinion	Gear
17/17	2.5	39,000	39,000	22,400	22,400	0.57	0.57
35/35	2.5	29,700	29,700	17,800	17,800	0.60	0.60
14/28	2.5	33,700	41,400	20,900	21,000	0.62	0.51
22/44	2.5	29,400	34,500	18,200	18,200	0.62	0.53
13/39	2.5	32,700	42,200	20,200	*	0.62	-
18/54	2.5	30,400	36,700	18,800	*	0.62	-
13/52	2.5	32,300	42,100	19,800	*	0.61	-
17/17	20	24,600	24,600	22,400	22,400	0.91	0.91
35/35	20	18,700	18,700	17,800	17,800	0.95	0.95
14/28	20	21,100	26,000	20,900	21,000	0.99	0.81
22/44	20	18,400	21,600	18,200	18,200	0.99	0.84
13/39	20	20,500	26,500	20,200	*	0.99	-
18/54	20	19,000	23,000	18,800	*	0.99	-
13/52	20	20,200	26,400	19,800	*	0.98	-

*Values are not available for q_k on the graph with the German standard.
A tooth layout would be required.

**Stress Ratio = $\frac{\text{German stress}}{\text{AGMA stress}}$

**TABLE XXIX. SPIRAL BEVEL GEARS WITH
20° PRESSURE ANGLE AND
35° SPIRAL ANGLE**

Gear Com- bination	DP	AGMA Method		German Method		**Stress Ratio	
		Pinion Stress (psi)	Gear Stress (psi)	Pinion Stress (psi)	Gear Stress (psi)	Pinion	Gear
17/17	2.5	43,800	43,800	29,500	29,500	0.67	0.67
35/35	2.5	26,400	26,400	25,600	25,600	0.97	0.97
14/28	2.5	36,500	36,500	29,700	29,800	0.81	0.82
22/44	2.5	27,000	27,000	26,500	*	0.98	-
13/39	2.5	32,000	32,000	28,400	*	0.89	-
18/54	2.5	25,100	25,100	27,000	*	1.07	-
13/52	2.5	27,000	27,000	28,400	*	1.05	-
17/17	20	27,500	27,500	29,500	29,500	1.07	1.07
35/35	20	16,600	16,600	25,600	25,600	1.54	1.54
14/28	20	23,000	23,000	29,700	29,800	1.29	1.29
22/44	20	17,000	17,000	26,500	*	1.56	-
13/39	20	20,000	20,000	28,400	*	1.42	-
18/54	20	15,700	15,700	27,000	*	1.72	-
13/52	20	16,900	16,900	28,400	*	1.68	-

*Values are not available for q_k on the graph with the German standard.
A tooth layout would be required.

**Stress Ratio = $\frac{\text{German stress}}{\text{AGMA stress}}$

TABLE XXX. SELECTED AUTOMOTIVE
SPIRAL BEVEL GEARS

Gear Combi- nation	DP	Pinion Torque (lb-in.)	Gear Torque (lb-in.)	AGMA Method		German Method		*Stress Ratio	
				Pinion Stress (psi)	Gear Stress (psi)	Pinion Stress (psi)	Gear Stress (psi)	Pinion	Gear
11/52	5.34	6,219	29,400	79,600	86,300	79,500	94,500	1.00	1.09
8/33	3.77	6,070	25,037	99,600	90,900	95,700	100,000	0.96	1.10
6/41	3.15	14,968	102,281	97,000	98,000	83,400	141,000	0.86	1.44

$$*Stress Ratio = \frac{\text{German stress}}{\text{AGMA stress}}$$

Table XXX lists three automotive ratios which were compared by the two methods. The biggest difference shows up on the 6/41 combination. Table XXXI gives life data for these three automotive ratios which were obtained from laboratory tests under controlled conditions. Figures 91 and 92 show the results of plotting these data. The broken lines in Figure 91 indicate the width of the scatter band in the standard AGMA method. It will be seen that these points all lie within the scatter band. Figure 92 is for the German method. There are insufficient data to show the width of the scatter band, and this graph does not show as consistent correlation as that shown by Figure 91.

Relative Strength of Straight Teeth Versus Spiral Teeth

A further comparison of straight bevel gears and spiral bevel gears in Tables XXVIII and XXIX shows that the German standard rates the straight bevel pinions 41 percent stronger than spiral bevel pinions, whereas the AGMA method rates the spiral bevel pinions 7 percent stronger than the straight bevel pinions (based on the average of the tabulated automotive ratios). These results by the German method do not appear to be reasonable.

Allowable Stresses and Strength Balance

The AGMA method tabulates the allowable stresses for most commonly used gear materials. Also included is an S-N diagram to show the relationship between calculated stress and gear life for stress levels above the endurance limit. With the aid of the diagram one can determine the required stress levels for gear and mating pinion that will result in equal gear life.

Determination of Gear Size

The AGMA method is supplied with allowable stress values and an S-N diagram relating the stress to the gear life, which provides the designer with the necessary information to determine the gear size that will be required to carry a sustained load for a given duration of time.

Comparison of Factors Considered in the AGMA and German Methods

Table XXXII gives a list of 16 factors affecting gear tooth strength. This table shows how these factors are treated in each of the above methods.

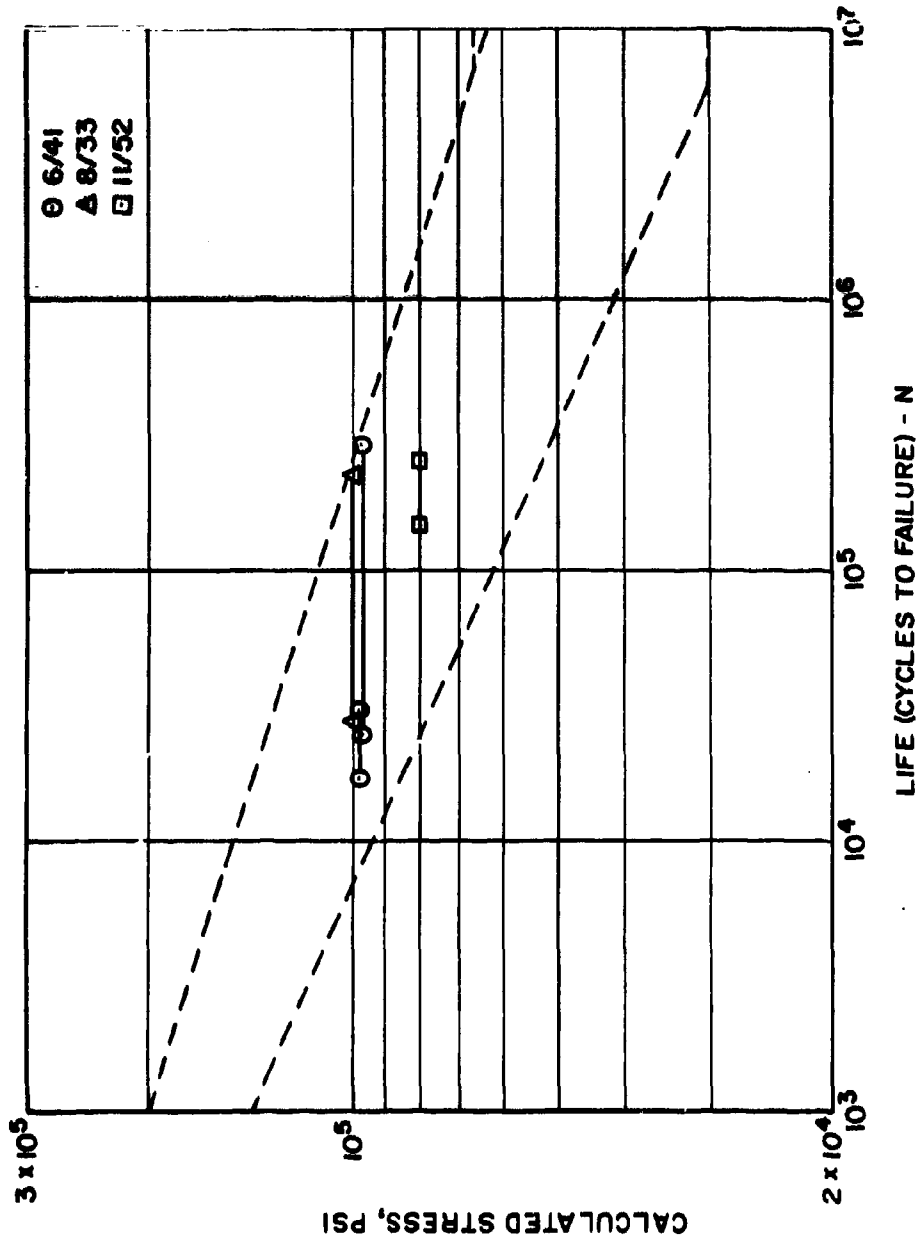
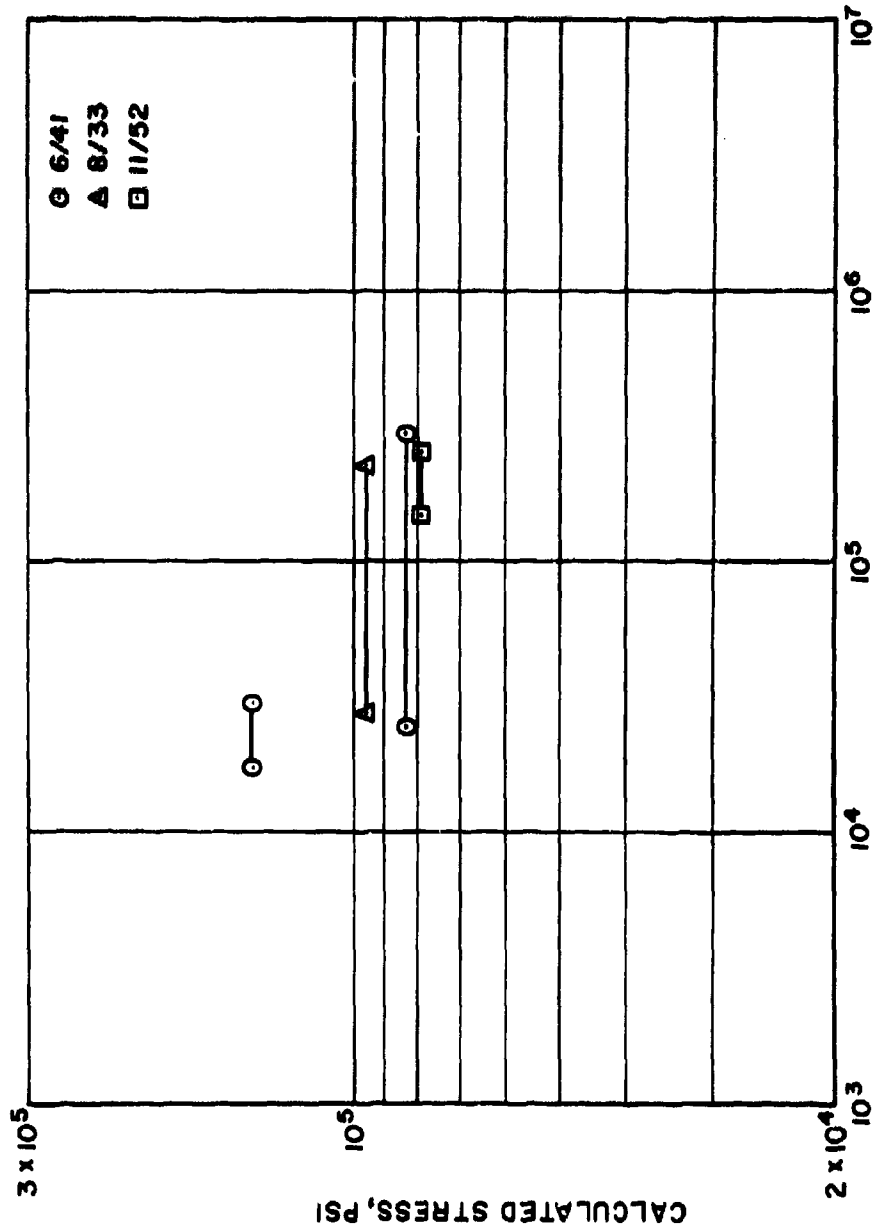


Figure 91. S-N Diagram Based on AGMA Method.



LIFE (CYCLES TO FAILURE) - N

Figure 92. S-N Diagram Based on German (DIN) Method.

Advantages of the AGMA Method

The AGMA method has been specifically engineered to give reliable design formulas for bevel gear teeth. It is backed by the results of extensive laboratory and field testing of gears in their mountings and shows remarkably consistent results.

It has been shown to give excellent results in balancing the thicknesses of pinion and gear teeth to give optimum life. Various designs may be easily and reliably compared.

This method is widely used throughout the world and is used as the industry standard in the U. S. A. For this reason it has been used as the starting point for further study in the present program.

TABLE XXXI. LIFE DATA FOR RATIOS IN TABLE				
Combination	Pinion Failures		Gear Failures	
	Life in Cycles	Number of Failures	Life in Cycles	Number of Failures
11/52	147,000- 253,000	4	-	None
8/33	27,400- 224,000	20	-	None
6/41	24,000- 294,000	8	17,000- 29,300	3

TABLE XXXII. FACTORS AFFECTING GEAR TOOTH STRENGTH

	American Method (AGMA Standards 222.02 & 223.01)	German Method (DIN Standard 3990)
1. Shape of the gear tooth.	Tooth strength is analyzed in mean normal cross section of the tooth, using the Lewis inscribed parabola for locating weakest section in root of tooth.	Tooth strength is analyzed in mean normal cross section of the tooth, using an inscribed equilateral triangle for locating weakest section in root of tooth.
2. Position of load when the tensile stress in the gear tooth will be a maximum.	Position of the point of load application is determined by taking into account not only the theoretical lines of contact but also the effects of lengthwise crowning and profile modification.	Position of point of load application is taken at tip of tooth.
3. Position of maximum stress.	Correction factor based on experimental studies to correct for position and magnitude at the point where the fillet meets the tooth bottom land.	No correction factor to correct for true stress.

TABLE XXXII - Continued

	American Method (AGMA Standards 222.02 & 223.01)	German Method (DIN Standard 3990)
4. Load sharing between teeth.	Amount of load carried by one tooth is based on an analysis of contact ratio and tooth bearing modification at critical point in mesh.	Amount of load carried by one tooth is assumed to be equal to the total transmitted load divided by the profile contact ratio. Tooth bearing modification is not considered, nor is the effect of spiral overlap included.
5. Radial component of normal load.	Radial component of normal load reduces the tensile stress in the tension fillet.	No consideration given to radial component of normal load.
6. Effective face width.	Effective face width is based on direction and length of line of contact on most heavily loaded tooth.	No effort is made to correct face width for effects of an oblique line of contact.
7. Stress concentration in root fillet due to notch effect.	Stress concentration factor is combined with stress correction factor listed in 3 above. This is based on experimental data.	No stress concentration factor is included in formulas.*

TABLE XXXII - Continued

	American Method (AGMA Standards 222.02 & 223.01)	German Method (DIN Standard 3990)
8. Strength balance between mating gears.	Strength balance is controllable to give desired results.	No mention made of strength balance.
9. Effect of gear mountings on gear stresses.	Load distribution factor based on evaluation of inaccuracies and deflections in the gear mountings under load.	No mention of gear mountings and their effect on gear stresses.
10. Dynamic factor that influences gear stresses.	Three dynamic factors: a. Overload factor to make allowance for roughness of both driving and driven units. b. Dynamic factor to reflect inaccuracies in the gears due to manufacturing tolerances. c. Inertia factor to acknowledge effects of a low contact ratio.	No dynamic factors included.

TABLE XXXII - Continued

	American Method (AGMA Standards 222.02 & 223.01)	German Method (DIN Standard 3990)
11. Effect of gear size on allowable stress.	Size factor included in formulas for calculated stress. Since this factor is a function of gear geometry, it has been applied to the calculated stress rather than to the allowable stress for convenience and simplicity.	No size factor is included. *
12. Effect of high temperatures on allowable stress.	Temperature factor to allow for reduction in allowable stress at high temperatures.	No consideration given to correction of allowable stress for temperature effects.
13. Relationship between calculated stress and fatigue life.	Life factor makes provision for an increase in allowable stress when required life is short.	No consideration given to effect of stress on life. †
14. Effect of stress reversal on allowable stress.	Stress reversal factor makes allowance for effects of stress reversal on idler gears.	No consideration given to effect of stress reversal. †

TABLE XXXII - Continued

	American Method (AGMA Standards 222.02 & 223.01)	German Method (DIN Standard 3990)
15. Factor of safety.	Factor of safety is included for use on critical applications or in cases where designer is not certain concerning the loads.	No factor of safety listed. *
16. Allowable stresses.	Allowable stresses are given for most common gear materials. These allowable stresses coincide with the fatigue endurance limit.	No allowable stresses are given, and no reference is made as to where these values can be obtained.
*Mention is made in the standard that this variable should be considered, but no formulas or rules are given.		

**BENDING STRESS FORMULAS ACCORDING TO THE GERMAN
STANDARD DIN 3990**

The formula for the bending stress is given as follows:

$$s_t = \frac{W_t K_o}{K_v} \cdot \frac{P_d}{F} \cdot \frac{q_k}{m_p \cos \psi} \cdot \left(\frac{A_o}{A} \right)^2 \quad (48)$$

where s_t = calculated tensile stress in psi

W_t = transmitted tangential load in pounds

K_o = overload factor

K_v = dynamic factor

P_d = diametral pitch at large end of tooth

F = face width in inches

q_k = strength factor (see below)

m_p = transverse (profile) contact ratio

ψ = mean spiral angle

A_o = outer cone distance in inches

A = mean cone distance in inches

In order to determine the value for the strength factor, q_k , either a tooth layout is required, Figure 93, or the attached graph, Figure 94, may be used, provided the normal pressure angle is 20° and the tooth working depth is $2.0 \cos \psi / P_d$. * To use the graph, the following values must be calculated:

*Graph based on symmetrical rack thickness proportions.

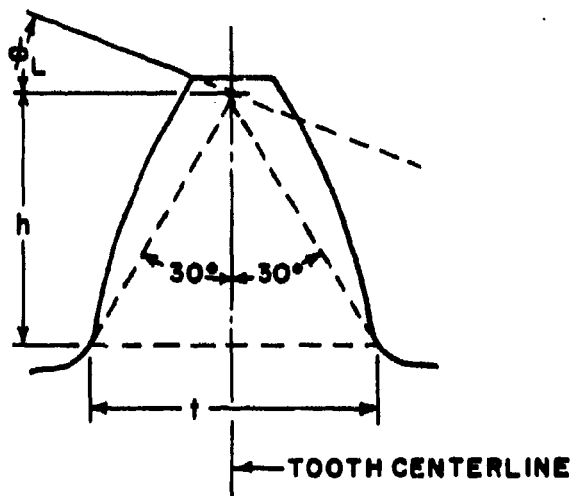


Figure 93. Tooth Layout Used to Determine Weakest Section by German Method.

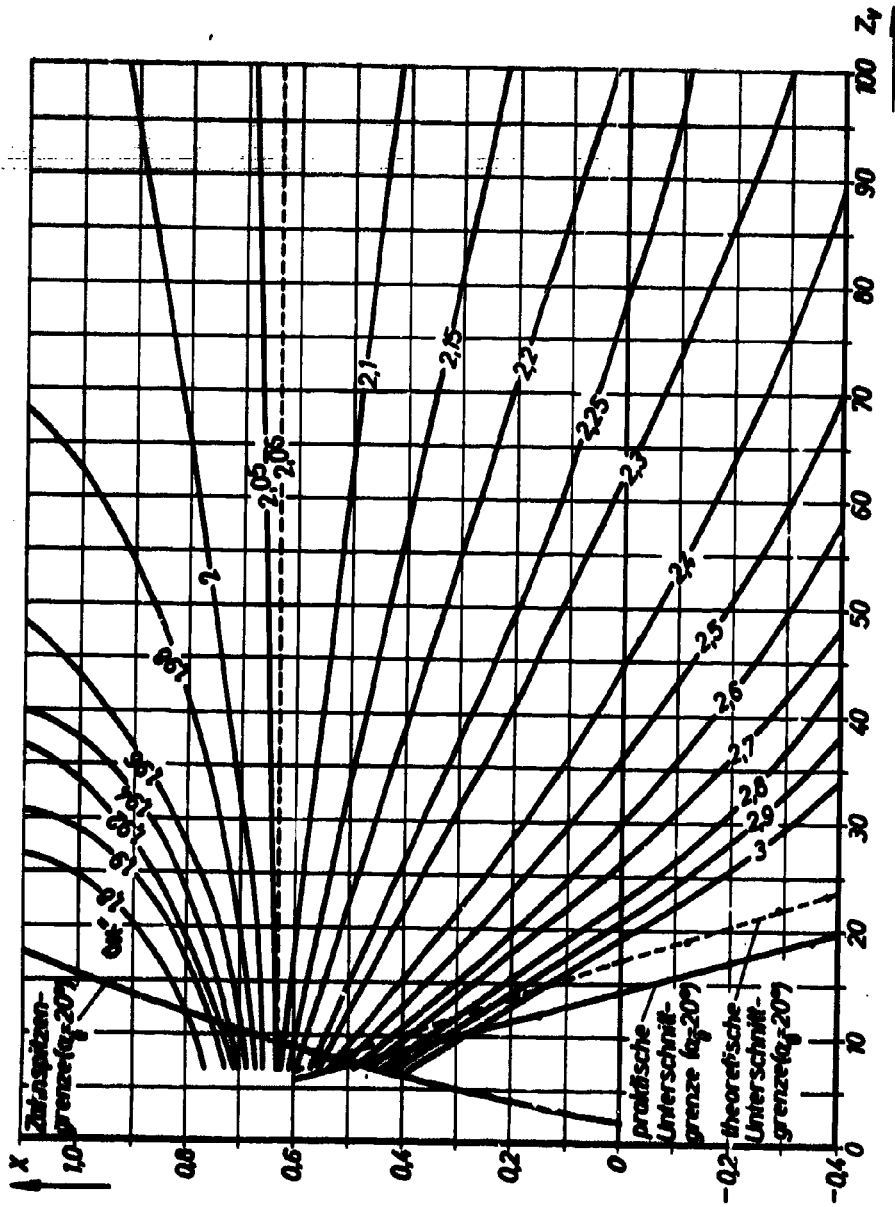


Figure 94. Graph Showing Strength Factor, q_k , in Terms of Tooth Number, Z_v , and Addendum Factor, x , for Gears With 20° Pressure Angle (From DIN 3990).

$$Z_{VP} = n \sec \gamma \sec^3 \psi \quad \text{equivalent number of teeth in pinion}$$

$$Z_{VG} = N \sec \Gamma \sec^3 \psi \quad \text{equivalent number of teeth in gear}$$

$$x_P = 0.460 \left(1 - \frac{1}{m_G^2}\right) \quad \text{pinion addendum factor (AGMA system)}$$

$$x_G = -x_P \quad \text{gear addendum factor}$$

$$m_G = \frac{N}{n} \quad \text{gear ratio}$$

n = number of pinion teeth

N = number of gear teeth

γ = pinion pitch angle

Γ = gear pitch angle

When a layout is made in the mean normal section to a scale of 1 DP (usual AGMA procedure), load is assumed to be applied at the tip of the tooth. The weakest section is determined by inscribing an equilateral triangle within the tooth outline such that the two sides are tangent to the fillet portion of the tooth at the base of the triangle. Then,

$$q_k = \frac{6h \cos \psi}{t^2} \frac{\cos \phi_L}{\cos \phi} \quad (49)$$

where q_k = strength factor

h = load height (radial distance from point where load line intersects tooth centerline to base of inscribed triangle) in inches

t = length of side of inscribed equilateral triangle in inches

ϕ_L = pressure angle at point of load application (angle between load line and a line perpendicular to tooth centerline at point where load line intersects tooth centerline)

ϕ = normal pressure angle

Unclassified
Security Classification

DOCUMENT CONTROL DATA - R & D

(Security classification of title, body of abstract and indexing annotation must be entered when the overall report is classified)

1. ORIGINATING ACTIVITY (Corporate author) Glesson Works 1000 University Avenue Rochester, New York 14603		2a. REPORT SECURITY CLASSIFICATION Unclassified	
2. REPORT TITLE ADVANCEMENT OF STRAIGHT AND SPIRAL BEVEL GEAR TECHNOLOGY		2b. GROUP	
3. DESCRIPTIVE NOTES (Type of report and inclusive dates) Final Technical Report			
4. AUTHOR(S) (First name, middle initial, last name) W. Coleman D. W. Mallis E. P. Lehmann D. M. Peel			
5. REPORT DATE October 1969	7a. TOTAL NO. OF PAGES 267	7b. NO. OF REFS 23	
6a. CONTRACT OR GRANT NO. DAAJ02-68-C-0032	6b. ORIGINATOR'S REPORT NUMBER(S) USAAVLABS Technical Report 69-75		
6. PROJECT NO. Task 1G1662204A01401	6c. OTHER REPORT NO(S) (Any other numbers that may be assigned this report) 4547 (GW No.)		
8. DISTRIBUTION STATEMENT This document is subject to special export controls, and each transmittal to foreign governments or foreign nationals may be made only with prior approval of US Army Aviation Materiel Laboratories, Fort Eustis, Virginia 23604.			
11. SUPPLEMENTARY NOTES		12. SPONSORING MILITARY ACTIVITY US Army Aviation Materiel Laboratories Fort Eustis, Virginia	
13. ABSTRACT The need for increased load capacity of bevel gears in aircraft applications has led to a review of existing methods for determining bevel gear tooth strength. Several methods were reviewed, but it was found that the existing AGMA method was basically the most sound. Fatigue testing of spiral bevel gears showed that vacuum-melt steel would permit higher stresses than those allowed by the present rating practices. A study of lengthwise tooth curvature (cutter diameter) showed that this factor has a significant effect on gear tooth strength. The use of small cutter diameters is shown to improve gear tooth strength by as much as 40 percent under the most favorable conditions. New formulas for effective face width and size factor were developed, which result in stress values more nearly equal to the true stresses in gear teeth. A change in the method for locating the most critical point of loading has resulted in an improved strength balance between the pinion and mating gear.			

DD FORM 1473
1 NOV 65

REPLACES DD FORM 1473, 1 JAN 64, WHICH IS OBSOLETE FOR ARMY USE.

Unclassified
Security Classification

Unclassified
Security Classification

14. KEY WORDS	LINK A		LINK B		LINK C	
	ROLE	WT	ROLE	WT	ROLE	WT
Spiral Bevel Gear Tooth Strength Bevel Gear Tooth Strength Gear Tooth Strength Fatigue Testing of Spiral Bevel Gears Vacuum-Melt Steel Lengthwise Tooth Curvature (Cutter Diameter) Effective Face Width Size Factor Point of Loading Strength Balance						

Unclassified
Security Classification

10466-69